PRODUCTION OF POLYHYDROXYALKANOATES FROM CASSAVA PEEL WASTE: AN INTEGRATED CHEMICAL AND BIOLOGICAL APPROACH

CARMEN HIERRO IGLESIAS

Doctor of Philosophy

ASTON UNIVERSITY

September 2023

Production of polyhydroxyalkanoates from cassava peel waste: an integrated chemical and biological approach

Carmen Hierro Iglesias

Doctor of Philosophy

Aston University

September 2023

Thesis abstract

Polyhydroxyalkanoates (PHA) are biodegradable polymers synthesised by microorganisms, offering a promising sustainable alternative to petroleum-based plastics because they can be synthesised from renewable resources such as biomass. A significant challenge in the industrial production of PHA is the high manufacturing cost, primarily associated with expensive commercial refined carbon sources used as feedstock. Therefore, the use of waste biomass resources to produce PHA has the potential to improve the economic feasibility. Cassava (*Manhiot esculenta*) is a crop widely cultivated in tropical regions. Cassava processing industries produce large amounts of cassava waste, of which 20% are cassava peels (CP), that are predominantly dumped into landfills, resulting in greenhouse gas emissions.

Therefore, this thesis aims to explore the potential of CP as biomass resource for efficient PHA production. Enzymatic and acid hydrolysis of CP were assessed. 97% of conversion from CP to fermentable sugars was achieved through a systematic approach using a design of experiments (DoE) to optimise acid concentration, time, and temperature in acid hydrolysis using H_2SO_4. Subsequently, cassava peel hydrolysates (CPH) were used as the sole carbon source at plate, shake flask, and benchtop stirred tank bioreactor scales for *Cupriavidus necator (C. necator)* growth and PHA production. Small-scale (plate and flask cultures) yielded up to 1.5 g/L of PHA, equivalent to approximately 30% (g_{PHA}/g_{DCW}). The optimization of the cultivation strategy in bioreactor, using defined media in the batch and CPH in the feeding phase, resulted in enhanced production, reaching 12.1 g/L of PHA, equivalent to 86% (g_{PHA}/g_{DCW}). An efficient process for producing PHA by integrating a chemical process for the hydrolysis of CP with a biological process for the conversion of CP into PHA using *C. necator* is presented. This work contributes to the advancement of efficient and sustainable PHA production in biorefinery platforms, and the replacement of petroleum-based plastics, toward achieving Net Zero targets.

Keywords: polyhydroxyalkanoates; waste upgrade; cassava peel; hydrolysis; fermentation; *Cupriavidus necator*; process optimisation.

A mi familia,

por su apoyo incondicional,

gracias por estar siempre a mi lado

Acknowledgments

I want to express my gratitude to my supervisor Dr. Alfred Fernandez-Castane; thank you so much for believing in my potential and trusting me for this PhD project, for your support and guidance during these four years. Your mentorship has not only enriched my academic journey but has also played a crucial role in shaping my evolution as a researcher. Gracias. A big thank you to my associate supervisors, Professor Patricia Thornley and Dr. Annie Chimphango, for giving me a different perspective on my project, and for all your support and motivation.

Thank you to all the staff who welcomed me to EBRI during my time here. A special mention is reserved to Dr. Paula Blanco-Sanchez, for her invaluable expertise in biomass pre-treatment and characterisation, as well as for her generous support and time. Clara, gracias por ayudar siempre en todo y por los ratos de conversación. Gracias también a Alberto, por tu tiempo y por ser un gran apoyo en momentos complicados durante este PhD. I am grateful to Dr. Jinesh Cherukkattu Manayil and Dr. Daniel Jozef Nowakowski for their assistance in resolving laboratory issues that arose during this period.

To all the PhD students in EBRI, especially to those who were there to face the initial difficulties of a PhD. Cris, mil gracias por ser mi primer apoyo, EBRI era mucho más divertido contigo. Filipe, my colleague of late working hours. Jorge, un millón de gracias no serían suficientes para agradecerte todo el apoyo durante estos años. Tu amistad es de lo mejor que me llevo de esta experiencia, te debo una cerve. But also, to those who arrived later and became real friends. Mpho, thank you for always being there to listen. Your support meant a lot to me. Y Marta, ¡ay Martita! La mejor compi de laboratorio que podría haber tenido, porque los dramas compartidos son menos dramas y sobre todo por estar siempre ahí, fuera y dentro del laboratorio. Suerte.

Thank you to all the members in the biolab who made this journey a bit easier. Special mention to Benjamin, for being my first colleague in this experience. To Cornelius, thanks for the help with characterisation techniques, and specially for bringing joy to the lab. To Lewis, in short time you have demonstrated to be un unvaluable member of the team. To all the masters and undergraduate students, especially to Bakhtawar. Mentoring you was such a rewarding

experience; I hope you could learn a lot too. Emma and Ricarda, although you stayed for a short time, it was wonderful to have you in the lab.

Thank you to all the RTs for believing in me and letting me be part of the team. It has been a real game-changer.

A massive thank you to my friends in Birmingham. Specially Marta, Lierni, Dani, Nelson, and Alberto. Echaré de menos los planes de miércoles y las noches de Catán. A mi compi de piso Marta, por ponernos al día en el Rudy's.

Por supuesto a todos mis amigos, los de siempre, que hacen que cuando vuelvo a casa siga siendo casa. No sabéis la suerte que tengo. Gracias por todos los viajes a Birmingham, sois los mejores. Balaguerins, tot i que no sigui de sempre, em feu sentir com si ho fos. Graciès. Mari, la caspolina más bonita. Eres lo mejor que me ha dado la Biotec.

Albert, gracias por todo, por hacer que un océano de por medio no separe, sino una. Por apoyarme cuando todo parecía imposible y hacer que confiara en mí. Ara comença tot.

Pero sobre todo gracias a mi familia, la mejor familia que podría imaginar. A la mejor hermana del mundo. Porque tus viajes a Birmingham y las incontables horas de videollamadas también forman parte de esta tesis. Y a mis padres, por dármelo todo, por la confianza, el esfuerzo y por ser el mejor ejemplo que se puede tener.

List of publications

2021:

"Magnetotactic Bacteria-Based Biorefinery: Potential for Generating Multiple Products from a Single Fermentation". **C. Hierro-Iglesias**, M. Masó-Martínez, J. Dulai, K.J. Chong, P.H. Blanco-Sanchez, A. Fernández-Castané. ACS Sustainable Chemistry & Engineering Vol 9 (2021) 10537–10546. https://doi.org/10.1021/acssuschemeng.1c02435.

2022:

"Opportunities for the development of cassava waste biorefineries for the production of polyhydroxyalkanoates in Sub-Saharan Africa". **C. Hierro-Iglesias**, A. Chimphango, P. Thornley, A. Fernández-Castané. Biomass and Bioenergy 166 (2022) 106600. 10.1016/j.biombioe.2022.106600.

2024:

"Process integration for efficient conversion of cassava peel waste into polyhydroxyalkanoates" **C. Hierro-Iglesias**, C.O Fatokun, A, Chimphango, P. Thornley, P.H. Blanco-Sanchez, R. Bayitse, A. Fernandez-Castane. Journal of Environmental Chemical Engineering (2024), 111815, 12 (1) https://doi.org/10.1016/j.jece.2023.111815.

"Valorising cassava peel waste into plasticized polyhydroxyalkanoates blended with polycaprolactone with controllable thermal and mechanical properties". E. Martinaud, **C. Hierro-Iglesias**, J. Hammerton, B. Hadad, R. Evans, J. Sacharczuk, D. Lester, M.J. Derry, P.D. Topham, A. Fernandez-Castane. Journal of Polymers and the Environment (2024) https://doi.org/ 10.1007/s10924-023-03167-4.

Manuscripts under preparation

“A strategy to enhance polyhydroxyalkanoates production from cassava peel waste in stirred tank bioreactor”

“Utilising cassava peel and volatile fatty acids from anaerobic digestion for sustainable polyhydroxyalkanoates production”.

List of Conference Presentations

2021

- BBNet annual conference: "Optimizing hydrolysis of cassava peels and conversion into polyhydroxyalkanoates by *Cupriavidus necator"* – Poster and flash presentation.
- Green Party Conference: "Production of bioplastics from cassava waste using biological pathways"- Oral presentation.

2022

- EUBCE Conference: "Optimization of the cultivation conditions of *Cupriavidus necator* for the production of polyhydroxyalkanoates from cassava peels waste"-Oral presentation.
- ERA Net Zero Doctoral Summer Showcase: "Polyhydroxyalkanoates from cassava waste: a sustainable alternative to petroleum-based plastics" – Oral presentation. Winner of best student oral presentation award.
- BBNet/HVB ECR Workshop: "From cassava peels to polyhydroxyalkanoates: hydrolysis optimization, microbial screening and process scale up"- Poster presentation.
- Net-Zero Heroes seminar: "From cassava waste to polyhydroxyalkanoates. The potential of biopolymers in achieving a Net-Zero future"- Oral presentation.

List of Contents

List of Abbreviations

μ	Specific growth rate (h^{-1})
3-HB	3-hydroxybutyrate
3-HV	3-hydoxyvalerate
ADF	Acid detergent fibre
ANOVA	Analysis of variance
CCD	Central composite design
CER	Carbon dioxide evolution rate
CP	Cassava peel
CPH	Cassava peel hydrolysate
cPHB	Conjugated polyhydroxybutyrate
DCW	Dry cell weight
DM	Defined media
DMSO	Dimethyl Sulfoxide
DNS	Di-nitrosalicylic acid
DoE	Design of experiments
DTG	Differential thermogravimetric
FCM	Flow cytometry
FSC	Forward scatter
FT-IR	Fourier Transform Infrared Spectroscopy
GC-MS	Gas chromatography-mass spectroscopy
GHG	Greenhouse gas
LCA	Life cycle analysis
LCL-PHA	Long-chain length polyhydroxyalkanoates
LDPE	Low-density polyethylene
MCL-PHA	Medium-chain length polyhydroxyalkanoates
Mt	Million tones
NDF	Neutral detergent fibre
NMR	Nuclear magnetic resonance
OR	Oxygen uptake rate
P(3HB)	Poly-3-hydroxybutyrate
P(3HB-co-3HHx)	Poly-3-hydroxybutyrate-co-3-hydroxyhexanoate

P(3HHx)	Poly-3-hydroxyalkanoate
P(3HV)	Poly-3-hydroxyvalerate
P(4HB)	Poly-4-hydroxybutyrate
PBS	Phosphate-buffered saline
PE	Polyethylene
PHA	Polyhydroxyalkanoates
PHB	Polyhydroxybutyrate
PHBV	poly(3-hydroxybutyrate-co-3-hydroxyvalerate)
PLA	Polylactic acid
pO_2	Partial pressure of oxygen (Dissolved oxygen)
PP	Polypropylene
P_{PHA}	Volumetric productivity of PHA (g/lh)
Pyr-546	Pyrromethene 546
RQ	Respiratory quotient
RSM	Response surface methodology
SCL-PHA	Short-chain length polyhydroxyalkanoates
SEM	Scanning electron microscopy
SSA	Sub-Saharan Africa
SSC	Side scatter
TEA	Techno-economic analysis
TEM	Transmission electron microscopy
TGA	Thermogravimetric analysis
TRS	Total reducing sugars
XRD	X-ray diffraction
$Y_{p/s}$	Product yield coefficient ($g_{product}/g_{substrate}$)
$Y_{x/s}$	Biomass yield coefficient ($g_{biomass}/g_{substrate}$)

List of Figures

List of Tables

Chapter 1. Introduction

1.1 Context of the thesis

The development of bio-based processes and products using renewable resources such as biomass, with a focus on low-carbon strategies, is motivated by the depletion of non-renewable resources and the need to tackle climate change [1,2]. Currently, 99% of plastics used in the globe are produced by the petrochemical industry, and at the end of their life cycle around 80% of these are abandoned in landfills to decompose. The decomposition process of petroleum-based plastics can take up to 1000 years if these are not managed appropriately [3]. Therefore, the poor management of plastic waste and the scarcity of fossil fuels are urging the need to develop more sustainable alternatives such as biodegradable biopolymers whereby polylactic acid (PLA) and polyhydroxyalkanoates (PHA) have attracted great interest [4].

PHA are biodegradable polymers produced by microorganisms and are presented as a promising alternative to petroleum-based plastics [5] because these can be synthesised from renewable resources such as biomass and can be biodegraded by microorganisms. Moreover, in contrast to other biopolymers, PHA can decompose in the aquatic environment, offering a solution not only to plastics dumped in landfills but also to those accumulated in the oceans [6]. The versatility of PHA in various applications is a key factor that positions them as a promising alternative to petroleum-based plastics. PHA have a wide range of applications, including commodity plastics for packaging, agricultural use (including as fertiliser), and medical applications [7].

In the domain of packaging, PHA arises as a viable sustainable solution, addressing the escalating need for environmentally friendly materials. Its ability to degrade naturally addresses the environmental issues linked with conventional plastics [8].

PHA serves a diverse role in agriculture beyond its use in biodegradable mulch films. It can also substitute conventional agricultural plastics such as crop covers and pots, offering an environmentally friendly alternative. Moreover, the potential of PHA as a fertiliser contributes to

the promotion of sustainable agricultural practices by facilitating a closed-loop system and contributing to the circular economy [9].

In the medical realm, the compatibility of PHA with biological systems renders it suitable for a multitude of applications, including but not limited to sutures, drug delivery systems, and tissue engineering. Despite its higher production cost, the use of PHA in valuable medical products justifies de expense. Its distinctive attributes, notably biodegradability and biocompatibility, position it favourably for medical applications where emphasis is placed on sustainability and tailored functionality, rather than product costs [10].

PHA synthesis involves the biotransformation of a carbon source into PHA by PHA-producing microorganisms. Despite the industrial production of PHA started in the 1980s, the interest in biopolymer production has increased in the last decades. One of the main challenges in the industrial production of PHA is the high cost of their manufacturing compared to petrochemical-derived plastics processes, mainly due to the feedstock price [11]. Because commercial synthetic carbon sources are expensive, the use of cheaper carbon sources from biomass resources has been proposed to improve the economic viability of the process [12]. Starchy crops are an interesting option as feedstock due to their high sugar content [13]. Cassava (*Manhiot esculenta*) is a starchy crop widely available in Africa, Asia, and South America. Notably, cassava processing industries produce large amounts of cassava waste that are predominantly dumped in landfills due to the lack of waste management policies in developing countries. Around 40 Mt of cassava waste are generated annually in Africa [14]. Cassava dry material is composed of 90% starch, which has approximately 20% of unbranched amylose and 80% of branched amylopectin, representing a carbohydrate-rich feedstock [15]. Starch can be hydrolysed into glucose, which can be used as the starting material to produce bioenergy and various bio-based products in biorefinery platforms, such as PHA (Figure 1.1).

Although the main focus of this thesis is on the synthesis of PHA from biomass, specifically cassava peel waste, it is important to acknowledge the larger picture of biomass utilisation [16]. Beyond PHA, biomass is a versatile feedstock that can be used to make biofuels and other chemicals with added value [17]. Numerous techniques, including fermentation, catalysis, and thermal conversion, can be used to produce these compounds [18]. While the main focus of this thesis is PHA production, it is important to recognise that biomass may also be used to produce additional value-added products including organic acids, platform chemicals, and bioplastics, as well as biofuels like bioethanol, biodiesel, and biogas. Within the context of sustainable development and circular economy activities, the wide range of products and processes related to biomass conversion provide an extensive picture of the possible uses and advantages of biomass utilisation [19].

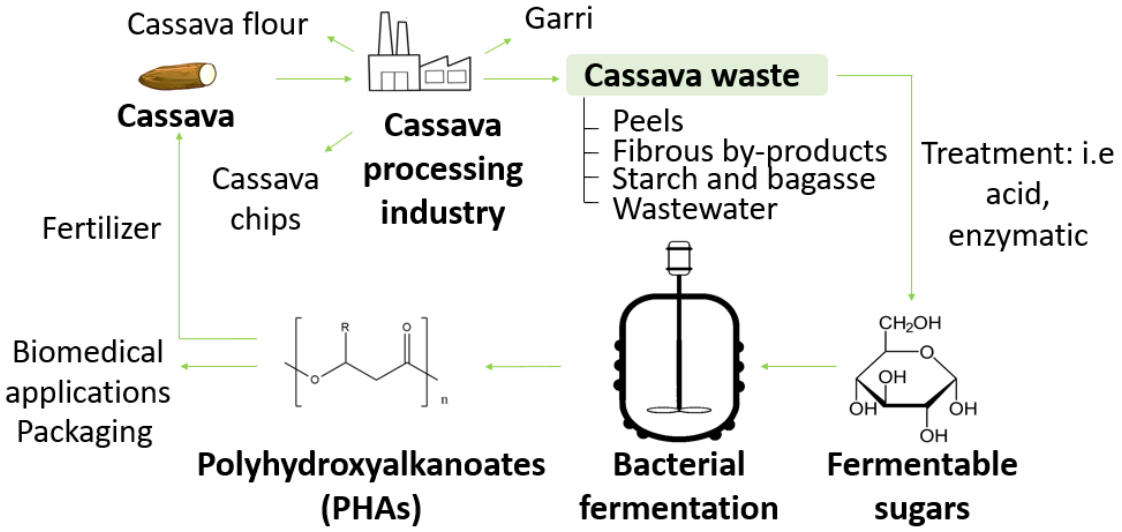

Figure 1. 1 Diagram of the circular economy process of cassava conversion into polyhydroxyalkanoates (PHA) through bacterial fermentation and their potential applications envisaged in this PhD thesis.

The utilisation of cassava waste as a renewable biomass resource for PHA production offers a potential solution to the cassava waste management issues whilst potentially decreasing the PHA production cost hence, promoting the replacement of petrochemical-based plastics, and avoiding the controversial use of edible crops.

1.2 State of the art

Despite more than four decades of extensive research into PHA production and the utilisation of various substrates from biomass and waste products, the quest for optimising this process to effectively replace petroleum-based plastics remains an ongoing challenge [20]. Currently, the primary focus of the scientific community engaged in PHA production centres around the development of sustainable processes, with an emphasis on utilising renewable sources as the primary feedstock [21]. A few studies have reported the utilisation of waste biomass, such as sugar cane molasses, for PHA production, as discussed in detail in *Chapter 2* of this thesis. However, it is important to note that although some of these studies achieved high PHA concentrations within bacteria, reaching levels up to 95% (g_{PHA}/g_{DCW}) [22], most of the developed processes have been constrained to small (flask) scale setups [15]. Consequently, these approaches have displayed limited productivity and are far from reaching the practicality required for commercial applications. However, the production of PHA from waste streams presents several challenges, as outlined by Marciniak and Mozejko-Ciesielska. These challenges include biological,

technological, and economic aspects. Biological challenges include the slow growth of microorganisms, the difficulty in genetically manipulating PHA-producing strains, the inability of bacteria to utilise various types of carbon sources, and the inability to accumulate PHA with desirable properties. Technological challenges involve the inconsistent chemical composition of the waste feedstocks, the optimisation of bioprocess parameters essential to achieve high PHA concentrations, the complexity of downstream processing and PHA recovery, and the variability in PHA properties. Lastly, they also highlighted some economic challenges that hinder commercialisation, including the high cost of carbon sources, the high PHA production cost, and the high cost of the final bioproduct. Addressing these challenges is crucial for advancing the feasibility and sustainability of PHA production from waste streams [23].

Concerning cassava, the selected feedstock for this thesis, it is important to highlight that very limited research has been conducted in this area. Globally, significant quantities of cassava waste are generated, as elaborated in detail in *Chapter 2* of this thesis. Specifically, cassava peel (CP) constitutes approximately 20% of the total waste generated, making it a readily available feedstock for sustainable conversion into value-added products [24]. Additionally, its high carbohydrate content positions it as a promising feedstock within biorefinery platforms. Furthermore, since CP are not typically consumed, their utilisation reduces the risk of competition with food production and the associated impact on vulnerable populations [25].

However, it is crucial to recognise the existence of inherent natural compounds in CP, such as phenolics and cyanides, which have the potential to impede microbial growth and influence the fermentation process. Phenolics hold the capacity to disrupt microbial activity and potentially affect the production of PHA. Similarly, cyanogenic glycosides present in CP pose a risk due to their ability to release cyanide, which could adversely affect microbial fermentation endeavours [26]. To overcome these challenges, it is important to explore methods aimed at mitigating the adverse effects of certain bioactive compounds on microbial growth and PHA production. One potential approach involves using solid-liquid extraction techniques to reduce the concentration of these compounds in CP before fermentation. Methods such as soaking CP in appropriate solvents or water can help to minimise the inhibitory effects on microbial cultures. By managing the presence of these compounds effectively, the conversion of CP waste into PHA via microbial fermentation can be optimised, maximising its potential as a sustainable bioprocess [27].

Recognising the diverse catalytic processes inherent in cassava, the primary emphasis in PHA production lies in exploring microbial fermentation pathways. Thus, while acknowledging the diverse potential for catalytic transformations in cassava utilisation, the current study of PHA production places the emphasis on the microbial fermentation approach.

As far as our knowledge extends, the studies using the cell factory presented here, *Cupriavidus necator (C. necator)* have been restricted to shake flask-scale cultures, and no assessment of cassava as the sole carbon source has been identified in the existing literature. Therefore, while limited research exists, the assessment of the use of cassava waste as a feedstock for PHA production using *C. necator* as the microbial factory has been identified as a notable gap in the literature that underscores the need for further investigation and exploration.

1.3 Aims and objectives of the thesis

The main aim of this thesis is to investigate the feasibility of using cassava peel waste as a sustainable resource for the biosynthesis of PHA by the bacterium species *C. necator*. This aims to answer the two following research questions:

"Can cassava peel waste be effectively employed as a renewable substrate for PHA production by *C. necator?"*

"What are the optimal process conditions and strategies to achieve efficient PHA biosynthesis?"

To achieve this aim, several objectives were set:

- To characterise the CP feedstock, to understand its properties and its potential to be metabolised by *C. necator*, ultimately targeting PHA production.
- To systematically assess diverse hydrolysis methodologies, encompassing both enzymatic and acid hydrolysis, for the efficient extraction of reducing sugars from CP.
- To perform an optimisation study to determine the best hydrolysis conditions employing design of experiments (DoE) and response surface methodology (RSM), specifically through a central composite design (CCD), aimed at maximising sugars recovery.
- To screen the potential of *C. necator* to grow and produce PHA using the cassava peel hydrolysates (CPH) obtained in the optimisation study, conducted at plate-scale.
- To identify the optimal hydrolysis conditions for highest microbial growth and PHA production.
- To upscale the process using the CPH derived from CP in the screening experiment, transitioning from plate to shake flask scale, in order to assess the suitability of CPH for microbial growth and PHA production at a higher scale.
- To further scale up the production of PHA from CPH, transitioning from flask-scale to bioreactor-scale, optimising the fermentation process, resembling industrial processing settings.

- To assess the applicability of flow cytometry as a rapid and efficient analytical tool to determine PHA biosynthesis.

Figure 1.2 depicts the overall process for the production of bioenergy and bioproducts from feedstocks rich in starch and lignocellulosic matter. This diagram depicts the sequential stages undertaken throughout this thesis to achieve the predefined objectives previously presented.

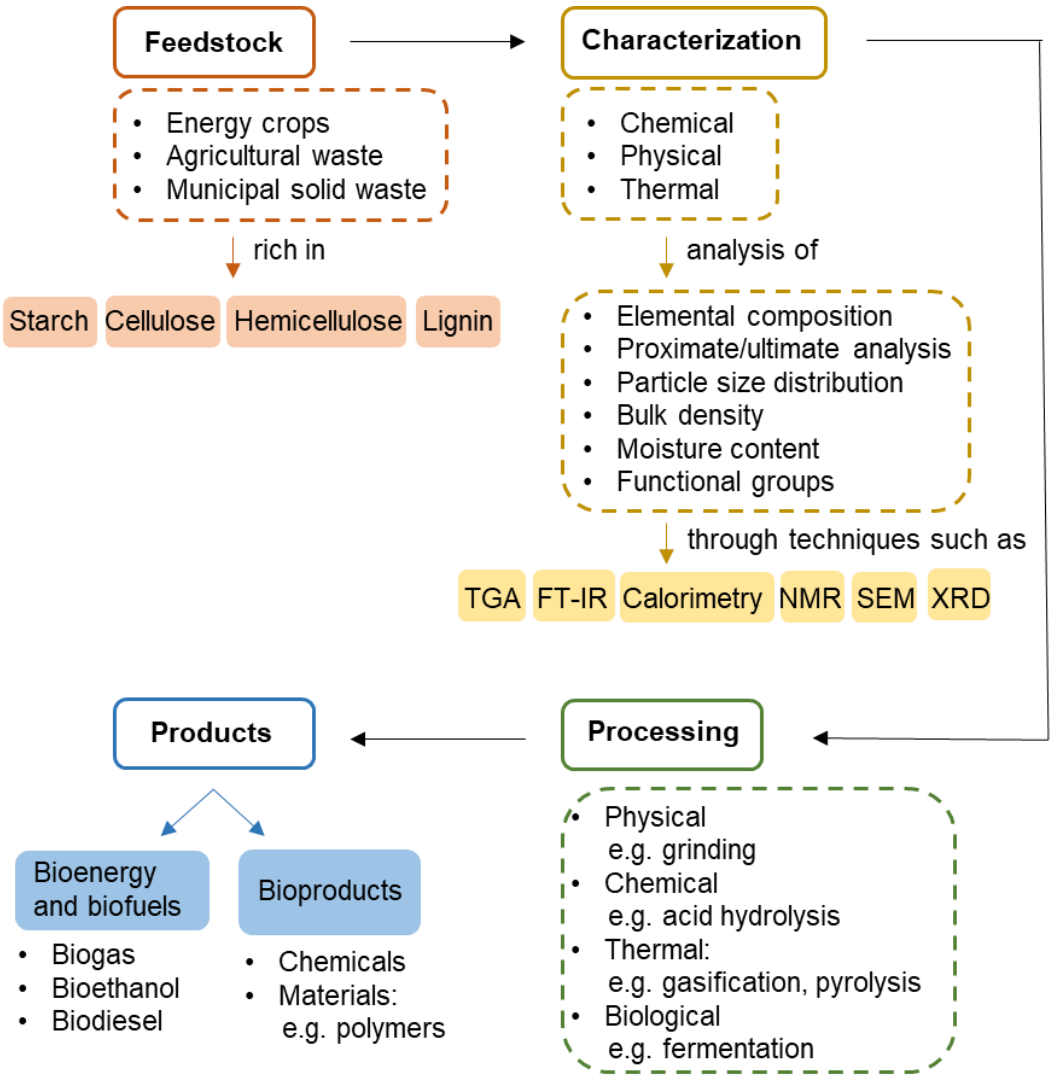

Figure 1. 2 Process diagram of bioenergy and bioproducts production from starchy and lignocellulosic feedstock, including characterisation and processing of biomass.

1.4 Structure of the thesis

This thesis is structured into seven chapters, each addressing different objectives:

- Chapter 1: This initial chapter sets the stage by providing an overview of the context and background that motivated the research presented in the thesis. Additionally, it briefly presents the current state of the art of the research topic and outlines the aims and objectives of the thesis. The chapter concludes by presenting a roadmap of the structure and content of the thesis.

- Chapter 2: This chapter offers a comprehensive literature review that addresses the fundamental concepts and ideas essential for readers to understand before they immerse themselves in the experimental sections. It contextualises the need for PHA development and underscores the significance of using CP as a feedstock. Additionally, this chapter provides insights within the framework of Sub-Saharan Africa (SSA) to elucidate the rationale behind selecting cassava as the substrate.

- Chapter 3: This chapter presents the characterisation of untreated and acid-hydrolysed CP, involving the physical, chemical, and structural properties of CP. This analysis aims to elucidate the alterations induced by acid hydrolysis on the feedstock and assess the potential of this feedstock for PHA production.

- Chapter 4: This chapter focuses on the pretreatment of CP and presents two methodologies for obtaining reducing sugars from CP: enzymatic and acid hydrolysis. Acid hydrolysis is subsequently subjected to optimisation utilising response surface methodology, specifically employing a central composite design to optimise key process parameters to achieve maximum reducing sugars recovery.

- Chapter 5: This chapter utilises the hydrolysates obtained in Chapter 4 to perform a screening of microbial growth and PHA production at plate scale. Following the identification of the most suitable hydrolysate, cultures are subsequently upscaled to shake flask.

- Chapter 6: In this chapter, the transition to bench-scale bioreactor is presented. Several cultivation fermentation strategies and varying process parameters are presented towards the enhancement of PHA production.

- Chapter 7: This final chapter presents the conclusions derived from the entire thesis and delineates potential directions for future research in order to enhance the outcomes achieved across this study.

Chapter 2. Literature review

The content of this chapter has been adapted from the following publication:

"Opportunities for the development of cassava waste biorefineries for the production of polyhydroxyalkanoates in Sub-Saharan Africa". **C. Hierro-Iglesias**, A. Chimphango, P. Thornley, A. Fernández-Castané. Biomass and Bioenergy 166 (2022) 106600. https://doi.org/10.1016/j.biombioe.2022.106600.

2.1 Introduction

The depletion of non-renewable resources and climate change are driving the development of bio-based processes and products using low-carbon-renewable biomass [1,2]. In 2019, 99% of plastics produced worldwide were obtained from non-renewable resources and the decomposition in landfills of petroleum-based plastic waste can take up to 1000 years [3]. It was estimated that between 1950 and 2015, 6300 Mt of plastic waste were generated [28]. Meanwhile, reductions in copper, gas, and oil demand resulted in an economic slowdown in Sub-Saharan Africa (SSA) in 2015 after 15 years of growth. Although Africa relies significantly on wood for its energy supply, there is also a high dependence on fossil fuels, with 80% of electricity produced in the continent coming from fossil fuels [29]. Sustainable technological and industrial development is needed in SSA to develop non-fossil-dependent sources of income [30]. In order to develop more sustainable production systems, the "circular economy" model is gaining interest [31] and biorefineries are proposed as production facilities that can potentially fulfill the implementation of such model [2]. In 2016, biomass represented more than 63.3% of Europe's total renewable energy production [32] and around 10% of the global energy supply [33]. The use of food processing waste in biorefineries to produce value-added products can potentially provide a solution to waste management challenges while developing greener economic models [25]. The SSA economy is largely based on agriculture and its derived products and these activities result in large quantities of organic waste, presenting a major issue that can be seen as an opportunity for the waste to be used as feedstock in biorefineries [34].

Sugarcane, cassava, palm oil, and jatropha are some of the most relevant crops with high production yields in SSA. This thesis focuses on cassava (*Manhiot esculenta*), which is an

important source of farm income in SSA [35]. Around 169 Mt of cassava are produced in Africa annually [36] resulting in 40 Mt of cassava waste [14], and each ton of cassava pulp abandoned in landfills releases between 195 and 361 kg of CO_2 equivalent to the atmosphere [37]. Cassava waste includes peels, bagasse, and wastewater; which have the potential for valorisation into products (i.e., starch, bioethanol, and biofuel) in biorefineries [38]. There has been practically no consideration of this in the research literature to date.

Household and industrial use of plastic increased by an estimated 50% in the world between 2000 and 2019 [39] though this differs around the globe. While the global yearly average plastic consumption per capita in 2015 was 43 kg, in South Africa and Nigeria this figure was only 24.5 and 4.4 kg, respectively. African society is experiencing a change in living habits and urbanisation. SSA is the world's fastest urbanising region, with urban areas expected to double their population in the next 25 years [40]. The production of polymers in SSA is scarce and the vast majority of plastic is imported [41]. Forecasts show that plastic imports in SSA will double by 2030 [41].

360 Mt of petroleum-based plastics are produced annually worldwide [42,43]. As illustrated in Figure 2.1A, 9% of the global plastic waste is recycled, 19% incinerated, 50% landfilled, and 22% evades waste management systems and goes into uncontrolled dumpsites [42]. If current production and waste management trends continue, roughly 12,000 Mt of plastic will be accumulated in landfills by 2050 [28]. Around 82 Mt of plastic waste was landfilled in Africa between 1990 and 2017 [41]. Therefore, the development of bio-based and bio-degradable polymers is a key priority [28], despite currently constituting only 1% of total plastic production. The remaining 99% are petroleum-based plastics such as polypropylene (PP) or polyethylene (PE). Bioplastic production shows an uneven geographic distribution. As depicted in Figure 2.1B, most of the production capacities are located in Asia and Europe, followed by North America and South America. African production of bioplastics is negligible [44] hence, indicating an opportunity for exploitation.

One of the most promising candidates for the sustainable development of environmentally friendly plastics is the biodegradable polyester polyhydroxyalkanoate (PHA), which can be produced from renewable resources [7]. These biopolymers can be used in a wide range of applications such as commodity plastics for packaging, agricultural use, and medical applications [45–49].

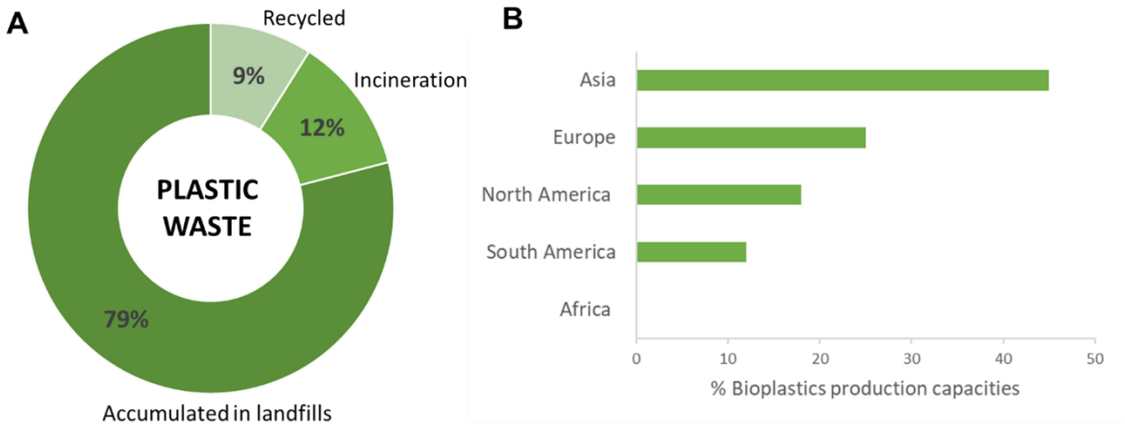

Figure 2. 1 (A) World waste plastic management in 2017 adapted from [41]; (B) Global production capacities of bioplastics in 2019 by continent, adapted from European Bioplastics (2019) [35].

Biopolymers offer many environmental advantages over petroleum-based plastics e.g., recent studies report c.a. 80% reduction in the global warming potential for production of 1 kg of PHA compared to the petrochemical alternative [47]. As a low-cost feedstock, cassava waste can help deliver cost-effective production, enabling the development of local circular economy systems in the SSA region by potentially including cassava-based products such as fertilisers during production.

This literature review, therefore, aims to determine the potential for the development of cassava waste integrated biorefineries to produce PHA in SSA with several objectives: (i) To identify the most appropriate biorefinery configurations: second-generation biorefineries along with the current development in SSA are reviewed in section 2. (ii) To assess the sustainable feedstock and scale-up potential: cassava production and cassava waste generation are considered in the third section as well as the potential for cassava to become a major resource for biorefineries by examining the most relevant bioproducts produced to date from cassava waste. (iii) To identify development opportunities and barriers: in the fourth section, biopolymers (especially PHA) are reviewed and opportunities to produce PHA from cassava waste are discussed. (iv) To support market strategies and planning, the feasibility of implementing cassava waste biorefineries for biopolymers production is evaluated and discussed in the fifth section through market analysis, techno-economic assessment, and life cycle analysis. (v) To integrate the above investigations to deliver a robust assessment of the future prospects of cassava waste biorefineries for biopolymers production in SSA, the above are synthesised in the sixth section.

2.2 Biorefineries

In the late 1990s, the concept of a biorefinery emerged as a result of increased awareness of climate change and fossil fuel scarcity [49]. The most distinctive feature of biorefineries compared to traditional petroleum-based processing plants is the use of biomass, and a key driver is that sustainable biorefineries can help minimize greenhouse gas (GHG) emissions and waste management problems associated with petrochemical refineries [50]. However, a wide range of possible substrates [51] and feedstocks must be selected to suit the product, target characteristics, and suitable conversion technologies [52]. Moreover, economic, social, and environmental aspects must be taken into consideration, including biomass availability in the region. The development of production facilities in less industrialized areas may entail additional benefits such as minimizing feedstock transportation as well as logistics and management considerations that may boost the local and regional economy [53]. Nevertheless, the replacement of petroleum with renewable feedstocks such as biomass requires changes in processing [31,54]. The integration of mature and emerging methods broadens the range of applications and products [52]. Section 2.2 summarises the four types of existing biorefinery concepts and analyses their development status with particular reference to SSA.

2.2.1 Types of biorefineries

Biorefineries are often categorised by the type of raw material used in the process: divided into first, second, third, and fourth-generation biorefineries [55] as depicted in Figure 2.2. First-generation biorefineries use crops as feedstock. The use of food products suitable for human consumption has led to controversy around these platforms due to ethical issues regarding food access in some global regions, potentially leading to competition between human consumption of food and biorefinery supply [56]. Therefore, the use of food crops raises sustainability concerns and first-generation biorefineries may compromise food availability in vulnerable areas [25,34].

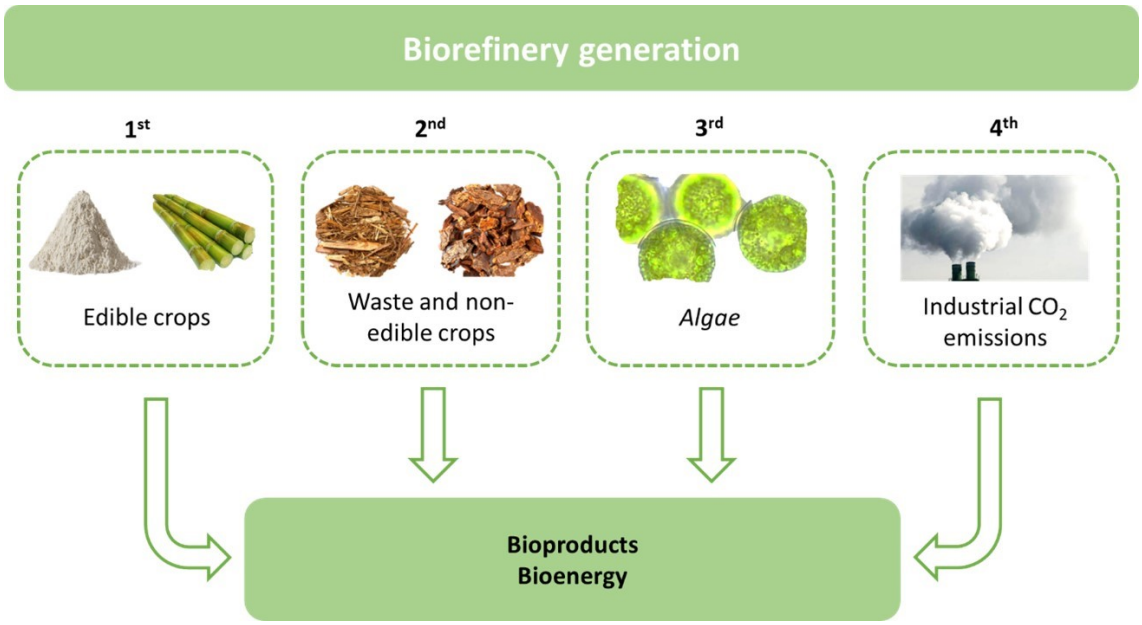

Figure 2. 2 Diagram depicting the types of biorefineries.

Second-generation biorefineries use biomass waste and non-edible crops as feedstock [57]. This includes waste streams generated in a wide range of industries and environments such as agro-industry, agriculture, forestry, and household activities [57]. This type of biorefinery presents some advantages over the first-generation e.g., lower cost of raw materials, alleviation of adverse effects arising from mismanaged waste and environmental pollution, and minimisation of the competition for land resources between food production and bioenergy and bioproducts production, and environmental benefit by valorising waste streams [58]. Various products such as biopolymers (i.e., PHA) [59] and chemicals (i.e., lactic acid, citric acid, hydroxymethylfurfural) [60] have been successfully produced following the 2nd generation biorefinery concept at laboratory scale.

Third-generation biorefineries use microbial cell factories to convert renewable energy and atmospheric CO_2 into value-added products and energy [61]. Many third-generation biorefineries are focused on the use of algae because these can assimilate CO_2 from freshwater, seawater, and wastewater for the production of a wide variety of fuels and products [62].

Lastly, fourth-generation biorefineries use CO_2 produced by other industries as a feedstock [62]. Such biorefineries aim to simultaneously produce value-added chemicals or fuels and store CO_2 during the production thus, reducing CO_2 emissions and achieving a carbon-negative process [63]. The production of bio-based products is well developed at laboratory and pilot scales. Nevertheless, very few products are commercially developed because of technological, environmental, and economic barriers [64].

Currently, the major industrial interest is focused on the development of second-generation biorefineries e.g., the AgriMax project aims to establish a biorefining process using crop waste to produce new bio-compounds for the chemical, bio-plastic, packaging, and agricultural sectors [64], and the OLEAF4VALUE project, aims to isolate high value-added bioactive compounds from olive leaves, with high market potential in the food, feed, chemical, and pharmaceutical sectors [65]. There are well-established industries that are mostly oriented to biofuels and bioenergy production. One example is Vivergo fuels (UK) [66], which produces ethanol from feed wheat. The production of other value-added products, such as bulk chemicals or biopolymers from waste biomass is still to be developed in the industrial landscape. The development of third and fourth-generation biorefineries is still very limited due to the relatively low yields when using microorganisms and the complexity of obtaining desired products from CO_2 [58].

2.2.2 Current developments of biorefineries in Sub-Saharan Africa

Biorefineries offer environmental advantages over traditional refineries, and they are emerging in many areas of the world, such as North America, Europe, Australia, and some areas of Asia. Biorefineries are also emerging in regions such as South America, but there has been very limited activity in Africa [67]. However, some countries in the continent have started developing strategies to promote their industrial implementation [68]. Ghana [69] and South Africa [70] are examples of countries that already published their own strategy to develop their bioeconomy through the exploitation of natural and renewable resources to contribute to economic growth and quality of life. *The bio-economy strategy* of South Africa states the potential of the development of biorefinery platforms for the co-production of a wide range of products and the benefits that this would entail to the country's economy [71].

In 2010 only 42% of the African population had access to electric power, and the increase in the oil price coupled with high population growth rates are hindering access to energy and basic goods [68]. With limited energy infrastructure, the development of biorefineries in SSA is mostly focused on biofuel production [40,72] since these offer a flexible and portable energy vector. Such development has the potential to alleviate fossil-fuel dependence in SSA as well as to promote infrastructure development. Additionally, biorefineries for biofuels can also help to boost the agricultural sector and thereby help tackle poverty [73].

Ghana is an example of a SSA country that has already made progress in this area since a government policy in 2010 that ordered a gradual replacement of petroleum-based fuels with biofuels [69]. Malawi developed a plan in 2006 where Jatropha oil seeds are used as feedstock

for biofuel production [74]. Various major cities in Malawi such as Lilongwe and Dwangwa have plants processing sugarcane molasses to obtain bioethanol [68] and there are biofuel production plants in Mozambique [75], Nigeria [68], Senegal [76] and Tanzania [77]. The use of bioresources for energy production in SSA countries is increasing e.g., 9 – 14% of South African energy needs were produced from biomass in 2016. However, the utilization of biomass for biofuel production is not always economically sustainable and value-added bioproducts can support this [78]. The choice of raw material must take into account the final product or combination of products, as well as the availability of feedstock and the main feedstocks used in the SSA region, which are mostly cassava, sugarcane, molasses, jatropha, and cashew [68]. However, the development of a biorefinery platform must also consider social and economic factors. Second-generation biorefineries are the preferred production plants in SSA due to the large cropped areas, resulting in large amounts of residues. The increasing global interest in moving away from petroleum-based chemicals could align well with the high availability of feedstocks in SSA if appropriate technologies are developed to enable the co-production of other bioproducts [79], which provide income that supports economic profitability e.g., jatropha press cake after biodiesel production has been used to obtain coatings, paints, adhesives, ethanol, binders and fertilizers in various African countries [80]. The International Energy Agency (IEA) estimated the production cost of biodiesel to be around US$0.8/l and the market price around US$1.09/l [81] in 2018. By comparison, the biopolymer polyhydroxybutyrate (PHB) has an estimated cost of US$5-6.11/kg and some companies such as Newlight Technologies claim to be able to produce them in the range of US$2-3/kg [82]. These differentials significantly impact profitability and drive the rationale for multiproduct integrated biorefineries rather than single-product strategies. Here, the co-production of high-value products within integrated biomass-processing facilities can potentially overcome some of the current economic challenges [71,83], since realizing higher sale values for small-volume products can support the overall economic viability of the multi-product biorefinery system. Second-generation biorefineries could then be a potential waste management solution, improving the region's economy through the co-production of various bioproducts and energy [84].

2.3 Cassava production in Sub-Saharan Africa

Cassava (*Manihot esculenta*) is the fourth most important crop for starch production in tropical and subtropical countries, after rice, sugar, and maize [85,86]. Its characteristics, such as endurance, resistance to disease and drought, and ability to grow in low-quality soils allow this crop to grow in different environments [15]. Cassava is a major food crop for more than 700 million people in the world, mostly in SSA and other developing countries such as Thailand,

Vietnam, and Indonesia. The vast majority of cassava production is located in Africa, Asia, and South America, as shown in Figure 2.3. In 2014, Africa was the top producer continent, with a 54.5% share of global production [87]. This crop offers a cheap source of carbohydrates in countries where most of the population faces poverty and hunger. Moreover, cassava can be grown both, at small scale - where there is no need for mechanisation and it is easy to harvest, allowing the growth in marginal areas with unfavourable weather conditions – and at large scale. Therefore, cassava properties make this crop very interesting and resistant to climate change, while promoting economic development in low and middle-income countries. Additionally, the development of local agro-industries for processing and trading cassava could decrease the need for imported crops and the associated high taxes. Therefore, this represents an opportunity to support local economies where cassava is yet underutilised due to the lack of technology to minimise post-harvest loss and the non-existent facilities to convert cassava residue into value-added products [88]. Water makes up 60% of the total cassava mass; while most of the dry material is starch, cellulose, and hemicellulose, making this a cheap source of carbohydrates. The use of cassava in biorefineries as feedstock can result in value-added products and income generation [15], but implementation has been limited due to the lack of industrial and technological capacity. Nigeria is the largest cassava producer in SSA and a global leader. The production in 2013 reached c.a. 55 Mt, representing 20% of the worldwide production [24]. However, only 7% of global production is used to obtain products such as organic acids and flavour compounds [89].

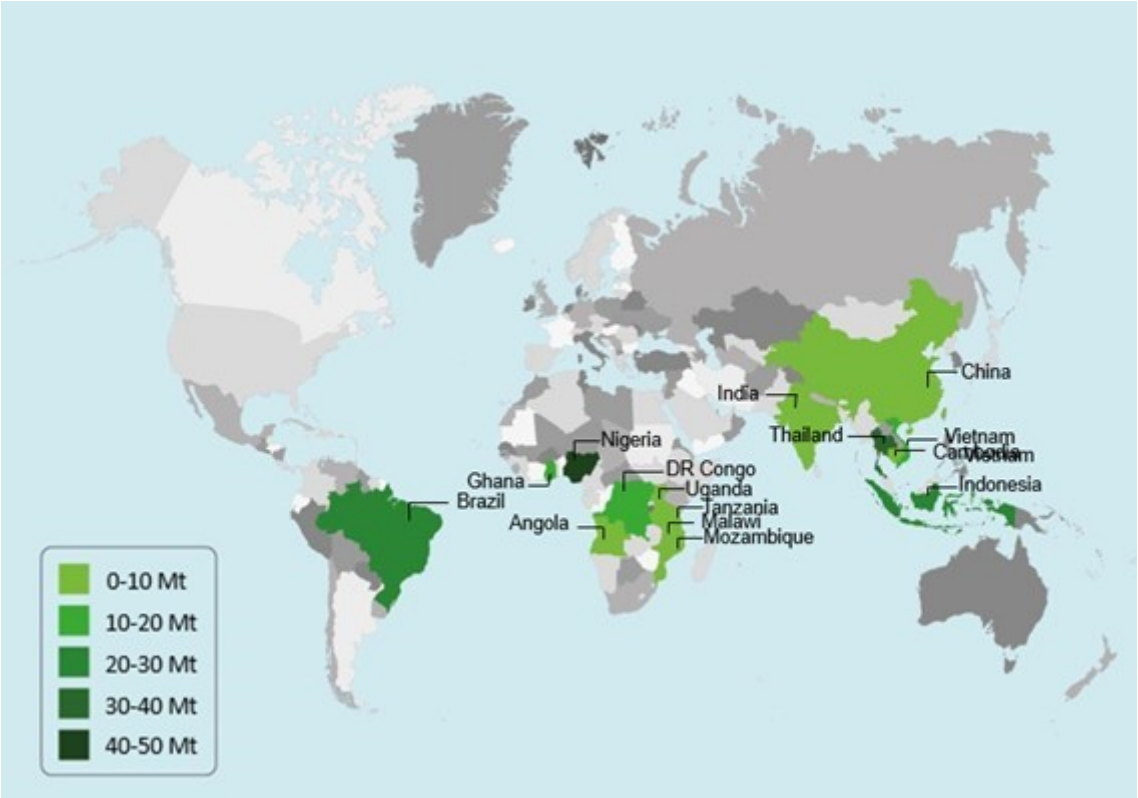

Figure 2. 3 Major cassava producer countries in 2014. Adapted from the joint FAO/IAEA division of nuclear techniques in food and agriculture report [78]. Mt: Million tons.

Cassava crops also present significant waste management challenges: waste generated after cassava harvesting and processing is usually left in the field or burnt, contributing to environmental pollution and human health hazards [90]. Understanding the different types of cassava waste is crucial in order to develop potential solutions. The main categories are: (i) peels from initial processing, (ii) fibrous by-products from crushing and sieving, (iii) settling starch residues and cassava processing bagasse, and; (iv) wastewater [91]. There are six cassava processing facilities in Nigeria, which generate 1.5 – 3 t and 3 – 6 m^3 of solid and liquid waste daily, respectively, from a supply of 6 – 8 t of cassava tubers. This results in approximately 40 Mt of cassava waste being generated in Africa annually [92]. Such waste is rich in organic compounds and can be potentially valorised and used as feedstock in biorefineries to produce fuels and chemicals [79]. If all the cassava waste generated in Africa in a year was to be converted into fuels, approximately 10^{14} kJ of energy could be produced annually, which would be enough to provide electric energy to Ghana for more than a year [93]. Cassava production has increased by an average of 2.2% per year in the last few decades, and the trend is expected to continue in the future, with the associated waste arising [94]. The development of cassava waste biorefineries in SSA, therefore, has the potential to help mitigate the environmental issues associated with waste disposal whilst promoting job creation and industrial activity [95].

2.3.1 Cassava waste valorisation into value-added products

2.3.1.1 Cassava composition, characterisation, and pre-treatment

The main types of cassava waste (peels, fibrous by-products, starch residues, and wastewater) have a similar composition to the fresh crop. This work focuses on the specific use of cassava peel (CP), which constitutes around 20% of the total waste produced during tuber processing. CP is a valuable biomass source for its high starch, cellulose, hemicellulose, and lignin concentrations. Previous authors characterized CP, revealing starch content of 44.5%, cellulose content of 9.1%, hemicellulose content of 7.5%, and lignin content of 9.2% [96]. Starch and cellulose are composed of glucose monomers and belong to the group of polysaccharides. In contrast, hemicellulose is a polysaccharide that can have a diverse range of monomers, including xylose, mannose, glucose, and galactose. Lignin, on the other hand, is a hydrocarbon composed of aliphatic and aromatic structures [97] (Figure 2.4).

The conversion of these molecules into value-added products [98], such as organic acids [99], ethanol [100], flavour and aroma compounds [101], methane [102], biogas [103], and biopolymers [15], among others, has significant potential. However, the efficient conversion of the polymeric components into their constituent monomers is a critical step due to the strong bonding within these structures.

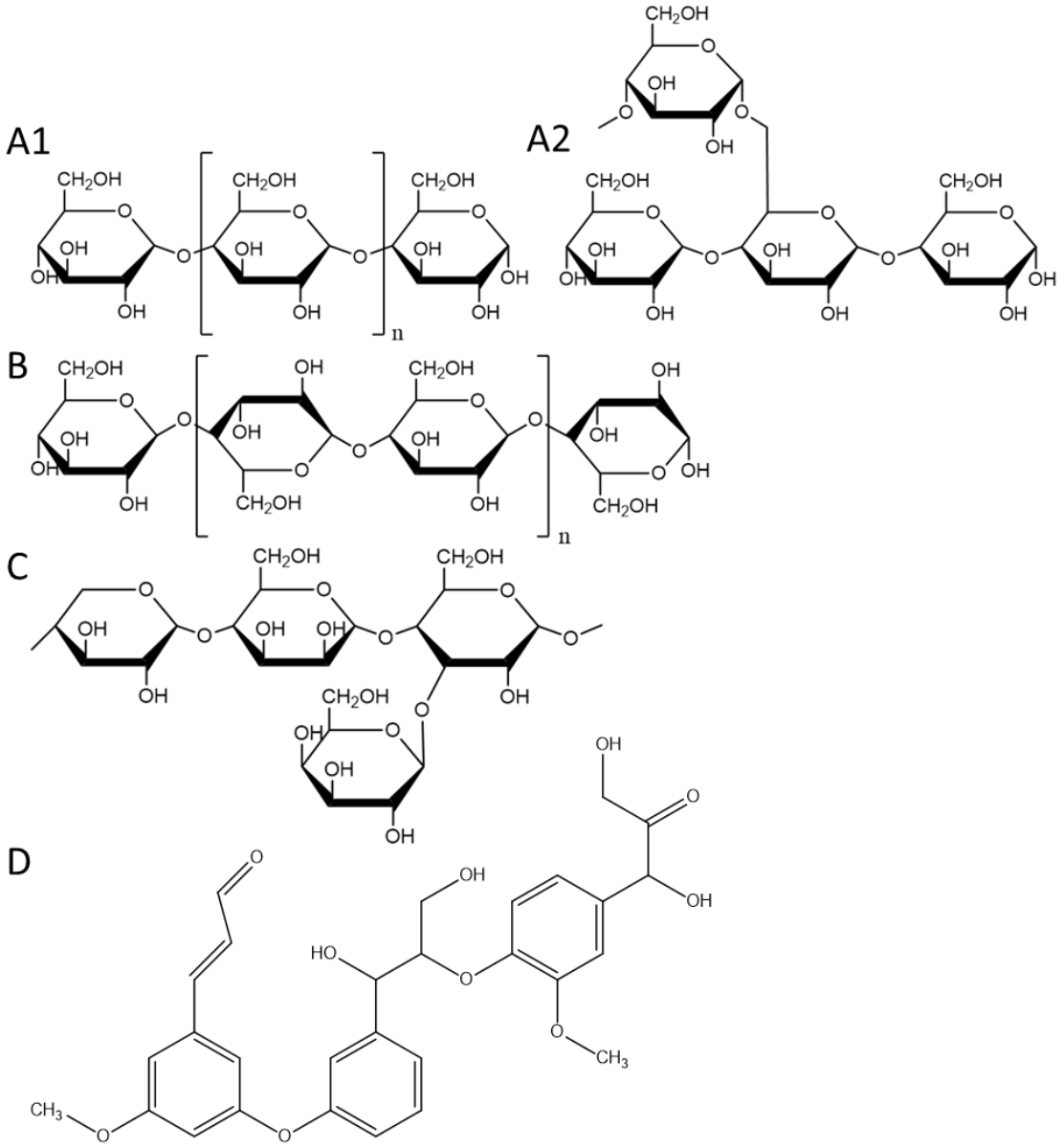

Figure 2. 4 Chemical structure of amylose (A1) and amylopectin (A2), constituents of starch (A); cellulose (B); an example of hemicellulose (C); and lignin (D) fractions. Molecular structures created using ChemDraw.

Apart from the portion of carbohydrates, CP include a wide range of bioactive substances, particularly phenolic compounds, which should be acknowledged and investigated due to their potential inhibition of microbial growth. Recent research has investigated different extraction techniques and provided information on the existence of these chemicals in CP [104]. The technique of phenolic compound extraction from biomass wastes, like CP, has the potential to significantly increase the value of this waste material and reduce the inhibitory activity in future fermentative processes. For instance, strategies employed in the fermentation of other agricultural waste, such as rapeseed meal, have demonstrated the efficacy of bioactive compound extraction in improving overall activity [105]. Therefore, investigating the composition of phenolic and

other bioactive compounds in CP and exploring extraction methods could offer new avenues for enhancing the utilisation of this abundant biomass resource.

However, the composition of biomass can fluctuate depending on factors such as the variety, source, and treatment method. Consequently, it is crucial to conduct biomass characterisation to understand its properties. This facilitates the identification of its potential for bioenergy and bioproduct production and allows for the selection of the most suitable conversion methods [106].

The characterisation process generally involves the evaluation of the chemical, physical, and thermal properties of biomass. Physicochemical methods are used to measure the elemental composition, proximate analysis, ultimate analysis, particle size distribution, bulk density, and moisture content of biomass. These methods can provide valuable insights into the physical and chemical properties of biomass. On the other hand, thermal characterization methods, such as thermogravimetric analysis (TGA) and calorimetry, can provide valuable information on the combustion or gasification behaviour of biomass [107,108]. In addition, spectroscopic techniques like Fourier Transform Infrared Spectroscopy (FT-IR) and nuclear magnetic resonance (NMR), provide information on the molecular structure and functional groups present in the biomass [109,110]. Alternative techniques, including scanning electron microscopy (SEM), and X-ray diffraction (XRD) analysis can be utilized to analyse the morphology of biomass [111]. By understanding these properties, the most suitable conversion technologies can be identified.

Using multiple and orthogonal characterisation methods is essential to obtain a comprehensive understanding of the biomass and ensure an accurate evaluation of its properties. However, the utilization of biomass waste in its natural form for the production of bio-based products is challenging due to its hygroscopic nature, high moisture content, high bulk volume, and low heating value. As a result, the processes involved are usually inefficient and costly [111]. Therefore, a pre-treatment step is necessary to modify the properties of the biomass feedstock, making it more suitable for conversion into value-added products [112]. Various pre-treatment techniques such as mechanical, thermal, and biological treatments are available, and their suitability and drawbacks are determined by the biomass composition and the target product [113]. Among those, enzymatic hydrolysis is one of the preferred methods. Amylolytic enzymes play a crucial role in the conversion of starch-rich substrates into reducing sugars and other products. The enzymatic hydrolysis of starch into glucose is a multi-step process that involves the use of several enzymes, including α-amylases and glucoamylases, which differ in their specificity and mode of action [114]. Figure 2.5 illustrates that the initial step in the process involves the gelatinisation of starch, typically conducted at a temperature range of 65-100 °C, which allows for greater accessibility of the enzymes to the substrate. Nevertheless, some authors have demonstrated that while this step enhances the effectiveness of the process, it is not an absolute

requirement to achieve high conversion values. An alternative approach proposed by previous authors involves skipping the gelatinisation step, as similar conversion rates have been observed with and without its implementation. Following gelatinisation, the next step in the process is liquefaction, typically performed at a pH of 6 and a temperature of 25 °C. It is noteworthy that while these temperatures are commonly used, there is a growing trend towards utilising thermostable enzymes in bioprocessing. Thermostable enzymes exhibit enhanced stability and activity at elevated temperatures, allowing for more efficient and cost-effective processes, particularly in industrial applications [115]. Liquefaction involves the partial hydrolysis of starch by α-amylases, cleaving the α-1,4 glycosidic bonds between glucose units. This enzymatic reaction results in dextrin, maltose, and a very limited amount of glucose. The constrained glucose production via α-amylase can be ascribed to various factors, encompassing the intricate configuration of starch molecules within CP, potentially impeding the accessibility of α-amylase to the substrate. Furthermore, the inherent substrate specificity and enzymatic activity of α-amylase may also contribute to the limited conversion of starch to glucose. Therefore, the capacity of α-amylase to produce high amounts of glucose from CP is limited [116]. The ultimate step of the process is saccharification, typically conducted at a pH of 6 and a temperature of 50 °C, during which the dextrin and maltose molecules produced in the liquefaction step undergo further hydrolysis by glucoamylase, leading to the generation of monomeric D-glucose. Specifically, glucoamylase cleaves the α-1,4 and α-1,6 bonds, thereby producing glucose [117].

Enzymatic hydrolysis offers several advantages over thermochemical techniques, including the generation of fewer hazardous wastes and lower energy consumption. Additionally, the high efficiency and specificity of enzymatic hydrolysis make it one of the preferred methods for the degradation of starchy feedstocks. However, large-scale processing may be limited due to long reaction times and costs [118].

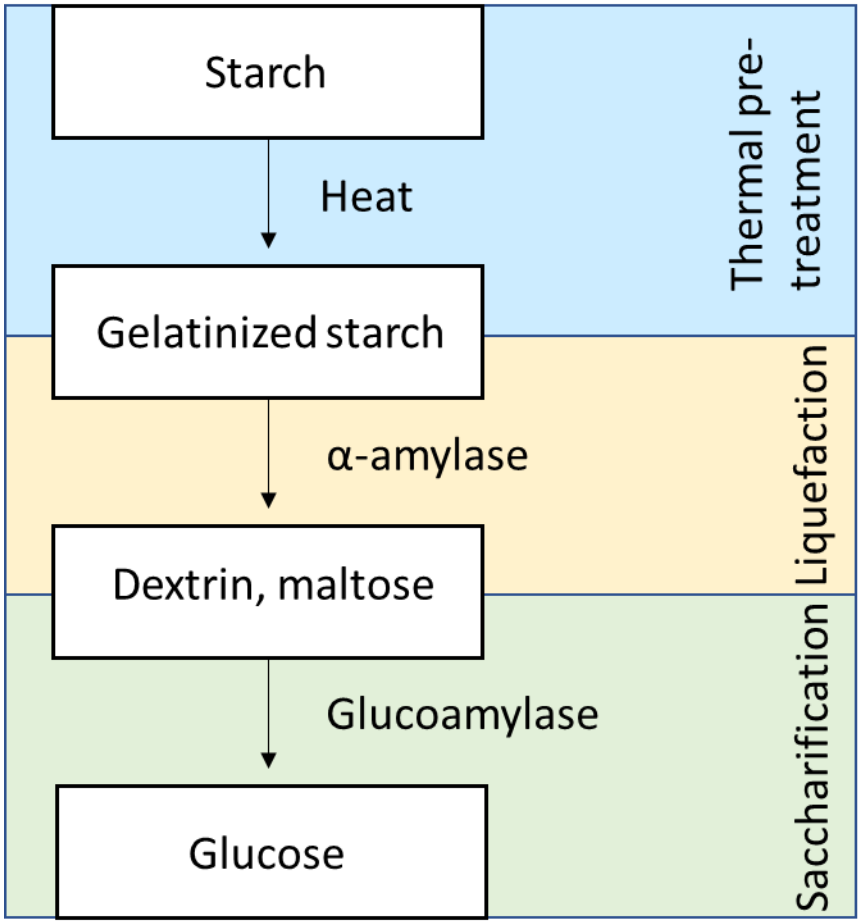

Figure 2. 5 Starch hydrolysis process using α-amylase and glucoamylase.

Other techniques are commonly employed in biomass pre-treatment, including the use of ionic liquids, extrusion pre-treatment, microwave-assisted technologies, and thermochemical processes such as carbonisation, gasification, hydrolysis, and pyrolysis, among others [106,119]. Among all the thermochemical methods, dilute acid hydrolysis appears to be the most prevalent technique for the recovery of reducing sugars from cassava. Moreover, dilute acid hydrolysis offers several advantages, including the need for low acid concentration (up to 3 – 4% (w/w)), which simplifies waste management compared to using highly concentrated acid solutions, resulting in a lower environmental impact [120]. Additionally, it is usually conducted at relatively low temperatures. While other techniques, such as carbonisation, gasification, and pyrolysis, require temperatures of 300, 700, and 500 °C [121–123], respectively, dilute acid hydrolysis is generally performed within the range of 60-200 °C [120,124]. Dilute acid hydrolysis has demonstrated time and cost advantages over enzymatic hydrolysis. While most studies performing enzymatic hydrolysis of CP require between 24 and 48 h [125,126] to achieve maximum conversion, dilute acid hydrolysis of CP only takes up to 2 h [126,127]. The cost of different methods for hydrolysing substrates has also been a topic of interest due to its implications on industrial processes. Woiciechowski and

co-workers conducted a study comparing the cost of enzymatic hydrolysis and acid hydrolysis of cassava bagasse. Their findings indicated that enzymatic hydrolysis resulted in a 70-fold increase in the final cost compared to acid hydrolysis [128]. Additionally, it is noteworthy that acid hydrolysis processes tend to produce a higher quantity of byproducts such as furfurals. These furfurals, while not directly contributing to the desired product, are important to consider due to their potential impacts on downstream processes and product purity in biorefinery operations [129].

2.3.1.2 Current status of cassava waste valorisation

Although the potential of cassava waste as a feedstock in biorefineries has yet to be fully exploited, the biotechnological approaches such as genetic engineering, that have been developed in recent decades facilitate significantly more efficient bio-based production from cassava waste [53, 54]. Countries such as Thailand, Cambodia, Brazil, Vietnam, India, and China are among the major producers and processors of cassava into a wide range of products [132]. Organic acid production from different agro-industrial waste streams is well described e.g., microbial transformation of cassava into citric acid was optimized in Brazil [99], lactic acid and ethanol were achieved at high yields in Thailand [133], and enhanced production of succinic acid is reported in China [134] The predominance of such countries may be not only due to the availability of feedstocks to be transformed into value-added products but also to the technological development that these countries have experienced in recent decades. Despite SSA being the most important cassava-producing region, there is a lack of industrial and technological development that hinders the bioconversion of biomass (e.g., cassava) into value-added products (i.e., biopolymers), and therefore, SSA remains distant from the leading world processors. Most of the cassava production in SSA is located in deprived areas [135]. Hence technological development of cassava valorisation into value-added chemicals such as biopolymers represents an economic opportunity as well as reducing dependence on fossil fuels. A few bioplastics have already been produced, showing promising results. Nevertheless, the biotransformation of cassava waste into biodegradable polymers is yet to be optimised [136].

2.4 Biopolymers

Biopolymers are a type of polymer produced from natural resources that represent an alternative to petroleum-based polymers. Biopolymers can be entirely synthesised by living organisms or chemically synthesised from a biological material [45]. A wide variety of characteristics such as the diverse structural composition and the alterable physical properties have turned biopolymers

into interesting products for a wide spectrum of applications from commodity plastics for packaging to pharmaceutical and medical uses (e.g., heart valves) [55]. Classification by biodegradability properties and origin results in three groups: the first category, bio-based polymers, comprise biopolymers based on renewable resources, which are not necessarily biodegradable, albeit most of them are. The second group, biodegradable polymers, comprises biodegradable biopolymers, which do not need to be based on renewable resources. The third type, bio-based and biodegradable polymers, consists of both, biopolymers based on renewable resources and biodegradable polymers [137].

Many biopolymers with similar properties to traditional petroleum-based plastics such as polypropylene (PP) or polyethylene (PE) are commercially relevant but are not biodegradable. Consequently, most of the current interest is centred on three types of polymers that belong to the bio-based and biodegradable polymers group. These biopolymers are polylactic acid (PLA), PHA, and starch-based polymers [4]. Another interesting characteristic of these biopolymers is their biocompatibility properties, which means they can be used in a variety of medical applications [138]. The following section focuses on the production and opportunities of PHA. Although the current worldwide production of biopolymers is dominated by PLA, recent publications show an increasing interest in PHA due to their faster and more reliable biodegradability times at lower temperatures [6]. PLA is a renewable polymer however; it does not offer the end-of-life advantages of PHA [6,139]. Additionally, emerging biopolymers such as polyethylene furanoate (PEF), derived from the polymerisation of 2,5-furandicarboxylic acid (FDCA), which can be obtained from biomass, are gaining attention. PEF presents promising properties for biodegradability and can contribute to the diversification of sustainable polymer options [140].

The biopolymers market is currently dominated by Europe and North America with Metabolix (USA) dominating global production, while production in the Asia Pacific and Latin America begins to evolve [141]. In contrast, there is little reported activity for the African continent, with very few companies producing biodegradable plastics; an exception is Hya Bioplastics in Uganda [142].

Production of PHA presents two major challenges: (i) the cost of the substrate needed for the synthesis of the biopolymer and (ii) the cost of purification and its associated technologies. Some manufacturers report the use of feedstocks such as castor oil, but limited feedstock data is publicly available. Therefore, biopolymers' commercialisation is hampered by economic factors [22].

2.4.1 Polyhydroxyalkanoates (PHA)

PHA (Figure 2.6A) are a wide family of polyesters that are produced by various microorganisms; both native and genetically modified. They are lipid-like molecules and have similar properties to some petroleum-based plastics such as polypropylene (PP) and low-density polyethylene (LDPE). PHA have become a promising alternative to petroleum-based plastics [5] as they can be synthesised from renewable resources and biodegraded by microorganisms [145]. PHA are hydrolysed by specific depolymerases, which are secreted by PHA-degrading microorganisms, hence the polymer is degraded extracellularly to water-soluble products [146]. The bio-based and biodegradable characteristics strongly support PHA market growth among bioplastics [8].

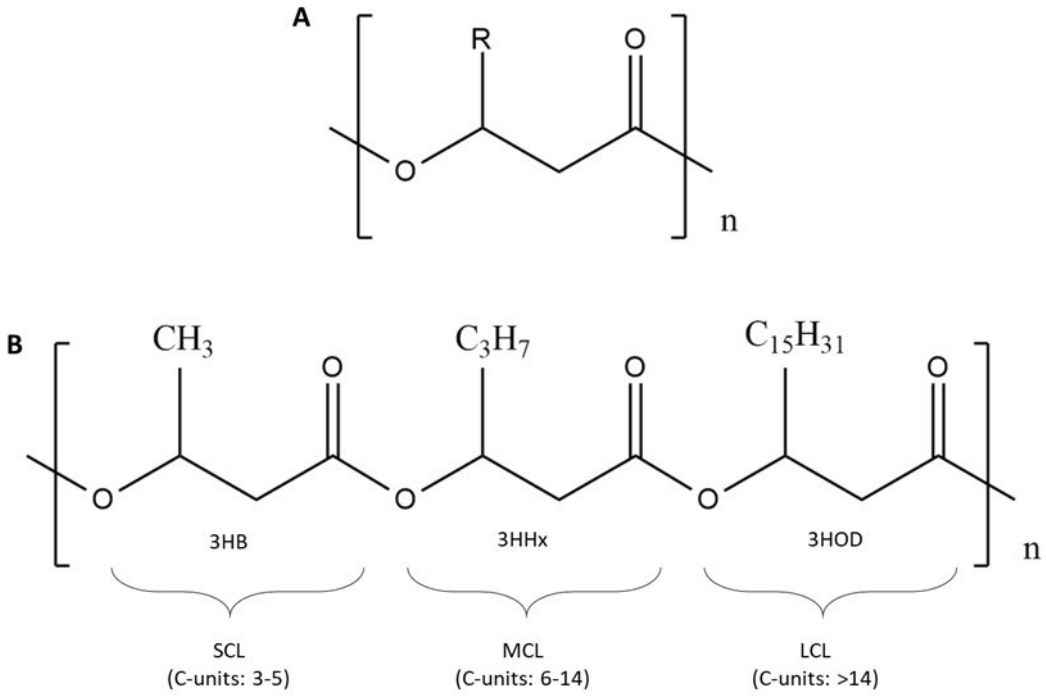

Figure 2. 6 General molecular structure of (A) Polyhydroxyalkanoates (PHA). (B) Examples of short-chain length (SCL), medium-chain length (MCL), and long-chain length (LCL)-PHA. Molecular structures created using ChemDraw. 3HB: 3-hydroxybutyrate acid; 3HHx: 3-hydroxyhexanoate acid; and 3HOD: 3-hydroxyactadecanoic acid.

More than 150 different PHA monomers have been described and different PHA polymers and copolymers can be obtained through combinations of single monomers depending on the carbon source used by the microorganism. Moreover, PHA show a wide diversity of characteristics and properties, therefore, allowing a broad range of applications. Widely studied PHA include polyhydroxybutyrate (PHB) which is one of the most abundant PHA homopolymers and; poly(3-hydroxybutyrate-co-3-hydroxyvalerate) (PHBV), a copolymer obtained after the combination of

3-hydroxybutyrate (3-HB) and 3-hydoxyvalerate (3-HV) [147,148]. PHA are divided into three categories depending on the number of carbon units: (i) short-chain length (SCL-PHA), (ii) medium-chain length (MCL-PHA), and (iii) long-chain length (LCL-PHA) (Figure 2.6B). The above-described monomers can be combined to form both, homopolymers and copolymers [138]. Table 2.1 shows the main characteristics of each category such as the number of carbon monomer units, the main properties, and potential applications.

Table 2. 1 Main characteristics of the three categories of polyhydroxyalkanoates (PHA).

Category	Carbon atoms	Main properties	Presence in nature	Relevant applications
SCL-PHA	4-5	Thermoplastic	Common	Packaging and textile [138,149]
MCL-PHA	4-14	Elastomeric	Common	Biomedical [149,150]
LCL-PHA	>14	Non-specific	Rare*	Bioplastics [151,152]

*LCL-PHA have been blended with SCL-PHA and mcl-PHA for application studies. SCL-PHA: short-chain length polyhydroxyalkanoates; MCL-PHA: medium-chain length polyhydroxyalkanoates; LCL-PHA: long-chain length polyhydroxyalkanoates.

PHA are only produced by microbes and they are stored as cytoplasmic granules which are insoluble in water [138], with a diameter ranging from 0.2 to 0.5 μm [138]. They can provide carbon and energy to the cell, enhancing the cell lifetime under starvation conditions [98,99]. Additionally, PHA enhances stress resistance and robustness of microbes when exposed to diverse environmental stressors, including but not limited to high or low temperature, freezing conditions, oxidative stress, and osmotic pressure [153]. On the surface of those granules, a considerable number of proteins are found. Although the function of some of these proteins has not been defined yet, the supramolecular complex of protein-PHA interactions has exploitation potential. Jendrossek proposed the designation “carbonosomes” to the complex organised structures containing proteins on the surface of PHA [154].

PHB is one of the most abundant and common PHA, which belongs to the SCL-PHA group. It consists of linear chains of (R)-3-hydroxybutyrate units. PHB has been divided into three groups based on the number of monomer units: (i) high molecular weight storage PHB, (ii) low molecular weight PHB and (iii) conjugated PHB (cPHB). Firstly, high molecular weight storage PHB includes PHB polymers containing more than 10^3 units, and they are also known as “storage PHB”. They are usually found in prokaryotes as inclusion bodies. Secondly, the low molecular weight PHB group comprises PHB polymers containing between 100 and 200 units of (R)-3-hydroxybutyrate. These types of polymers may be found in all organisms [138]. Lastly,

conjugated PHB (cPHB) includes PHB polymers containing less than 30 units of (R)-3-hydroxybutyrate covalently linked to proteins [155].

The biochemical pathway for PHB synthesis comprises three main steps: (i) the condensation of two molecules of acetyl-Co A to acetoacetyl-CoA by a β-ketothiolase (PhaA); (ii) the acetoacetyl-CoA reduction into 3-hydroxybutyryl-CoA (monomeric precursor of the biopolymer) by an acetoacetyl-CoA reductase (PhaB) and; (iii) 3-hydroxybutyryl-coA polymerization to obtain PHB, conducted by a PHB synthase (PhaC) (Figure 2.7) [156].

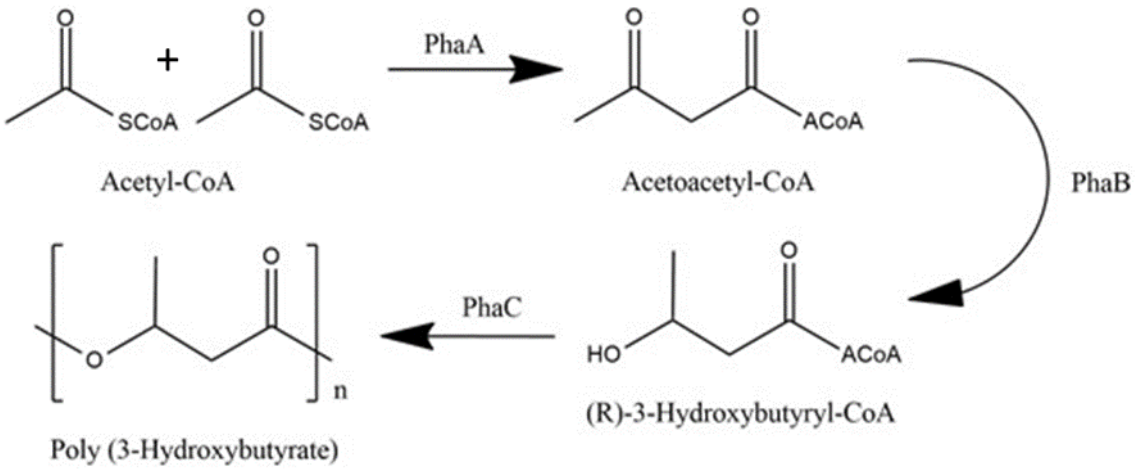

Figure 2. 7 Schematic illustration of the enzyme-catalysed polyhydroxybutyrate (PHB) synthesis system. Molecular structures created using ChemDraw.

2.4.2 Polyhydroxyalkanoates production

PHA are bio-based and biodegradable biopolymers that are entirely produced by various types of microorganisms. It has been reported that PHA are produced in response to carbon oversupply, resulting in carbon and energy reserves inside the cells. Nevertheless, carbon oversupply is not the only stimulus for the microbes to produce PHA: the limited supply of other nutrients such as nitrogen or oxygen restricts bacterial growth and leads to PHA synthesis [157,158]. PHA synthesis requires a carbon source that the microorganism uptakes and subsequently transforms into PHA. All PHA are synthesised from CoA-activated precursors by the action of PHA synthases that catalyse the polymerisation [155]. Depending on the microorganism, different carbon sources can be used such as glucose, fructose, maltose, or xylose. Nevertheless, not only sugars can be used as feedstock in PHA production. Vegetable oil derivatives have also shown promising results in lab-scale studies [13]. Despite the industrial production of PHA started in the 1980s, the interest in biopolymer production has increased in the last decades. One of the main problems detected in

PHA production is the high process cost compared to petrochemical-derived plastics. In 2017, PHA cost was estimated to be $5-6.11/kg which is 3 to 4 -fold higher than their petrochemical competitors, while polymers such as polypropylene (PP) or polyethylene (PE) cost approximately $1.3-1.9/kg [22, 23]. One of the most limiting steps in PHA production is the feedstock price. Commercial synthetic carbon sources are expensive hence, using cheaper carbon sources from biomass resources has been proposed to improve the economic viability of the process [12]. Other factors directly influencing the high cost of the process are the production yield and PHA recovery efficiency in the downstream process [13]. PHA yield depends on different variables such as the bacterial species, components of the culture media, and culture conditions [159]. The following sections analyse two key variables of the PHA production process: the microbial cell factory, and the raw material used as feedstock.

2.4.2.1 Microbial cell factories commonly used for the production of PHA

PHA can be produced by many microorganisms natively whereas others can be genetically modified in order to synthesise biopolymers. Most of the native producers accumulate PHA as intracellular carbon and energy reserves [148]. A wide variety of microorganisms have been used to date to efficiently produce PHA for industrial applications. Gram-positive and negative bacteria and some eukaryotes have been reported to produce PHA [138]. Table 2.2 presents relevant studies showing different carbon sources (feedstock) and cultivation strategies for PHA production. As can be observed, PHA production can be as high as 95% of the bacterial dry cell weight under optimised conditions [22]. *Cuapriavidus necator* (*C. necator* – formerly known as *Wautersia eutropha, Ralstonia eutropha,* and *Alcaligenes eutrophus*) is a gram-negative facultative chemolithoautotrophic bacterium widely studied for its ability to efficiently produce PHA. *C. necato*r produces PHA natively, mainly PHB, in the presence of an excess of carbon and under nutrient stress [160]. *C. necator* exhibits a versatile metabolism capable of utilising various carbon sources, including sugars, alcohols, and fatty acids. It possesses key metabolic pathways such as the glycolytic pathway, the tricarboxylic acid (TCA) cycle, and the β-oxidation pathway for lipid metabolism [161]. PHA production in C. necator unfolds through a series of intricate biochemical steps. Commencing with substrate uptake and metabolic processing, precursor molecules such as acetyl-CoA and synthesised and subsequently polymerised into PHA chains within the bacterial cell as depicted in Figure 2.7 [162]. This particular PHA-producing microorganism has three genes that are required for PHA synthesis which are clustered in a transcriptional unit called phaCAB operon. PHA can be produced under autotrophic conditions using H_2 as an electron donor and O_2 as an electron receptor thus, reducing CO_2 [155]. Although

PHB is the most abundant biopolymer synthesized by *C. necator*, this bacterium can also produce copolymers such as poly (3-hydroxybutyrate-co-3-hydroxyvalerate). The resulting biopolymer composition depends on different variables such as the carbon source or the biochemical pathway utilised [163]. Researchers have endeavoured to exploit the innate capabilities of *C. necator* for the industrial- scale production of PHA. Strategic interventions encompassing optimisation of growth conditions and genetic manipulation have been employed to enhance PHA yields, fostering advancements in sustainable bioplastic production. *C. necator* plays a critical role in promoting the search for environmentally viable plastics because of its innate metabolic flexibility. The investigation into PHA production stands as a compelling area for further exploration, as researchers delve into its intricate metabolism processes. Positioned at the intersection of sustainability and biotechnology, these academic pursuits offer a propitious pathway for pushing the boundaries of bioplastics production forward while adhering to the principles of scholarly rigor and integrity [161].

Advances in genetic engineering have enabled the development of novel PHA-producing strains [164]. An interesting example is *E. coli*, whereby genes from *C. necator* were inserted to produce PHB [165]. Other microorganisms have also shown promising PHB production rates after genetic manipulation. Remarkably, all the studies depicted in Table 2.2 were carried out in technologically and industrially developed countries. In contrast, most countries in SSA have not developed the technology to achieve similar production titres. Knowledge transfer from developed to developing countries, as well as the need for advanced technology provision, can help to develop the SSA economy and development.

Table 2. 2 Relevant microbial systems used for the production of polyhydroxyalkanoates (PHA).

Cell factory	Carbon source	Cultivation strategy	PHA content (% (g_{PHA}/g_{DCW})	Reference
NATIVE				
C. necator	Waste rapeseed oil + whole cheese whey hydrolysate	Batch	95.4	[166]
B. sacchari	Saccharose	Fed-batch	72.6	[167]
P. putida	Decanoic acid + glucose	Fed-batch	74	[168]
Ideonella sp. O-1	Syngas	Batch	77.9	[104]
B. megaterium	Sugarcane molasses	Fed-batch	45.8	[169]
V. proteolyticus	Fructose	Batch	54.7	[170]
RECOMBINANT				
E. coli	Glycerol	Fed-batch	67.9	[171]
H. bluephagenesis	Crude corn extract liquid + glucose	Fed-batch	79.5	[172]
M. extorquens	Methanol	Fed-batch	24.7	[173]

2.4.2.2 Use of cassava waste as feedstock for PHA production

Feedstock price is one of the major burdens in the process of PHA production [174]. With the objective of reducing the total production cost of PHA, a wide range of feedstocks have been tested as an alternative to synthetic commercial sugars (Table 2.3). The highest production values (in terms of intracellular PHA accumulation) are generally achieved using pure sugars (i.e., glucose) followed by alternative feedstocks with high content of carbohydrates such as cassava and sugarcane. The use of synthetic sugars as carbon sources results in high process costs and therefore, researchers are working to find more efficient routes by using waste streams as carbon sources [151]. Waste biomass has a high potential to be used as feedstock for the production of PHA. For example, lignocellulosic biomass can be pre-treated to release fermentable sugars that bacteria can use as the carbon source to grow and produce PHA [175]. On the other hand, starchy materials from crops or wastewater are interesting resources because they are cheap, renewable, and locally available [13]. Cassava waste has been seldom used as feedstock for PHA production with limited published work (Table 2.3).

Table 2. 3 Production of polyhydroxyalkanoates (PHA) using relevant substrates and microbial systems.

Substrate	Cell factory	Process limitation	Polymer	Cultivation strategy	PHA content (% (gPHA/gDCW))	Ref.
Glucose	*C. eutrophus B10646*	Nitrogen	P(3HB/3HV/4HB) and P(3HB/3HV/3HHx)	Batch	80.0	[176]
Cassava starch hydrolysate	*Cupriavidus sp. KKU38*	Nitrogen	PHB	Batch	61.6	[15]
Cassava waste	*H. borinquense*	n.a	P(3HB-co-3HV)	Batch	44.7	[177]
Cassava extract + andiroba oil	*P. oleovorans*	Oxygen	P(3HB-co-3HV)	Batch	74.0	[178]
Cassava starch	*P. aeruginosa*	n.a	PHB	Batch	57.7	[136]
Paperboard mill wastewater	*Actinobacteria*	Phosphorous and nitrogen	n.a	Batch	15.4	[179]
Acetate	*n.a*	n.a	n.a	Batch	34.2	[180]
Sugarcane molasses and corn steep liquor	*B. megaterium*	Nitrogen	PHB	Batch	46.2	[181]
Acetate and soft drinks wastewater	n.a	n.a	n.a	Fed-batch	79.0	[182]

P(3HB): poly-3-hydroxybutyrate; P(3HV): poly-3-hydroxyvalerate; P(4HB): poly-4-hydroxybutyrate; P(3HHx): poly-3-hydroxyalkanoate.

2.5 Potential development of cassava waste biorefineries in Sub-Saharan Africa

2.5.1 Market analysis

The current global market of plastics relies mostly (99%) on petroleum-based plastics [42]. Nevertheless, thanks to the properties and advantages of bioplastics, the biopolymers market is expected to grow and diversify considerably in the following years. The global PHA market is expected to grow at a compound annual growth rate (CAGR) of c.a 6.3% over the next decade to reach approximately $119.15 million by 2025 [42,183]. The latest market data compiled by *European Bioplastics* and the research institute Nova-Institute reports that bioplastics production capacity will increase from 2.11 Mt in 2020 to 7.4 Mt in 2028 [184]. Some of the prominent areas that are driving the increase in biopolymer demand are the healthcare industry, the renewable materials market, and the recent advances in PHA manufacturing technologies [141]. Although

the above reports show promising market data for the near future, they are mostly focused on North America, Europe, and the Asia Pacific. Currently, Europe and North America are the two largest biopolymers-producing areas and these regions are expected to continue leading the ranking thanks to public and private investment in R&D. Nevertheless, the Asia Pacific market is also likely to witness significant gains [185]. Although more than 150 polyhydroxyalkanoates (PHA) have been identified to date, the high production cost hinders their commercialisation, hence commercial production of bioplastics is currently limited to a few types of PHA. During the 1970s, the oil crisis raised the interest in bioplastics and Imperial Chemical Industries (ICI, UK) became the first company to commercialise PHA. Currently, the most produced PHA are poly-3-hydroxybutyrate (P(3HB)) and poly-3-hydroxybutyrate-co-3-hydroxyvalerate (P(3HB-co-3HV)), and Metabolix (USA) is the largest market player, with an annual production capacity of 50,000 tonnes and with facilities in the USA and Europe. Another large company that focuses on P(3HB) and P(3HB-co-3HV) production is Monsanto (USA), which in 2004 rejected the idea of microbial production and moved into PHA production using plants. Nevertheless, they have not reported yet any plant-based PHA. Furthermore, PHA production using plants is controversially linked to the use of genetically modified crops. Other companies are increasing their production capacity of biopolymers, such as CJ CheilJedang (Korea), which acquired the intellectual property on bioplastics production from Metabolix. However, P(3HB) and P(3HB-co-3HV) are not the only biopolymers with commercial interest. Kaneka (Japan), P&G (USA), and Danimer Scientific (USA) are interested in Poly-3-hydroxybutyrate-co-3-hydroxyhexanoate P(3HB-co-3HHx) production. Other companies such as Tianjin Green Bio (China), Bluepha (China), TianAn Biopolymer (China), BioCycle (Brazil), Biomer (Germany), Mango Materials (USA), and Newlight Technologies (USA) are currently developing commercial-scale PHA production facilities [164]. The above analysis shows that the biopolymers market is growing, and it is likely to further grow at higher rates but with the same geographical distribution. Furthermore, some countries such as China and India are expected to have a positive impact on the biopolymers (mainly PHA) market in the near future. However, Africa does not have an existing bioplastics market and limited growth projections in the near future [185]. Higher investment in research and innovation will be needed to develop the global bioplastics market opportunity for the SSA economy albeit, there is a clear market niche with huge potential in the region.

2.5.2 Techno-economic analysis: A case study of a cassava waste biorefinery for the production of energy and bioproducts

Cassava waste has been demonstrated to be a potential feedstock for PHA production. In the biorefinery context, feedstock production and biopolymer manufacture should be co-located to minimize costs associated with transport as exposed in Section 2.4.2.2 and therefore, realize the potential and associated economic benefits [186]. SSA is the major cassava producer in the world, but most countries have very limited technological and industrial resources, constraining the biopolymers market development. Techno-economic analysis may be useful to evaluate the feasibility of cassava biorefinery platforms; the few reports that have been carried out to date focused on the feasibility of integrated biorefineries to co-produce bioproducts such as succinic acid, glucose syrup, and bioethanol in combination with heat and power production [187]. Other relevant works report the potential use of cassava-based industrial waste in biorefineries to produce several products such as biofuels, biogas, or biosurfactants [50], and future perspectives on the integration and use of cassava in the bioproducts industry [38].

In this section, the work published in 2020 by Padi and Chimphango [188] is showcased as a case study. This work focuses on two major questions: "*What are the opportunities of cassava waste biorefineries to provide significant energy supply in SSA?*" and "*Is there potential for product diversification in a cassava waste biorefinery?*". Different by-products can be obtained from cassava waste [38]. Biogas, bioethanol, succinic acid, and glucose syrup are some of the products with high commercial and industrial interest [188]. Consequently, succinic acid was chosen as the main by-product of interest to study the techno-economic feasibility of a cassava waste biorefinery [188]. This organic acid and its derivatives are used extensively in the plastic, polymer, and pharmaceutical industries [189]. Padi and Chimphango studied the feasibility of commercial waste biorefineries for cassava starch industries using South African fiscal conditions as a model of cassava-producing regions in SSA. Five scenarios were considered for their integration into a cassava starch plant. For each scenario, different cassava waste types were used, and diverse by-products were obtained. All scenarios assumed cassava bagasse and cassava wastewater are to be supplied by the plant, and cassava stalks are recovered from the fields. Figure 2.8 shows the process diagram of a cassava waste biorefinery that targets zero wastewater and solids disposal. In this biorefinery platform, cassava bagasse, cassava wastewater, and 10% of cassava stalks were used for the co-production of succinic acid and bioethanol combined with the production of heat and power from the 90% of cassava stalks remaining [188]. The main parameters and assumptions employed in this techno-economic analysis (TEA) study were (i) the percentage of cassava stalks available for the biorefinery, (ii) models for obtaining mass and

energy balances as well as (iii) equipment costing and sizing, and plant life. The analysis revealed that the biorefinery plant has the potential to meet the energy demand for both, the biorefinery and cassava starch process, showing a surplus of 121-200 MW of electricity, which is the net power produced in the biorefinery plant minus the power needed by the starch process. The potential surplus power for all scenarios suggests opportunities for energy self-sufficiency in integrated waste biorefineries [188]. On the other hand, the annual production of succinic acid projected in this integrated biorefinery is within the industrial scale capacities range (10-30 Gg SA/ a). The outcome of this work shows that the exposed approach has realistic commercial potential. The use of wastewater not only represents an advantage as a carbon source but also aids in reducing the consumption of fresh water and thus, mitigating environmental problems [188]

Among the five scenarios, the model simulating the co-production of succinic acid, bioethanol, heat, and power using 10% cassava stalks, cassava bagasse, and cassava wastewater as feedstock; required higher total capital investment values than all the other four scenarios studied. The biorefinery throughput was projected at 7.29 Mg/h, 377.83 Mg/h, and 450.89 Mg/h when using cassava bagasse, cassava wastewater, and cassava stalks, respectively. The other four scenarios were: scenario (I): the combination of cassava bagasse and cassava starch wastewater for biogas production and cassava stalks for producing combined heat and power; scenario (II): the combination of cassava bagasse and cassava wastewater for the production of bioethanol with all cassava stalks used for production of combined heat and power; scenario (III): the combination of 10% of cassava stalks, cassava bagasse and cassava wastewater for bioethanol production with 90% of the cassava stalks used for combined heat and power production and scenario (IV): the combination of 10% of the cassava stalks, cassava bagasse and cassava wastewater for co-production of glucose syrup, bioethanol with 90% of the cassava stalks used for combined heat and power production, demonstrated promising profitability, thanks to the integration of the succinic acid production in the process.

This work confirmed that feedstock price is a major determinant factor for a biorefinery process as has been discussed in section 2.4.2.2. This study shows encouraging results for cassava waste biorefineries in SSA. Although TEA will be key for a PHA production plant using cassava waste, and such studies are still scarce for this particular bioproduct; the above-exposed case study paves the way to develop further feasibility studies for the development of cassava waste biorefineries. Due to the lack of techno-economic studies in this field, estimations of the capacity of the process were performed by our research group (non-published results). Considering the total amount of cassava waste generated in Africa in a year, 40 Mt [92], and based on previous data for the production and extraction of PHA from biomass sources with similar starch composition, a resulting quantity of 4 Mt of PHA could potentially be obtained annually in a biorefinery platform. Such estimations were made based on 62%, 65%, and 25% recovery yields for the pre-treatment,

fermentation, and downstream processes, respectively [7]. On the other hand, around 19.5 Mt of petroleum-based plastics are currently being used every year in the African continent [41]. The estimated production of PHA from cassava waste would represent 20% of the usage of total plastic in Africa. This can potentially facilitate the replacement of a significant portion of petroleum-based plastics for biodegradable and bio-based ones. In addition, this will contribute to reducing plastic waste management needs, which is a current challenge in the continent.

Integration of the cassava processing plant with the biorefinery reduces costs, leading to a more profitable process, and self-supply of energy contributes to substantial avoided costs, contributing to financial viability where it displaces conventional fuel or electricity in an energy-intensive process. This could e.g., be in traditionally high energy consumption systems such as wood processing, sugar, or tea production, or growth sectors such as cement. While there are not currently significant cassava-biopolymer industries in SSA, the rapid urbanisation of the continent and economic development provides an opportunity for expansion, since obtaining products of industrial interest enables a potential increase in profitability where market opportunities exist. Thus, the development of cassava waste biorefineries producing not only PHA but also relevant by-products such as succinic acid (which has an estimated market value of USD 6-9/kg [190] and market size of USD 181.6 million [191]) or bioethanol (which has an estimated value of USD 0.9-1.1/L and a market size of USD 64.8 billion [192]) could support profitability [188].

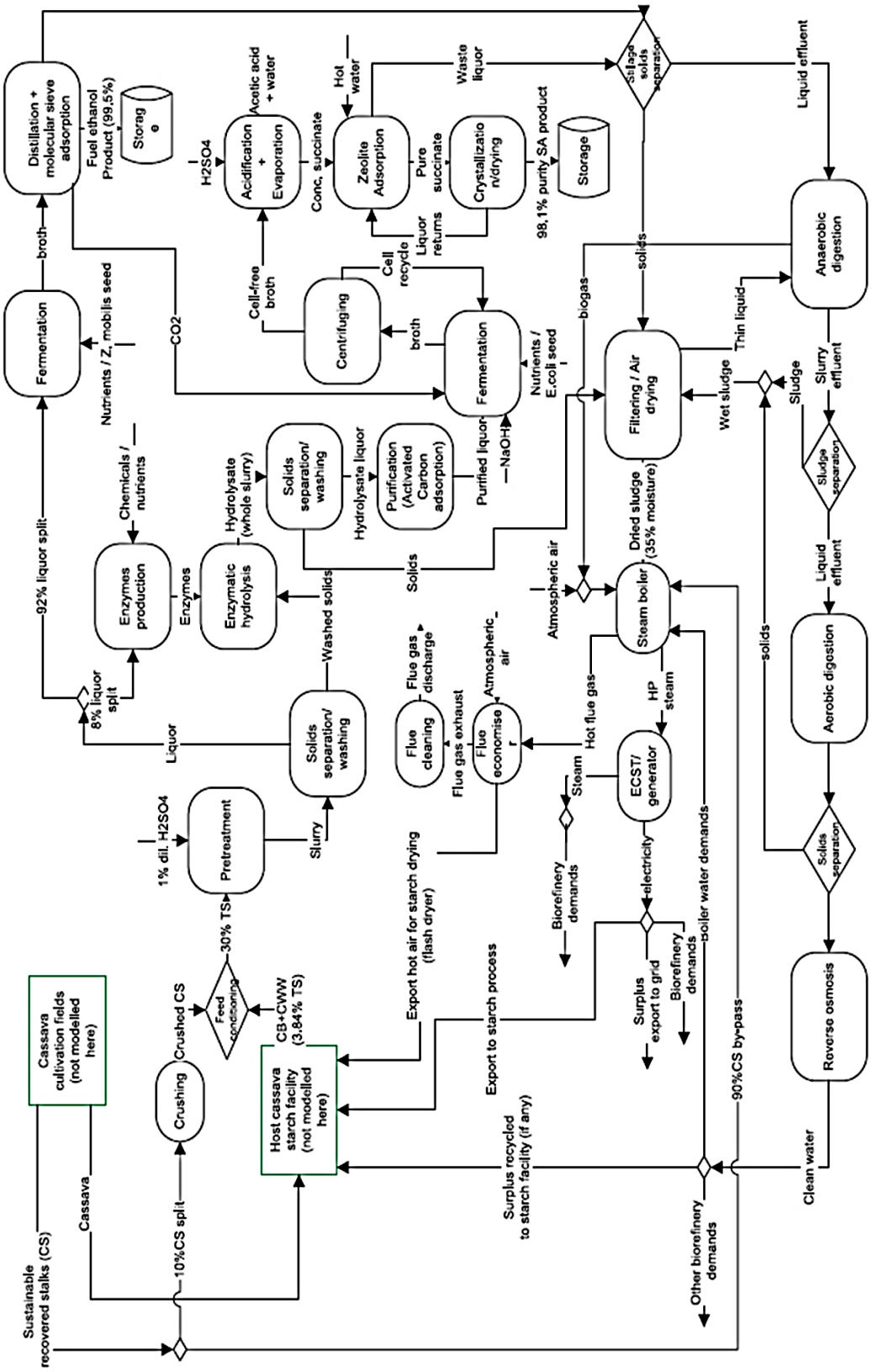

Figure 2. 8 Cassava waste biorefineries for heat, power, and succinic acid, integrated in cassava starch processing. Reproduced with permission from Padi & Chimphango [172].

2.5.3 Life cycle analysis (LCA)

The interest in biopolymers has significantly increased in recent decades due mainly to the environmental benefits they offer compared to their petrochemical-derived counterparts. In particular, biopolymers which are both bio-based and biodegradable, such as PHA, are the most interesting [193]. The production from renewable resources and biodegradability properties make them an environmentally friendly alternative to petrochemical polymers [7]. However, farming practices to produce those feedstocks often incur significant embodied energy and therefore, there is a need to consider the environmental impacts based on the life cycle analysis (LCA) of PHA in comparison to petrochemical polymers. Most LCA studies of PHA are based on simulations and laboratory or small-scale production plants. Albeit there are several significant studies, the pioneering LCA on PHA was published only in the early 2000 and concluded that PHA production required more energy than the polymers obtained from petroleum [194]. However, the knowledge and the technology available two decades ago have evolved [137]. Interestingly, an LCA of PHA produced from corn grain revealed that PHA production offers environmental advantages both in terms of GHG emissions and non-renewable energy consumption over petroleum-based plastics. The residues generated in the study after the fermentation step to produce PHA and the recovery process were used as fuel in a cogeneration power plant [195]. Another study compared PHA and petrochemical polymers concluding that GHG emission from the production of 1kg of PHA was 0.25 – 0.5 kg of CO_2 whereas petroleum-based plastics production resulted in 2 – 3kg of CO_2 emissions. The low CO_2 emissions from PHA production were attributed to the fixation of CO_2 by the feedstock biomass and bacterial respiration during the fermentation process [47]. Furthermore, another recent study analysed the LCA of PHA obtained from two different feedstocks – glucose and cheese whey – and PHA obtained using genetically engineered plants. The study concluded that genetically modified plants do not show any advantages over the microbial process using renewable resources. Although the PHA recovery process involves much fewer energy requirements in genetically modified plants compared to microbial fermentation, the global process using genetically modified organisms requires 4.5-fold more energy [196]. Although biopolymers have been considered to have a lower environmental impact than petroleum-based plastics, a more recent study analysed different biopolymers, including PHA, and concluded that none of the commercial biopolymers, including those currently under development, were environmentally sustainable [197]. In contrast, the use of land for feedstock production can contribute to an increase in competition due to the crops being harvested for food use. Consequently, this can lead to an increase in poverty and issues related to food access. This may be the case in SSA despite the SSA region offering large crop cultivation fields and capacities. The use of waste crops can potentially contribute to promoting the production of biopolymers without affecting the food supply [198]. Although the literature is scarce, some authors have

already published studies analysing the LCA of PHA produced from waste. For example, Kedall and co-workers showed that PHA production from the cellulosic fraction of residual materials, that otherwise is disposed of in the environment, requires half of the energy needed for PHA obtained from a dedicated agricultural feedstock [199]. Here, the key factor is whether the feedstock is a dedicated crop or a waste by-product. Developing more sustainable processes for biopolymer production may be supported by the development of more efficient practices in crop cultivation, technological improvements during the production process, and the use of fermentable residues, such as waste crops originating from different food industries [199,200]. This will not only contribute to bioplastics manufacturing sustainability but also, to a circular economy by decreasing the energy demand for materials production and the reduction of waste, thus, contributing to solving important environmental issues [54]. A key issue with most LCAs of agricultural residues is devising a methodology that appropriately treats the residue and allocates proportionate emissions from the main feedstock production. It is possible to obtain very favourable results if it is assumed that emissions associated with the disposal of the waste residue are avoided and thereby credited to the biopolymer; whereas higher emission intensities will result if it is assumed that the agrochemical and other inputs associated with crop production should be allocated to the cassava residues on a mass or energetic basis. These assumptions should be guided by consideration of the overall production, markets, and trends and the methodology adapted accordingly.

However, regardless of the methodology chosen further development of PHA obtained from agricultural residues and cassava-based biorefineries must consider the life cycle and environmental impacts to identify process hotspots, isolate preferred process schemes, and, optimize these environmentally and economically.

2.6 Conclusions

A range of solutions can be implemented to reduce the cost of PHA production such as the use of genetically modified strains (i.e., PHA-overproducing strains or strains capable of utilising substrates more efficiently) by developing the use of waste biomass resources as low-cost feedstock as an alternative to the use of synthetic sugars. The use of alternative substrates to commercial sugars has attracted much attention because it contributes to the circular economy principles. Waste crops and in particular, cassava waste, can be considered an adequate resource for the development of integrated biorefineries for bioenergy and bioproducts in SSA, which is the major cassava producer worldwide. The development of bioenergy strategies and policies in SSA countries (particularly South Africa and Nigeria) will be key in the implementation of biorefinery approaches alongside the utilization of key enabling technologies. Studies regarding

the techno-economic feasibility of a cassava waste biorefinery in South Africa indicate that the development of integrated biorefineries for the production of value-added products has great potential to provide positive economic and social impact provided that self-supply of energy is achieved. Although a promising and feasible scenario can be envisaged, technologies for biopolymers production from waste crops must be further optimised to return both, environmental and economic benefits. Nevertheless, the present study confirms the practical conversion potential, enabling mass-energy balance and techno-economic assessments.

An important step toward this objective is the implementation of processing plants near the production areas to avoid transportation and consequently, decrease associated costs. To achieve this, a social analysis of cassava biorefinery mobilisation should be carried out to ensure appropriate acceptance in SSA. Importantly, government-driven policies to promote cleaner production systems and reduce plastic waste and pollution will be necessary to promote the transition to a more sustainable bioeconomy. Knowledge transfer and capacity building between countries with developed technologies and the SSA region will also be essential to realize the potential of cassava waste biorefineries for PHA production. Ethical aspects and regulations are to be considered: cassava is an edible crop representing one of the major sources of calories in SSA but, the dietary driver remains constant in the face of climate change and urbanisation. Finally, there is a need to consider a holistic perspective on sustainability: going beyond environmental LCA to also consider the impact of cassava processing and biorefinery establishment on livelihoods, farming practices, projects, and community scale economics to establish the most appropriate development trajectories for appropriate demonstration and innovation programs to stimulate the sector and its potential benefits.

Considering the potential of CP as feedstock for PHA production, and the limited existing research on this subject, the following chapters of this thesis present an experimental approach designed to assess the practical feasibility of this process.

Chapter 3. Characterisation of untreated and acid-hydrolysed cassava peel

The content of this chapter has been adapted from the following manuscript:

"Process integration for efficient conversion of cassava peel waste into polyhydroxyalkanoates" **C. Hierro-Iglesias**, C.O Fatokun, A, Chimphango, P. Thornley, P.H. Blanco-Sanchez, R. Bayitse, A. Fernandez-Castane. Journal of Environmental Chemical Engineering (2024), 111815, 12 (1) https://doi.org/10.1016/j.jece.2023.111815.

3.1 Introduction

Cassava cultivation in tropical and subtropical regions generates significant amounts of peel waste. Around 40 Mt of cassava waste are generated annually in Africa [14]. CP is a valuable biomass source for its high starch, cellulose, hemicellulose, and lignin concentrations. Previous authors characterized CP, revealing starch content of 44.5%, cellulose content of 9.1%, hemicellulose content of 7.5%, and lignin content of 9.2% [96].These polymers comprise a diverse range of monomers, with starch and cellulose-containing glucose as the sole constituent, while hemicellulose shows a more varied composition, containing also other monomers such as xylose, mannose, and galactose. Additionally, lignin features aromatic and aliphatic structures (Figure 2.4). However, the variety and cultivation conditions are examples of factors that can affect the biomass composition. Therefore, biomass characterisation is essential for the optimum conversion of biomass into the desired value-added products.

The utilisation of biomass derived-molecules for bioenergy and bioproduct production holds significant potential, but pre-treatment methods are necessary to convert the polymers into fermentable and available molecules [113]. Dilute acid hydrolysis stands out as a commonly used

and cost-effective pre-treatment method for recovering sugars and other valuable molecules from polymeric biomass. Some authors have previously performed acid hydrolysis on CP using various acids, with H_2SO_4 and HCl being the most commonly used due to their effectiveness and availability [127,201]. It is noteworthy that during acid hydrolysis of CP, the generation of furfurals such as 5-hydroxymetylfurfural may occur, which are indicative of the breakdown of polysaccharides [202]. In addition to chemical hydrolysis, pretreatment methods may also involve mechanical processes such as particle size reduction and cleaning, optimising biomass accessibility for subsequent conversion processes. Considering the holistic approach to pretreatment methods ensures comprehensive biomass utilisation and enhances the overall efficiency of bioenergy and bioproducts production [203].

Some studies have conducted physicochemical characterisation of CP using various techniques such as FT-IR, SEM, XRD, proximate and ultimate analysis, and TGA, among others [204–208]. For example, Widiarto and co-workers analysed cellulose nanofibers from CP using FT-IR, TEM, XRD, and TGA, after an alkaline and bleaching process [208]. Kayiwa and co-workers analysed the bulk density, water-binding capacity, and lignocellulosic composition and performed a proximate and ultimate analysis of CP [207]. Other studies, such as the one performed by Daud and co-workers, used SEM to determine the morphological characteristics of CP [206].

While some studies have investigated the physicochemical properties of CP, there is limited available research on the changes in these properties before and after acid hydrolysis. This chapter aims to address this gap by examining the physicochemical properties of CP before and after an acid treatment to extract sugars. Multiple characterisation techniques, including TGA, proximate and ultimate analysis, FT-IR, and SEM, were employed to provide a comprehensive understanding of biomass characteristics and its potential.

3.2 Materials and methods

3.2.1 Feedstock

Milled CP were kindly provided by Dr Richard Bayitse from Council for Scientific and Industrial Research (CSIR) in Ghana. CP were collected from a cassava processing plant in Bawjiase, Ghana, soaked in water for 30 min to ease the removal of the brown skin, and subsequently dried overnight at 60 ºC before being milled. Bayitse and co-workers previously characterised CP, revealing a total carbohydrate composition of 88% (DM) [125].

3.2.2 Pre-treatment of cassava peel

Acid hydrolysis of CP was performed using 0.6 M H_2SO_4 (>95%, CAS 7664-93-9) for 58 min at 107 ºC, in 20 mL reaction volume containing 10% (w/v) of CP. Hydrolysis was performed in a Starfish workstation (Radleys, Essex, UK) (Figure 3.1). Two-neck round bottom 50 mL pressure flasks (Aldrich®, Merck, Darmstadt, Germany), were used to perform the reactions. Flasks were sealed to maintain them pressurized and stirred at 280 rpm. After the reaction, samples were cooled down and vacuum filtrated through a cellulose 11µm filter paper (Whatman, Cytiva, Washington D.C, United States). The solid portion (treated CP) was air-dried and stored at room temperature until analysis.

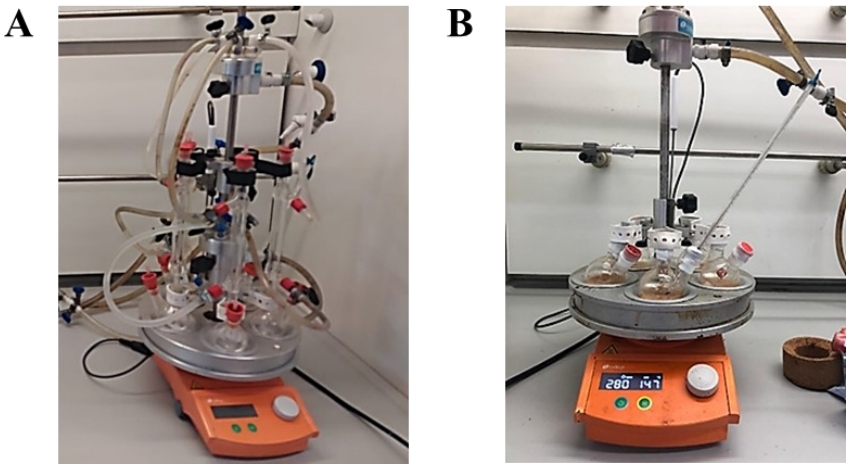

Figure 3. 1 Starfish workstation (Radleys, Essex, UK) used for acid hydrolysis of cassava peel with fitted condensers (A); and sealed flasks (B).

3.2.3 Thermogravimetric analysis

A thermogravimetric analyser TGA/DSC3+ STARe System (Mettler Toledo, Ohio, USA) was utilised to assess the thermal degradation of both untreated and treated CP. Alumina crucibles were loaded with 3 mg of each sample and subjected to a temperature range from 25 to 900 °C at a heating rate of 10 °C/min under a nitrogen atmosphere (30 mL/min) to maintain an inert atmosphere. The sample mass was recorded and used to determine the mass loss and mass loss rate percentage as follows:

$$\text{Mass loss (\%w/w)} = \frac{\text{Mass of sample}}{\text{Mass sample 25°C}} \text{ x } 100 \quad \text{(Eq. 3.1)}$$

$$\text{Mass loss rate (\%w/(w min))} = \frac{\Delta\text{mass}}{\Delta\text{time}} \text{ x } 100 \quad \text{(Eq. 3.2)}$$

3.2.4 Proximate analysis

Data obtained from the TGA was used for the proximate analysis to determine moisture and volatile matter as follows [209]:

$$\text{Moisture (\% (w/w))} = \frac{\text{Mass of sample at 25 °C- Mass of sample dried at 105 °C}}{\text{Mas of sample at 25 °C}} \text{ x } 100 \quad \text{(Eq. 3.3)}$$

$$\text{Volatile matter (\% (w/w))} = \frac{\text{Mass of dried sample at 105 °C- Mass of sample dried at 900 °C}}{\text{Mass of dried sample at 105 °C}} \text{x} 100 \quad \text{(Eq.3.4)}$$

Ash content was determined by the ignition of samples in a muffle furnace at 575 °C for 3 h according to ASTM E-1755-01 standard method. The remaining residue after combustion of the organic material represented the ash content and was calculated as follows [209]:

$$\text{Ash content (\%w/w)} = \frac{\text{Mass of sample at 575 °C}}{\text{Mass of sample at 105 °C}} \text{x } 100 \text{ (Eq. 3.5)}$$

The fixed carbon (FC) was calculated by difference as follows [209]:

FC(% (w/w))=100-(moisture (%)+ volatile matter (%)+ ash (%)) (Eq. 3.6)

3.2.5 Ultimate analysis

Ultimate analysis was carried out to determine the elemental composition. A FLASH 2000 CHNS/O analyser (ThermoFisher, Waltham, USA) was used to determine Carbon (C), Hydrogen (H), Nitrogen (N), and Sulphur (S) content. The oxygen (O) content was determined as follows:

O (%w/w))= 100 - (C (%)+ H (%)+ N (%) + S(%)) (Eq. 3.7)

3.2.6 Functional group analysis

Fourier Transform Infrared (FT-IR) spectroscopy was carried out using a NICOLET iS50 (ThermoFisher, Waltham, USA) equipped with attenuated total reflectance (ATR) to characterise chemical functional groups. Spectra were recorded at a wavenumber range of 400-4000 cm^{-1} with a resolution of 4 cm^{-1}. Signals were assigned to specific functional groups based on the literature [96,208,210,211].

3.2.7 Surface morphology analysis

The surface morphology of the untreated and treated CP was evaluated using scanning electron microscopy (SEM) (JSM-7800F Prime, JEOL, Japan). Images were acquired at 1200x magnification at 5.0 kv.

3.3 Results and discussion

3.3.1 Thermal characterisation

Thermogravimetric analysis (TGA) and differential thermogravimetric (DTG) curves for untreated and treated CP are shown in Figure 3.2. The main components of CP, starch, cellulose, hemicellulose, and lignin exhibit different thermal degradation behaviours due to their distinct chemical structures and compositions (Figure 2.4). According to previous research, the degradation of starch initiates at 228 °C and extends up to 393 °C, while cellulose undergoes degradation within the range of 300-400 °C. Hemicellulose, on the other hand, degrades within the temperature range of 180-350 °C, whereas lignin undergoes degradation between 250 °C and 800 °C [212,213]. Hemicellulose, due to its amorphous structure, is readily susceptible to degradation, leading to the lowest thermal degradation temperature [214]. Starch and cellulose, both comprising elongated glucose polymers, exhibit a similar initial degradation temperature, although the thermal degradation range of cellulose is wider than that of starch. The lower degradation temperature of starch is attributed to the presence of branched amylopectin within its molecular structure [214,215]. Additionally, cellulose presents hydrogen bonds, which increase its thermal stability. Finally, lignin possesses high thermal stability due to its elevated molecular weight and the presence of benzene-propane units [214].

The TGA results, as illustrated in Figure 3.2, reveal three primary stages of degradation, stage 1 (25-150 °C), stage 2 (150-450 °C), and stage 3 (450-900 °C). Stage 1 (25 – 150 °C) shows a 4% mass loss in both samples, which can be attributed to the evaporation of humidity and degradation of light compounds [216]. Notably, despite the use of dried biomass, a 4% mass loss was observed in both samples within this temperature range [21]. The sharper peak emerging in the treated CP at 100 °C (Figure 3.2B) may correspond to the degradation of light compounds, such as sulphur groups, that appeared after the acid hydrolysis of the sample.

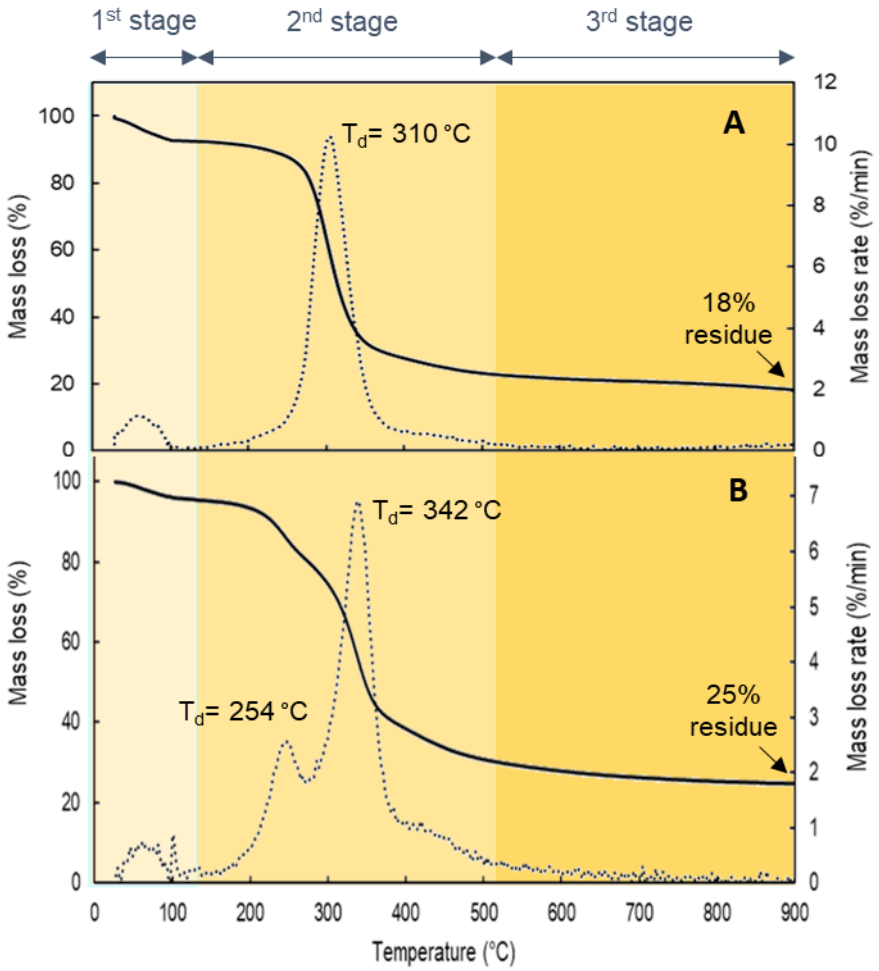

Figure 3. 2 Thermogravimetric (black line) and derivative thermogravimetric (dotted line) curves of the untreated (A) and treated (B) cassava peels. Td: degradation temperature.

Stage 2 (150 to 450 °C) corresponds to the degradation of volatile substances, such as hydrocarbons, H_2, CO, CH_4, and incombustible gases [217], including the major constituents of cassava (starch, cellulose, hemicellulose, and lignin), showing a degradation temperature (T_d) of 310 °C [16,22]. Both samples exhibited a weight loss of approximately 60% in stage 2 (Figure 3.2). In Figure 3.2A, the presence of a single peak (150 to 450 °C) is likely due to overlapping degradation temperatures of cassava constituents [22]. Given the overlapped temperature ranges of thermal degradation for starch, cellulose, hemicellulose, and lignin, it is not possible to differentiate these constituents in the untreated CP sample. This is evident from the presence of a single peak at 310 °C (Figure 3.2A). As noted in previous research, the degradation peaks of the major constituents of cassava may overlap in the TGA spectrum [218]. According to previous authors, in order to distinguish among these molecules several steps should be performed. The first step involves separating starch from the lignocellulosic material through enzymatic methods [219]. Cellulose is usually quantified using acid hydrolysis, while hemicellulose is quantified

using alkaline hydrolysis [220,221]. Furthermore, the neutral detergent fibre (NDF) method and the acid detergent fibre (ADF) method are commonly used together to quantify both cellulose and hemicellulose. Finally, lignin can be quantified using the Klason lignin method [222].

In contrast, the treated CP sample displayed two degradation temperatures (T_d), in Stage 2, between 254 and 342 °C (Figure 3.2B). This can be explained by the presence of less thermally stable components resulting from the acid hydrolysis whereby CP undergoes changes due to the breakdown of complex carbohydrates into simpler sugars. For example, the appearance of a peak at 254 °C might correspond to the degradation of simpler sugars, such as glucose, formed during acid hydrolysis, whereas the peak at 342 °C might be related to the degradation of remaining components, such as starch, cellulose or lignin, in the treated CP [223]. Furthermore, the potential incomplete degradation of biomass cross-linkages between lignin and cellulose and hemicellulose can affect the degradation temperature, causing a shift in the peaks towards higher temperatures compared to the untreated sample [224].

Stage 3 (450 to 900 °C), is often associated with char formation. A biomass loss of 12% and 13% was observed for untreated (Figure 3.2A) and treated (Figure 3.2B) CP, respectively. The loss of mass corresponds to the degradation of the remaining lignin, and minerals, and the production of char following devolatilization [225].

A remaining residue of 18% and 25% was observed for untreated and treated CP, respectively (Figure 3.2). The increased residue in the treated CP may be due to the effect of the acid hydrolysis on the CP constituents. Lignin has higher thermal stability than starch, cellulose, and hemicellulose. Therefore, when the treated biomass is subjected to TGA, the remaining lignin contributes to a higher overall residue than the untreated biomass and these observations are in agreement with previous studies [226].

Overall, the primary organic materials in CP were decomposed below 450 °C and these findings are consistent with the previous studies suggesting temperatures around 500 °C for the thermal degradation of cassava [218,225].

3.3.2 Proximate analysis

Table 3.1 presents the proximate analysis of CP, including moisture content, volatile matter, ash content, and fixed carbon composition of the biomass. The treated CP had a lower moisture content (3.8%) than the untreated CP (7.4%). Idris et al. reported [15] similar moisture content as the treated CP. Other works also reported comparable moisture contents for the untreated CP [207,225,227,228]. The moisture content of biomass can be variable, as it depends on different conditions such as storage, drying conditions, and variety of feedstock [229].

The moisture content from the proximate analysis was compared to the TGA analysis (Figure 3.2) results, showing 4% moisture content in both samples. The treated CP exhibited consistent moisture content between TGA and proximate analysis. However, the untreated CP had a moisture content of 7.4% in proximate analysis.

Table 3. 1 Proximate properties of untreated and treated cassava peels (CP) (n=3).

Sample	Moisture (%)	Volatile matter (%)	Ash (%)	Fixed carbon (%)
Untreated CP	7.4 ± 0.2	80.0 ± 0.3	6.7 ± 0.1	5.9 ± 0.0
Treated CP	3.8 ± 0.0	74.1 ± 0.0	4.4 ± 0.5	18.2 ± 0.0

The untreated and treated CP showed volatile matter concentrations of 80 and 74%, respectively. TGA analysis estimated a volatile composition of approximately 60% for both samples (Figure 3.2). The variation is attributed to differences in the methodology used in each technique.

The volatile matter results presented in Table 3.1 align with most values documented in the literature [93,207,218]. However, due to the influence of various factors, such as the origin and processing, on volatile matter content, it is critical to characterise biomass to achieve its optimal utilisation [229].

The ash concentration of untreated and treated CP was 6.7% and 4.4%, respectively, consistent with previous studies [96,207,230–232]. Other studies found an 8-19% decrease in ash content when the peels were subjected to hydrolysis [233,234].

The fixed carbon concentration of the untreated and treated CP was 5.9 and 18.2%, respectively. The results of this study indicate that treated CP has higher fixed carbon than untreated CP. This finding aligns with previous studies that found an increase in fixed carbon concentration following biomass hydrolysis. The increase is attributed to the removal of inorganic materials, resulting in a decrease in ash content [207,235].

3.3.3 Ultimate analysis

Table 3.2 displays the ultimate analysis of untreated and treated CP showing carbon, hydrogen, nitrogen, sulphur, and oxygen abundances. The values observed in all elements (except hydrogen) are consistent with previous literature. The carbon concentration has been reported in the range of 36.96% [236] to 54.9% [207], the hydrogen concentration in the range of 3.98 [236] to 10.19 [207], the nitrogen concentration in the range of 0.26 [207] to 3.32 [236], the sulphur concentration in the range of 0.04 to 0.18 [228], and the oxygen concentration in the range of

32.27 [207] to 44.68 [228]. The presence of sulphur in the treated sample can be attributed to the diffusion of sulphuric acid into the biomass during the acid hydrolysis process, as suggested elsewhere [237]. Additionally, partial sulfonation may contribute to the observed sulphur content in the treated sample [238]. Furthermore, the emergence of a new peak in the DTG spectra at 105 °C (Figure 3.2B), potentially associated with the degradation of light compounds, can be related to the new sulphur groups in the sample. Furthermore, alongside the noted alterations in sulphuric content, the detection of nitrogen within the CP could imply the existence of nitrogen-based compounds, potentially encompassing proteins. Although the nitrogen levels within CP seem comparatively elevated, it is imperative to acknowledge that CP harbours a multitude of nitrogenous compounds aside from proteins, including amino acids, and nucleic acids. Additionally, nitrogen content within CP may also emanate from alternative origins, such as residual soils components or microbial processes. Therefore, the presence of nitrogen in the treated sample may be attributed to various factors beyond just protein content. This nuanced understanding provides a more comprehensive perspective on the nitrogen composition in the treated biomass [239].

Table 3. 2 Ultimate properties of untreated and treated cassava peels (CP) (n=3).

Sample	C (%)	H (%)	N (%)	S (%)	O (%)
Untreated CP	40.0 ± 0.3	6.4 ± 0.1	1.3 ± 0.1	0.0 ± 0.0	52.4 ± 0.4
Treated CP	46.2 ± 0.1	6.3 ± 0.0	2.2 ± 0.1	0.2 ± 0.0	45.2 ± 0.1

3.3.4 Functional group analysis

Untreated and treated CP were characterised by FT-IR to determine the alterations in functional groups that occurred following acid hydrolysis. CP, being a biomass source with high amounts of both starch and lignocellulosic material, is a rich source of functional groups, including but not limited to alcohols, ketones, and aromatics (Figure 2.4.) [208]. Figure 3.3 displays the corresponding spectra whereby the emergence of distinctive absorption peaks can be observed. Some shifts in the peak position were also observed when comparing the untreated and treated CP.

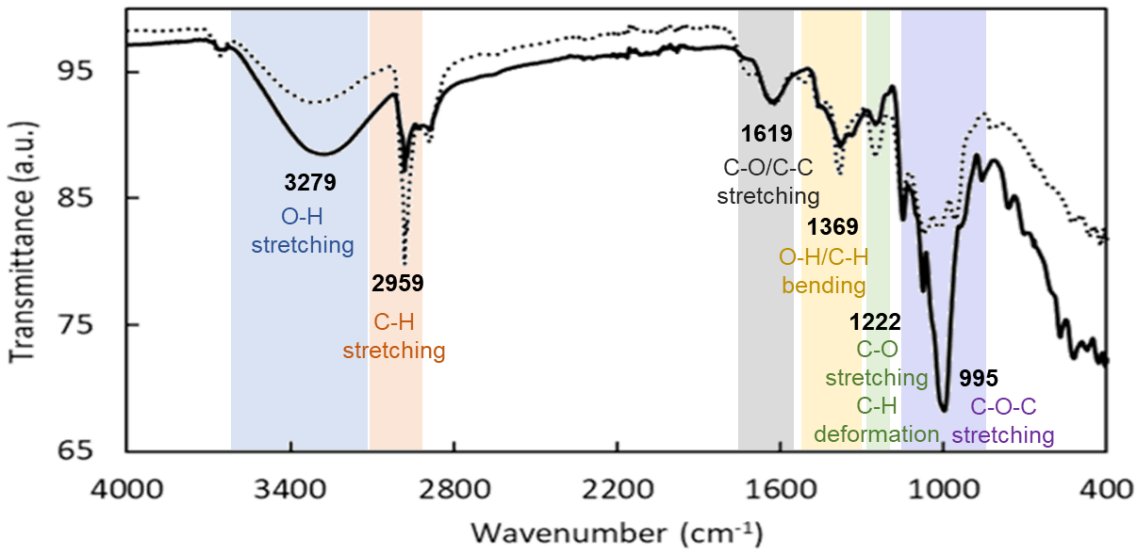

Figure 3. 3 FT-IR spectra of untreated (black line) and treated (dotted line) cassava peels. a.u.: arbitrary units (n=3).

The peak observed at 3279 cm^{-1} corresponds to the O-H stretching, which is likely associated with the hydroxylic groups present in both starch and cellulose [96,208]. The reduction in the peak intensity in the treated sample might be linked to the reduced moisture content and is in line with the results presented in Figure 3.2A. This result aligns with the moisture content results from the proximate analysis presented in Table 3.1. It has been proposed that this peak may be a result of sample dehydration [218]. The presence of a distinct peak at 2959 cm^{-1} suggests the stretching vibration of C-H in CH_2 and CH_3 groups that are present in starch, cellulose, hemicellulose, and lignin [210]. The intensified peak 2959 cm^{-1} in the treated sample indicates an increase in the presence of C-H bonds, likely due to the solubilisation of starch, cellulose, and hemicellulose in the form of fermentable sugars following acid hydrolysis. This process results in the release of fermentable sugars from the biomass [210]. A small peak was observed at approximately 1700 cm^{-1} in the treated sample. This peak may correspond to a conjugated aldehyde, suggesting the presence of molecules such as furfural and 5-hydroxymetyl furfural [240]. The peak detected at 1619 cm^{-1} indicates the existence of C=O bonds, and C=C functional groups, which are present in lignin [208,211]. This peak may also be attributed to the carbonyl groups that may arise from the oxidation of starch and hemicellulose [210]. The peak detected at 1369 cm^{-1} may represent the O-H bending vibration of starch and cellulose [241]. Additionally, it may also be associated with the C-H bending vibration of the carboxylic groups [211]. The peak observed at 1222 cm^{-1} may correspond to the C-O stretching of hemicellulose and lignin, as well as the deformation of C-H in aromatic rings [211]. The increase of this peak may be due to the presence of pseudo-lignin, which is formed through re-polymerisation of degradation products of polysaccharides. The formation of pseudo-lignin is a characteristic phenomenon associated with dilute acid

hydrolysis [96,242]. The signal detected at 995 cm^{-1}, which exhibits the greatest intensity in the untreated CP disappears entirely following acid treatment, and might be associated with the C-O-C stretching of the β-glycosidic linkage in cellulose and lignin. The absence of this peak in the treated sample may be due to the breakdown of cellulose into reducing sugars during the acid hydrolysis process.

Aruwajoye et al. conducted an analysis of the functional groups of CP before and after an acid pre-treatment using 3.68% v/v HCl for 2.57 h and at 69.62 ºC [96] and confirmed that acid hydrolysis alters the structural composition and properties of CP. The acidic environment leads to the cleavage of the chemical bonds in polysaccharides, resulting in an increased concentration of smaller molecules, such as reducing sugars, and a reduced concentration of polysaccharides and larger molecules such as starch, cellulose, hemicellulose, and lignin [243]. Furthermore, other structures, such as pseudo-lignin, can be formed due to a repolymerization process. The impact of different hydrolysis conditions (e.g., acid concentration, hydrolysis time, hydrolysis temperature, etc.) on CP can result in differences in the biomass degradation, resulting for example in the variable presence of reducing sugars hence, affecting the process yields whilst affecting the structural integrity and properties of the resulting hydrolysate.

3.3.5 Surface morphology analysis

SEM was employed to characterise the surface of untreated and treated CP (Figure 3.4).

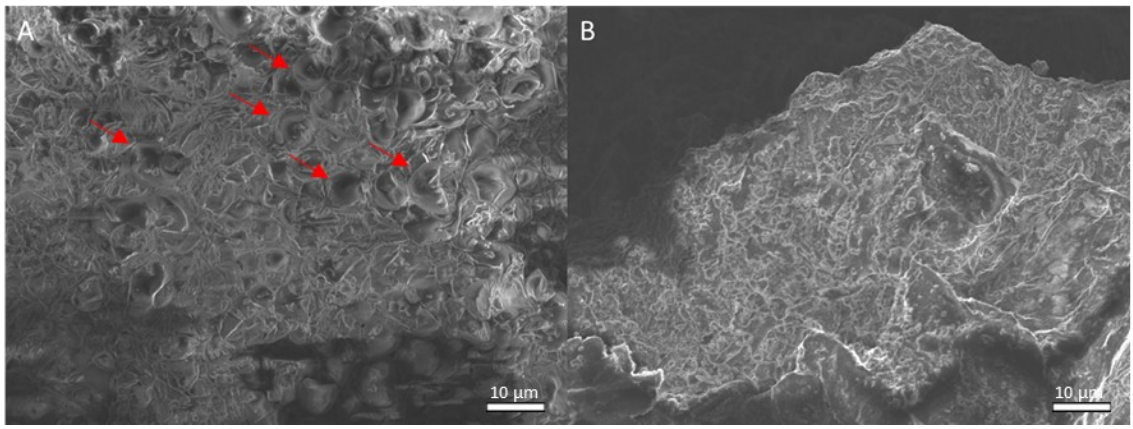

Figure 3. 4 Scanning electron microscopy (SEM) characterization of (A) untreated, and (B) treated cassava peel (CP). Red arrows indicate some of the starch granules.

Starch granules can be observed in the untreated CP, which contribute to the non-uniform surface of the sample. This result is supported by previous authors, who observed globular starch granules

covering the surface of cassava peel [244]. However, starch granules are less noticeable in the treated CP, indicating the effect of the acid pre-treatment in breaking down the polysaccharides. Aruwajoye et al. observed a similar effect upon acid and thermal pre-treatment of CP [96]. Our results confirm the surface structural changes in polysaccharides resulting from acid hydrolysis, as it offers detailed images of the surface morphology of biomass.

3.4 Conclusions

The study aimed to characterise untreated and treated CP through multiple and complementary techniques. TGA was used to analyse the degradation stages of the sample, which were found to correspond to moisture, volatiles, and biochar formation. While the three degradation stages were identified in both untreated and acid hydrolysed samples, the treated CP exhibited additional peaks at lower degradation temperatures, indicating that the hydrolysis process broke down the constituents of the CP into smaller insoluble molecules. The ultimate and proximate analysis revealed disparities between the two samples, thereby supporting the impact of the pre-treatment. The functional group analysis provided evidence for the degradation of cellulose into reducing sugars following the acid hydrolysis, and the SEM images demonstrated the breakdown of starch granules, which were not discernible after the hydrolysis process. The findings presented in this chapter agree with prior research on the characterization of CP. Nevertheless, some minor differences were noted, emphasising the importance of employing multiple techniques to characterise biomass both before and after treatment.

The results confirm the degradation of intricate polysaccharides into smaller, more readily fermentable sugars after acid pretreatment. Consequently, acid hydrolysis enables the subsequent conversion of these sugars into value-added products, thereby resulting in the valorisation of CP waste.

Chapter 4. Pre-treatment of cassava peel waste: investigating the potential of enzymatic and acid hydrolysis for the release of fermentable sugars

Part of the content of this chapter has been adapted from the following publication:

"Process integration for efficient conversion of cassava peel waste into polyhydroxyalkanoates" **C. Hierro-Iglesias**, C.O Fatokun, A, Chimphango, P. Thornley, P.H. Blanco-Sanchez, R. Bayitse, A. Fernandez-Castane. Journal of Environmental Chemical Engineering. (2024), 111815, 12 (1) https://doi.org/10.1016/j.jece.2023.111815.

4.1 Introduction

Cassava peel (CP) contains approximately 45% of starch and 17% of cellulose and hemicellulose [125]. Starch, cellulose, and hemicellulose can be hydrolysed to glucose and other sugars e.g., xylose, arabinose, or fructose, which can then be further used for the co-production of bioenergy and a range of bio-based products such as biopolymers [15]. Several studies have reported the hydrolysis of cassava into sugars using various techniques, among which enzymatic and dilute acid hydrolysis stand out.

The enzymatic hydrolysis of starch into glucose is presented in Figure 2.5 [3]. Although the initial step in the process involves the gelatinisation of starch, some authors have demonstrated that while this step enhances the effectiveness of the process, it is not an absolute requirement to

achieve high conversion values [245]. Conversion yields of 79% [246] and 75% [126] were achieved using a mix of α-amylases and glucoamylases from cassava in previous studies.

The liquefaction and saccharification of starch can be performed simultaneously as a single step or as two separate steps. In the simultaneous process, α-amylase and glucoamylase are added to the substrate as a cocktail, which simplifies the process and reduces the overall reaction time [247]. However, the separate liquefaction and saccharification of starch, where each enzyme is added separately at their optimal conditions, is the most widely used approach as it offers better control over the reaction conditions [128,201,245,247,248]. The choice between these strategies depends on the specific requirements of the application and the available resources [249].

Previous studies have also utilised dilute acid hydrolysis as a pre-treatment technique for CP. Conversion yields of CP into reducing sugars using dilute acid hydrolysis are comparable to enzymatic hydrolysis. For example, conversions of 66% [126] and 95% [127] were achieved using H_2SO_4 0.1 M and 1.5 M, respectively. HCl 0.25 M and 1.6 M was also tested reaching 63% [126] and 93% [96] of conversion, respectively.

An appropriate experimental design is crucial for maximising information and optimising the response of interest in a study. The experimental design allows assessing the interaction effects of multiple factors on the response, ensuring precise and objective analysis. By selecting an appropriate experimental design, the impact of non-significant variables can be minimised. Ultimately, a valid, reliable, and reproducible study is guaranteed [250]. Although there are numerous studies on the acid hydrolysis of CP, most of them only examined narrow ranges within the studied variables, with limited attention given to the factor of time. Furthermore, the interaction effects between more than two variables, including time, have not been comprehensively studied, leading to an incomplete understanding of the factors that affect the process [127,201].

Therefore, the main objective of this chapter is to develop a hydrolysis strategy aimed at maximising the yield of reducing sugars obtained from CP. To achieve this, enzymatic and dilute acid hydrolysis were compared and evaluated. Enzymatic loading, simultaneous and separate liquefaction and saccharification steps, and different thermal pre-treatments were evaluated in the enzymatic hydrolysis to maximise the recovery of the reducing sugars. The effect of two acids, HCl and H_2SO_4, was assessed for the acid hydrolysis. Furthermore, a design of experiments (DoE) based on the response surface methodology (RSM) using a central composite design (CCD) was used to determine the optimum conditions for dilute acid hydrolysis using H_2SO_4.

4.2 Materials and methods

4.2.1 Feedstock

Milled CP were kindly provided by Dr Richard Bayitse from the Council for Scientific and Industrial Research (CSIR) in Ghana. CP were collected from a cassava processing plant in Bawjiase, Ghana, soaked in water for 30 min to ease the removal of the brown skin, and subsequently dried overnight at 60 ºC before being milled. Bayitse and co-workers previously characterised cassava peels, revealing a total carbohydrate composition of 88% with starch representing 42.3% of the sample [125].

4.2.2 Enzymatic hydrolysis

Enzymatic hydrolysis of CP was performed using α-amylase from *Aspergillus oryzae* (9000-90-2, Merck KGaA, Darmstadt, Germany) for liquefaction and glucoamylase from *Rhizopus sp.* (9032-08-0, Merck KGaA, Darmstadt, Germany) for saccharification.

The biomass loading used in this study was selected based on previous literature. Several studies have reported CP concentrations ranging from 1.5 to 20% (w/v) (DW) [126,248,251]. However, after conducting an extensive review of the literature, 10% (w/v) (DW) was found as the preferred choice for reducing sugars recovery [125,247,252] and consequently adopted in this study. Therefore, a concentration of 10% (w/v) (DW) of CP in 20 mL of sodium acetate buffer 16 mM at pH 6 was used in this study.

Various enzyme concentrations (1-420 U/g_{starch}), hydrolysis times (1-72 h), and hydrolysis temperatures (25-50ºC) were tested. Ranges of enzymatic concentrations and hydrolysis times were chosen based on the literature. α-amylase and glucoamylase were used in a 1:1 ratio in all cases. Enzyme concentrations were chosen based on the study conducted by Ruiz et al., who demonstrated conversion yields of up to 86% using amylolytic enzyme concentrations from 5.9 U/g to 212 U/g_{strach}. This study was chosen as a benchmark for enzyme dosage for several reasons. Firstly, the authors optimised the enzyme loading to achieve high conversions. Secondly, to the best of our knowledge, this study provides the most comprehensive and detailed explanation of the enzyme dosage used [245].

Following the determination of the best enzymatic concentration, two hydrolysis approaches were examined. The first one involved simultaneous liquefaction and saccharification of CP, as previously reported in the literature [245,247]. The second approach consisted of two distinct steps, the liquefaction reaction, followed by saccharification. The latter method has been more extensively used in previous research [128,201,245,247,248]. The reaction temperature was

selected based on the manufacturer instructions for the enzymes used in the study. Given that α-amylase and glucoamylase had distinct optimal temperatures of 25 ºC and 50 ºC, respectively, these temperatures were applied during the separate liquefaction and saccharification phases of the process. For the simultaneous liquefaction and saccharification process, an intermediate temperature of 38 ºC was selected as the operational temperature.

Reactions were performed in a Thermo Mixer HC (Starlab, Blakelands, UK) at 500 rpm. After the reaction, samples were vacuum filtrated through a cellulose 11µm filter paper (Whatman, Cytiva, Washington D.C, United States) followed by another filtration step using a PVDF 0.45 µm filter (Whatman, Cytiva, Washington D.C, United States) and the CPH were stored at -20 ºC.

4.2.3 Acid hydrolysis

Acid hydrolysis of CP was performed using a range of HCl and H_2SO_4. For the evaluation of HCl and H_2SO_4, concentrations of 0.025, 0.05, and 0.25 M were tested at 120 ºC for 60 min. For the optimization of the acid hydrolysis using H_2SO_4, the range of acid concentrations, times, and temperature tests is shown in Table 4.1. Reactions were performed in 20 mL containing 10% (w/v) of CP. CP concentration was chosen based on the literature [128,253,254]. HCl and H_2SO_4 solutions were prepared from commercial stocks (HCl 37% (w/w) CAS 7647-01-0 Y) and (H_2SO_4 >95%; CAS 7664-93-9). The hydrolysis was conducted in a Starfish workstation (Radleys, Essex, UK) (Figure 3.1). Hydrolysis reactions were performed in two-neck round bottom 50 mL pressure flasks and stirred at 280 rpm (Aldrich®, Merck, Darmstadt, Germany). To avoid evaporation sample loss, experiments below 100 ºC were fitted into a condenser. Pressure was released by inserting a needle in one of the necks of the flask. In order to achieve temperatures above 100 ºC, flasks were maintained pressurised. After the reaction, samples were vacuum filtrated through a cellulose 11µm filter paper (Whatman, Cytiva, Washington D.C, United States) followed by another filtration step using a PVDF 0.45 µm filter (Whatman, Cytiva, Washington D.C, United States) and the CPH were stored at -20 ºC.

4.2.4 Experimental design

A design of experiments (DoE) based on the response surface methodology (RSM) was used to determine the optimal conditions for hydrolysing CP with H_2SO_4. RSM is a useful tool comprised of mathematical and statistical techniques commonly used to optimize one or several responses of a process, in which different variables interact affecting the response of interest [255]. While there exists various types of experimental designs, including factorial, fractional factorial, and central composite designs (CCD), RSM with CCD is particularly suitable for this study due its

ability to efficiently explore the response surface and identify optimal conditions within the experimental range. Additionally, CCD allows for the construction of second-order (quadratic) models and reduced third-order (cubic) models, which are essential for accurately modelling complex relationships between variables [256]. A circumscribed CCD was used to assess the effect of three variables (H_2SO_4 concentration (*[H_2SO_4]*, M); time (*t*, min); and temperature (*T*, ºC)) on the responses total reducing sugars (*TRS*) concentration (g/L) and glucose concentration (g/L). Since the optimisation of the model for the glucose concentration response was not reached in this study, the DoE for the glucose concentration response is provided in Appendix A1.

CCD is frequently used to develop models whose behaviour can be explained by polynomial equations. Generally, CCD consists of factorial, axial, and central points. The factorial points were represented by *[H_2SO_4]* (0.6-2.4 M), *t* (58-182 min), and *T* (72-108 ºC) in the experimental setup. Central points were repeated six times to obtain a close approximation of the experimental error. Table 4.1 displays the independent variables and levels used in the design. The independent variables and their ranges were chosen based on preliminary experiments (not published) and literature data [126,127].

Table 4. 1 Independent variables and their levels used in the central composite design (CCD).

Independent variables	Units	Notation	Factor level				
			-1.68	-1	0	1	1.68
H_2SO_4 concentration ([H_2SO_4])	(M)	x_1	0.01	0.60	1.50	2.40	3.00
Time (t)	(Min)	x_2	15	58	120	182	225
Temperature (T)	(ºC)	x_3	60	72	90	108	120

Experiments were conducted towards the construction of a mathematical model. The TRS concentration (*y*) was predicted using the following polynomial equation (Eq. 4.1) [257]:

$$y=\beta_0+\sum_{i=1}^{k}\beta_i X_i+\sum_{i=1}^{k}\beta_{ii}X_i^2+\sum_{i=1}^{k}\sum_{i,j}^{k}\beta_{ij}X_iX_j \qquad \text{(Eq. 4.1)}$$

where *y* is the response variable; x_i, x_j and x_k are the corresponding actual values of the variables; β_0 is the regression coefficient of the fitted response at the centre point of the design; β_i is the linear term coefficient, β_{ii} is the regression coefficient for quadratic effects and β_{ij} and β_{ji} are the interaction terms coefficients.

Subsequently, non-significant factors were removed from the equation using the backward elimination methodology, followed by the addition of higher degree factors to the polynomial equation [258].

The effect and regression coefficients of individual linear, quadratic, and interaction terms were determined using analysis of variance (ANOVA). The RSM was applied to the experimental data using a commercial statistical package, Design-Expert version 11.1.2.0. A confidence interval of 95% was chosen, hence p-values lower than 0.05 were considered statistically significant [255].

4.2.3 Analysis of total reducing sugars (TRS) and glucose concentration

Glucose concentration in CPH was measured using a YSI 2500 biochemical analyser (Xylem Inc., Nottingham, UK). Prior to the analysis, samples were filtered using a PVDF 0.45 μm filter (Whatman, Cytiva, Washington D.C, United States).

TRS concentration in CPH was determined using the DNS (Di-nitrosalicylic acid) test, adapted from Miller (1959) [259]. The DNS reagent composition was as follows (% (w/v)): 0.63 DNS; 0.5 NaOH; 18.2 $KNaC_4H_4O_6 \cdot 4\ H_2O$; 0.5 $Na_2S_2O_5$ and 0.5 % (v/v) C_6H_6O. 0.5 mL of sample was mixed with 0.5 mL of DNS reagent. Samples were then boiled in water for 5 min and subsequently cooled down to room temperature. The absorbance was measured at 575 nm using a Jenway 6310 Spectrophotometer (Keison Products, Chelmsford, UK). The choice of wavelength for absorbance measurements was based on its optimal sensitivity for detecting the colour change associated with the formation of reducing sugars in the DNS reaction. This wavelength has been widely used in similar studies due to its compatibility with the absorbance spectra of reaction products [259]. To calculate sample concentrations, absorbance values were interpolated based on a calibration curve prepared using pure synthetic D-(+)-glucose (CAS 2280-44-6). A calibration curve and a picture presenting 4 samples containing different sugar concentrations are presented in Appendix A2.

4.3 Results and discussion

4.3.1 Enzymatic hydrolysis of cassava peel

4.3.1.1 Evaluation of enzymatic loading

The present study assessed the effect of α-amylase and glucoamylase in the enzymatic hydrolysis of CP under different conditions. One of the objectives was to determine the optimal amount of enzyme to maximise the hydrolysis process. Despite conducting an exhaustive review of existing literature on enzymatic hydrolysis of cassava (Table 4.2), no clear information was found regarding the quantity of enzyme employed in most of the studies. While most research indicates

the volume of the enzymatic cocktail utilized, there is no information available on the specific enzymatic activity units. Furthermore, most suppliers provide minimal information about their enzyme products. Also, prior research investigating the enzymatic hydrolysis of CP commonly used enzymatic cocktails provided by Novozymes, which include thermostable enzymes. This study initially aimed to use the same enzymatic cocktails provided by Novozymes, which were Liquozyme supra 2.2X and Extenda peak 1.5 extra. However, due to the COVID-19 pandemic, the company was unable to provide these products, leading us to explore alternative options. The alternative enzymatic products used were α-amylase and glucoamylase, separately. It is important to note that these enzymes were not thermostable, unlike most of those used in previous research. Due to the lack of information available on the enzymatic activity and the limited availability of enzymatic products, our study evaluated a wide range of enzymatic loadings, specifically within the range of 1 to 420 U/g.

Table 4. 2 Summary of enzymatic hydrolysis studies on cassava: reaction conditions and conversion yields.

Feedstock	Catalyst	Temperature (°C)	Time (h)	Conversion (%)	Reference
CP	α-amylase + Glucoamylase	90 50	2 24	75.4	[126]
	Cellulases	50	24	43	
	Xylanase	50	9	2.6	
	Pectinase	40	3	9	
CB	α-amylase + Glucoamylase	90 60	1 24	97.3	[128]
CS	α-amylase + Glucoamylase	90 60	1 48	96	[248]
CS	α-amylase + Glucoamylase	80 70	0.75	86	[245]
CP	Cellulase + β-glucanase	50	120	88	[260]
CPU	α-amylase + Glucoamylase + β-glucanase	50	24	62	[261]
CS	Pectinase + α-amylase + Glucoamylase	45 95 60	1 1 4	98	[262]
CP	Cellulase + β-glucanase + amyloglucosidase + α-amylase	54.75	43.15	54.48	[249]

Cassava peels (CP); Cassava bagasse (CB); Cassava starch (CS); Cassava pulp (CPU)

Figure 4.1 presents the results of the glucose concentration and conversion of starch into glucose obtained after the simultaneous liquefaction and saccharification of CP using enzymatic loadings of 1, 4, 8, and 13 U/g_{starch} at 38 ºC for 24 h. The results shown in Figure 4.1 indicate that a maximum glucose conversion of 8.4% was attained after 24 h of hydrolysis using 13 U/g_{starch} of our enzymatic cocktail, which is significantly lower than the values reported in the literature by various authors. As illustrated in Table 4.2, studies using α-amylase and glucoamylase have reported conversion efficiencies from 75 to 97% [126,245,247,248,251]. However, it should be noted that these investigations employed different initial cassava sources, such as cassava starch, peels, and bagasse, which may have impacted the overall conversion efficiency. The studies that yielded the highest conversions, ranging from 86% to 97, employed cassava starch and bagasse. Conversely, investigations that utilised CP, which are more analogous to our study, resulted in lower conversion rates, ranging from 75% to 88%. Despite this, the results of our study, 8.4% of conversion, exhibit 10 times lower conversion than those reported in previous studies using CP.

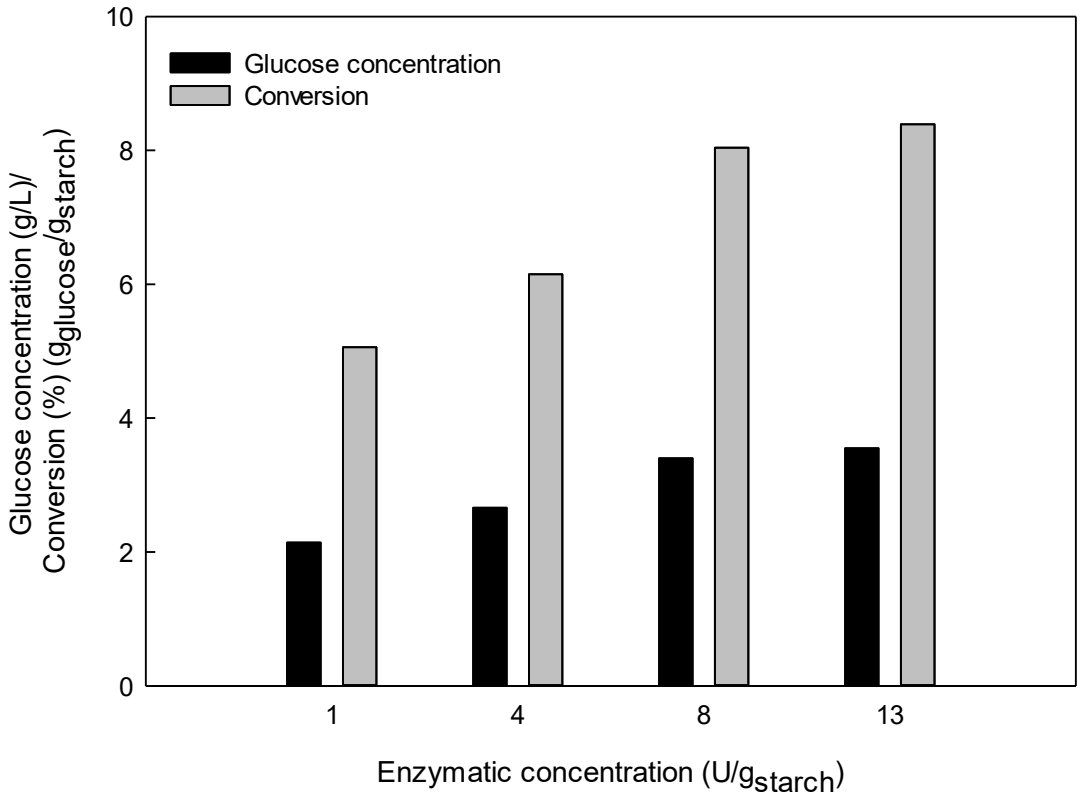

Figure 4. 1 Glucose concentration (g/L) (black bar) and starch conversion into glucose (%) (grey bar) after enzymatic hydrolysis of cassava peel (CP) using α-amylase and glucoamylase (1:1 ratio) after 24 h (n=1) Temperature: 38 ºC; pH 6; sodium acetate buffer 16 mM

Although the conversion obtained in the experiment was low, Figure 4.1 shows that a higher enzymatic loading led to a greater conversion. Specifically, increasing the enzymatic loading from

1 to 13 U/g resulted in a 39.7% increase in the conversion of starch to glucose. Ruiz and co-workers investigated a wider range of enzymatic loadings to achieve high conversions, identifying 130.5 U/g_{starch} of α-amylase and 81.5 U/g_{starch} of glucoamylase as the optimal enzymatic loadings [245]. Building on this work, the present study tested enzymatic dosages of 40, 80, 210, and 420 U/g_{starch}, and the results are presented in Figure 4.2. Given that very low conversion values were obtained after 24 h (Figure 4.1), and previous studies reported longer enzymatic hydrolysis durations of 43h [249] and 48h [248], the enzymatic hydrolysis using 40, 80, 210, and 420 U/g_{starch} was evaluated at 48 h. As illustrated in Figure 4.2, an increase in enzymatic loading and hydrolysis time was found to be positively correlated with higher glucose concentration and conversion. In an enzymatic assay without substrate limitation, the reaction rate is expected to increase with an increase in enzyme concentration. However, it is important to consider other factors that could affect the reaction rate, such as the interactions between the enzyme and substrate or products, pH, or temperature [249]. Other researchers have reported a positive correlation between the reaction rate and enzymatic dosage. For example, Barati and co-workers conducted a CCD and confirmed that increasing the hydrolysis time and enzyme dosage had a positive effect on the glucose content extracted from CP [263]. The maximum glucose concentration of 19.6 g/L corresponding to a 46.4% conversion were obtained using an enzymatic loading of 210 U/g_{starch} for 48h. However, the maximum glucose conversion achieved using 420 U/g_{starch} of enzymes was 37.7%, indicating that the highest enzyme concentration did not result in the highest conversion. An explanation for this may be that although the reaction rate can be accelerated by increasing the enzyme concentration, when all substrate molecules are bound to enzymes, the reaction rate will no longer increase despite a further increase in enzyme concentration, due to the lack of available substrate molecules [264]. Furthermore, kinetics based on initial rates can overlook the effects that accumulate over long reaction times. A process with lower initial enzyme activity may have a shorter duration of effectiveness and result in lower ultimate yield. Therefore, it is important to consider not only the initial rate of enzyme activity but also the yield achieved over time when evaluating the productivity of a process [265].

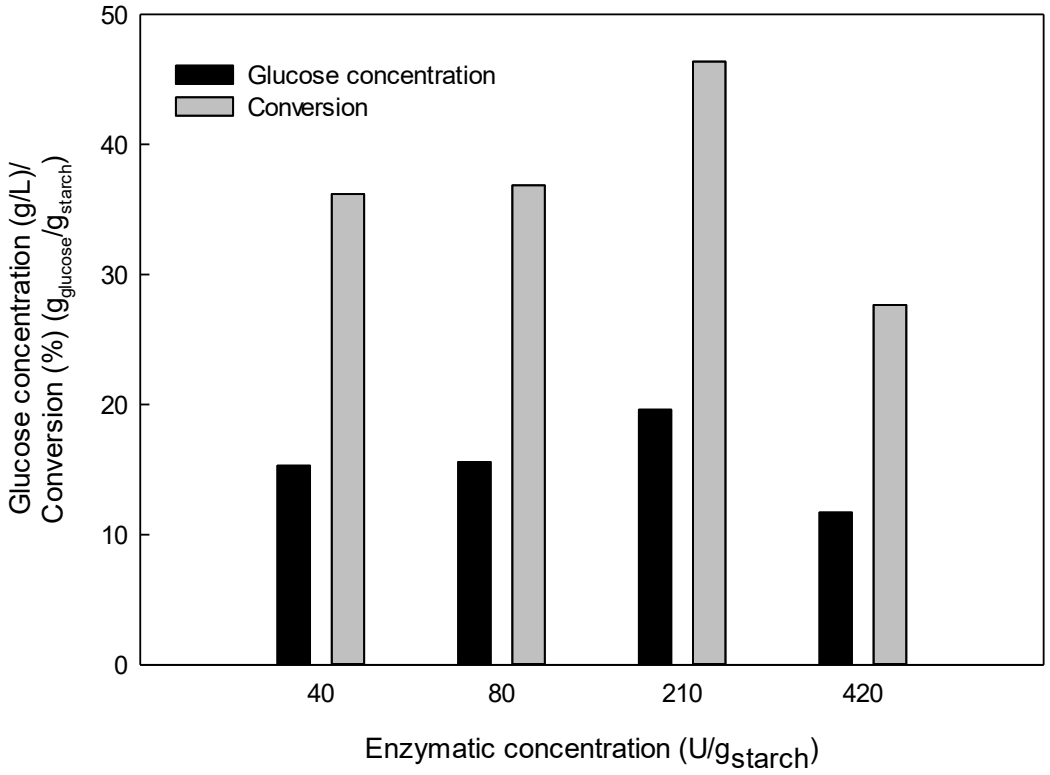

Figure 4. 2 Glucose concentration (g/L) (black bar) and starch conversion into glucose (%) (grey bar) after enzymatic hydrolysis of cassava peel (CP) using α-amylase and glucoamylase (1:1 ratio) after 48 h (n=1) Temperature: 38 ºC; pH 6; sodium acetate buffer 16 mM.

After testing various enzyme concentrations, we determined that the most efficient concentration was 210 U/g, which consisted of 105 U/g of α-amylose and 105 U/g of glucoamylase. These findings were higher than those reported by Ruiz et al. and Virunanon et al., who reported maximum enzymatic dosages of 130.5 U/g [245] and 50 U/g [261], respectively. The differences can be attributed to several factors such as the chemical characteristics of the substrate, the reaction conditions, and the origin of the enzymes [266,267]. Moreover, certain authors have noted that variations in the morphology of the substrate may contribute to differences in hydrolysis [268,269]. Increasing the duration of the hydrolysis process from 24 to 48h and increasing the enzyme loading from 13 to 210 U/g led to an important improvement in conversion, which rose from 8.5% to 46.3%. Nevertheless, despite this significant increase, the highest conversion achieved in the study (46.3%) remained lower than the rates reported in the studies outlined in Table 4.2.

However, it is crucial to take the practical consequences of these conclusions into account. Increased enzyme dosages can result in higher conversion rates, but they also increase the cost of

operation. In contrast, reducing enzyme loading may result in slightly lower conversion rates but substantially improves the overall cost-effectiveness of the process [270].

Drawing from our data, it is evident that there exists a trade-off between conversion efficiency and cost-effectiveness in enzymatic hydrolysis procedures. The optimisation of enzyme dosages necessitates finding a delicate equilibrium between attaining satisfactory conversion rates and guaranteeing economic feasibility and scalability.

In practical terms, achieving a slightly lower conversion efficiency may be acceptable if it leads to significant cost savings in enzyme usage. This approach resonates with the practicalities of industrial-scale bioprocessing, where the overarching goal is to maximise productivity while simultaneously maximising operational expenses.

After evaluating various enzyme dosages in enzymatic hydrolysis processes, our study reveals that enzyme quantity significantly influences conversion efficiency. While higher enzyme dosages result in higher conversion rates, they also incur higher operational costs. Conversely, reducing enzyme loading may lead to slightly lower conversion rates but substantially improves cost-effectiveness.

Based on our data, we conclude that the optimal conditions for enzymatic hydrolysis of our substrate involve using 80 U/g_{starch} of enzyme, which resulted in a conversion efficiency of 36.9%. This finding demonstrates that achieving a balance between conversion efficiency and cost-effectiveness is essential for practical implementation in industrial-scale processes.

Our results, which defy initial predictions, indicate that using greater enzyme concentrations, 210 U/g_{starch}, which produce 46.4% conversion efficiency, might not be the most financially viable choice because of the significant rise in operating expenses. As a result, selecting an enzyme dosage of 80 U/g_{starch} offers a more economical option without appreciably lowering conversion efficiency.

As illustrated in Figure 2.5, the hydrolysis of starch involves several steps. Liquefaction results in dextrin and maltose molecules that are then hydrolysed to glucose monomers during the saccharification step. Since all dextrin, maltose and glucose are reducing sugars and to evaluate the effect of each enzyme, a DNS test to quantify the total amount of reducing sugars in samples hydrolysed using different concentrations of enzymes (40, 80, 210, and 420 U/g_{starch}) was conducted after 48h of hydrolysis and results are presented in Figure 4.3.

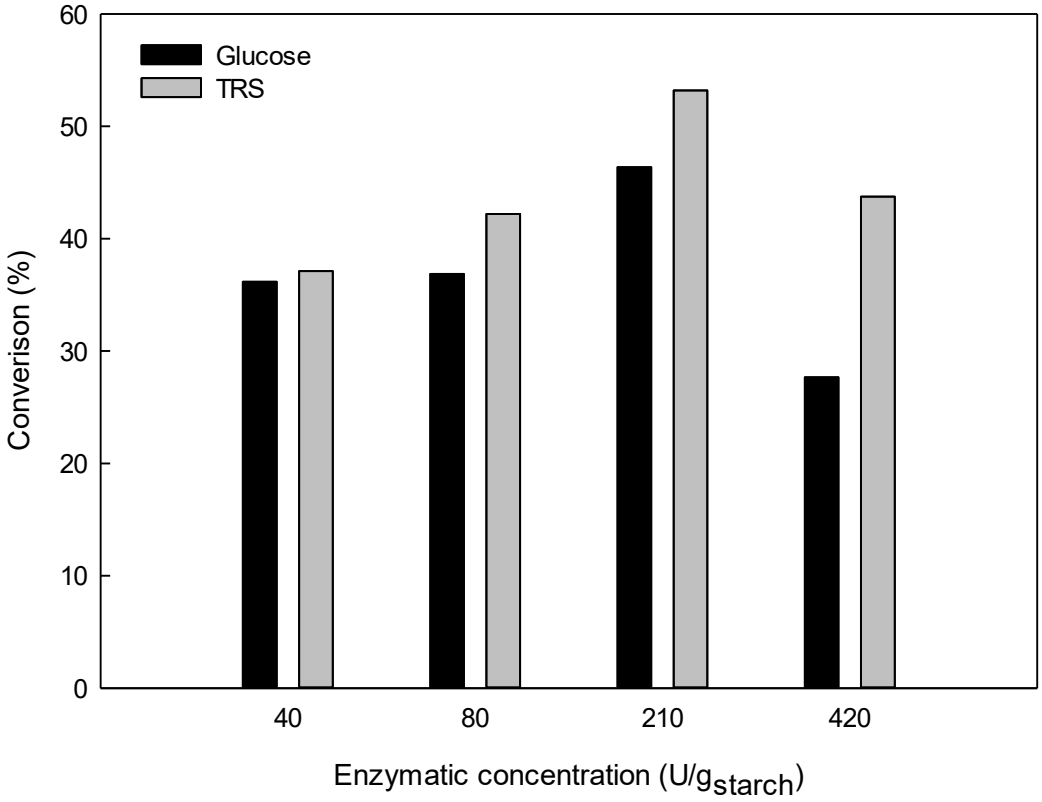

Figure 4. 3 Black column, cassava peel starch conversion into glucose (%); and grey column, cassava peel starch conversion into total reducing sugars (TRS) concentration (%) after enzymatic hydrolysis of cassava peel using α-amylase and glucoamylase (1:1 ratio) (n=1) Temperature: 38 ºC; pH 6; sodium acetate buffer 16 mM.

Figure 4.3 shows that glucose accounted for 63% to 97% of the TRS. As α-amylase and glucoamylase are enzymes specifically utilised for starch degradation, the hydrolysis of starch should only produce glucose monomers. The presence of a higher concentration of TRS in comparison to glucose may imply that dextrin and maltose were not fully hydrolysed into glucose. This observation suggests that the use of both enzymes in a 1:1 ratio may not be optimal. Although α-amylase appears to have a significant effect resulting in a high percentage of reducing sugars, the concentration of glucoamylase may not be optimal, leading to the accumulation of dextrin and maltose molecules that remained undegraded [271]. However, due to time constraints and enzyme availability, further experiments were not conducted to determine the optimal ratio of α-amylase and glucoamylase. This should be the focus of future work, as a thorough investigation of the effect of varying enzyme ratios on the degree of hydrolysis, provides valuable insights for improving the efficiency of the process. Increasing the amount of glucoamylase used during the hydrolysis process might result in the complete hydrolysis of dextrin and maltose. These results are not in agreement with those reported by Ruiz et al., who observed that the ratio of amylase

and glucoamylase needed was 1:0.6, implying that glucoamylase should be added at lower concentrations. This discrepancy can be attributed to variations in experimental conditions, such as the starch content of the feedstock and the origin of the enzymes [266,267].

4.3.1.2 Evaluation of simultaneous and separate liquefaction and saccharification

Simultaneous liquefaction and saccharification of CP has previously been reported, and conversion rates of 79% [247] and 86% [245] were achieved using cassava as feedstock. However, the separation of the liquefaction and saccharification steps has been more commonly used, showing conversion rates of over 75% [128,201,245,247,248]. To compare the effectiveness of the two methods, liquefaction and saccharification were performed separately using 105 U/g of each enzyme. Specifically, α-amylase was added at 25 ºC, and glucoamylase was added at 50 ºC, as recommended by the supplier's specifications. The outcomes of this experiment, presented in Table 4.3, demonstrated that the maximum conversion of starch to glucose after 48 h of hydrolysis using the separate liquefaction and saccharification method only reached 11.2 g/L of glucose, representing 26.5% of conversion. This value is lower than the glucose yield obtained using simultaneous liquefaction and saccharification, which resulted in a conversion of 46.3% after the same hydrolysis time and using the same enzymatic concentration. Based on the results of this study, it can be concluded that the simultaneous process of liquefaction and saccharification was more effective in converting starch into glucose compared to conducting each step separately at their respective optimum temperatures. Our findings are consistent with those reported by Virunanon and co-workers, who demonstrated that the simultaneous liquefaction and saccharification of cassava pulp and wastewater utilizing α-amylase, glucoamylase, and β-glucanase resulted in higher concentrations of reducing sugars than the stepwise sequential hydrolysis using the same enzymes [261].

Table 4. 3 Glucose concentration (g/L) and conversion (%) of starch into glucose carrying out simultaneous and separate liquefaction and saccharification using 210 U/g of α-amylase and glucoamylase for 48 h. Temperature: Simultaneous 38 ºC, Separate: Liquefaction: 25 ºC, Saccharification 50 ºC; pH 6; sodium acetate buffer 16 mM.

Liquefaction and saccharification	Glucose concentration (g/L)	Conversion (%)
Simultaneous	19.6	46.3
Separate	11.2	26.5

4.3.1.3 Evaluation of thermal pre-treatment

Numerous studies have reported the positive impact of thermal pre-treatment on the enzymatic hydrolysis of starchy feedstocks [272,273]. Cassava starch was reported to have a gelatinization temperature of 66-73ºC [248], and some studies report the use of such temperature as the thermal pre-treatment for cassava enzymatic hydrolysis [245]. However, other studies have conducted the pre-treatment at higher temperatures of 95ºC [247] and 100ºC [128], which also led to high conversions. Thus, following the determination of the optimal enzyme loading of 210 U/g during simultaneous liquefaction and saccharification, the impact of two different pre-treatment temperatures was examined. Hence in order to promote the effectiveness of α-amylase, CP were incubated at 66 ºC and 99 ºC for 30 min. Table 4.4 shows that the hydrolysis process did not improve with the incubation of cassava peels at 66 ºC. This pre-treatment method resulted in a reduced conversion rate in comparison to the conversion achieved without any pre-treatment. Conversely, pre-treatment at 99 ºC resulted in a higher conversion. After 48 h of hydrolysis, a glucose concentration of 29.6 g/L was achieved, representing a conversion of 70%. The obtained results in this study validate that thermal pre-treatment-induced gelatinization of starch improved the enzymatic access to the substrate and conversion rate.

Table 4. 4 Glucose concentration (g/L) and conversion (%) of starch into glucose doing simultaneous liquefaction and saccharification using 210 U/g of α-amylase and glucoamylase for 48 h with different pre-treatment methods. Temperature: 38 ºC; pH 6; sodium acetate buffer 16 mM.

Pre-treatment method	Glucose concentration (g/L)	Conversion (%)
Untreated	19.6	46.3
66 ºC	10.6	25.1
99 ºC	29.6	70.0

The hydrolysis process here presented using α-amylase and glucoamylase was enhanced to achieve a final conversion of 70%. This result falls within the range of the study previously conducted by Yoonan and Kongkiattikajorn, who reported a conversion of 75.4%. Although most of the studies reported higher conversions than the present investigation, this may be due to the use of thermostable enzymes. As shown in Table 4.1, most studies achieving yields greater than 80% used hydrolysis temperatures between 60 and 100 ºC. Those studies explicitly specified the use of thermostable enzymes in the process. Despite our effort to acquire thermostable enzymes (Liquozyme supra 2.2X and Extenda peak 1.5 extra) from Novozymes, due to the impact of the COVID-19 pandemic it was not possible. Consequently, utilizing the aforementioned enzymes outlined in the *4.2 Materials and methods* section was the alternative option selected.

While other enzymes have been evaluated in the literature to hydrolyse cassava, α-amylase, and glucoamylase are the most commonly utilized enzymes. Yoonan and Kongkiattikajorn investigated the effect of cellulases, xylanases, and pectinases, achieving conversions of 43%, 2.6%, and 9%, respectively. These values were considerably lower compared to the use of α-amylase and glucoamylase, which resulted in 75.4% of conversion [126]. Since the major polysaccharide present in cassava peels is starch, the utilization of individual enzymes such as cellulases, pectinases, xylanases, and β-glucanases alone is not likely to produce higher conversions than those achieved using amylolytic enzymes. Notwithstanding, some studies have reported that combining different enzymes can lead to high conversions. For example, a combination of amylolytic enzymes and pectinases yielded a conversion of 98% [262]. Additionally, Bayitse and co-workers achieved a conversion of 88% using cellulases and β-glucanases [125]. Although the glucose recovery in our study represented 70% of the initial starch, it only represented 29.6% of the CP weight. Therefore, future studies could explore the use of a combination of amylolytic enzymes with cellulases and β-glucanases, considering the presence of cellulose and hemicellulose in CP.

4.3.2 Acid hydrolysis of cassava peel

4.3.2.1 Evaluation of HCl and H_2SO_4 effect on the hydrolysis of cassava peel

An extensive literature review was conducted to examine previous works on the acid hydrolysis of cassava, and these are presented in Table 4.5. Table 4.5 illustrates that various acids have been used for the hydrolysis of cassava, with H_2SO_4 and HCl being the preferred options, achieving conversions up to 94.5% [127,128]. Nonetheless, other acids, such as H_3PO_4 and CH_3COOH, have also been used, resulting in conversions of 35.4% and 30.4%, respectively [126,254]. The hydrolysis process has been conducted at temperatures ranging between 69 °C and 135 °C, with reaction times ranging from 3 to 154 min.

Table 4. 5 Summary of acid hydrolysis studies on cassava: reaction details and conversion yields.

Feedstock	Catalyst	Temperature (°C)	Time (min)	Conversion (%)	Reference
CP	1.5 M H_2SO_4	110	120	94	[127]
CP	1.1 M H_3PO_4	121	3	35.5	[254]
CP	0.5 M H_2SO_4	100	60	38	[274]
CP	0.1 M H_2SO_4	135	90	66.3	[126]
	0.025 M HCl			63.3	
	0.25 M CH_3COOH			30.4	
CB	0.4 M HCl	120	10	94.5	[128]
CP	0.6 M H_2SO_4	90	30	25	[269]
CP	1.2 M HCl	69	5	93	[96]
		121	70		
CP	0.4 M H_2SO_4	121	70	22	[275]

Cassava peel (CP); Cassava bagasse (CB)

Based on the information provided in Table 4.5 and to reduce the scope of our experiment, HCl and H_2SO_4 were chosen to hydrolyse CP at 120 °C for 60 min and results are shown in Figure 4.5. Figure 4.5 shows that the glucose concentration obtained using HCl at the tested concentrations resulted in approximately 25 g/L, corresponding to a conversion efficiency of 25%. This observed glucose release is attributed not only to the hydrolysis of starch, as discussed earlier, but also to the effective breakdown of cellulose and hemicellulose within the CP. The hydrolysis process demonstrates its capability to liberate glucose from both starch, cellulose, and hemicellulose present in the biomass [276]. Conversely, using the same concentrations of H_2SO_4, the conversion efficiencies were 51, 52, and 53%, respectively. The results showed that H_2SO_4 was more effective than enzymatic hydrolysis and HCl in converting CP into glucose. Specifically, using 0.25 M H_2SO_4 at 120 °C for 60 min resulted in a 2-fold increase in glucose conversion compared to HCl and a 45% increase compared to the best enzymatic hydrolysis condition presented in *4.3.1.3 Evaluation of thermal pre-treatment*. Therefore, H_2SO_4 was chosen as the catalyst for further optimization of the hydrolysis of CP.

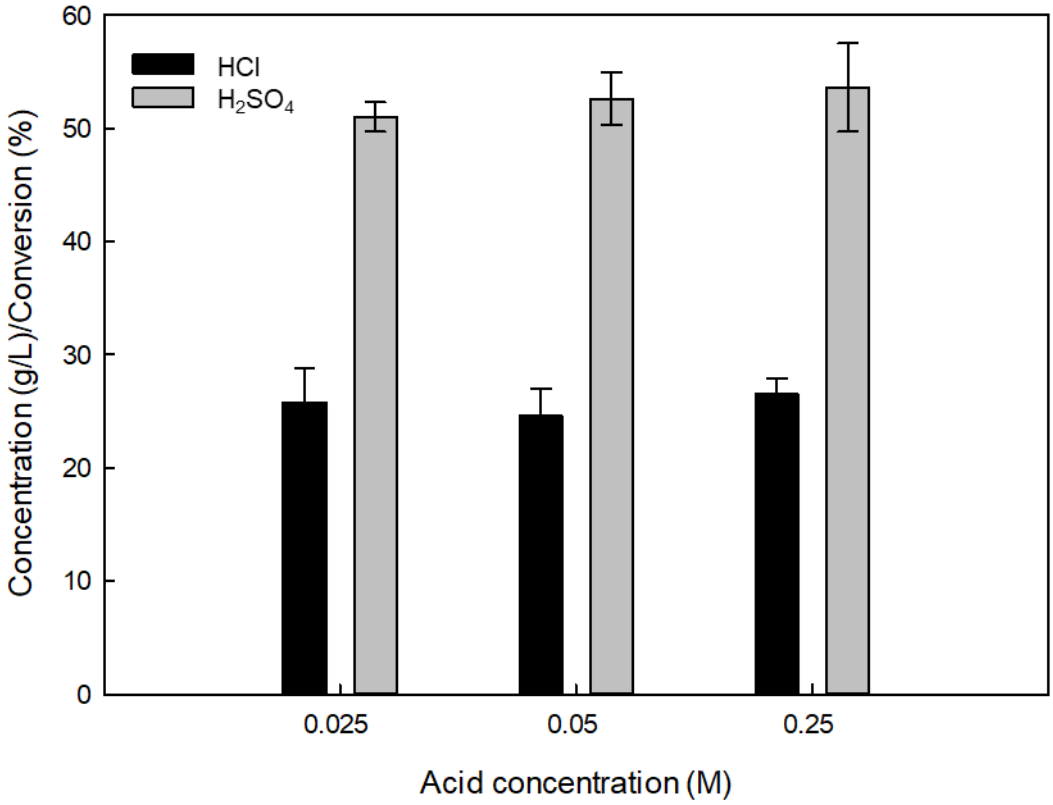

Figure 4. 4 Glucose concentration and cassava peel conversion into glucose after hydrolysis using HCl (black column), and H_2SO_4 (grey column) at 120 °C for 60 min (n=3).

While some studies have been conducted on the acid hydrolysis of cassava, most of them do not perform a systematic optimization of the process. Additionally, studies that investigate the interaction between more than two variables or the effect of the hydrolysis time in the process, are scarce. To the best of our knowledge, the study conducted by Aruwajoye et al. is the most comprehensive. The authors investigated five factors on the hydrolysis of CP using HCl as the catalyst. However, this study required a thermal pre-treatment of the CP in the presence of the acid followed by the reaction in an autoclave [96]. Our aim is to develop a simpler system with a unique hydrolysis step for high sugar recovery using H_2SO_4.

4.3.2.2 Acid hydrolysis optimisation using response surface methodology

To reduce the number of experimental trials, a CCD was performed to determine the optimum conditions for the hydrolysis of CP. The effect of three variables on the TRS concentration in the

hydrolysate was investigated: H_2SO_4 concentration, hydrolysis time, and hydrolysis temperature. Experimental results and independent factors are shown in Table 4.6.

Table 4. 6 Central Composite Design (CCD) used in this study for the optimization along with experimental values of the response total reducing sugars (TRS) concentration.

Run	Factor x_1 [H_2SO_4] (M)	Factor x_2 Time (min)	Factor x_3 Temperature (°C)	Response TRS concentration (g/L)
1	0.6	182	72	17.1
2	0.6	182	108	62.0
3	0.6	58	108	82.1
4	0.6	58	72	14.2
5	2.4	58	108	72.1
6	2.4	58	72	37.9
7	2.4	182	72	82.1
8	2.4	182	108	60.0
9	0.01	120	90	3.5
10	3	120	90	85.7
11	1.5	15	90	77.0
12	1.5	120	60	12.4
13	1.5	120	120	72.9
14	1.5	225	90	78.3
15	1.5	120	90	66.4
16	1.5	120	90	65.0
17	1.5	120	90	54.6
18	1.5	120	90	73.4
19	1.5	120	90	66.3
20	1.5	120	90	72.1

Results from Table 4.6 were analysed by Design Expert using analysis of variance (ANOVA) and the fitted equation model was obtained. Table 4.7 shows the results of the ANOVA test, which indicate that the model is highly significant, with an F-value of 28.6 and a p-value lower than 0.0001. Such values imply that an F-value of this magnitude is only 0.01% likely to occur due to noise. Furthermore, the F-value of 0.94 and p-value of 0.51 of the lack of fit imply that this is not significant relative to the pure error. Since the fit of the model is desirable, the insignificance of the lack of fit means that the model has good predictability. A coefficient of variation (CV) of 13.1% was obtained, which lies below an acceptable limit of 15% [277]. The fitness of the model was also assessed by the coefficient of determination R^2. In this case, an R^2 of 0.97 was obtained, indicating that the variables account for more than 96% of the variation and that the model cannot explain less than 3% of the total variance. Adequate precision measures the signal-to-noise ratio and values greater than 4 are desirable. The ratio of 16.2 indicates that the signal is adequate for

the model which can be used to navigate the design space. The adjusted R^2 (0.91) is in reasonable agreement with the predicted R^2 (0.80), showing a difference lower than 0.2 [255].

Table 4. 7 Analysis of variance (ANOVA) for the central composite design reduced cubic model. x_1: H_2SO_4 concentration; x_2: time; x_3: temperature.

Source	Sum of squares	df	Mean square	F-value	p-value
Model	12442.36	10	1244.236	28.6	<0.0001
x_1	3406.78	1	3406.78	78.2	<0.0001
x_3	3787.83	1	3787.83	86.9	<0.0001
x_1x_2	303.32	1	303.32	7.0	0.027
x_1x_3	1267.06	1	1267.06	29.1	0.0004
x_2x_3	789.63	1	789.63	18.1	0.002
x_1^2	890.83	1	890.83	20.4	0.001
x_3^2	1047.60	1	1047.60	24.0	0.0008
$x_1x_2^2$	759.42	1	759.42	17.4	0.002
Residual	692.21	9	76.91	-	-
Lack of fit	168.38	4	42.1	0.94	0.51
Pure error	223.83	5	44.77	-	-
Cor Total	12834.57	19	675.5	-	-

C.V = 13.1%; R^2 = 0.97; Adj R^2 = 0.91; Pred R^2 = 0.80; Adeq Precision = 16.2

Table 4.7 also shows the statistics of the individual factors and the interactions between them. To obtain an improved model, backward elimination of the insignificant factors of the quadratic model was performed. Although the backward elimination technique slightly improved the model, an enhanced model was achieved by adding a higher degree term to the polynomial equation, $x_1 x_2^2$, thus, resulting in a reduced cubic model. Equation 4.2 (Eq. 4.2) shows the enhanced polynomial model for the estimation of TRS concentration:

$$y=69.49+24.85x_1+16.69x_3+6.16x_1x_2-12.59x_1x_3-9.94x_2x_3-8.39x_1^2-8.96x_3^2-15.25x_1x_2^2 \quad \text{(Eq. 4.2)}$$

The coefficient sign (±) defines the direction of the relationship between each of the factors and the response. A positive coefficient means that as the value of the independent variable increases, the dependent variable will also increase. A negative coefficient indicates that as the independent variable rises, the dependent variable falls [278].

In conclusion, the ANOVA analysis confirms the significance and good predictability of the fitted equation model. The obtained results, indicate that the variables accounted for a significant proportion of the variation and the model can be reliably used for navigating the design space.

The predicted versus actual values plot (Figure 4.5A) shows that the predicted values are in agreement with the experimental results. All points are very close to the line, indicating an excellent fit where x=y. The strong fit of this model confirms that the reduced cubic model can be used to estimate and optimise the TRS concentration in the CPH.

Table 4.7 shows that the factors H_2SO_4 concentration and temperature had significant linear, quadratic and interactive effects on the model. Nevertheless, the linear (x_2) and quadratic (x_2^2), effects of time were removed from the model due to their insignificance. However, the interactions of time with H_2SO_4 concentration and temperature (x_1x_2, x_2x_3, and $x_1x_2^2$) produced p-values below 0.05 indicating their significance to the model. Figure 4.5B, which examines the single effect of the three factors involved in the design, further supports these findings. The increase in H_2SO_4 concentration and temperature results in an increase in TRS concentration. However, time shows a reduced effect at all ranges, confirming its non-significance in the model as a single factor.

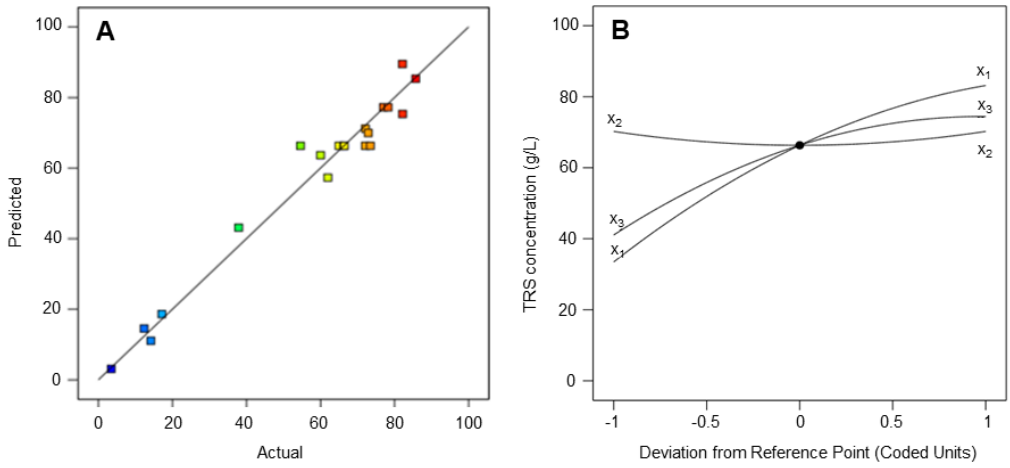

Figure 4. 5 (A) Total reducing sugars (TRS) concentration predicted vs. actual values plot; (B) Perturbation plot over the total reducing sugars (TRS) concentration (g/L). (x_1) H2SO4 acid concentration; (x_2) time; (x_3) temperature.

The analysis of the interactions between variables was further investigated based on the contour and 3D response surface plots presented in Figure 4.6.

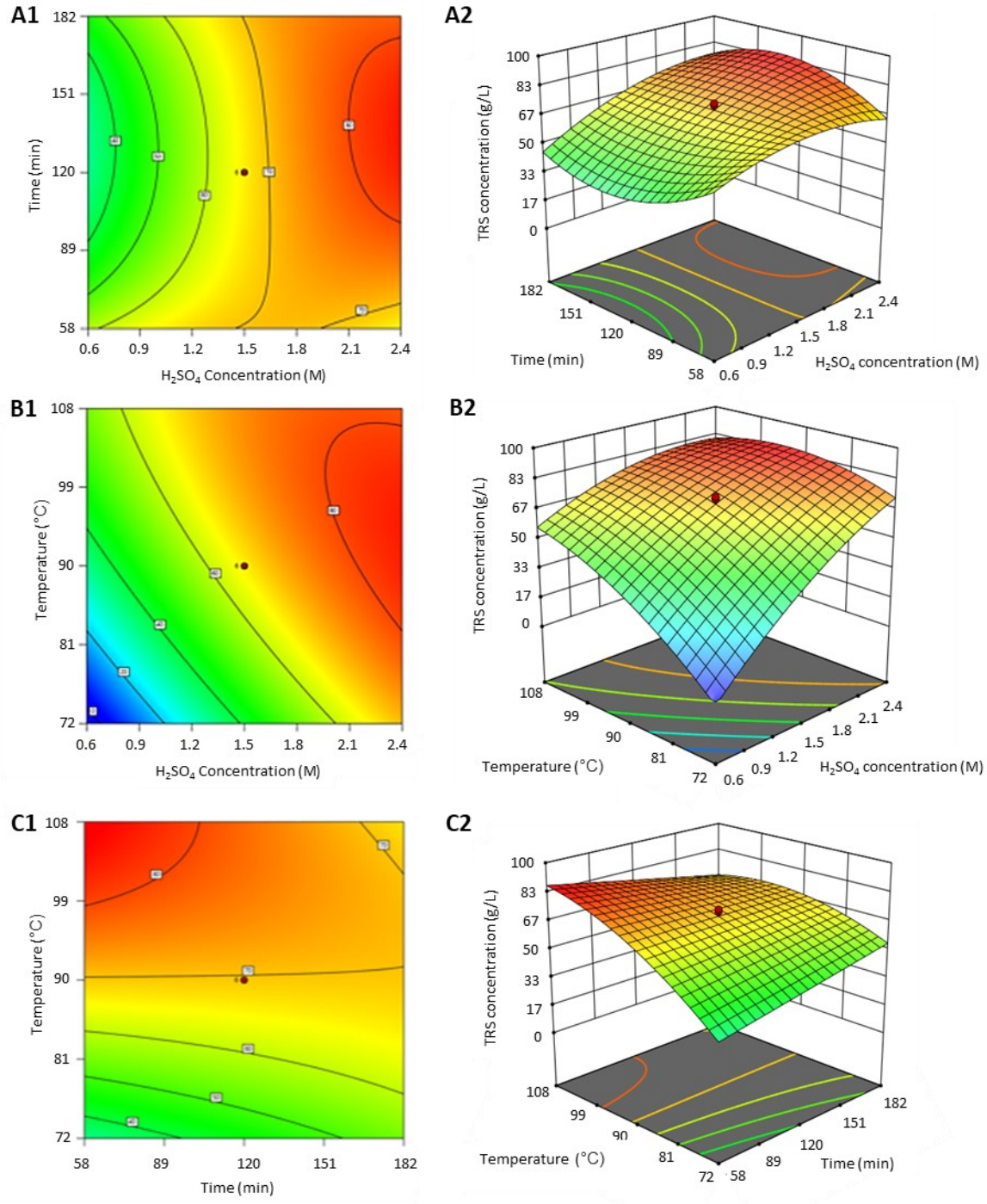

Figure 4. 6 Contour plots (1) and 3D response surface plots (2) representing the effect over total reducing sugars (TRS) concentration (g/L) of (A), H_2SO_4 concentration (M) and time (min); (B), H_2SO_4 concentration (M) and temperature (ºC) and (C), time (min) and temperature (ºC).

Each pair of plots (A, B, and C) depicts the response as a function of two parameters while maintaining the third parameter at a fixed central level. As can be seen, TRS concentrations

exceeding 80 g/L can be achieved through various combinations of the independent variables. Figure 4.6A illustrates the interaction between H_2SO_4 concentration and time, where the highest TRS concentrations were obtained by using H_2SO_4 concentrations from 2 M for a range of time between 90 and 175 min. Figure 4.6B shows the interaction between H_2SO_4 concentration and temperature, where H_2SO_4 concentrations from 2M and temperatures ranging from 80 ºC and 105 ºC resulted in TRS concentrations higher than 83 g/L. Finally, Figure 4.6C shows the interaction between temperature and time, indicating that the maximum TRS concentration was achieved by using hydrolysis temperatures exceeding 99ºC within 90 min. Overall, our results indicate that increasing H_2SO_4 concentration and temperature leads to higher TRS concentration. Therefore, it can be concluded that the duration of the hydrolysis reaction, in combination with the other two independent variables, has a significant impact on the TRS concentration, and this finding is supported by both graphical (Figure 4.6) and statistical analyses (Table 4.7). Onyelucheya and co-workers used H_3PO_4 to hydrolyse CP and found that increasing the acid concentration led to a reduction in the required hydrolysis time [254]. However, their study did not provide a systematic approach to optimise the hydrolysis of CP nor explore optimal conditions. In contrast, our study, employing a DoE approach, revealed a more intricate interaction between acid concentration and hydrolysis time. The analysis of the 3D and contour plots presented in Figure 4.6 revealed that H_2SO_4 concentrations from 2 M, time between 70 and 175 min, and hydrolysis temperatures from 85 °C yield over 80 g/L of TRS.

We carried out an independent experiment to validate our model employing 2.2 M H_2SO_4, 150 min reaction time, and 102 °C, achieving 80.3 g/L of TRS. The predicted TRS concentration was 80.7 g/L, being an acceptable error of 0.5% between the experimental and the predicted value.

Considering the initial carbohydrate concentration of 88% in the CP [125], a maximum conversion of 97% of carbohydrates into reducing sugars was achieved in the CPH in this study. Upon comparison with other studies (Table 4.5), hydrolysis with H_2SO_4 has been reported to yield 66 to 94% TRS conversion from CP at 110 °C [127] and 135 °C [126]. Nevertheless, these works show disparities in the optimal concentration of acid and did not conduct a systematic study. Our research shows that H_2SO_4 concentrations higher than 2 M and temperatures around 85 °C led to conversion yields of 97%. Ajala and co-workers reported an optimum H_2SO_4 concentration of 1.5 M to achieve 94% conversion, being in close agreement with our findings [127]. In contrast, Yoonan and Kongkiattikajorn report 0.1 M of H_2SO_4 as the optimal concentration for the hydrolysis of CP. However, the authors only achieved 66% conversion [126], significantly lower than our results.

Focusing on the reaction time, we found that conducting the hydrolysis between 70 and 175 min led to conversions up to 97%. The aforementioned studies used hydrolysis times of 120 min and

90 min respectively [126,127]. Nevertheless, the optimisation of the process variable time and the interaction of the three different factors was not described. While our process requires slightly higher concentrated H_2SO_4, theirs employs a higher temperature. The interest in using lower temperatures and times is not only due to the lower energy demand but also to the mitigation of sugar degradation. High temperatures and prolonged reaction times can lead to the degradation of sugars, which may lead to lower conversion yields [254]. Furthermore, our study employs a systematic optimisation approach, considering three variables simultaneously, whereas the study performed by Ajala and co-workers employed a fixed time [127].

The present study was optimised to hydrolyse CP using H_2SO_4 as the catalyst. However, other acids can be used to show similar conversion rates. Table 4.5 shows a number of relevant studies on the acid hydrolysis of cassava. Various authors report HCl of various concentrations to achieve conversions of 94.5 and 93% [96,128]. It is important to consider that the variations in the findings of different studies may be attributed to the variations in the properties of cassava, as well as differences in the acid used, acid concentration, reaction time, and reaction temperature used in the hydrolysis process. For example, due to its chemical structure, starch is more easily digested than cellulose. This is because the α-1,4 and α-1,6 glycosidic bonds of starch are not as strong as the β-1.4-glycosidic bonds of cellulose and hemicellulose, hence they are more resistant to dilute acids. Therefore, the hydrolysis of cellulose and hemicellulose usually requires more severe conditions than starch [279]. Some authors have suggested that the total conversion of cellulose and hemicellulose into reducing sugars is not possible [280], which may explain the presence of 3% undegraded carbohydrates in our study. To the best of our knowledge, our study yielded the highest conversion from cassava to reducing sugars achieved to date, while also presenting an optimised hydrolysis process.

4.4 Conclusions

The aim of this research was to assess and compare the effectiveness of enzymatic and acid hydrolysis techniques for the conversion of CP into reducing sugars. The optimal enzymatic conditions were determined using a thermal pre-treatment of the CP at 99 ºC for 30 min, followed by simultaneous liquefaction and saccharification at 38 ºC, using a combination of α-amylase and glucoamylase at a concentration of 210 U/g in a 1:1 ratio for 48 h. This condition yielded a conversion of 70% of starch into glucose. However, it is important to note the practical considerations of the process. While this high conversion is promising, it must be balanced against the associated operational costs, particularly regarding the high enzyme dosage required. Therefore, while this optimal condition demonstrates the potential for high conversion efficiency, further analysis is warranted to explore cost-effectiveness alternative. In conclusion, our study

underscores the importance of optimising enzymatic conditions for efficient glucose production from CP. Moving forward, future research should focus on refining these conditions to strike a balance between conversion efficiency and cost-effectiveness, ultimately facilitating the implementation of enzymatic hydrolysis processes on a industrial scale.

Conversely, the optimisation of the acid hydrolysis yielded a conversion of 97% from CP to reducing sugars using 3 M H_2SO_4 for 120 min at 90 ºC. Further optimization indicated that minor alterations in hydrolysis conditions, such as using 2.6 M H_2SO_4 for 133 min and 90 ºC could result in a complete conversion of polysaccharides to reducing sugars.

Overall, acid hydrolysis demonstrated a higher degree of efficiency compared to enzymatic hydrolysis. Despite achieving a Pyr-546 for conversion with enzymatic hydrolysis, the final concentration of glucose in the CPH was only 29.6 g/L. In contrast, acid hydrolysis yielded a TRS concentration of 85.7g/L. This significant difference can be attributed to the specificity of each catalyst. The amylolytic enzymes used in the study only act on the α-1,4 and α-1,6 glycosidic bonds of starch, releasing glucose monomers, whereas H_2SO_4 cleaves all bonds present in starch, cellulose, and hemicellulose, allowing higher conversion and a wider range of reducing sugars. However, it is important to note that the optimisation was only performed for the acid hydrolysis, which likely contributed to the better results obtained with this method. Therefore, a more complete comparison of the two hydrolysis methods will require the optimisation of both techniques and further investigation into the factors that affect their respective efficiencies.

While the addition of other enzymes such as cellulases and β-glucanases may potentially improve the conversion yields of acid hydrolysis by breaking down cellulose and hemicellulose, they were not utilised in the present study due to economic considerations. The choice of amylolytic enzymes was based not only on the starch content of CP but also on the efficiency of the different enzymes. As previously reported, 40 to 100 times higher enzymatic concentration is needed to break down cellulose than starch [281]. The combination of both methodologies should also be further investigated.

When considering large-scale biomass conversion processes, it is essential to take into account the cost and environmental impact of the methodologies. Although acid hydrolysis is typically less expensive than enzymatic hydrolysis, it has environmental impacts, mainly due to the generation of acid waste. However, the results of this study suggest that acid hydrolysis should be considered as the preferred method for the conversion of CP into reducing sugars. The ease of operation of scalability of acid hydrolysis make it a practical option for industrial applications, where high yields and efficiency are critical factors for consideration.

To the best of our knowledge, our study has documented the highest TRS recovery observed to date. While our results closely align with the 94% recovery achieved by Ajala and co-workers [127], our study slightly enhanced the process. This improvement was achieved by incorporating a more comprehensive DoE, which introduced the variable time into the study, thus contributing to the improvement of the TRS recovery process.

Chapter 5. Screening of the potential of *Cupriavidus necator* for cassava peel valorisation into polyhydroxyalkanoates

Part of the content of this chapter has been adapted from the following manuscript:

"Process integration for efficient conversion of cassava peel waste into polyhydroxyalkanoates" **C. Hierro-Iglesias**, C.O Fatokun, A, Chimphango, P. Thornley, P.H. Blanco-Sanchez, R. Bayitse, A. Fernandez-Castane. Submitted to Journal of Environmental Chemical Engineering.

5.1 Introduction

The valorisation of waste-biomass into value-added products has significant importance in the context of sustainable development and resource management [88]. Cassava, as elaborated on earlier and in more depth within Chapters 2, 3, and 4 of this thesis, is one of the most important crops in tropical and subtropical countries, resulting in high volumes of cassava waste. Employing cassava waste in biorefinery platforms to produce value-added products offers the potential to address challenges in cassava waste management, while simultaneously substituting non-renewable resources in energy and product manufacturing [24]. The production of several products, including ethanol [100], flavour and aroma compounds [101], methane [102], biogas [103], and biopolymers [15] from cassava has been previously documented.

Polyhydroxyalkanoates (PHA) are biopolymers with great potential as an alternative to petroleum-based plastics [5]. They can be produced from renewable resources and biodegraded by microorganisms [145]. PHA are produced exclusively by microbes and stored as cytoplasmic granules [282], providing carbon and energy to the cell, enhancing cell viability, e.g., during starvation [283,284]. PHA show diverse properties and finds applications in packaging,

agriculture, and medicine [7,11,45,46]. *Cupriavidus necator (C. necator)* is the model organism for producing PHA, under conditions of excess carbon and nutrient stress [160].

An important barrier in the commercialisation of PHA is their high manufacturing cost in comparison to petrochemical-derived plastics [11], with PHA cost estimated at 3 to 4-fold higher than their petrochemical counterparts [285]. Slow microorganism growth, energy costs, and downstream strategies impede cost-effective PHA production [286,287], with carbon sources constituting 40% of total annual operating cost [288]. The utilisation of sugar cane molasses and corn cob, has yielded PHA concentrations of 46% and 52% (g_{PHB}/g_{DCW}), respectively [12,289], indicating potential for PHA production from various types of waste biomass, including cassava waste.

Another challenge in PHA production is the absence of rapid and reliable techniques for quantifying PHA [290]. Gas chromatography coupled to mass spectrometry (GC-MS), the prevailing method, requires laborious sample preparation, which is time-consuming and involves hazardous chemicals [291]. Given that real-time monitoring is essential for process optimisation, it hinders the development of optimized PHA production strategies [292]. Flow cytometry (FCM), offers a rapid and comprehensive approach for monitoring PHA production. It provides a real-time analysis of single cells, utilising different lasers to generate diverse signals that inform about several characteristics of the cell, including size and complexity [293]. By using specific fluorophores, such as Nile-red, which binds to intracellular lipidic compounds, PHA detection becomes efficient [294–297]. While Nile-red accelerates analysis compared to GC-MS, it requires centrifugation and 30 min fluorophore incubation, contributing to time consumption [294]. As an alternative, pyrromethene-546 (Pyr-546), is a lipophilic dye that enters bacteria and stains PHA green [298]. Pyr-546 offers a compelling substitute for Nile-red, avoiding sample preparation and prolonged incubation. Although not widely adopted and requiring further optimisation, some studies have employed Pyr-546 for PHA detection [283,298].

This chapter builds upon the work presented in Chapter 4*,* where the optimisation of the acid hydrolysis of CP was conducted resulting in 15 different CPH of varying composition. This chapter focuses on evaluating the ability of *C. necator* to utilise the reducing sugars from CPH to grow and produce PHA. A screening of the 15 CPH from Chapter 4 was conducted to culture *C. necator* at small scale (1 mL). The optimal condition determined during the screening was subsequently applied to flask scale, where baffled and non-baffled flasks were tested. Moreover, the optimisation of the staining protocol using Pyr-546 was performed.

The utilisation of different types of tanks, particularly baffled and non-baffled configurations, plays a crucial role in microbial growth and biotechnological processes, notably impacting the availability of oxygen in the medium. The design of the cultivation flasks, including the presence

or absence of baffles, significantly influences oxygen transfer rates, mixing efficiency, and ultimately, microbial growth dynamics. Baffled tanks are characterised by the presence of internal baffles or impellers, which promote better mixing within the culture medium [299,300]. On the other hand, non- baffled tanks lack these internal structures, leading to less efficient mixing and potentially stratified oxygen distribution. Gaining understanding of how tank designs affect oxygen availability is essential to optimising culture efficiency and efficiently grow microbial processes for industrial use [300].

5.2 Materials and methods

5.2.1 Feedstock and feedstock pre-treatment

Milled CP were kindly provided by Dr Richard Bayitse from the Council for Scientific and Industrial Research (CSIR) in Ghana. CP were collected from a cassava processing plant in Bawjiase, Ghana, soaked in water for 30 min to ease the removal of the brown skin, and subsequently dried overnight at 60 ºC before being milled.

CP were pre-treated with varying H_2SO_4 concentrations (0.01, 0.6, 1.5, 2.4, and 3 M) (>95%, Fisher Scientific, Loughborough, UK, CAS 7664-93-9), times (15, 58, 120, 182, and 225 min), and temperatures (60, 72, 90, 107 and 120 ºC) as shown in Table 4.1. Reactions were performed in a 20 mL reaction volume containing 10% (w/v) of CP. Hydrolysis reactions were conducted in a Starfish workstation (Radleys, Essex, UK) using two-neck round bottom 50 mL pressure flasks and stirred at 280 rpm (Aldrich®, Merck, Darmstadt, Germany) (Figure 3.1). To avoid sample loss due to evaporation, experiments below 100 ºC were fitted with a condenser. Pressure was released by inserting a needle in one of the necks of the flask. In order to achieve temperatures above 100 ºC, flasks were maintained pressurised. After the reaction, samples were vacuum filtrated through a cellulose 11µm filter paper (Whatman, Cytiva, Washington D.C, United States) followed by another filtration step using a PVDF 0.45 µm filter (Whatman, Cytiva, Washington D.C, United States).

5.2.2 Strain and cultivation strategies

C. necator H16 was used to perform the biotransformation from sugars to PHA. *C. necator* H16 was originally a fructose consumer. However, for the purposes of this research, it was mutated to obtain a glucose-utilising strain via adaptive evolution. Bacteria and mutation protocol were kindly provided by Dr Katalin Kovacs from the University of Nottingham.

For the control experiment, *C. necator* was cultivated in defined media (DM) consisting of mineral salt media (MSM) containing (g/L): 10 glucose; 1 $(NH_4)_2SO_4$; 1.5 KH_2PO_4; 9 Na_2HPO_4 $2H_2O$; 0.2 $MgSO_4 \cdot 7H_2O$; 9 citric acid; and 1 ml/L trace element solution [12]. The pH of the medium was adjusted to 7 with NaOH and the media was sterilised by autoclaving at 121ºC for 20 min in a Priorclave® autoclave (Priorclave Ltd, London, UK). Glucose and phosphates were autoclaved separately to avoid the Maillard reaction. Trace element solution was added after autoclaving and sterilised by filtration through 0.22 µm cellulose filters (Sartorius Stedim UK Ltd, Surrey, UK). Trace element solution had the following composition (g/L): 10 $FeSO_4 \cdot 7H_2O$; 2.25 $ZnSO_4 \cdot 7H_2O$; 1 $CuSO_4 \cdot 5H_2O$; 0.5 $MnSO_4 \cdot 5H_2O$; 2 $CaCl_2 \cdot 2H_2O$; 0.23 $Na_2B_4O7 \cdot 10H_2O$; 0.1 $(NH_4)_6Mo_7O_{24}$; and 10 ml/L 35% HCl [12].

Screening of microbial growth was performed using the 15 CPH described in Chapter 4 as the sole source of nutrients. 1 mL cultures using DM and CPH were performed in triplicates using 24-well microplates (Figure 5.1A). CPH were neutralised to pH 7 using NaOH and sterilised by filtration through 0.22 µm cellulose filters (Sartorius Stedim UK Ltd, Surrey, UK) and cultured for 72 h at 30 ºC and 250 rpm in a shaker incubator (Incu-Shake MAXI®, SciQuip Ltd, Newtown, UK). Cultures were performed in triplicates.

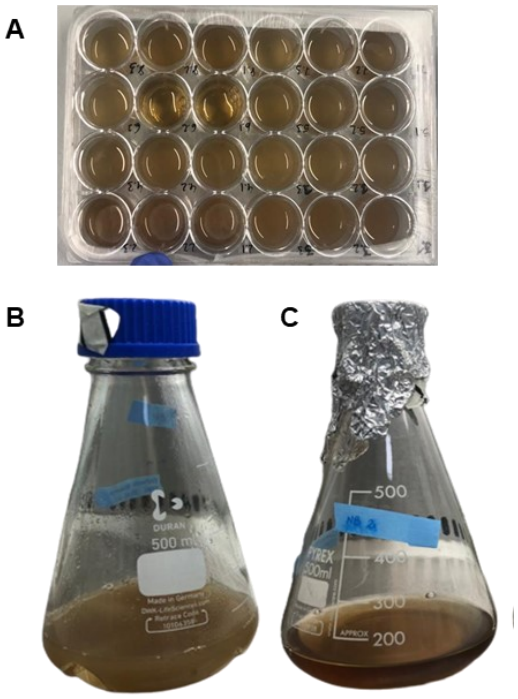

Figure 5. 1 Cultures performed at (A) plate scale (1mL); (B) baffled flasks (100 mL); and (C) non-baffled flasks (100mL).

Following the evaluation of the CPH composition for *C. necator* growth and PHA production, the scale-up to shake flask was performed. DM and CPH obtained under the hydrolysis conditions of 0.6 M H_2SO_4, 58 min, and 107 ºC were used as culture media. CPH was diluted to a glucose concentration of 10 g/L and sterilised by filtration through 0.22 µm cellulose filters (Sartorius Stedim UK Ltd, Surrey, UK). Furthermore, considering the ability of *C. necator* to enhance the production of PHA under O_2-deprived conditions, baffled (Figure 5.1B) and non-baffled (Figure 5.1C) flasks were used in the study. 100 mL volume cultures were performed in 500 mL flasks and cultured for 72 h at 30 ºC and 250 rpm in a shaker incubator (Incu-Shake MAXI®, SciQuip Ltd, Newtown, UK). Cultures were performed in triplicates.

All cultures were inoculated at an OD_{600} of 0.1 using an inoculum culture and incubated for 72 h, 30 ºC, and 250 rpm in a shaker incubator. For the inoculum cultures, one loop of cryostock, stored at - 80 ºC in 15% (w/w) glycerol, was aseptically added into 10 mL of inoculum culture media containing (g/L): 10, peptone; 10, beef extract and 5, NaCl [12]. The pH of the medium was adjusted to 7 using NaOH and subsequently sterilised by autoclaving at 121 ºC for 20 min. Inoculums were cultured overnight at 30 ºC and 250 rpm in a shaker incubator. Inoculum cultures were used for the optimisation of the Pyr-546 staining protocol in *C. necator.*

5.2.4 Microbial growth and PHA production

Microbial growth was analysed by optical density at a wavelength of 600 nm using a Jenway 6310 Spectrophotometer (Keison Products, Chelmsford, UK). Bacterial concentration determined in cell/mL was quantified using a flow cytometer BD Accuri™ C6 Plus Flow Cytometer (Becton, Dickinson and Company, Oxford, UK) in the screening experiments and a first-order correlation between OD_{600} and bacterial concentration was established. Biomass dry cell weight (DCW) was determined in one of the flask experiments. For this purpose, 2 mL of bacterial culture underwent centrifugation at 13,000 g for 2 min using an AccuSpin Micro 17 centrifuge (Thermo Fisher Scientific, Massachusetts, USA). The resulting pellet was subsequently resuspended in 2 mL of distilled water to remove impurities, followed by another round of centrifugation using the same conditions, and this step was repeated twice. Subsequently, the supernatant was discarded and pellets were transferred to pre-dried and pre-weighted weighting boats. Samples were then subjected to 24 h drying at 100 ºC in an oven (Memmert, Schwabach, Germany). Following this, samples were weighted to establish the DCW. A correlation curve between DCW and OD_{600} was calculated, and this curve is provided in Appendix B1.

PHA optimisation from microtiter samples was adapted from the method used by Fernandez-Castane et al. [283]. The optimization of the staining protocol for *C. necator* using pyrromethene-

546 (Pyr-546) was performed. Concentrations of 0/100, 20/80, 40/60, and 60/40 % (v/v, Ethanol (EtOH)/Dimethyl sulfoxide (DMSO)) were tested. Furthermore, pyr-546 concentrations of 0.05, 0.1, and 0.2 mg mL^{-1} were also tested, resulting in 12 conditions.

Briefly, bacterial samples were resuspended in phosphate-buffered saline (PBS) and stained with pyr-546 (Exciton, Lockbourne, USA). Pyr-546 stocks were stored at 4 ºC in 20/80% (v/v, EtOH/DMSO) and added to the bacterial solution at a concentration of 5 µg/mL. Stained samples were incubated for 1 min and analysed using a flow cytometer BD Accuri™ C6 Plus Flow Cytometer (Becton, Dickinson and Company, Oxford, UK) using a 488 nm solid-state laser and fluorescence was detected using the 533/30 BP filter (FL1-A).

PHA quantification was performed by acid propanolysis followed by GC-MS analysis, adapted from elsewhere [301]. Briefly, the bacterial pellet was freeze-dried in a Lablyo benchtop freeze dryer (Frozen in Time Ltd, York, UK) at -50 °C and 1-5 Pa, overnight. Propanolysis was performed using 5 mg of lyophilized bacteria in 1 mL of chloroform and 1 mL of 1-propanol containing 15% of 37% (v/v) HCl in an 8 mL glass tube (Duran®, Mainz, Germany). 50 µL of 1 mg/mL solution of benzoic acid in 1-propanol was added as the internal standard. The mixtures were incubated for 2 h at 100°C in an oven (Memmert, Schwabach, Germany). After cooling to room temperature, 2 mL of distilled water was added followed by vortexing for 30 s, and left standing for 5 min to allow for phase separation. The upper aqueous phase was discarded, and the washing step was repeated to eliminate impurities. 1 mL of the organic phase containing derivatised PHA was filtered with 0.2 µm nylon filters (Fisher Scientific, Loughborough, UK) and transferred to a GC-MS vial. The standard sample of poly (3-hydroxybutyric acid-*co*-3-hydroxyvaleric acid) (PHBV, 80181-31-3, Merck, Darmstadt, Germany) was used to prepare the standard calibration curves for PHB and PHV. These calibration curves and a representative GC-MS chromatogram of a standard sample and a culture sample are included in Appendix B2. Analysis was performed using a Single quadrupole gas chromatograph-mass spectrometer GCMS-QP2010 (Shimazu, Milton Keynes, UK). One µL was injected into an analyser with a 30 m SH-Rtx-5MS column (Shimazu, Milton Keynes, UK) at 280°C. The flow rate was set at 1.25 ml/min and the ionization detector at 240 °C. Column temperature was programmed from 40 to 250 °C at a rate of 5 °C/min. The total measurement time for each sample was 40 min. PHBV was identified using the internal libraries NIST17s and NIST17-1 available in GC-MS Postrun Analysis Software (Shimazu, Milton Keynes, UK). PHBV amount of each sample was normalised by the weight of the lyophilised bacteria and expressed as a percentage of polymer weight/cell dry weight.

A correlation between PHA concentration (%) assessed through GC-MS and fluorescence values obtained from Pyr-546-stain cells was conducted to calculate the concentration of PHA from FCM

data. This experiment was carried out using flask-scale cultures and employed DM. The correlation curve is available in Appendix B3.

5.2.5 Optical microscopy images

Bacteria stained with Pyr-546 were observed and imaged using a Zeiss Axiolab microscope (Carl Zeiss Ltd., Cambridge, UK) fitted with a Zeiss AxioCam ICm1 camera, and the images were processed in auto-exposure mode with the aid of Zeiss ZEN Lite 2012 software. Samples were excited with a Zeiss VHW 50f-2b ultraviolet light source and a 520 LP filter was employed for detection of fluorescence.

5.2.6 Analysis of total reducing sugars (TRS) and glucose concentration

Total reducing sugars (TRS) concentration was determined using the DNS (Di-nitrosalicylic acid) test, which was adapted p-from Miller (1959) [259]. The reagent composition was as follows (% (w/v)): 0.63 DNS; 0.5 NaOH; 18.2 $KNaC_4H_4O_6 \cdot 4\ H_2O$; 0.5 $Na_2S_2O_5$ and 0.5 % (v/v) C_6H_6O. 0.5 mL of sample were mixed with 0.5 mL of DNS reagent. Samples were placed in boiling water for 5 min and cooled to room temperature. The absorbance was measured at 575 nm using a Jenway 6310 Spectrophotometer (Keison Products, Chelmsford, UK). A calibration curve (Appendix 4.1) was prepared using pure synthetic D-(+)-glucose (Fisher Scientific, Loughborough, UK, CAS 2280-44-6), and absorbance values were interpolated to calculate sample concentrations (Appendix A2).

Glucose concentration was measured using the YSI model 2500 biochemical analyzer (Xylem Inc., Nottingham, UK). Samples were previously filtered through a PVDF 0.45 µm filter (Whatman, Cytiva, Washington D.C, United States).

5.3 Results and discussion

5.3.1 Optimisation of bacterial polyhydroxyalkanoates staining

In order to detect PHA present in the bacteria, samples were stained with Pyr-546, and fluorescence was measured by FCM. To determine the optimal conditions for the staining process, a unique sample of *C. necator* was consistently analysed throughout the study.

Figure 5.2 depicts the fluorescence intensity corresponding to the different staining conditions examined within the experiment and FCM histograms can be found in Appendix B4. As shown in Figure 5.2, the different staining preparations yielded varied fluorescence values, from 373.8 AU for the sample stained with 0.05 mg/mL of Pyr-546, diluted in 40/60 (%v/v EtOH/DMSO) without incubation time, to 3305.5 AU for the sample stained with 0.05 mg/mL of Pyr-546 diluted in 20/80 (%v/v EtOH/DMSO) and incubated for 5 min. This difference represents a 9-fold increase between the aforementioned samples.

Despite achieving the highest fluorescence intensity using 0.05 mg/mL of Pyr-546 diluted in 20/80 (%v/v EtOH/DMSO), and incubated for 5 min, a remarkably similar result was obtained using the same staining parameters but with an incubation time of 1 min (Figure 5.2B). The difference in fluorescence intensity between these two conditions is 5%. Given this low difference, and in order to minimise data acquisition timeframe, 1 min incubation time was chosen as the preferred incubation time using 0.05 mg/mL of Pyr-546 diluted in 20/80 (%v/v EtOH/DMSO). Furthermore, this staining condition represents a 46-fold increase over the control sample, which indicates the presence of lipid-like molecules, such as PHA inside the bacteria.

Although the fluorescence intensity was not as high as with the use of 0.05 mg/mL of Pyr-546 diluted in 20/80 (%v/v EtOH/DMSO), and incubated for 1 min, comparable intensity values were obtained using 0.2 mg/mL of Pyr-546 diluted in 100 (% v/v DMSO), and incubated for 1 min. However, it is important to note that this condition required higher fluorophore concentration, resulting in increased process costs. Consequently, 0.05 mg/mL of Pyr-546 diluted in 20/80 (%v/v EtOH/DMSO), and 1 min incubation time was chosen as the optimal staining condition to detect PHA in *C. necator* using Pyr-546. This choice provides a balance between fluorescence intensity, economy, and time efficiency.

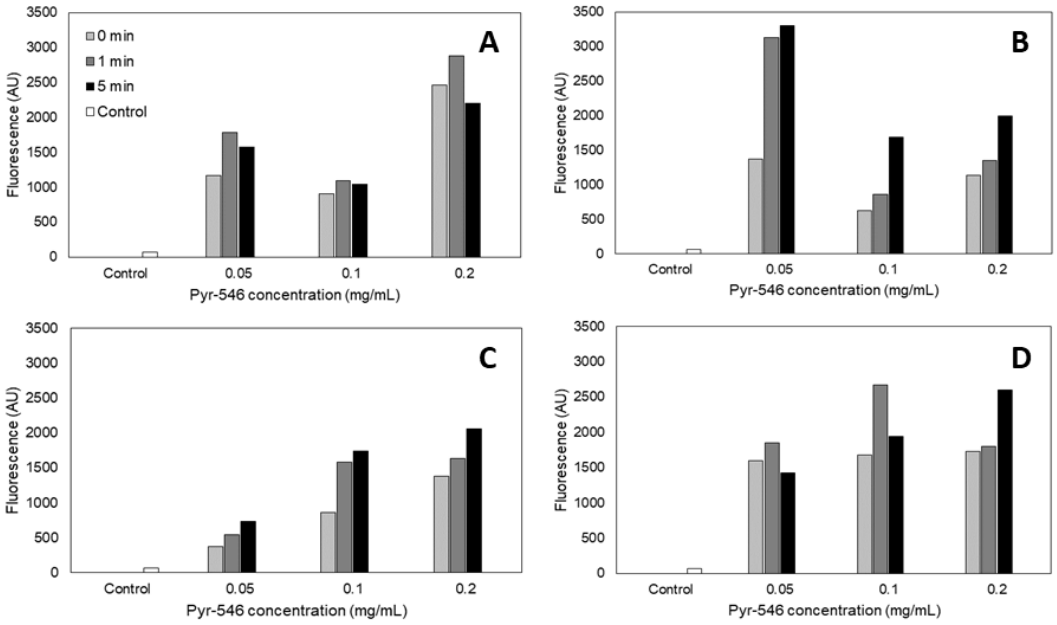

Figure 5. 2 Fluorescence of Cupriavidus necator H16 stained with Pyrromethene-546 (A) 0/100 EtOH/DMSO (%v/v); (B) 20/80 EtOH/DMSO (%v/v); (C) 40/60 EtOH/DMSO (%v/v); (D) 60/40 EtOH/DMSO (%v/v). AU: Arbitrary Units. n=1.

5.3.2 Screening of *Cupriavidus necator* growth and polyhydroxyalkanoates production from cassava peel hydrolysate

5.3.2.1 Determination of microbial growth

The 15 resulting CPH obtained from the CCD presented in Ch*apter 4*, with different TRS and glucose concentrations were tested to assess the growth of *C. necator* and its ability to produce PHA. Results are shown in Figure 5.3 together with a control experiment using DM. As depicted, *C. necator* was able to metabolise all the CPH after 48h of culture to different extent. However, significant differences can be observed. Growth varied from as little as OD_{600} 0.69 using the CPH obtained under the hydrolysis conditions of 1.5 M H_2SO_4, 15 min, and 90ºC, to OD_{600} 15.8 using the CPH obtained under the following conditions: 0.6 M H_2SO_4, 58 min, and 107 ºC. The highest growth obtained in this study using CPH was compared to the culture using DM, which reached an OD_{600} 8.6 after 48 h of cultivation. As depicted in Figure 5.3, among the 15 cultures conducted using CPH, three exhibited higher growth compared to the culture using DM. This increased growth might be attributed to the presence of additional reducing sugars, such as fructose, xylose, mannose, and arabinose, within the CPH.

In order to understand what factors might be affecting microbial growth, the inhibitory effect of glucose concentration on the growth of *C. necator* was investigated. To the best of our knowledge, there have been no previous studies addressing this question. However, previous research has examined substrate inhibition using other sugars in *C. necator*. Notably, Dey and Rangarajan conducted a study revealing that concentrations exceeding 20 g/L of sucrose in the culture media adversely affected the growth of *C. necator* [302]. However, after contrasting Figures 5.3A and B, substrate inhibition was disregarded in our study. Figure 5.3B shows that the culture that produced the greatest growth corresponds to the CPH containing 75.2 g/L of TRS. However, the initial sugar concentration in the culture had no beneficial impact on the growth either. The culture presenting an OD_{600} of 14.4 had a starting TRS concentration of 27.6 g/L. Nevertheless, the CPH obtained under 1.5 M H_2SO_4, 15 min and 90ºC resulted in OD_{600} lower than 1 with an initial sugar concentration of 66.4 g/L. These findings demonstrate that the glucose concentration does not negatively affect *C. necator* growth.

The sugar composition of CP has been previously reported in the literature, with glucose accounting for approximately 95% of the TRS and xylose and arabinose representing the remaining amount [125]. However, as shown in Figure 5.3C, the glucose concentration over the TRS of the CPH in the present study was in the 14-89% range. Despite obtaining a wide range of glucose concentrations, no clear correlation was found between the TRS composition and microbial growth. When Figures 5.3A and C are compared, it is clear that the CPH containing 66.5% glucose resulted in the highest microbial growth (OD_{600} 15.8). A CPH containing 66.9% of glucose, on the other hand, resulted in the least amount of growth (OD_{600} 0.69). Although only glucose was identified and quantified from all the potential sugars in the CPH, the results show that the sugar composition of the CPH is not a critical factor in the growth of *C. necator*.

Figure 5.3A shows the quantified amount of alkali used to neutralise the culture media. All the CPH obtained using 0.6 M presented the highest growth results. All these experiments required NaOH concentrations lower than 2 M to be neutralised. Cultures that needed less alkali grew more on average. CPH produced under 0.01 M H_2SO_4, 120 min, and 90 ºC did not require a neutralisation step. However, the growth only reached OD_{600} 5.2. This might be a result of the low availability of sugars in the media, 3.5 g/L (Figure 5.3B). When more alkali is added to an acidic solution, salt is likely to form in the media, and high salt concentrations may prevent bacterial growth [303].

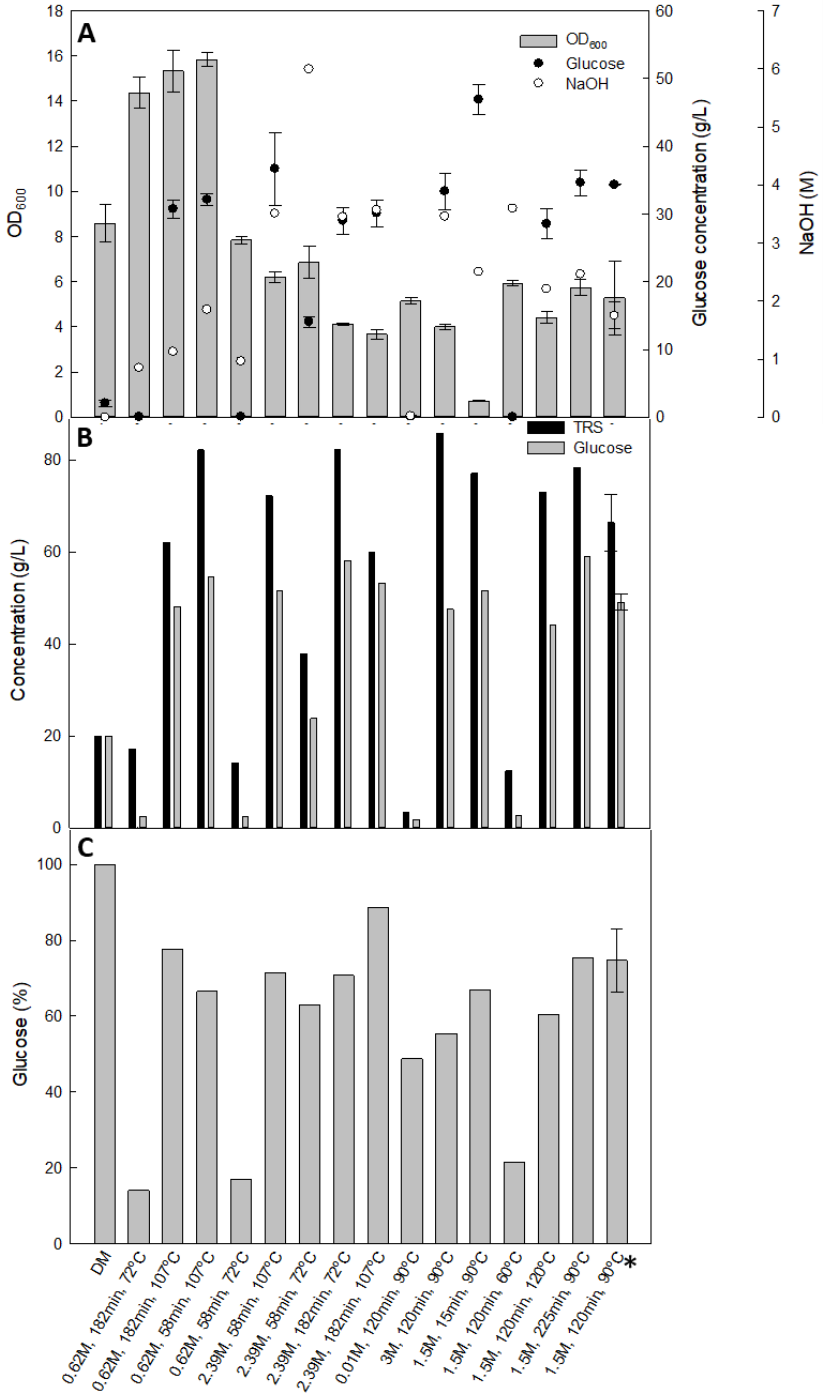

Figure 5. 3 Utilisation of CPH by *C. necator.* (A) Grey column, OD_{600}; (●) residual glucose concentration (g/L) after 48 h of culture (n=3); and (○) NaOH (M) used for pH neutralization. (B) Black column, Total reducing sugars (TRS) concentrations and; grey column, glucose concentrations obtained from each hydrolysis condition. (C) Glucose as a percentage of total reducing sugars from each hydrolysis condition from the DoE matrix. DM: defined media (*) Average and standard deviation values are given for the central point (1.5M, 120min, and 90 °C) (n=6).

5.3.2.2 Determination of polyhydroxyalkanoates production

FCM was used to rapidly assess relative PHA content within the individual bacteria. The lipophilic fluorophore Pyr-546 was used to stain bacteria and the fluorescence intensities are shown in Figure 5.4. As shown in the correlation between PHA concentration (%) quantified using GC-MS and fluorescence values from FCM, higher fluorescence values mean higher PHA content (Appendix B3).

Figure 5.4 reveals that the lowest H_2SO_4 concentrations tested, specifically 0.01 M and 0.6 M, yielded the highest PHA production. 0.6 M H_2SO_4, 58 min, and 107 ºC was the best CP hydrolysis condition for the further production of PHA by *C. necator*, which aligns with the optimal hydrolysis condition for microbial growth. Similar to the findings from the previous growth study, the results indicate that the H_2SO_4 concentration used in the hydrolysis process had a direct effect on the production of PHA, which might be also due to the salts availability in the media. However, no correlation was observed between hydrolysis time and temperature with the PHA production. As depicted in Figure 5.4, PHA concentration obtained in the experiment using DM are in line with some values obtained using CPH. However, the disparity in PHA concentration among samples might be attributed to different compositions of the respective culture media, leading to differential fluorescence outcomes, and therefore different PHA concentrations. Therefore, the application of FCM represents a valuable technique, enabling efficient assessment of PHA production when employing identical culture media.

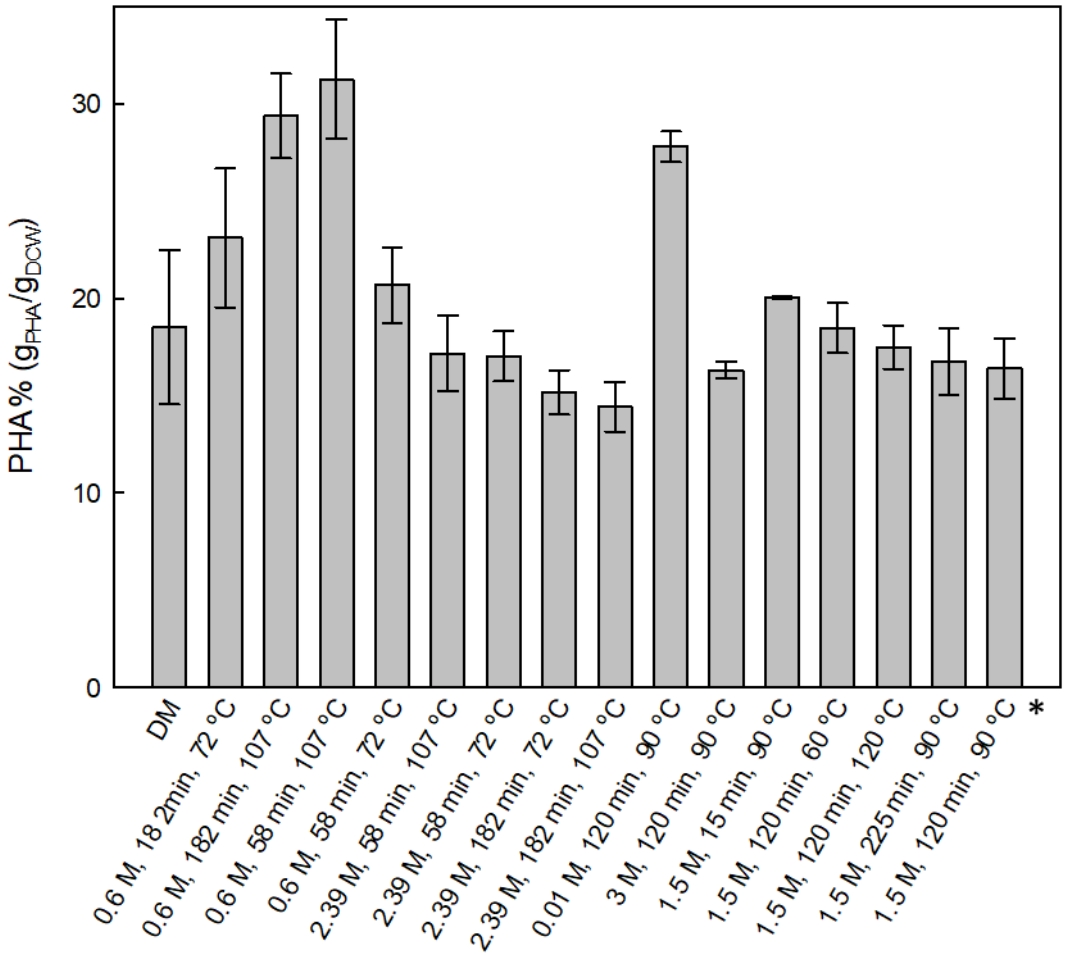

Figure 5. 4 Polyhydroxyalkanoates (PHA) concentration (% g_{PHA}/g_{DCW}) from cassava peels hydrolysates (CPH) using *Cupriavidus necator*. X axes corresponds to the hydrolysis conditions from the DoE matrix and defined media (DM) (n=3). (*) Average and standard deviation values are given for the central point (1.5 M, 120 min, and 90 °C) (n=6).

Figure 5.5 A1 and B1 exhibit fluorescence microscope images showing representative samples with low and high fluorescence values from Pyro-546-stained bacteria grown on CPH (0.01 M, 120 min, and 90 ºC) and CPH (0.6 M, 58 min, and 107 ºC), corresponding to PHA accumulation of 10 and 31 % PHA (g_{PHA}/g_{DCW}), respectively (Appendix B3). Vega-Castro and co-workers reported the production of 0.064 g/L of PHA using acid-hydrolysed CP [275]. Our work whereby 31% PHA corresponds to 1.5 g/L of PHA, clearly shows improved yields than the previously published.

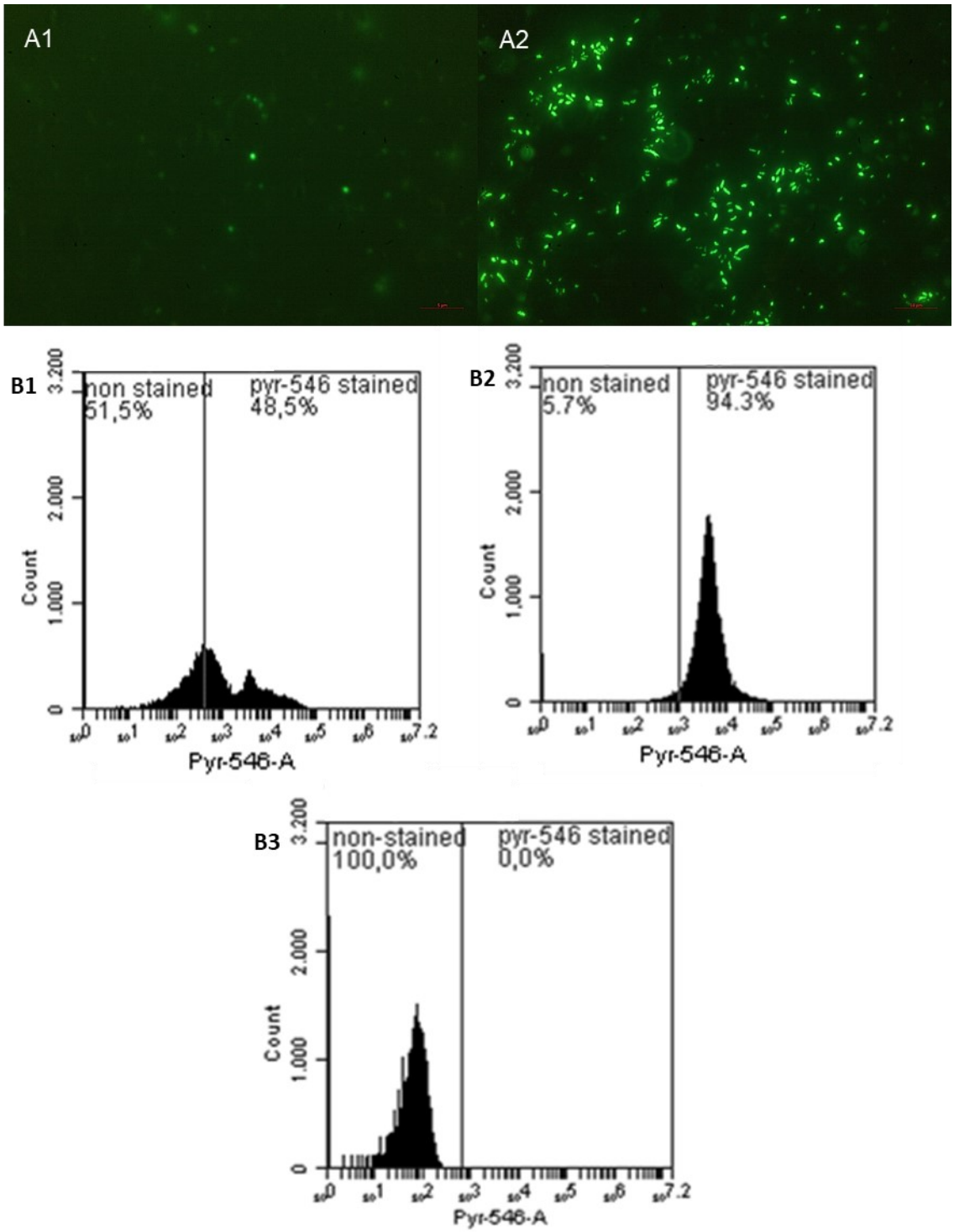

Figure 5. 5 Fluorescence microscopy images (A) and fluorescence flow cytometry (FCM) plots (B) of Pyro-546-stained *Cupriavidus necator* (*C. necator*) showing polyhydroxyalkanoates (PHA) production from cassava peels hydrolysate (CPH) obtained under hydrolysis conditions of 0.01 M, 120 min and 90 ºC (B1); and 0.6 M, 58 min and 107 ºC (B2); and non-stained sample used as control for Pyr-546 fluorescence (B3).

Furthermore, figure 5.5 A2 and B2 display the corresponding FCM plots of the fluorescence intensity of each sample. The FCM fluorescence plots of all 15 samples can be found in Appendix

B5. As depicted in Figure 5.5, higher fluorescence values obtained using FCM correspond to higher fluorescence observed in the fluorescence microscope images. Additionally, Figure 5.5 B1, which corresponds to the lowest fluorescence value, shows a heterogeneous distribution of fluorescence among the bacteria, indicating that only 48.5% of the bacteria contained PHA. Conversely, Figure 5.5 B2, corresponding to the highest fluorescence value, displays a unique and sharper peak, indicating a homogeneous distribution of fluorescence among the cells. Remarkably, in this sample 94.3% of the bacteria contained PHA. As can be observed in Appendix B5, with the exception of the sample hydrolysed using 0.01 M H_2SO_4, all other samples presented between 75 and 99% of bacteria containing PHA. Therefore, we have employed FCM analysis as a rapid and high-throughput method to screen the formation of PHA in *C. necator* grown on CPH. Although some studies have reported the production of PHA from CP, to the best of our knowledge, only Vizcaino and co-workers have used pyr-546 to relatively assess the production of PHA in *C. necator* from an alternative feedstock. The use of FCM in this study confirmed the ability of *C. necator* to produce PHA from CPH and the suitability of FCM as a rapid and high-throughput method to rapidly assess PHA production.

After analysing Figures 5.3 and 5.4, the CP hydrolysis conditions of 0.6 M, 58 min, and 107 ºC were determined to be the optimal ones for *C. necator* growth and PHA production. Under these conditions, an OD_{600} of 15.8, equivalent to a biomass concentration of 4.6 g/L was achieved, and the fluorescence values corresponded to the maximum PHA formation of 31% PHA (g_{PHA}/g_{DCW}), equivalent to 1.5 g/L of PHA.

5.3.2.3 Analysis of *Cupriavidus necator* morphology

The analysis of bacterial morphology using FCM with forward scatter (FSC) and side scatter (SSC) measurements was employed to track the size and shape of *C. necator* cultured with CPH. FSC and SSC, which collect light scatter at different angles, provide valuable information about bacterial size and granularity, respectively. The granularity of a population is defined by the optical complexity caused by particulate material within the cell [283]. The results of this study (Figure 5.6) reveal clear distinctions in population composition within the examined cultures. Specifically, cultures grown with CPH obtained using 0.6 M H_2SO_4 showcased a uniform and homogeneous population regarding size (Figure 5.5 A1). However, a diverse range of complexity is evident within this condition. Figure 5.6 B1 shows a smaller and less complex population, accounting for less than 2% of the total bacteria and labeled as P2. Conversely, the principal and larger population, labelled as P1, displays considerable complexity, manifested by the elongated shape in the plot. On the other hand, the utilization of CPH obtained using higher H_2SO_4 concentrations (2.4 M and 3 M) exhibited more heterogeneous growth with two separate

populations regarding both size and complexity (Figure 5.6 A2 and B2). Remarkably, the only condition that displayed three different populations was the one using 0.01 M H_2SO_4 (Figure 5.5 A3 and B3). These results suggest that the CPH samples examined in this study led to three distinct growth patterns. Figure 5.6 presents representative samples illustrating each growth pattern, and FCM plots of all samples can be found in Appendix B6. Notably, the growth patterns were primarily influenced by the H_2SO_4 concentration used during the hydrolysis process. However, no clear correlation was observed between bacterial growth and either the time or temperature used to recover the reducing sugars from CP.

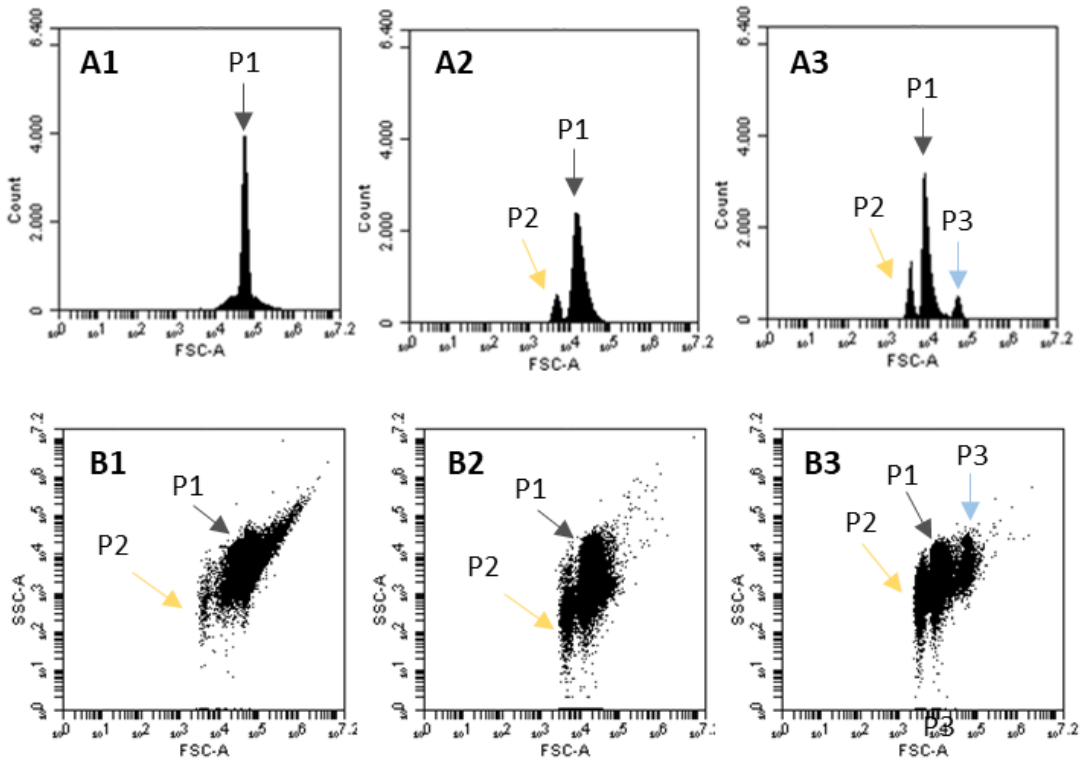

Figure 5. 6 Analysis of Cupriavidus necator (C. necator) morphology using flow cytometry (FCM). (A) Relative cell size using forward scatter (FSC) and (B) FSC vs and granularity through side scatter (SSC) of cultures grown using cassava peels hydrolysate (CPH) obtained under hydrolysis conditions of 0.6 M, 58 min, 107 ºC (1); 2.4 M, 182 min, 72 ºC (2); and 0.01 M, 120 min, 90 ºC (3) (n=3).

Given that SSC provides information about the complexity of bacteria, and considering that PHA accumulation influences light scatter, thus affecting SSC values, a linear correlation between SSC and Pyr-546 fluorescence values was performed, as illustrated in Figure 5.7. The correlation discerns that the higher fluorescence values correspond to increased cell complexity, confirming

that PHA accumulation enhances bacterial complexity. Although with a different microorganism, this observation has been previously highlighted by Fernandez-Castane and co-workers [304].

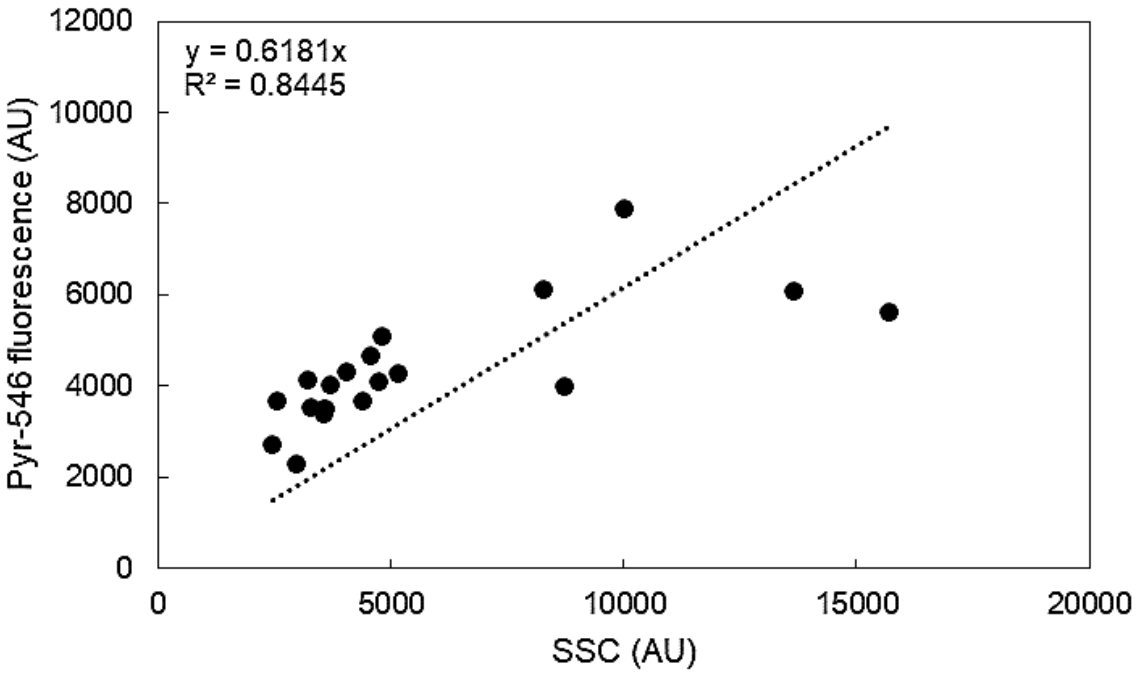

Figure 5. 7 Correlation between Pyrromethene-546 (Pyr-546) and side scatter (SSC). (AU: arbitrary units).

5.3.2.4 Correlation of OD_{600} and microbial concentration measurements

FCM has previously been reported in the literature as a valuable technique for the quantification of bacterial concentrations [283]. Therefore, FCM was used in this study for the absolute counting of bacteria and the subsequent calculation of bacteria concentration expressed as cell/mL. The analysis was conducted using the cultures derived from the screening experiment using CPH. This approach enabled the comparison of bacterial concentration data obtained with FCM with OD_{600} measurements, thereby establishing a correlation between these two analytical techniques. As depicted in Figure 5.8, a strong correlation (R^2>0.9) between OD_{600} and FCM cell count was observed for *C. necator*, with 1 OD_{600} equivalent to 3.25 x 10^8 cell/mL. This correlation is higher than Nicolaisen and co-workers' correlation of 1 x 10^8 CFU/mL [305]. Notably, FCM offers advantages over CFU counting methods, as mentioned by previous researchers, due to the ability of FCM to detect viable but not culturable cells [283]. Furthermore, these variations could

potentially be attributed to fluctuations in the intracellular PHA concentration. Although no study was found for *C. necator*, previous authors have observed that the accumulation of PHA within *Burkholderia thailandensis* can influence the optical density readings of the culture [306]. However, it remains an unexplored aspect whether this effect leads to an overestimation or underestimation of the OD_{600} measurements. Limited investigation has been undertaken in this context and OD_{600} remains the preferred methodology to assess *C. necator* growth.

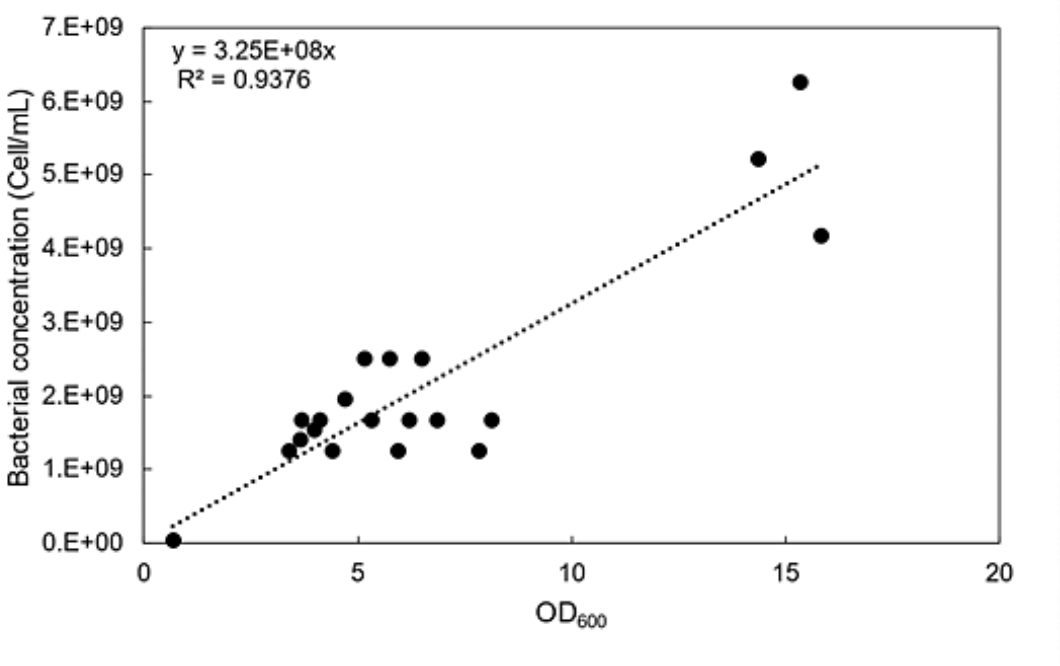

Figure 5. 8 Correlation of OD_{600} values and cell/mL concentration obtained by spectrophotometry and by flow cytometry (FCM), respectively; 1 OD_{600}= 3.25 x10^8 cell/mL.

5.3.3 Flask scale cultivation

Acknowledging the importance of scaling up processes in bioproduction, we initiated this study by assessing the effect of the CPH composition on *C. necator* growth and PHA production at plate scale. This preliminary experiment is crucial for transitioning laboratory findings to practical, flask-scale applications. Flask and bench bioreactor-scale cultures bridge the gap between small-scale experimentation and potential industrial use, ensuring that processes can be adapted to larger-scale productions [307].

Therefore, having established the hydrolysis reaction using 0.6 M H_2SO_4, 58 min, and 107 ºC, as the optimal CP hydrolysis conditions for the growth of *C. necator* and production of PHA at plate scale, flask scale experiments with a 100-fold volume increase were performed. Baffled and non-

baffled flasks were used to evaluate the influence of aeration on the production of PHA by *C. necator* and results are presented in Figure 5.9.

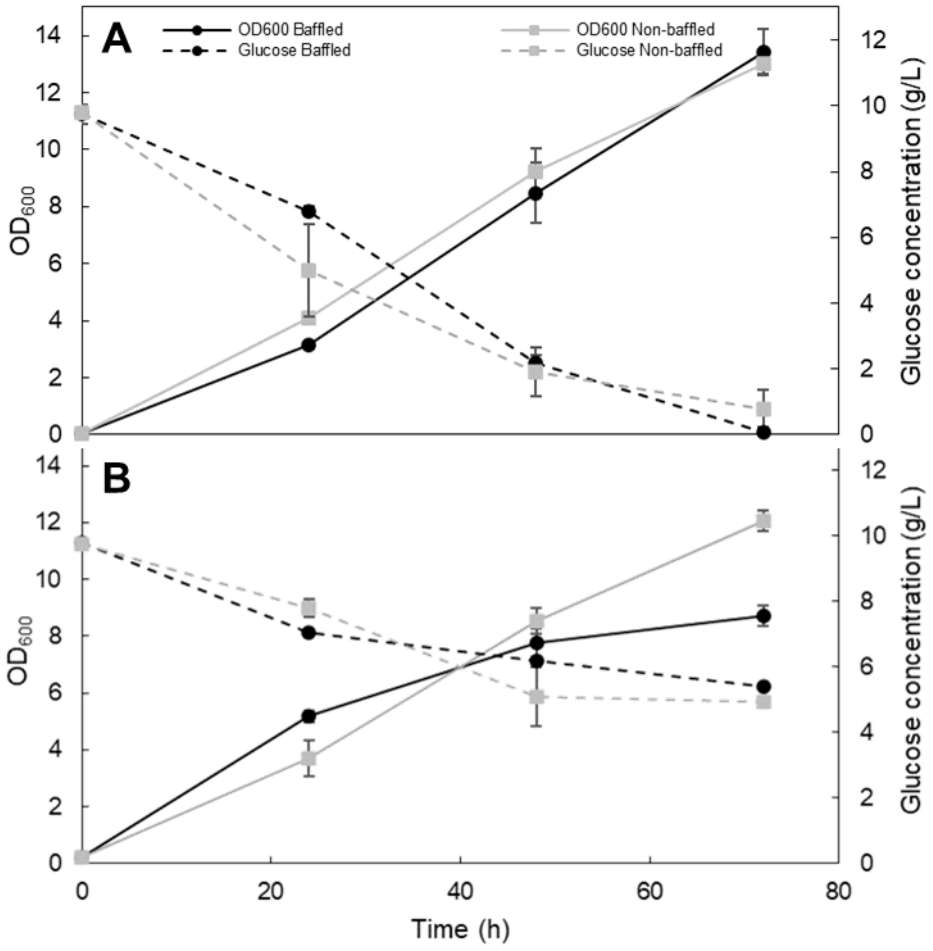

Figure 5. 9 *Cupriavidus necator (C. necator)* growth (solid line) and glucose concentration (dashed line) in baffled (black) and non-baffled (grey) flask cultures using defined media (A) and diluted cassava peel hydrolysate (B).

As depicted in Figure 5.9, the utilization of DM resulted in OD_{600} of 13, equivalent to 3.8 g/L of DCW, using both baffled and non-baffled flasks. Conversely, using CPH led to OD_{600} values of 9 and 12, equivalent to 2.6 and 3.5 g/L of DCW, in baffled and non-baffled flasks, respectively. The shift from plate to flask yielded a 5-unit OD_{600} increase when using DM, whereas CPH exhibited a reduction of 3 OD_{600} units under the same conditions. Given that the screening experiment showed a glucose concentration of 32 g/L after 72 h of culture (Figure 5.3A), indicating the utilization of only 15 g/L, a decision was made to dilute the CPH. This dilution aimed to match the glucose concentration employed in DM, which was 10 g/L. Therefore, despite only approximately half of the available glucose being consumed at flask scale (Figure 5.9), the

reduction in growth might be attributed to the dilution of other potentially unidentified nutrients present in the CPH.

The comparison between baffled and non-baffled flasks revealed no differences when using DM, while 3 OD_{600} units difference was observed using CPH. An improved growth was expected using baffed flasks because limited oxygen availability might result in the reduction of microbial metabolism [308]. However, higher growth was obtained using the non-baffled flasks. This observation indicates that the non-baffled flasks may offer sufficient aeration capabilities for *C. necator* growth. The number of reports evaluating the glucose consumption behaviour of non-native *C. necator* glucose-consuming strains is scarce. A study conducted by Sen and co-workers reported a maximum OD_{600} of 10 after 80 h of culture [12]. Our findings, in contrast, demonstrate improved growth within a shorter timeframe using the same initial glucose concentration. Despite the similarity in culture media composition between the two studies, there were slight variations in the culture set-up. In our study, 500 mL conical flasks with a 100 mL working volume were used, whereas the aforementioned study employed a working volume of 400 mL. This difference in working volume might account for the enhanced growth observed in our study, suggesting that 400 mL working volume in a 500 mL flask may not provide sufficient aeration for the culture. In another study, a DCW of 4.28 g/L was achieved [15], surpassing our OD_{600} of 13, which corresponds to a DCW of 3.8 g/L. However, their utilization of 20 g/L of glucose represents a 2-fold increase in the carbon source concentration compared to our study. Despite their higher final biomass concentration, their substrate-to-biomass yield ($Y_{x/s}$) was 0.22 $g_{DCW}/g_{glucose}$, whereas ours reached 0.38 $g_{DCW}/g_{glucose}$. Although both studies employed similar working volume and culture media composition, there were differences in agitation levels. They conducted shaking at 150 rpm, while our study employed a higher agitation rate of 250 rpm. This disparity in agitation intensity may explain the increased substrate-to-biomass yield observed in our study, as higher shaking rates facilitate the aeration and mass transfer within the culture [309]. Therefore, subtle variations in culture setup, such as working volume and agitation intensity, can significantly influence biomass yield and growth kinetics.

More limitations regarding the availability of studies are encountered when utilizing CPH as the carbon source for *C. necator* growth. In the study conducted by Poomipuk and co-workers, they used cassava starch hydrolysate (CSH) produced under enzymatic hydrolysis, resulting in a DCW of 5.97 g/L. Their approach started from 20 g/L of glucose in the CSH, obtaining a $Y_{x/s}$ of 0.318 $g_{DCW}/g_{glucose}$. In contrast, our higher $Y_{x/s}$ using CPH reached 0.740 $g_{DCW}/g_{glucose.}$ It is important to note that our $Y_{x/s}$ calculation is exclusively based on glucose consumption, whereas we acknowledge that our sample's composition included approximately 30% of different sugars which *C. necator* might also have utilised for growing. To the best of our knowledge, this is the

only study in which a waste product from the cassava industry has been used for the cultivation of *C. necator* at flask scale using *C. necator*.

5.3.3.1 Determination of polyhydroxyalkanoates production by *Cupriavidus necator* in baffled and non-baffled flasks.

Polyhydroxyalkanoates, specifically poly (3-hydroxybutyrate-co-3-hydroxyvalerate) (PHBV), were quantified through GC-MS and results are presented in Figure 5.10.

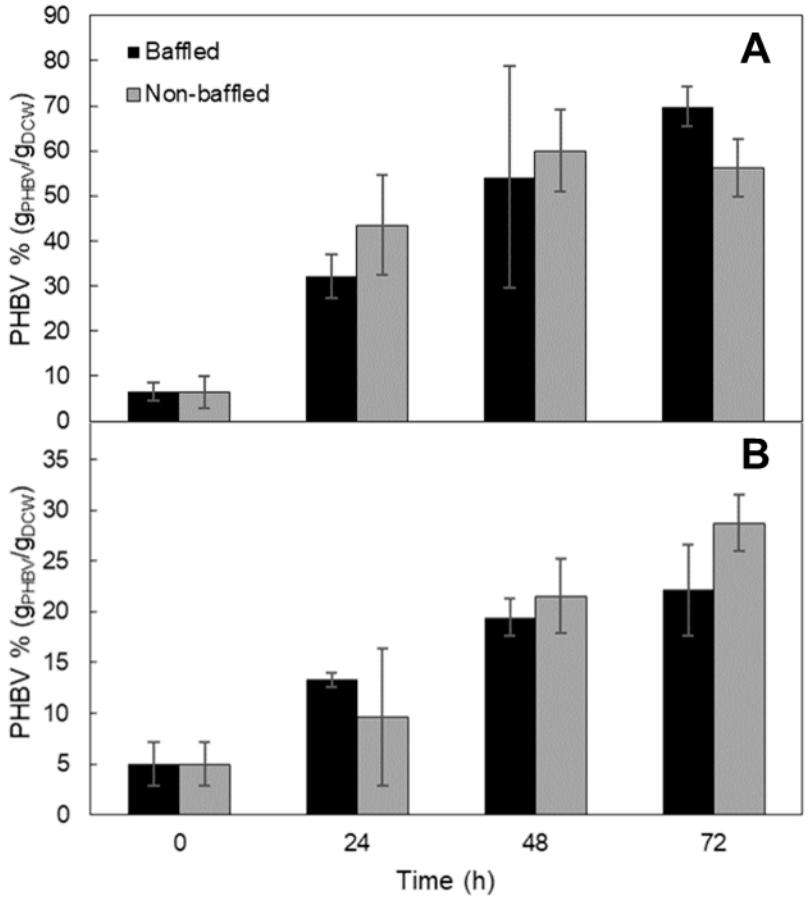

Figure 5. 10 Polyhydroxyalkanoates production by Cupriavidus necator measured using GC-MS in baffled (black) and non-baffled (grey) flask cultures using defined media (A) and cassava peel hydrolysate (B).

The use of DM yielded a final concentration of 69.8% and 56.2% of PHA (g_{PHA}/g_{DCW}), equivalent to 2.7 and 2.1 g/L, in baffled and non-baffled flasks, respectively. In contrast, the use of CPH led to PHA concentrations of 22.2% and 28.8% of PHA (g_{PHA}/g_{DCW}), equivalent to 0.58 and 1 g/L, in baffled and non-baffled flasks, respectively. Although according to the literature a higher PHA production was expected when an O_2 limitation is present in the culture, our experimental observations are contradicting. This discrepancy highlights the complexity of PHA production

dynamics and its response to varying sources and aeration conditions. However, upon joint analysis of Figure 5.9 and Figure 5.10, a potential explanation emerges: while baffled flasks enhance aeration, the lack of O_2 limitation conditions in non-baffled flasks is also noticeable. This deduction is based on the absence of any effects on both growth and PHA production that would be indicative of true O_2 limitation. Therefore, based on our findings, the use of baffled flasks would be more suitable when using DM. Conversely, non-baffled flasks appear to be the optimal choice for PHA production by *C. necator* from CPH. To the best of our knowledge, no prior research has explored these particular conditions, and the existing studies in this field lack specifications regarding the type of flasks used.

Table 5.1 summarises OD_{600} values, biomass concentration (g/L), PHA content within the bacteria (g_{PHA}/g_{DCW}), and PHA concentration (g/L) in the shake-flaks cultures presented in this section, as well as the best condition obtained in the screening experiment in plate.

Table 5. 1 Biomass concentration (OD_{600} and dry cell weight (g/L)), and polyhydroxyalkanoates concentrations (PHA% (g_{PHA}/g_{DCW}) and PHA (g/L)) in varying culture strategies.

Culture	**OD_{600}**	**Biomass concentration (g/L)**	**PHA% (g_{PHA}/g_{DCW})**	**PHA concentration (g/L)**
Plate DM	8.6	2.5	18	0.45
Plate CPH	15.8	4.6	31	1.5
Baffled flask DM	13	3.8	69.8	2.7
Non-baffled flask DM	13	3.8	56.2	2.1
Baffled flask diluted CPH	9	2.6	22.2	0.58
Non-baffled flask diluted CPH	12	3.5	28.8	1.0

PHA: polyhydroxyalkanoates; DCW: dry cell weight; DM: defined media; and CPH: cassava peel hydrolysate.

Our results using DM align with the findings of Sen and co-workers, who achieved around 60% of PHA (g_{PHA}/g_{DCW}), equivalent to 1.5 g/L [12], and Poomipuk and co-workers, who obtained a final PHA concentration of 73.9% [15], equivalent to 3 g/L using glucose as the sole carbon source. The latter study also employed CSH as the carbon source for PHA production, achieving a final concentration of 61.6% of PHA (g_{PHA}/g_{DCW}), equivalent to 2.4 g/L. This result represents a 2-fold increase compared to our results. However, it is noteworthy to consider that while they used CSH as the carbon source, they enriched the media with all the essential nutrients to support *C. necator* growth. In contrast, our study exclusively employed CPH to minimise process costs. No other study was found at flask scale that specifically addresses the biotransformation of any cassava waste type into PHA *by C. necator.* However, other microorganisms, such as *Halogeometricum borinquense*, have been used for similar objectives, achieving a final

concentration of 44.7% of PHA (g_{PHA}/g_{DCW}), equivalent to 1.6 g/L [177]. Although this result surpasses our findings, it is important to acknowledge that the authors of that study also supplemented the cassava waste with essential nutrients to support microbial growth. Furthermore, the use of a different microorganism for the bioconversion makes direct comparisons challenging. This underscores the importance and novelty of our study, wherein we demonstrate PHA conversions of up to 28.8% (g_{PHA}/g_{DCW}), equivalent to 1g/L, solely using CPH as the carbon source at flask scale. This approach contributes to cost reduction, addressing one of the major limitations in the industrial PHA production process.

5.4 Conclusions

The screening of *C. necator* growth and PHA production using the different CPH samples examined in this study demonstrated the ability of this microorganism to effectively utilise the available reducing sugars to grow and produce PHA. The H_2SO_4 concentration used in the hydrolysis reaction showed a direct influence on bacterial growth and PHA production, likely influenced by the presence of potential inhibitors generated during acid hydrolysis. However, hydrolysis time and temperature did not show any clear effect on growth and PHA production. The impact of H_2SO_4 concentration could be attributed to variations in osmotic pressure caused by the neutralisation of the CPH. In addition, the H_2SO_4 concentration used in the hydrolysis reaction also influenced the morphology of *C. necator*. Specifically, the hydrolysates obtained using 0.6 M H_2SO_4 not only yielded the highest results in terms of growth and PHA production but also resulted in the most homogenous populations regarding morphology and PHA concentration within the bacteria.

Furthermore, this study highlights the efficiency of FCM as a valuable and rapid technique to assess bacterial morphology and PHA production. The utilisation of 0.6 M H_2SO_4 in the hydrolysis process led to more than 75% of the bacteria presenting PHA. Among the various hydrolysis conditions tested, the optimal combination to enhance *C. necator* growth and PHA production was determined to be 0.6 M H_2SO_4, 58 min, and 107 ºC. Based on these findings, this specific hydrolysis condition was used to explore PHA production in *C. necator* at flask scale.

At flask scale, there were no discernible differences between the use of baffled and non-baffled flasks. This suggests that non-baffled flasks supplied adequate aeration for *C. necator* to grow, and O_2 limiting conditions, which could have enhanced PHA production, were not attained. The flask scale cultures reached similar growth to previous studies and achieved up to 28.8% (g_{PHA}/g_{DCW}) of PHA, equivalent to 1g/L, using CPH as the unique carbon source. To the best of our knowledge, this is the first study that employs CPH as the sole carbon source, without nutrient

enrichment, for the production of PHA at flask scale. Furthermore, this study represents a benchmark for future optimisation of PHA production, paving the way for further enhancements in the process. The addition of supplementary components to the media and the scaling-up of the production process will contribute to improve PHA production. These advancements will contribute to the development of more efficient and sustainable PHA production strategies.

Chapter 6. Process scale-up: polyhydroxyalkanoates production from cassava peel hydrolysate by *C. necator* in stirred-tank bioreactors

6.1 Introduction

The transition from laboratory assays to industrial implementation involves a significant shift from flask-scale experiments to bioreactor-scale production. This transition offers numerous advantages, including the continuous regulation of operating conditions, improved process reproducibility, and increased cultivation efficiency [310]. However, the scale-up process entails numerous challenges that are to be addressed. For example, parameters like agitation, aeration, and pH, play crucial roles in microbial fermentation and need to be adapted to the specific process requirements. While agitation can be regulated at flask scale, bioreactors are preferred for their enhanced and continuous control of process parameters. However, the increased shear stress that can arise during bioreactor operation can lead to a decrease in productivity. Therefore, an optimisation of process conditions at bioreactor-scale needs to be performed [311].

A diverse array of bioreactor types exists, including bubble column bioreactors, continuous stirred tank bioreactors, fluidized bed bioreactors, packed bed bioreactors, and photobioreactors. Stirred-tank bioreactors are among the preferred choices for many microbial fermentations of industrial products such as bioethanol [312] and enzymes [313], due to their ability for effective fluid mixing, oxygen transfer capabilities, and ease of maintaining homogeneous conditions [314].

Moreover, various process strategies, including batch, fed-batch, and continuous processes, can be performed based on the ultimate aim of the process. The batch process, wherein all nutrients are introduced at the beginning of the cultivation, is suitable e.g., for optimising process parameters such as agitation, aeration, temperature, and dissolved oxygen concentration. However, this approach is associated with limitations on product yields [315]. Conversely, the fed-batch strategy, entailing a continuous supply of nutrients throughout cultivation, facilitates the achievement of higher product yields [316]. Finally, continuous strategy, characterised by the constant supply of medium and the concurrent removal of culture, offers advantages such as reducing product inhibition and facilitating a deeper comprehension of the process through the establishment of a steady state [317].

The scaling up of microbial cultures poses a variety of challenges, with aeration emerging as a significant component determining process performance. As reactor capacities increase, the effective delivery of oxygen to the microbial culture becomes more complex and may lead to oxygen gradients and dissolved oxygen level restrictions. These difficulties may have a major effect on the metabolism, product production, and growth dynamics of microorganisms. This, it is crucial to understand the dynamics of aeration in bioreactors in order to maintain ideal process conditions and produce the targeted product yields [318].

As mentioned in Chapter 5, limited research has been conducted on the production of PHA from cassava waste using *C. necator* at flask scale. Furthermore, to the best of our knowledge, no studies have been published addressing larger-scale production in bioreactors. Some authors have explored different waste feedstocks for PHA production using *C. necator* at bioreactor scale. For example, 51.2 g/L of PHA were achieved using waste glycerol [319], and 11.7 g/L of PHA were achieved from sugarcane vinasse and molasses [320]. Conversely, cassava waste has been employed for PHA production using other microorganisms, however, final PHA productions are significantly lower. *Pseudomonas aeruginosa* produced 0.94 g/L of PHA from cassava starch hydrolysate [136]. This underscores a notable gap in the research involving *C. necator* for PHA production from cassava waste.

This chapter aims to scale up the shake flask cultures presented in Chapter 5 to bench-scale 1-L bioreactor experiments to enhance the production of PHA from CPH using *C. necator.* To achieve this, different parameters such as culture media, pH regulation strategies, aeration, as well as various operation (batch and fed-batch) strategies are explored.

6.2 Materials and methods

6.2.1 Feedstock and feedstock pre-treatment

Milled CP were kindly provided by Dr Richard Bayitse from the Council for Scientific and Industrial Research (CSIR) in Ghana. CP were collected from a cassava processing plant in Bawjiase, Ghana, soaked in water for 30 min to ease the removal of the brown skin and subsequently dried overnight at 60 ºC before being milled.

CP were pre-treated with 0.6 M H_2SO_4 (>95%, Fisher Scientific, Loughborough, UK, CAS 7664-93-9), for 58 min at 107 ºC. The reaction was performed in 20 mL reaction volume containing 10% (w/v) of CP. The hydrolysis was conducted in a Starfish workstation (Radleys, Essex, UK) (Figure 3.1). Hydrolysis reaction was performed in two-neck round bottom 50 mL pressure flasks (Aldrich®, Merck, Darmstadt, Germany) and stirred at 280 rpm. In order to achieve the temperature above 100 ºC, flasks were maintained pressurised. After the reaction, samples were vacuum filtered through an 11 µm cellulose filter paper (Whatman, Cytiva, Washington D.C, United States). Liquid fraction was neutralized to pH 7 using 12.5 M NaOH.

6.2.2 Microbial fermentation: culture media and cultivation strategies

Microbial fermentations were performed in 1-L bioreactors containing 700 mL as the starting working volume. A Biostat B (Sartorius Stedim UK Ltd, Surrey, UK) automated laboratory 1-L jacketed bioreactor equipped with four baffles and an agitator with two six-bladed Rushton turbines was used. Dissolved oxygen in the medium (pO_2) was measured online using an OxyFerm FDA VP 160 probe (Hamilton, Bonaduz, Switzerland). pH was measured online using an Easyferm plus PHI VP 160 Pt100 Probe (Hamilton, Bonaduz, Switzerland. Agitation was maintained between 300 and 1200 rpm.

Bioreactors were inoculated at OD_{600} of 0.2 from a seed culture. Seed culture media composition was as follows (g/L): 10 glucose; 1 $(NH_4)_2SO_4$; 1.5 KH_2PO_4; 9 Na_2HPO_4 $2H_2O$; 0.2 $MgSO_4 \cdot 7H_2O$; 9 citric acid and 1 ml/L trace element solution. The pH of the medium was adjusted to 7 and the media was sterilised by autoclaving at 121 ºC for 20 min in a V60-BASE Priorclave® autoclave (Priorclave Ltd, London, UK). Glucose and phosphates were autoclaved separately. Trace element solution was added after autoclaving and sterilised by filtration through 0.22 µm cellulose filters (Sartorius Stedim UK Ltd, Surrey, UK). Trace element solution had the following composition (g/L): 10 $FeSO_4 \cdot 7H_2O$; 2.25 $ZnSO_4 \cdot 7H_2O$; 1 $CuSO_4 \cdot 5H_2O$; 0.5 $MnSO_4 \cdot 5H_2O$; 2 $CaCl_2 \cdot 2H_2O$; 0.23 $Na_2B_4O7 \cdot 10H_2O$; 0.1 $(NH_4)_6Mo_7O_{24}$ and 10 mL/L of 35% HCl [148]. Seed

cultures were inoculated at OD_{600} 0.2 from an inoculum culture and cultivated for 8 h at 30 ºC and 250 rpm in a shaker incubator (Incu-Shake MAXI®, SciQuip Ltd, Newtown, UK). For the inoculum cultures, one loop of cryostock, stored at - 80 ºC in 15% (w/w) glycerol, was aseptically added into 10 mL of inoculum culture media containing (g/L): 10, peptone; 10, beef extract and 5, NaCl [12]. The pH of the medium was adjusted to 7 using NaOH 1 M and subsequently sterilised by autoclaving at 121 ºC for 20 min. Inoculums were cultured overnight at 30 ºC and 250 rpm in a shaker incubator.

Three batch experiments were performed. The first batch, named B20DM, was used as a benchmark culture. Defined media (DM) with synthetic glucose as the carbon source was used as the culture media. The DM composition was as follows (g/L): 20 glucose; 4.5 KH_2PO_4; 4 $(NH_4)_2SO_4$; 1.2 $MgSO_4 \cdot 7H_2O$; 1.7 citric acid and 10 mL/L trace element solution [321]. Culture media was sterilised by autoclaving. Glucose and phosphates were autoclaved separately to avoid the Maillard reaction. The trace element solution was added after autoclaving and sterilised by filtration using 0.22 µm cellulose filters (Sartorius Stedim UK Ltd, Surrey, UK). The pH was maintained at 7 through the addition of 2 M ammonia and 1 M HCl. Ammonia was selected as the pH regulator due to its dual role as an alkali pH regulator and a nitrogen source, to avoid nitrogen limitation in the culture. The pO_2 was maintained above 20% using a cascade control for the aeration using compressed air at 1 vvm. The second batch, named B50CPH, exclusively comprised the neutralised CPH containing 75 g/L of TRS, with 50 g/L accounting for glucose content. CPH was sterilised by filtration using 0.22 µm cellulose filters (Sartorius Stedim UK Ltd, Surrey, UK). The initial pH was 7 and no pH control was performed. The pO_2 was maintained above 20% using a cascade control for the aeration using compressed air at 1 vvm. In the third batch, named B20CPH, the CPH was diluted to a glucose concentration of 20 g/L, aligning with the glucose concentration in the benchmark batch. B20CPH culture media comprised 30 g/L of TRS, of which 20 g/L were glucose. The pH was maintained at 7.00 through the addition of 2 M NaOH and 1 M HCl. Yeast extract at a concentration of 10% (w/v) was added to the culture after 21 h, when the microbial growth rate decreased. pO_2 was maintained above 20% using a cascade control for the aeration using compressed air at 1 vvm.

Three fed-batch experiments were performed. For the first fed-batch, named FBDM20PO, DM was used throughout the batch phase until complete glucose consumption, when a feeding containing CPH was added. CPH feeding contained 75 g/L of TRS, with 50 g/L being glucose. The feeding addition rate was 0.09 mL/min. The pH was maintained at 7 through the addition of 2 M NaOH and 1 M HCl. The pO_2 was maintained between 0 and 20% via intermittent air pulses. The second fed-batch, named FBDM3PO, replicated the parameters of the prior fed-batch, FBDM20PO, with the exception of pO_2 regulation. In FBDM3PO, the pO_2 was maintained between 0 and 3% using a cascade control for the aeration using compressed air at 1 vvm. The

final fed-batch, named FB20CPH, replicated the previous experiment, FBDM3PO, with the exception of the culture media during the batch phase. In this case, CPH diluted to 20 g/L of glucose was used. Table 6.1 summarises all the varying parameters employed among the cultures.

Table 6. 1 Fermentation parameters of the batch and fed-batch cultures performed

Fermentation	Batch culture media	Feeding	pH regulator	pO_2 (%)	pO_2 control
B20DM	DM	n.a	2 M Ammonia 1 M HCl	>20	Cascade
B50CPH	CPH	n.a	n.a	>20	Cascade
B20CPH	Diluted CPH	Yeast extract	2 M NaOH 1 M HCl	>20	Cascade
FBDM20PO	DM	CPH	2 M NaOH 1 M HCl	0-20	Air pulses
FBDM3PO	DM	CPH	2 M NaOH 1 M HCl	0-3	Cascade
FB20DM	Diluted CPH	CPH	2 M NaOH 1 M HCl	0-3	Cascade

Defined media (DM); Cassava peel hydrolysate (CPH)

Representative pictures of the bioreactor containing different culture media are presented in Figure 6.1.

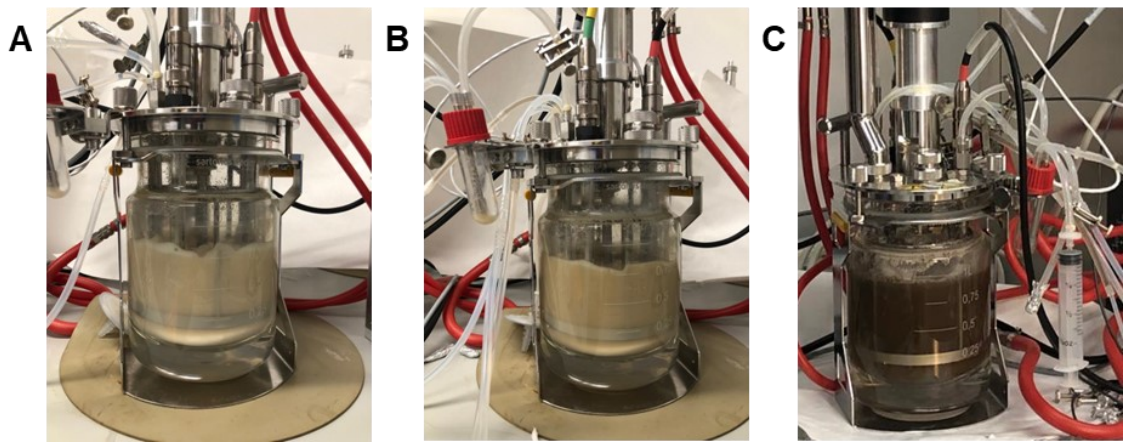

Figure 6. 1 Bioreactors containing defined media (DM) (A); DM and cassava peel hydrolysate (CPH) (B); and CPH (C).

6.2.3 Microbial growth and polyhydroxyalkanoates concentration

Microbial growth was analysed by optical density at a wavelength of 600 nm using a Jenway 6310 Spectrophotometer (Keison Products, Chelmsford, UK) in all experiments.

The Pyr-546-staining protocol developed in *Chapter 5* was employed for PHA determination in FCM. Briefly, bacterial samples were resuspended in phosphate-buffered saline (PBS) and stained with Pyr-546 (Exciton, Lockbourne, USA). Pyr-546 stocks were stored at 4 ºC in 20/80% (v/v, EtOH/DMSO) and added to the bacterial solution at a concentration of 5 µg/mL. Stained samples were incubated for 1 min and analysed with a flow cytometer BD AccuriTM C6 Plus Flow Cytometer (Becton, Dickinson and Company, Oxford, UK) using a 488 nm solid-state laser and fluorescence was detected using the 533/30 BP filter (FL1-A).

PHA quantification was performed by acid propanolysis followed by GC-MS analysis, adapted from elsewhere [301]. The bacterial pellet was freeze-dried in a Lablyo benchtop freeze dryer (Frozen in Time Ltd, York, UK) at -50 °C and 1-5 Pa, overnight. Propanolysis was performed using 5 mg of lyophilised bacteria in 1 mL of chloroform and 1 mL of 1-propanol containing 15% of 37% (v/v) HCl in an 8 mL glass tube (Duran®, Mainz, Germany). 50 µL of 1 mg/mL solution of benzoic acid in 1-propanol was added as the internal standard. The mixtures were incubated for 2 h at 100 °C in an oven (Memmert, Schwabach, Germany). After cooling to room temperature, 2 mL of distilled water was added followed by vortexing for 30 s, and left standing for 5 min to allow for phase separation. The upper aqueous phase was discarded, and the washing step was repeated to eliminate impurities. 1 mL of the organic phase containing derivatised PHA was filtered with 0.2 µm nylon filters (Fisher Scientific, Loughborough, UK) and transferred to a GC-MS vial. The standard sample of poly (3-hydroxybutyric acid-*co*-3-hydroxyvaleric acid) (PHBV, 80181-31-3, Merck, Darmstadt, Germany) was used to prepare the standard calibration curves for PHB and PHV. These calibration curves and representative GC-MS chromatograms of a standard sample and a culture sample are included in Appendix 5.2. Analysis was performed using a Single quadrupole gas chromatograph-mass spectrometer GCMS-QP2010 (Shimazu, Milton Keynes, UK). One µL was injected into an analyser with a 30 m SH-Rtx-5MS column (Shimazu, Milton Keynes, UK) at 280°C. The flow rate was set at 1.25 mL/min and the ionization detector at 240°C. Column temperature was programmed from 40 to 250°C at a rate of 5°C/min. The total measurement time for each sample was 40 min. PHBV was identified using the internal libraries NIST17s and NIST17-1 available in GC-MS Postrun Analysis Software (Shimazu, Milton Keynes, UK). PHBV amount of each sample was normalised by the weight of the lyophilised bacteria and expressed as a percentage of polymer weight/cell dry weight.

6.2.4 Process productivity parameters determination

Specific growth rate (μ), biomass yield coefficient ($Y_{x/s}$), product yield coefficient ($Y_{p/s}$), and volumetric productivity of PHA (P_{PHA}) were calculated for the six fermentations presented in this chapter.

μ is defined by equation 6.1 (Eq 6.1)

$$\mu = d(\ln(X))/dt$$

Where X is the biomass concentration and t is time.

The $Y_{x/s}$ of the exponential growth phase of the cultures is defined by equation 6.2 (Eq. 6.2). The slope of its integrated form, as shown in equation 6.3, represents the $Y_{x/s}$ value.

$$Y_{x/s}\,(g_{biomass}/g_{substrate}) = -\,(d_x/d_s) \quad \text{(Eq. 6.2)}$$

$$Y_{x/s}\,(g_{biomass}/g_{substrate}) = (X - X_o) / (S_o - S) \quad \text{(Eq. 6.3)}$$

Where X is the biomass concentration; X_o is the initial biomass concentration; S is the substrate concentration; and S_o is the initial substrate concentration.

The $Y_{p/s}$ of the stationary growth phase of the cultures is defined by equation 6.4 (Eq. 6.4). The slope of its integrated form, as shown in equation 6.5, represents the $Y_{p/s}$ value.

$$Y_{p/s}\,(g_{PHA}/g_{substrate}) = -\,(d_p/d_s) \quad \text{(Eq. 6.4)}$$

$$Y_{p/s}(g_{PHA}/g_{substrate}) = (P - P_o) / (S_o - S) \quad \text{(Eq. 6.5)}$$

Where P is the PHA concentration; P_o is the initial PHA concentration; S is the substrate concentration; and S_o is the initial substrate concentration.

The volumetric productivity of PHA (P_{PHA}), is given by the ratio between the amount of PHA produced in g/L and the fermentation time. Therefore, it is calculated by establishing a correlation between the PHA concentration versus time.

Linear regression analyses were performed using Microsoft Office Excel 2021.

6.2.5 Optical microscopy images

Bacteria stained with Pyr-546 were observed and imaged using a Zeiss Axiolab microscope (Carl Zeiss Ltd., Cambridge, UK) fitted with a Zeiss AxioCam ICm1 camera, and the images were processed in auto-exposure mode with the aid of Zeiss ZEN Lite 2012 software. Samples were

excited with a Zeiss VHW 50f-2b ultraviolet light source and a 520 LP filter was employed for detection of fluorescence.

6.3.6 Transmission electron microscopy (TEM)

Bacterial samples were deposited onto lacey carbon-supported 300-mesh copper grids coated with graphene oxide (GOLC300Cu50, EM Resolutions, Sheffield, UK) and subsequently subjected to vacuum drying prior to analysis. Transmission Electron Microscopy (TEM) images were acquired using a JEM-2100F microscope (JEOL, Herts, UK) operating at 200 kV, which was equipped with a Gatan Orius CCD camera (Pleasanton, USA).

6.2.7 Analysis of total reducing sugars (TRS) and glucose concentration

Total reducing sugars (TRS) concentration was determined using the DNS (Di-nitrosalicylic acid) test, which was adapted from Miller (1959) [259]. The reagent composition was as follows (% (w/v)): 0.63 DNS; 0.5 NaOH; 18.2 $KNaC_4H_4O_6 \cdot 4\ H_2O$; 0.5 $Na_2S_2O_5$ and 0.5 % (v/v) C_6H_6O. 0.5 mL of sample were mixed with 0.5 mL of DNS reagent. Samples were placed in boiling water for 5 min and cooled to room temperature. The absorbance was measured at 575 nm using a Jenway 6310 Spectrophotometer (Keison Products, Chelmsford, UK). A calibration curve (Appendix 4.1) was prepared using pure synthetic D-(+)-glucose (Fisher Scientific, Loughborough, UK, CAS 2280-44-6), and absorbance values were interpolated to calculate sample concentrations (Appendix A2).

Glucose concentration was measured using the YSI model 2500 biochemical analyzer (Xylem Inc., Nottingham, UK). Samples were previously filtered through a PVDF 0.45 μm filter (Whatman, Cytiva, Washington D.C, United States).

6.2.8 Gases analysis

Oxygen and carbon dioxide concentrations (%) in the exhaust gas were measured by BlueInOne Ferm Gas analysers and monitored through the BlueVis software (BlueSens gas sensor GmbH, Herten, Germany). Gas concentrations were used to calculate the carbon dioxide evolution rate (CER) (Eq.6.5) and the oxygen uptake rate (OUR) (Eq. 6.6). These parameters were then used to calculate the respiratory quotient (RQ) (Eq. 6.7).

$$CER\ \left(\frac{mol}{Lh}\right) = \frac{F_{gas}\ x\ P}{V_f\ x\ R\ x\ T} x\ \left(\frac{1\text{-}O_2\%\ in\text{-}CO_2\%in}{1\text{-}O_2\%out\text{-}CO_2\%out}\ x\ CO_2\%out\text{-}CO_2\%in\right) \text{(Eq. 6.5)}$$

$$OUR\ \left(\frac{mol}{Lh}\right) = \frac{F_{gas}\ x\ P}{V_f\ x\ R\ x\ T} x\ \left(O_2\%in\ -\ \frac{1\text{-}O_2\%\ in\text{-}CO_2\%in}{1\text{-}O_2\%out\text{-}CO_2\%out}\ x\ O_2\%out\right) \text{(Eq. 6.6)}$$

$$RQ = \frac{CER}{OUR} \text{(Eq. 6.7)}$$

Where F_{gas} is the inlet gas flow rate (L/h); P is the normal pressure (bar); V_f is the working volume in the bioreactor (L); R is the gasses constant (bar L/K mol); T is temperature (K); O_2% in is the oxygen composition in the inlet gas (%); CO_2%in is the carbon dioxide composition in the inlet gas (%); O_2%out is the oxygen composition in the outlet gas (%); and CO_2%out is the carbon dioxide composition in the outlet gas [322].

6.3 Results and discussion

This chapter focuses on the examination of the scalability of the process to bench-scale bioreactor after conducting an initial screening to evaluate the potential of *C. necator* to grow and produce PHA from CPH, which was presented in *Chapter 5*, at both plate and flask scales. Various parameters, including the cultivation strategy, aeration, CPH concentration, and pH regulation, are assessed in the following sections to evaluate *C. necator* growth, PHA biosynthesis, and cellular physiology.

6.3.1 Assessment of *Cupriavidus necator* growth in bioreactor

Three batch bioreactor cultures were performed, and the results are shown in Figure 6.2. Figure 6.2A shows the results of the benchmark culture, B20DM, in which synthetic glucose at 20 g/L was used as the carbon source without any nutrient limitation. Figure 6.2B presents the results of the B50CPH batch, where CPH containing an initial concentration of 50 g/L of glucose and 75 g/L of TRS was used as the sole carbon source. This culture operated without any additional nutrients throughout fermentation, including pH regulation. Finally, figure 6.2C shows the B20CPH batch, wherein CPH was diluted to a concentration of 20 g/L of glucose and 30 g/L of TRS. Nutrient limitations might have occurred prior to the addition of yeast extract. As can be observed, the three batches reached a maximum OD_{600} of 12, equivalent to a microbial concentration of 3.5 g/L of DCW. While the benchmark culture exhibited complete glucose consumption by the end of the fermentation, residual glucose and TRS concentrations of 36.1 of 63.8 were detected in B50CPH. In the case of B20CPH, there were 7.7 g/L of glucose and 13.9 g/L of TRS remaining in the culture. These results indicate that 13.9 and 12.3 g/L of glucose were consumed in B50CPH and B20CPH, respectively. The cessation of growth before the complete

consumption of sugars might suggest that *C. necator* utilised all the essential nutrients available in the media, or potential inhibitor byproducts were accumulated in the culture. Examples of these inhibitors include organic acid (e.g, acetic acid, formic acid), furan derivatives (e.g., furfural, 5-hydroxymetylfurfural), phenolic compounds (e.g., sytingaldehyde, vanillin), ammonia, amines, aldehydes (e.g., formaldehyde), and ketones (e.g., acetone). These compounds can be generated during biomass pretreatment or microbial metabolism and have been shown to inhibit microbial growth and interfere with the fermentation process [323].

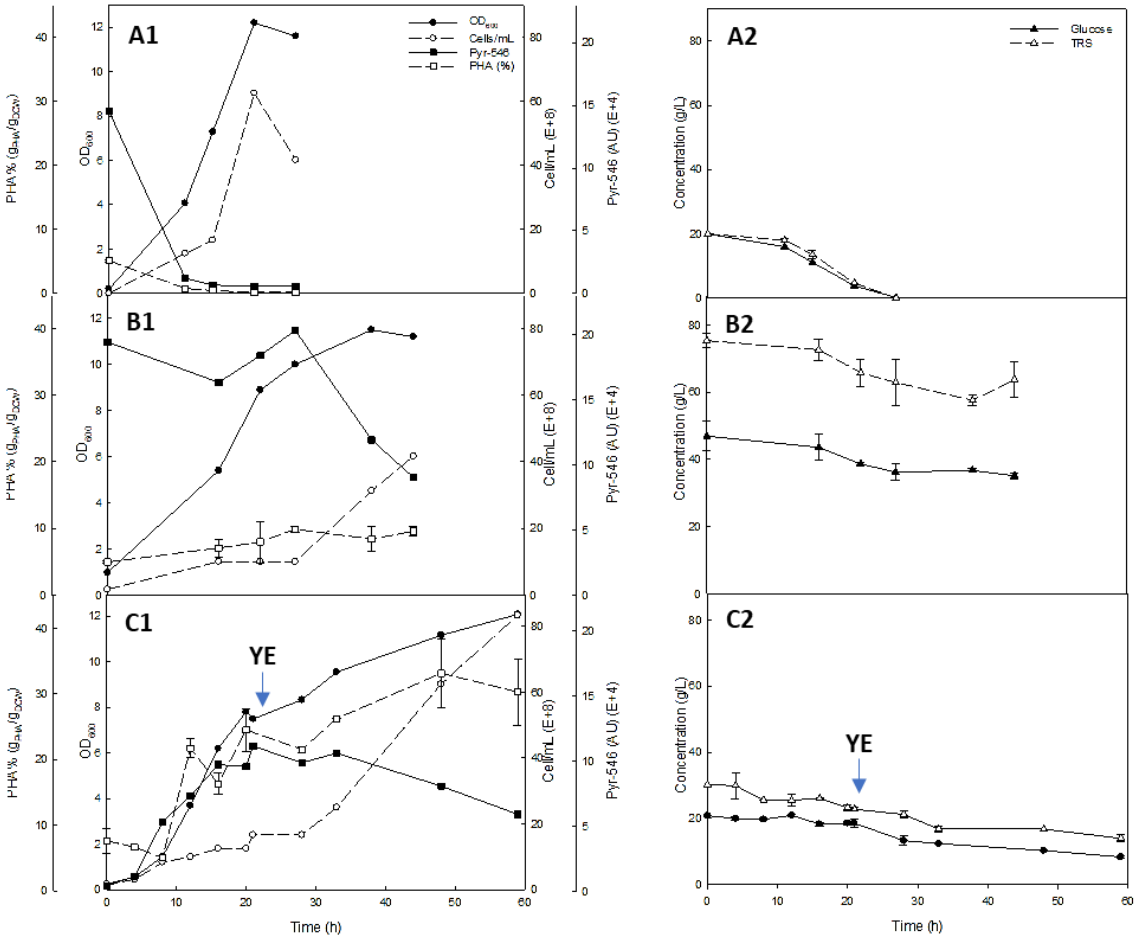

Figure 6. 2 Comparison of the growth and PHA (polyhydroxyalkanoates) production by *C. necator* *(*Cupriavidus necator) and sugars concentration in batch experiments using different culture media: (A) B20DM (Defined media, 20 g/L of glucose); (B) B50CPH (cassava peels hydrolysate, 50 g/L of total sugars); and (C) B20CPH (cassava peels hydrolysate, 20 g/L of total sugars). (—●—) OD_{600}; (--○--) cell/mL; (—■—) fluorescence Pyr-546 (pyrromethene 546)-stained cells; (--□--) PHA (polyhydroxyalkanoates) %; (—▲—) glucose (g/L) and (--Δ--) TRS (total reducing sugars) (g/L). AU: arbitrary units; YE: yeast extract (n=3).

After achieving a maximum growth of OD_{600} 12, equivalent to 3.5 g/L, using both DM and CPH in batch cultures, and with the aim of increasing the productivity of the process [324], three fed-batch cultures were conducted. The results of these fed-batch cultures are presented in Figure 6.3.

Figure 6.3A shows the results of FBDM20PO, where DM was used during the batch phase, and CPH was added as the feeding when the growth rate began to decline. The culture achieved an OD_{600} of around 30, equivalent to 8.8 g/L, at the end of the batch phase. Notably, the growth in this culture surpassed that observed in the batch experiment performed using DM (Figure 6.1A), where an OD_{600} of 12 was achieved. However, some differences between the two experiments are noteworthy. In the previous batch, ammonia was used to regulate pH and ensure nitrogen surplus, whereas in this case NaOH was selected as the pH regulator to limit nitrogen availability. Additionally, the pO_2 concentration in this culture was maintained between 0 and 20% while in the previous batch, pO_2 was consistently over 20%.

After the addition of CPH in FBDM20PO, the OD_{600} reached 39.5, equivalent to 11.6 g/L of DCW. However, it is important to note that the growth rate markedly decelerated during this phase, reaching 0.012 h^{-1}, in contrast to the batch phase, which exhibited a growth rate of 0.14 h^{-1}. While the batch phase in FBDM20PO extended to 46 h, compared to the 27 h duration observed in B20DM, it is noteworthy that the restriction of oxygen and nitrogen availability resulted in more than a 3-fold increase in microbial growth. Hence, a decision was made to undertake another fed-batch culture, further constraining oxygen availability to 3%.

In this fed-batch, FBDM3PO (Figure 6.3B), the batch phase extended for 38 h, achieving an OD_{600} of 23.9, equivalent to 7 g/L od DCW. Although the growth in FBDM3PO was lower than that obtained with higher oxygen availability (FBDM20PO), the addition of the feeding resulted in an OD_{600} of 48.7, equivalent to 14.3 g/L of DCW, after 95 h of culture. Specifically, during the batch phase, a growth rate of 0.16 h^{-1} was observed, whereas a growth rate of 0.015 h^{-1} was attained post-feeding. Remarkably, this alteration led to a 1.2-fold enhancement in growth, underscoring the impact of reduced oxygen concentration.

A final fed-batch, FB20CPH, was conducted and is presented in Figure 6.3C. For this experiment, diluted CPH was utilised during the batch phase, and CPH was incorporated as the feeding. During the batch phase, which extended for 29 h, an OD_{600} of 15.2, equivalent to 4.5 g/L of DCW was achieved. This fermentation can be compared to the B20CPH fermentation (Figure 6.2C), where an OD_{600} of 7.8 was accomplished within 20 h, before the addition of yeast extract, representing a growth rate of 0.23 h^{-1}. Although this growth rate was higher than a growth rate of 0.15 h^{-1} obtained during the batch phase of FB20CPH, it led to a lower final microbial growth. Consequently, it can be concluded that the reduction of the oxygen concentration in the media enhanced microbial growth using both DM and CPH.

While in FBDM20PO and FBDM3PO nearly all the glucose was consumed by the end of the batch phase (Figure 6.3 A2 and B2), in FB20CPH, 15.6 g/L and 21 g/L of glucose and TRS, respectively, remained in the culture, meaning that only 4.7 g/L of glucose were consumed. In

this case, the addition of the CPH feeding did not improve microbial growth, indicating that essential nutrients for microbial growth were depleted after 41 h of culture, or byproduct inhibitors were accumulated in the culture. Therefore, the addition of CPH did not enhance growth in FB20CPH.

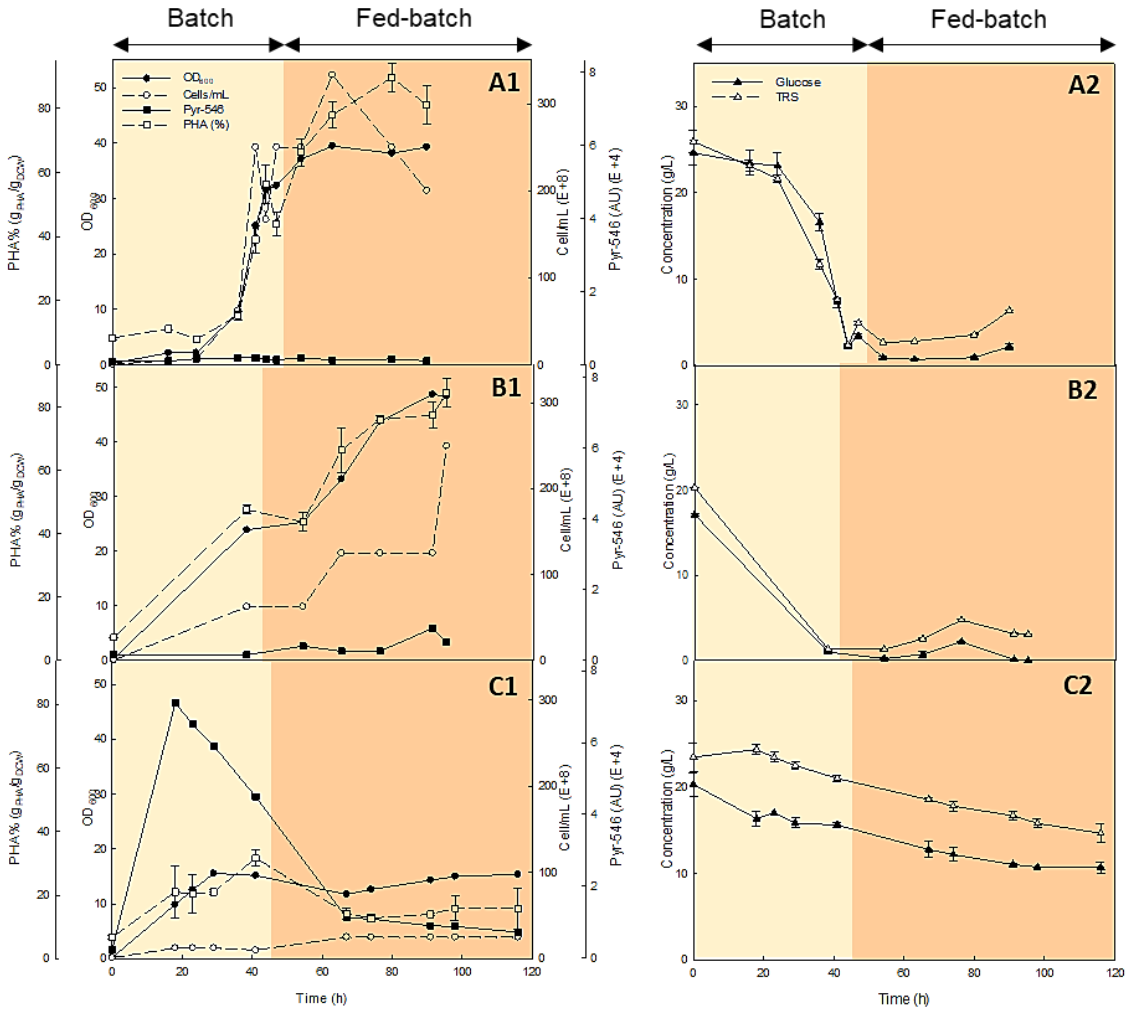

Figure 6. 3 Comparison of the growth and PHA (polyhydroxyalkanoates) production by *C. necator (*Cupriavidus necator) and sugars concentration in fed-batch experiments using different culture media and dissolved oxygen concentration (pO_2): (A) FBDM20PO (Batch with defined media (DM), 20 g/L of glucose; fed-batch with cassava peel hydrolysate (CPH); pO_2: 0-20%); (B) FBDM3PO (Batch with DM, 20 g/L of glucose; fed-batch with CPH; pO_2: 3%); and (C) FB20CPH (Batch with diluted CPH, 20 g/L of glucose; fed-batch with CPH; pO_2: 3%). (—●—) OD_{600}; (--○--) cell/mL; (—■—) fluorescence from the fluorophore Pyr-546 (pyromethene 546); (--□--) PHA (polyhydroxyalkanoates) %; (—▲—) glucose (g/L) and (--Δ--) TRS (total reducing sugars) (g/L). AU: arbitrary units; YE: yeast extract. (n=3).

Although the batch cultures in this study achieved comparable growth to the flask cultures detailed in *Chapter 5.3.3.1 Determination of Cupriavidus necator growth in baffled and non-baffled flasks*, the improvement of the aeration and the implementation of feeding strategies in the fed-batch experiments yielded a 4-fold increase in *C. necator* growth. This enhancement

resulted in an OD_{600} of 48.5, equivalent to 14.3 g/L of DCW, specifically when DM was employed in the batch phase and, CPH feeding containing 43 g/L of glucose was used.

Figure 6.4 illustrates, as an example, the time profile of the process parameters for the FBDM3PO fermentation.

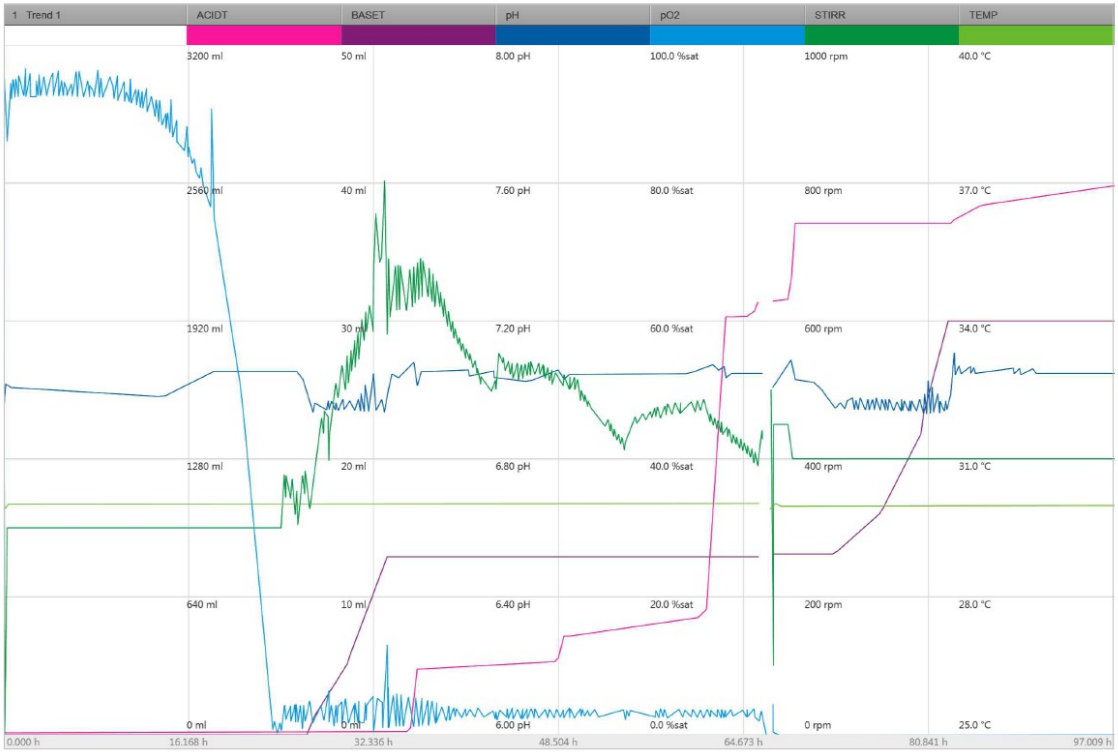

Figure 6. 4 Evolution of the fermentation parameters in FBDM3PO fermentation. Acid (pink); base (purple); pH (dark blue); pO_2 (light blue); stirring (dark green); and temperature (light green).

6.3.2 Assessment of *Cupriavidus necator* polyhydroxyalkanoates production in bioreactor

6.3.2.1 Polyhydroxyalkanoates quantification using GC-MS

The quantification of PHA using GC-MS in the batch and fed-batch cultures is presented in Figure 6.2 and 6.3, respectively.

Figure 6.2 reveals that, as previously reported in the literature, nutrient limitation in the culture enhances PHA production [158]. Notably, B20DM fermentation resulted in negligible PHA. This benchmark experiment aligns with prior findings in the literature, where the utilisation of glucose under non-limiting conditions yielded only around 1% of PHA [325]. In contrast, B50CPH achieved a PHA production of 10% (g_{PHA}/g_{DCW}), equivalent to 0.3 g/L of PHA, under conditions

that potentially restricted nutrients availability, as no additional nutrients were supplemented to the culture (Figure 6.2 B1). Figure 6.2 C1 shows the results of the B20CPH fermentation, wherein the PHA concentration increased up to 28.6% (g_{PHA}/g_{DCW}) after 48 h of culture, corresponding to 1 g/L of PHA. In this culture, yeast extract was added to the media after 21 h, when a cease in microbial growth was detected. However, no previous nutrient addition was performed. Before the addition of yeast extract, around 20% (g_{PHA}/g_{DCW}) of PHA was accumulated within the bacteria, confirming that nutrient limitation promotes PHA production. Following the yeast extract addition, a slight decrease of the PHA production was observed, coinciding with an increase in microbial growth. However, 12 h after the addition of yeast extract, the PHA concentration slightly increased. Nevertheless, the PHA production rate was slower than during the initial stages of the culture. While the addition of nutrients did not entirely halt PHA production, it was confirmed that the production rate decreased in comparison to the nutrient-limitation phase. B20CPH fermentation shows similar results as those obtained in *Chapter 5.3.3.2 Determination of polyhydroxyalkanoates production by Cupriavidus necator in baffled and non-baffled flasks*, where a PHA concentration of 28.8% (g_{PHA}/g_{DCW}), equivalent to 1 g/L of PHA was achieved after 72 h of culture.

On the other hand, FBDM20PO (Figure 6.3 A1) achieved a PHA concentration of 53.6% (g_{PHA}/g_{DCW}), at the end of the batch phase, using DM. This result is similar to the result of the non-baffled flask culture using DM presented in *Chapter 5.3.3.2 Determination of polyhydroxyalkanoates production by Cupriavidus necator in baffled and non-baffled flasks.* However, this concentration was increased up to 86.3%, equivalent to 9.7 g/L, at 80 h of culture, following the addition of the CPH feeding. The reduction of pO_2 performed in FBDM3PO led to a slightly lower concentration of PHA within bacteria of 84.7% (g_{PHA}/g_{DCW}) (Figure 6.3 B1). However, this reduction in pO_2 also resulted in an enhanced microbial growth, hence yielding a PHA concentration of 12.1 g/L within the culture after 95 h.

In the case of FB20CPH (Figure 6.3 C1), a maximum PHA concentration of 31.7% (g_{PHA}/g_{DCW}), equivalent to 1.5 g/L of PHA, was obtained at the end of the batch phase. This result is in agreement with the PHA production observed in the B20CPH batch (Figure 6.2 C1) and flask-scale cultures presented in *Chapter 5*. However, the addition of a CPH feeding did not improve the production. As previously discussed, the addition of CPH did not promote microbial growth, suggesting that a significant nutrient deficit emerged within the culture, or high inhibitors concentration was accumulated. These inhibitors could originate from the CPH itself, such as lignin-derived compounds or byproducts of the acid hydrolysis process, or they could be formed by the bacteria during the fermentation process, including organic acid or metabolic products [326]. Further analysis is warranted to elucidate the specific nature and origin of these inhibitors,

as well as their impact on PHA production dynamics. These potential limitations might have hampered both bacterial growth and PHA production in FB20CPH.

Table 6.2 provides a concise overview of the OD_{600}, PHA concentration inside bacteria (%), and PHA concentration in the culture (g/L) for all the fermentations presented in this chapter.

Table 6. 2 Growth and polyhydroxyalkanoates (PHA) production by *Cupriavidus necator* produced under different fermentation strategies.

Fermentation	OD_{600}	PHA % (g_{PHA}/g_{DCW})	PHA (g/L)
B20DM	12.2	0.5	0.01
B50CPH	12.1	9.6	0.30
B20CPH	12.1	32.9	0.90
FBDM20PO	39.5	89.6	9.7
FBDM3PO	48.7	84.7	12.10
FB20DM	15.6	31.7	1.36

In this study, the maximum PHA concentration reached among the cultures was 12.1 g/L of PHA, equivalent to 84.7% (g_{PHA}/g_{DCW}). This peak PHA production was achieved through a sequential approach, performing a batch phase with DM followed by the introduction of a feeding phase comprising CPH containing a glucose concentration of 43 g/L. Furthermore, the impact of oxygen restriction on bacterial metabolism and its consequential enhancement of PHA production underscore the importance of understanding the metabolic responses of *C. necator* to varying oxygen concentrations. This observation aligns with findings from previous studies where enhanced PHA production under oxygen limitation conditions has been demonstrated, indicating the potential for further optimisation of PHA production processes through oxygen control strategies [327].

In the metabolic dynamics of *C. necator,* oxygen assumes a fundamental role, intricately modulating a sophisticated interplay of biochemical pathways. This metabolism is highly dependent on oxygen availability, as oxygen-limiting circumstances encourage the synthesis of PHA [327].

For the production of ATP and the upkeep of cells, *C. necator* depends on oxygen as the terminal electron acceptor during respiratory activities in aerobic settings [328]. On the other hand, when oxygen is not present, bacterial metabolic pathway shift to produce PHA, since PHA is a better carbon and energy storage than other molecules. The suppression of aerobic respiratory pathways and the activation of genes encoding essential enzymes required for PHA production pathways are examples of this metabolic adaptation [327].

Consequently, oxygen limitation not only prompts metabolic reprogramming but also enhances carbon flux towards PHA accumulation. This adaptive response highlights the versatile metabolic capabilities of *C. necator*, underscoring its potential for efficient PHA production under varying conditions [329].

A thorough comprehension of the metabolic modifications manifested by *C. necator* in oxygen-limited environments will provide significant understanding of the control of PHA production pathways. This understanding will facilitate the development of customised strategies aimed at enhancing PHA production in various biotechnological applications.

Samples from this experiment were analysed using TEM microscopy and Figure 6.5 shows the accumulation of PHA granules in *C. necator* cells using TEM and fluorescent microscopy.

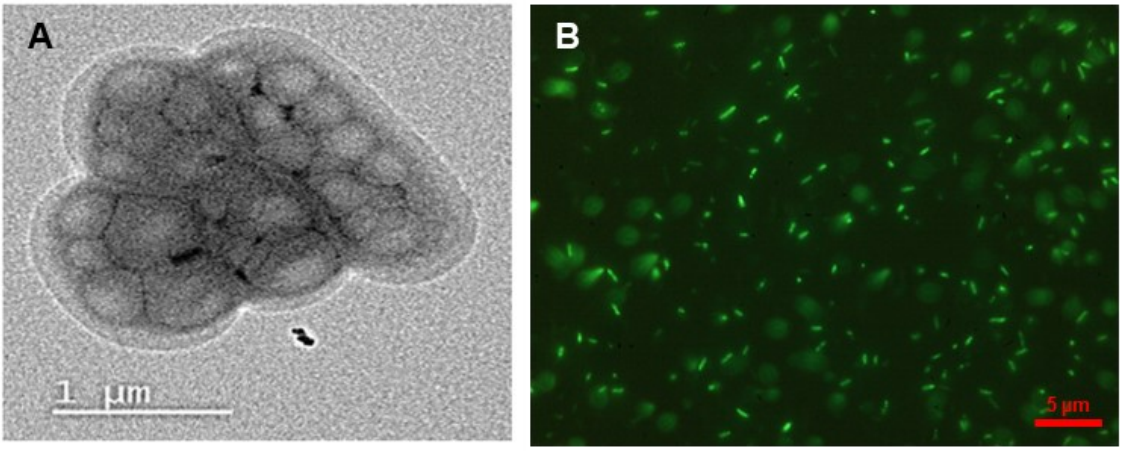

Figure 6. 5 *Cupravidus necator* cells containing PHA granules produced from cassava peel hydrolysate: (A) TEM image and (B) Fluorescent microscopy image of Pyr-546-stained cells.

While specific bioreactor-scale research on PHA production from cassava waste using *C. necator* is negligible, our findings can be compared with studies utilising various waste sources and microorganisms. Concentrations of 14.5 g/L of PHA (95.5 % (g_{PHA}/g_{DCW})) were obtained using waste rapeseed oil and cheesy whey with *C. necator* [22]. Additionally, the use of sugarcane vinasse and molasses yielded 11.7 g/L of PHA (56% (g_{PHA}/g_{DCW})) [320]. The result of these studies closely aligns with our findings.

When cassava waste was used as a substrate, PHA concentrations of 2 g/L of PHA (74%) [178] and 0.035 g/L of PHA (58% (g_{PHA}/g_{DCW})) [136] were reported using *P. oleovorans* and *P. aeruginosa*, respectively. Although using a different microorganism, our results yielded a 6-fold increase from previous results using cassava waste as feedstock for the production of PHA.

To the best of our knowledge, Cavalheiro and co-workers achieved the highest reported PHA production to date at bioreactor scale using waste sources with *C. necator*. They accomplished 51.2 g/L of PHA (95% (g_{PHA}/g_{DCW})) of PHA from waste glycerol by *C. necator* [319]. While PHA content per bacteria was lower in their study, the final concentration of PHA in the culture was 4 times higher than the result obtained in our study. However, it is important to acknowledge that a key factor contributing to this variation might be the substantial difference in the feedstock used between the two studies.

Additionally, 100 g/L of PHA (79.5% (g_{PHA}/g_{DCW})) was achieved from crude corn extract liquid using *H. bluephagenesis* [330], and 10.5 g/L of PHA (88.7% (g_{PHA}/g_{DCW})) was obtained from palm oil effluent using *B. licheniformis* [331]. However, due to the utilisation of different feedstocks and microorganisms, drawing comparisons between these results can be challenging.

6.3.2.2 Polyhydroxyalkanoates assessment using flow cytometry

FCM was employed to assess Pyr-546 fluorescence, enabling the relative detection of PHA concentration inside bacteria. The fluorescence values are presented in Figures 6.2 and 6.3. Additionally, Figure 6.6 depicts the Pyr-546 fluorescence histograms for the highest fluorescence value observed in each fermentation experiment.

Figures 6.2 and 6.3 depict a broad range of fluorescence values observed across the fermentations, reflecting variations in PHA accumulation within the bacterial populations, reaffirming our earlier hypothesis regarding the influence of culture media and cultivation conditions on the fluorescence values. Furthermore, in Figure 6.6, the histograms display distinct peaks, each representing different levels of PHA accumulation within the bacteria.

A sharp, singular peak, as observed in Figure 6.6A for the B20DM culture, indicates uniform PHA accumulation among all bacteria within the culture. Although 99.5% of the bacteria in this culture were stained, the fluorescence values were residual, a finding that is consistent with the GC-MS results, which revealed PHA content below 1%.

On the other hand, Figure 6.6B, C, and F, which corresponds to the cultures employing CPH in both the batch and feeding phases, exhibit multiple sharp peaks, suggesting distinct subpopulations of bacteria with varying PHA concentration. Although in these cases most of the bacteria (94%) were stained, the PHA content per bacteria was around 30%.

Furthermore, Figure 6.6D and E, representing fermentation experiments using DM in the batch phase and CPH in the feeding, display broader peaks, indicating heterogenous PHA accumulation

among the bacterial population. This variability suggests that different groups of bacteria within the culture harbour varying concentrations of PHA. This variability might be attributed to the addition of CPH during the feeding phase. Although these cultures resulted in the highest PHA content per bacterium, Figure 6.6 illustrates that less than 80% of the cells were stained.

In summary, the fluorescence peaks in the histograms provide insights into the homogeneity of PHA accumulation within the bacterial populations. Sharp, singular peaks indicate uniform PHA distribution, while multiple sharp peaks suggest distinct subpopulations with varying PHA concentrations. Broader peaks signify heterogeneous PHA accumulation, reflecting varying concentrations of PHA among the bacteria in the culture.

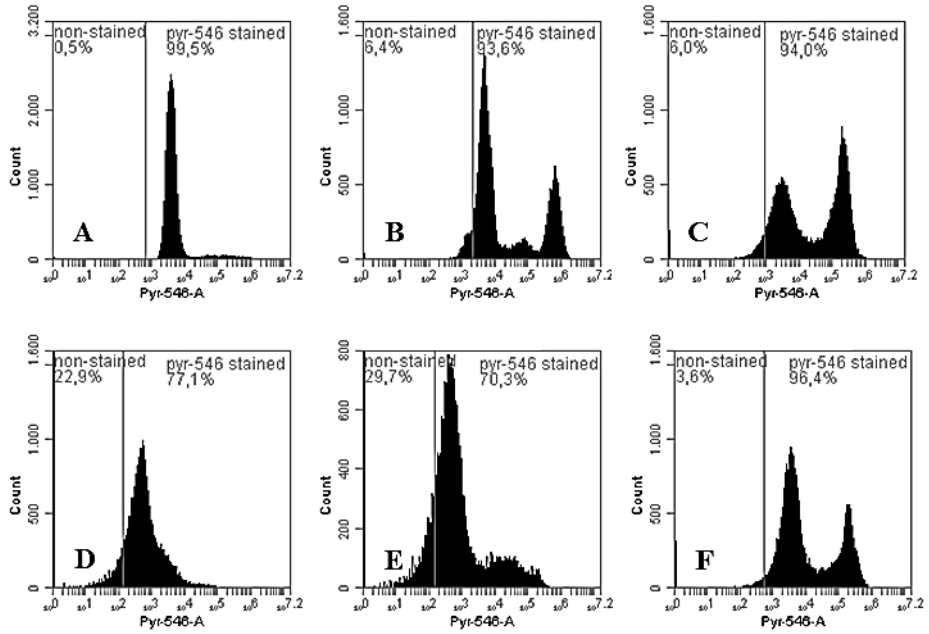

Figure 6. 6 Analysis of polyhydroxyalkanoates (PHA) production by *Cupriavidus necator (C. necator)* after Pyr-546 staining in B20DM (A); B50CPH (B); B20CPH (C); FBDM20PO (D); FBDM3PO (E); and FB20CPH.

The investigation of the relationship between PHA concentration measured using GC-MS and Pyr-546 fluorescence, as illustrated in Figures 6.2 and 6.3, provides significant insights. A clear correlation between the two techniques is observed in B20DM, where no PHA were produced. Conversely, Figure 6.2 B1 and C1 illustrate a similar behaviour of both methods during the exponential growth phase, with fluorescence declining as the culture progressed into the stationary phase. In contrast, the fed-batch experiments (Figure 6.3) show no discernible correlation in results between the two methods. This discrepancy can be potentially attributed to

the diverse culture media and cultivation strategies employed, resulting in a broad range of fluorescence values. Prior experiments conducted by our research group have demonstrated that varying media composition can result in a wide range of fluorescence values. Additionally, to the best of our knowledge, the mechanisms governing the entry of the fluorophore into the bacteria have not been thoroughly explored. Therefore, it remains uncertain whether damage to the bacterial membrane might influence the binding of the fluorophore. Consequently, a universal correlation between these techniques is not feasible, necessitating individual analyses for each experiment. However, under consistent parameters, a specific correlation for a given experiment can be established and used as a reference. It is important to acknowledge that while these techniques may not present a perfect correlation, Pyr-546 can serve as valuable tool for preliminary and on-line assessments of PHA production progression within a culture, facilitating real-time assessments without compromising the precision and reliability offered by established quantification techniques such as GC-MS.

6.3.3 Correlation between OD_{600} and flow cytometry cell counting

Following the discussion regarding the correlation between OD_{600} and cell counting in FCM presented in *Chapter 5.3.2.4 Correlation of OD_{600} and microbial concentration measurements*, the bioreactor experiments in this chapter were employed to establish a similar a correlation. Previous literature has highlighted that the production and accumulation of PHA within the bacteria can affect light scattering properties, thereby influencing OD_{600} values [306]. In this context, given that B20DM yielded no PHA production (Figure 6.2A), a correlation analysis was carried out for this experiment and compared with all other fermentations in which PHA were produced. The outcomes of this analysis are depicted in Figure 6.7.

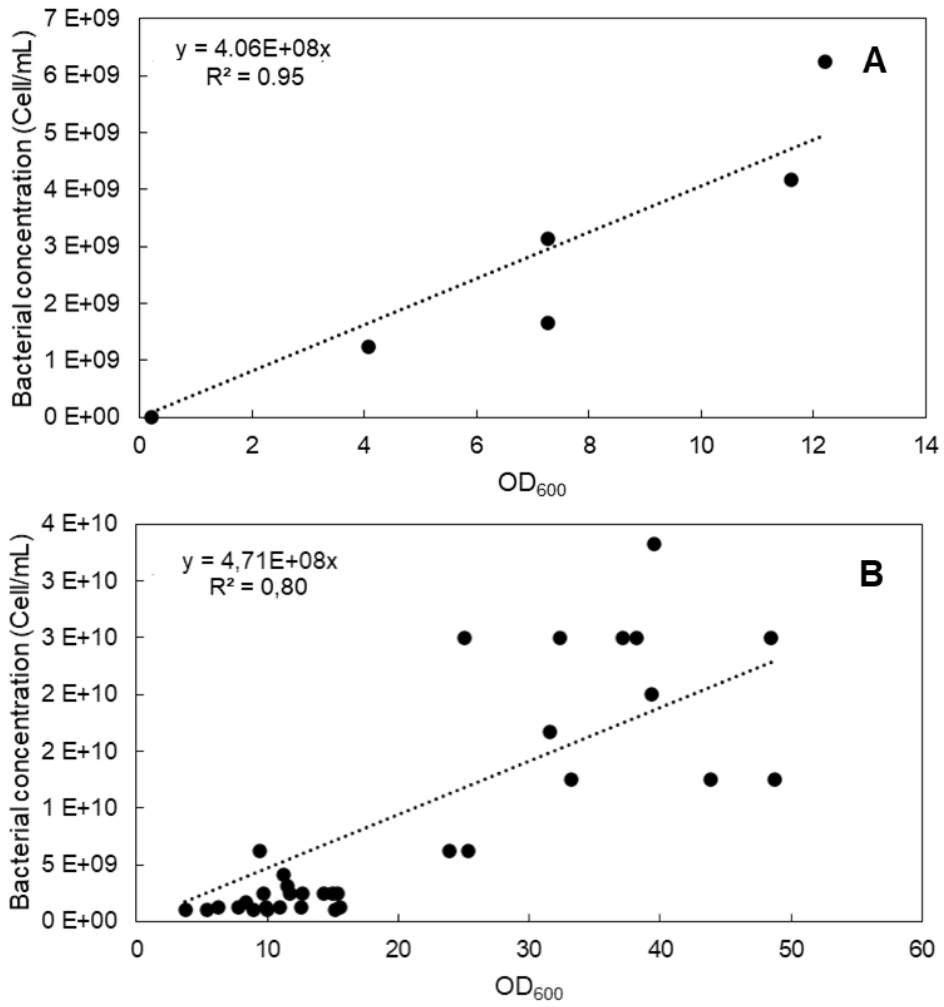

Figure 6. 7 Correlation of OD_{600} values obtained by spectrophotometry and cell/mL counting by flow cytometry (FCM) in non-producing polyhydroxyalkanoates (PHA) culture (A); and producing PHA cultures (B).

Figure 6.7A shows a robust correlation ($R^2 > 0.95$) between OD_{600} and bacterial concentration for the non-PHA producing culture. Hence, it can be established that 1 OD_{600} corresponds to 4.06 x 10^8 cell/mL. In contrast, Figure 6.7B, displays a less robust and more dispersed correlation (R^2=0.8), albeit acceptable. This lower correlation may be attributed to the fact that it was computed using data from five different fermentation experiments, each employing varied cultivation conditions and strategies. Additionally, the PHA concentration of the sampled points used in this correlation ranged from 5% to 86%, having a different effect on light scattering. In this scenario, 1OD_{600} equates to 4.71 x 10^8 cell/mL. While the disparity between the PHA-producing and non-PHA-producing experiments is relatively low, it can be inferred that the accumulation of PHA within the bacteria leads to a subtle overestimation of the growth of the culture when assessed using OD_{600} values. However, slopes are very similar and to the best of our

knowledge, there is no prior research addressing this phenomenon. Consequently, further research would be required to compare and validate the data presented in this thesis.

6.3.4 Determination of process productivity parameters

The six fermentation experiments presented in this chapter were utilised to compute various process parameters (μ_{X1}, $Y_{X/S}$, $Y_{P/S}$, and P_{PHA}), the outcomes of which are outlined in Table 6.3. These parameters offer valuable insights into the efficiency and productivity of each experiment.

Table 6. 3 Comparison of process productivity parameters from fermentation experiments

Fermentation	μ_{batch} (h^{-1})	$\mu_{feeding}$ (h^{-1})	$Y_{X/S}$ ($g_{biomass}/g_{substrate}$)	$Y_{P/S}$ ($g_{PHA}/g_{substrate}$)	P_{PHA} (g_{PHA}/Lh)
B20DM	0.18	n.a	0.22	0.000	0.000
B50CPH	0.12	n.a	0.18	0.004	0.005
B20CPH	0.23	n.a	0.27	0.03	0.017
FBDM20PO	0.14	0.012	0.41	0.35	0.11
FBDM3PO	0.16	0.015	0.39	0.49	0.16
FB20DM	0.15	0.006	0.26	0.03	0.03

Specific growth rate (μ), a fundamental parameter in microbial fermentation, serves as a vital indicator of the rate at which microorganisms multiply and proliferate. Table 6.3 reveals slight variations in growth rates, ranging from 0.12 h^{-1} in the batch containing non-diluted CPH to 0.23 h^{-1} in the batch containing diluted CPH. The observed highest growth using CPH compared to DM might be attributed to the presence of various sugars in the media and additional nutrients derived from the CP hydrolysis, which could favour microbial growth. Conversely, the lowest growth rate in B50CPH could be explained by the nitrogen limitation and a more concentrated media. Non-diluted CPH resulted in higher sugar content but elevated salt amounts [303] and potential growth inhibitors produced after the CP hydrolysis [332]. The concentration of these inhibitors decreased in B20CPH after media dilution, potentially resulting in a higher growth rate. Furthermore, when comparing results in Table 6.3, it becomes evident that while the reduction in pO_2 favoured the PHA production, it led to lower growth rates. Previous studies using glucose as substrate to grow *C. necator* have reported specific growth rates of around 0.2 h^{-1} [333], which are comparable with the findings presented in this study [28].

The $Y_{x/s}$ quantifies the efficiency of the microorganism in converting the substrate into biomass. The results ranged from 0.18 g/g in B50CPH to 0.41 g/g in FBDM20PO. Notably, despite the lower growth rate, the $Y_{x/s}$ was higher for the two fed-batch experiments that used DM in the batch phase compared to those using CPH. These variations in $Y_{x/s}$ across the experiments can be

attributed differences in nutrient composition, oxygen availability, and the presence of potential inhibitors and byproducts in the culture. The yields obtained in this study are consistent with previous research using *C. necator,* where $Y_{x/s}$ values up to 0.47 g/g were achieved using fructose [334,335].

Efficiency in PHA production was assessed through the $Y_{p/s}$ and P_{PHA} coefficients, with results presented in Table 6.3. Notably, two fermentation experiments stand out for their high $Y_{p/s}$ values, indicating their efficiency in PHA production. These are the two fed-batch experiments that employed DM during the batch phase and CPH as the feeding. With a value of 0.49 g/g, the experiment with the lowest pO_2 (FBDM3PO) proved to be the most efficient strategy for PHA production. These findings are in line with previous studies using *C. necator* to convert various substrates into PHA, where $Y_{P/S}$ values over 0.4 g/g were achieved using substrate like fructose [335] and sesame seed oil [336].

The highest P_{PHA} value obtained in our study, 0.16 g/L, also corresponds to the FBDM3PO fermentation. Notably, this value is slightly higher than the results obtained in the aforementioned studies using fructose and sesame seed oil, where values of 0.12 and 0.11 were achieved, respectively [335,336]. However, it is important to acknowledge that different substrates are expected to yield varying results in PHA production processes.

Therefore, our findings, while in line with existing literature, offer valuable insights due to the utilization of CPH, a relatively unexplored feedstock for the production of PHA. The efficiency and productivity coefficients here presented suggest that FBDM3PO emerged as the most promising fermentation to enhance PHA production.

6.3.5 Morphology analysis using flow cytometry

The evaluation of bacterial morphology was conducted using FCM and the results are presented in Figure 6.8. The depicted samples correspond to the final stage of each fermentation process. As illustrated in Figure 6.8, the samples exhibiting the less uniformity in terms of size (FSC) correspond to B50CPH and FB20CPH, which employed non-diluted CPH, and the diluted CPH in the batch phase along with non-diluted CPH as the feeding, respectively. Conversely, the fermentations using DM and diluted CPH presented a more homogeneous growth pattern, characterised by a predominantly uniform population and a small, less complex residual population.

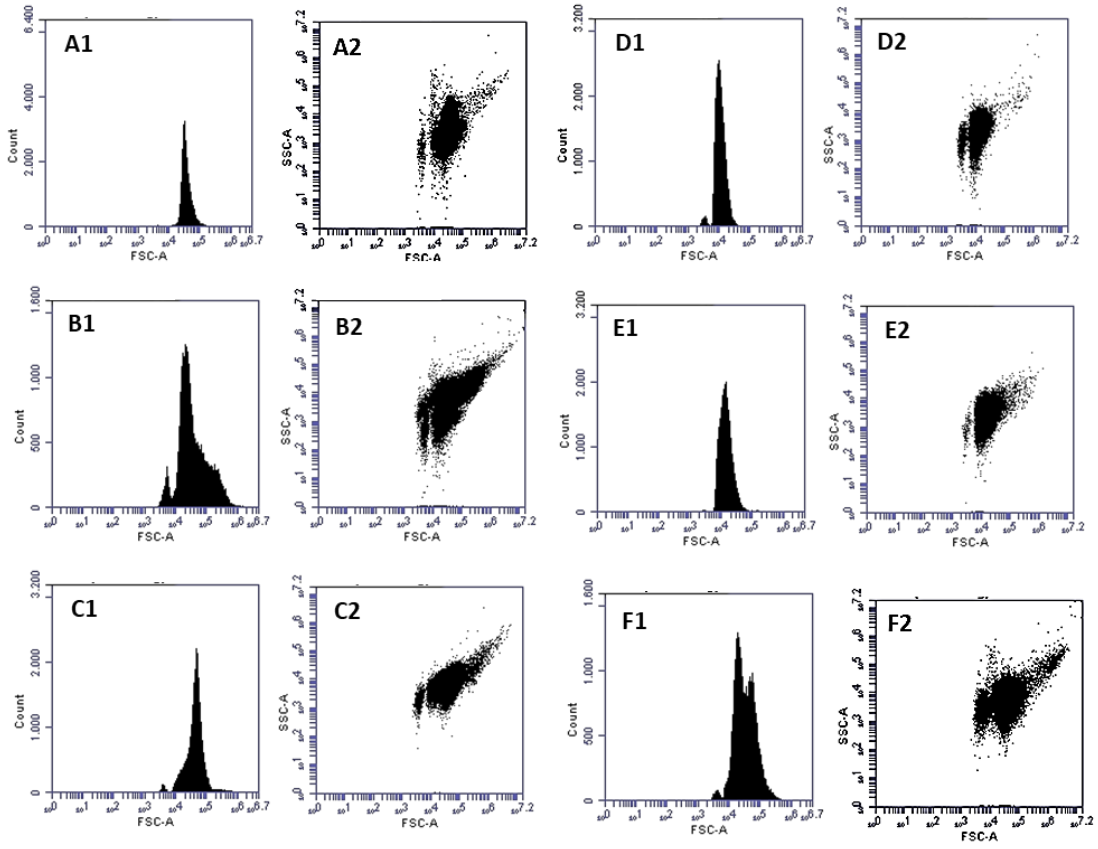

Figure 6. 8 Analysis of *Cupriavidus necator (C. necator)* size through forward scatter (FSC-A axis) (1) and complexity through size scatter (SSC-A axis) (2) using flow cytometry (FCM) of B20DM (A); B50CPH (B); B20CPH (C); FBDM20PO (D); FBDM3PO (E); and FB20CPH (F).

A similar pattern is observed in the plots depicting the complexity of bacteria (SSC). Specifically, plots A2, D2, and E2, reveal populations that are less complex and more uniform. Notably, all these samples share a common factor, which is the use of DM during the batch phase of the culture. However, the fact that samples D and E, corresponding to the fermentations resulting in the highest PHA production exhibit less complex populations, is somehow contradictory. This discrepancy is particularly based on our findings in *Chapter 5.3.2.3 Analysis of Cupriavidus necator morphology,* where the correlation between Pyr-546, indicative of PHA accumulation, and complexity measured by SSC was assessed (Figure 5.7), as well as in previous literature [304]. Conversely, plots B, C and E demonstrate high complexity, although their PHA production did not exceed 35%.

Therefore, it can be concluded that the complexity observed in these plots may be attributed more to the effect of CPH on microbial growth than to the impact of PHA accumulation. This highlights the importance of independently assessing FCM data separately for each specific experimental

condition, thus avoiding the assumption of a universally applicable behaviour pattern, as previously mentioned throughout this thesis.

6.3.6 Respiratory quotient and metabolism

Measurements of the CO_2 production and O_2 consumption were conducted using a gas analyser in two of the fermentations presented in this chapter, FBDM3PO and FB20CPH. While FBDM3PO was chosen as a representative fermentation of a high-PHA production process, FB20CPH was representative of a low-PHA production process. CO_2 and O_2 measurements were subsequently employed to calculate the RQ for each culture, and the results are graphically presented in Figure 6.7.

As depicted in Figure 6.9, the RQ values for the FB20CPH fermentation ranged between 0.98 and 1.03 throughout the entire fermentation process. This value means that 1 mol of CO_2 is produced for every mol of O_2 consumed, a characteristic feature of aerobic fermentation on sugars [337]. This culture, representative of low-PHA-producing cultures, was compared to an investigation involving a non-PHA-producing *C. necator* strain, in which RQ values around 1 were consistently observed throughout the culture [334].

Conversely, the RQ values of the FBDM3PO fermentation raged between 0.92 and 1.01, meaning that the O_2 consumption is higher than the CO_2 generation. The sharpest decrease in the RQ occurred after the addition of the feeding to the culture. This case, representative of high-PHA production was compared to previous studies, where RQ values below 1 were obtained during the PHA production phase [338,339]. This reduction in the RQ might be attributed to the redirection of the carbon away from respiration and towards PHA synthesis, leading to reduced CO_2 production [334].

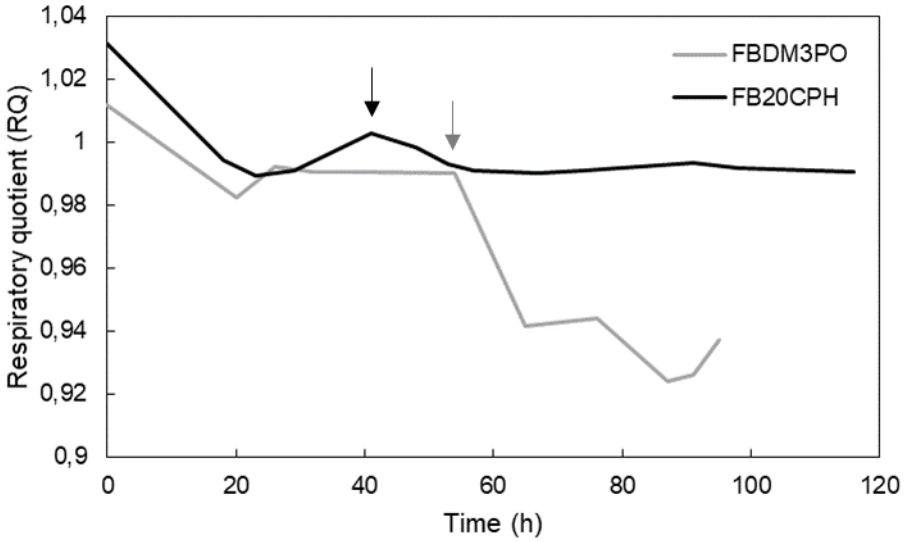

Figure 6. 9 Evolution of respiratory quotient (RQ) of FBDM3PO (grey line); and FB20CPH (black line) fermentation throughout time. Arrow in the represent the addition of feeding to the FBDM3PO (grey arrow); and FB20CPH (black arrow) fermentation.

6.4 Conclusions

The exploration of PHA production scale-up from shake flasks to benchtop bioreactors in this chapter has yielded significant insights. By comparing various batch and fed-batch experiments employing different culture media and fermentation parameters, we have identified a promising fermentation strategy. Specifically, utilizing CPH in the feeding phase after a batch phase with DM, led not only to the highest microbial growth, with an OD_{600} of 48.7, but also to the highest PHA production, 12.1 g/L. Our examination of the process productivity parameters confirms the effectiveness of this chosen strategy among the tested conditions.

Our findings align with previous research, emphasising that restricting oxygen availability in the culture enhances PHA production. Although further optimization is warranted for the complete utilisation of CPH as the sole carbon source, our investigation highlights its considerable potential. Notably, the introduction of CPH during the feeding stage of the FBDM3PO fermentation resulted in a remarkable 40-fold increase in PHA production compared to the batch phase employing DM.

To the best of our knowledge, this is the first study at bioreactor scale addressing the use of CP for PHA production using *C. necator.* The PHA concentration of 12.1 g/L achieved in the study confirms the potential of this feedstock to be valorised into PHA. Our results are in line with previous works producing PHA from alternative sources using *C. necator*. Furthermore, this study showcases a 6-fold increase in the PHA production when compared to previous studies procuring

PHA from cassava waste using alternative microorganisms. Consequently, the findings presented in this study not only demonstrates the potential for more efficient and sustainable PHA production strategies, but also establish a significant benchmark study for future optimisation of the process.

Chapter 7. General conclusions and future perspectives

7.1 Conclusions

This thesis has extensively explored the utilisation of cassava peel (CP) waste as a sustainable feedstock for polyhydroxyalkanoates (PHA) production, using *Cupriavidus necator (C. necator)* across several scales (from mL to L scales). The findings presented herein not only contribute to the field of PHA production but also offer valuable insights into waste valorisation and pre-treatment of CP.

Various analytical techniques, including TGA, proximate and ultimate analysis, FT-IR, and SEM, were employed to comprehensively characterise CP. In order to gain insights into the effect of acid hydrolysis on CP. Both untreated (native) CP and acid-hydrolysed CP were extensively characterised. The outcomes reveal marked differences between the two samples, confirming the degradation of intricate polysaccharides into smaller, more readily fermentable sugars. This conversion was further quantified through total reducing sugars (TRS) and glucose analysis, enabling the quantification of the sugar concentration within the cassava peel hydrolysate (CPH). The significance of this polysaccharide degradation lies in the non-fermentable nature of these polymers, which require depolymerisation into monomer (fermentable) sugars for their subsequent conversion into PHA.

Furthermore, this study comprehensively investigated two different hydrolysis techniques. Enzymatic hydrolysis, using α-amylases and glucoamylases, reached a final conversion of 70% from the starch present in CP to glucose. This outcome was achieved using a thermal pre-treatment of the CP at 99 ºC for 30 min, followed by simultaneous liquefaction and saccharification at 38 ºC, using a combination of α-amylase and glucoamylase at a concentration of 210 U/g in a 1:1 ratio, conducted for 48 h. Although this enzymatic conversion falls within the range of previous studies using the same enzymes, acid hydrolysis yielded better results with significantly shorter reaction times. Acid hydrolysis led to a remarkable 97% conversion from

polysaccharides to reducing sugars following optimisation performed through a design of experiments (DoE) using response surface methodology (RSM). This conversion was achieved using 3 M H_2SO_4 for 120 min and 90 ºC. To the best of our knowledge, the systematic approach presented in this thesis to optimise sugars recovery from CP represents the highest conversion achieved to date.

The screening experiment, using the 15 CPH resulting from the DoE, revealed the ability of *C. necator* to grow and produce PHA using CPH as the sole carbon source. In our study, the hydrolysis condition of 0.6 M H_2SO_4, 58 min, and 107 ºC, resulted in the CPH yielding the highest growth, with an OD_{600} of 15.8, and PHA production reaching 1.5 g/L (31% (g_{PHA}/g_{DCW})) at small (1mL) scale. To the best of our knowledge, this study represents the first investigation into the utilisation of CP as the exclusive carbon source for PHA production with *C. necator*, paving the path for future process optimisation.

The transition to shake-flask cultures resulted in a slight decrease in growth, with an OD_{600} of 12 and a PHA concentration of 1 g/L. This observed decline might be attributed to the reduction in nutrient concentration during the scale-up process. After assessing glucose consumption in the screening experiment, it was observed that sugars were not completely depleted at the end of the culture. Consequently, a strategic decision was made to reduce the sugar concentration to equate the concentration of the cultures performed using defined media (DM). This dilution might have impacted the availability of other essential nutrients required for bacterial growth. Furthermore, the reduced PHA concentration can also be attributed to the dilution effect. Extensive literature has documented that an excess of carbon in the culture media promotes PHA production. Therefore, the dilution might have resulted in reduced PHA concentration at the expense of consuming all available sugars.

Several bioreactor fermentations were conducted, and the effect of nitrogen and oxygen in the culture were assessed. Firstly, an excess of nitrogen was found to lead to negligible PHA production. Secondly, the restriction of oxygen availability was observed to promote PHA production.

The scaling up to bioreactor resulted in an OD_{600} of 15.2 and PHA production of 1.5 g/L when using CPH as the sole carbon source. These results are similar to those obtained at flask-scale. The presence of unidentified inhibitors within the CPH or the accumulation of by-products formed during the fermentation process, might have prevent bacteria from further growth and PHA production.

However, alternative fermentation strategies were explored. It was found that using defined media (DM) during the batch phase and adding CPH as the feeding, while maintaining the pO_2

levels between 0-3%, reached an OD_{600} of 48.7 and a PHA concentration of 12.1 g/L (84.7% (g_{PHA}/g_{DCW})). This result aligns with the findings of numerous studies using *C. necator* for PHA production from a wide range of waste feedstocks. Notably, this thesis presents the first study performed using cassava waste for the production of PHA at bioreactor scale using *C. necator.* Furthermore, our study showcases a 6-fold increase in PHA production when compared to previous studies using *Pseudomonas* species for PHA production from cassava waste.

The use of flow cytometry (FCM) provided valuable insights into bacterial morphology, a critical aspect of the culture, aiding in our understanding of the impact of CPH on bacterial physiology. Additionally, this thesis introduces an innovative approach to detect PHA within bacteria using the fluorophore pyrromethene-546 (Pyr-546). This approach has received minimal attention in the existing literature. Our research further optimised the fluorophore staining protocol for *C. necator*, and applied this staining method across all our experiments. It was concluded that Pyr-546 can serve as a valuable tool for preliminary and on-line assessment of PHA. However, it was detected that slight variations in the culture media composition and cultivation conditions led to fluctuations in the measured fluorescence values. Therefore, a *one-size-fits-all* correlation between the fluorescence values and PHA concentration is unfeasible, highlighting the need for individual assessment across diverse experimental setups. To the best of our knowledge, this is the first study that highlights the influence of the culture media and cultivation conditions on Pyr-546 staining.

In conclusion, over 12 g/L of PHA were successfully achieved in this thesis, integrating chemical and biological processes, thereby highlighting the importance of multidisciplinary research and paving the way for future efficient PHA production using CP. Furthermore, the use of *C. necator,* a native producer of PHA, simplifies the process eliminating the need for genetic engineering. However, while this research demonstrates the potential of native PHA production pathways, it also acknowledges the promising role of genetic engineering for further enhancing PHA production, improving media tolerance, and optimising metabolic pathways in *C. necator*. Future research efforts could explore these avenues to push the boundaries of PHA production further.

The results obtained across this thesis give a positive answer to the first research question presented in *Chapter 1: "Can cassava peel waste be effectively employed as a renewable substrate for PHA production by C. necator?".*

Regarding the second research question: *"What are the optimal process conditions and strategies to achieve efficient PHA biosynthesis?",* it is important to note that while our research reports a PHA concentration of 12 g/L, several strategies are discussed throughout the thesis that have the potential to enhance process productivity. These strategies are compiled in the next section.

This study contributes valuable insights to both the PHA production and the cassava waste management fields, offering solutions to two pressing global challenges in the contemporary society: the need to replace petroleum-based plastics and the efficient management of agricultural waste. Moreover, this study aligns with the Sustainable Development Goals (SDGs) set forth by the United Nations and holds significant potential to contribute towards achieving Net Zero targets.

However, the establishment of these processes near to the feedstock production areas carries the potential to foster the advancement of more environmentally sustainable practices. These areas often pertain to developing countries, and knowledge and technological transfer to develop these processes will mitigate the need for long-distance transportation of feedstock, concurrently boosting the economic prospects of these countries. An example is Sub-Saharan Africa, where high amounts of CP waste are generated. African countries may solve many difficulties and simultaneously contribute to the UN SDGs by utilising locally accessible resources, such as CP waste, and putting biorefinery technologies into practice.

7.2 Limitations and future work

In light of the substantial contributions presented in this thesis, it is equally important to recognise the inherent limitations of the study and identify promising avenues for future research. This section serves as a critical reflexion on the boundaries of our work and an exploration of the possibilities in this field.

- Regarding the characterisation of our feedstock, the compositional analysis to quantify the starch, cellulose, hemicellulose and lignin content would provide valuable information for the subsequent pre-treatment process.

- Although the results achieved in the enzymatic study presented in this thesis align with those presented in literature, there is room for optimisation. Firstly, due to the limitations we encountered obtaining the desired enzymes due to the impact of the COVID-19 pandemic, an alternative and limited product was employed. Given this constraint and time limitations, replicates of the enzymatic reactions were not performed. We acknowledge the importance of replicates for higher reliability of the experiments here presented. Furthermore, and related to the previous point, a compositional analysis will help to develop a more effective strategy incorporating additional enzymes, such as cellulases, to enhance sugars recovery. Finally, implementing a comprehensive enzymatic optimisation through a DoE would contribute to increase the hydrolysis yields and facilitate a more robust comparison between the enzymatic and the acid processes. This

comprehensive approach should aim to optimise the ratio of enzymes used in the process, with the objective of minimising the enzyme concentration to reduce costs.

- Further research into the mechanism by which Pyr-546 enters bacteria is essential to gain a better understanding of its potential applications. This can contribute to the development of an improved staining method for bacteria and the establishment of a more universally applicable correlation between Pyr-546 fluorescence and PHA concentration. Such development could streamline the analysis and expedite research efforts.

- Finally, the PHA production from CPH could potentially be further enhanced by investigating diverse factors that might influence bacterial growth and PHA production, such as substrate composition, pH levels, temperature, oxygen availability, and the presence of potential inhibitors. Exploring these factors in more detail could provide valuable insights into optimising PHA production processes and maximising yields. In this study, the effect of oxygen was assessed, and the oxygenation was optimised to enhance PHA production. Furthermore, it was observed that an excess of nitrogen led to no PHA production. However, the analysis of nitrogen content in the CPH was not performed. Having precise information about the nutrients, such as nitrogen or phosphorous, which are known to affect PHA production, in the CPH could help to develop more effective PHA production strategies. Moreover, a comprehensive analysis of the CPH will provide insights into the available sugars and the preferred ones for this *C. necator* strain to grow and produce PHA. The analysis of potential inhibitors and by-products present in the CPH, as well as their accumulation and in the culture over time, could contribute to the development of a strategy for their elimination or reduction. Lastly, the development of culturing continuous strategy in bioreactor might contribute to avoid product inhibition. This, in turn, may lead to higher bacterial concentrations and increased PHA production.

In conclusion, the implementation of the strategies discussed in this section holds the potential to reduce the reliance on DM in the process and increase the utilisation of CPH. By enhancing the efficiency of CPH utilisation and reducing the dependence on DM, these approaches offer promising avenues to decrease the production cost of PHA. Consequently, this can potentially make PHA production more competitive with the widely used petroleum-based plastics, contributing to a more sustainable alternative.

List of references

[1] F. Feed, B.C. Materials, IEA Bioenergy 29th update, Biomass Bioenergy 31 (2007) I–VII. https://doi.org/10.1016/s0961-9534(07)00106-7.

[2] S.K. Maity, Opportunities, recent trends and challenges of integrated biorefinery: Part I, Renewable and Sustainable Energy Reviews 43 (2015) 1427–1445. https://doi.org/10.1016/j.rser.2014.11.092.

[3] A. Chamas, H. Moon, J. Zheng, Y. Qiu, T. Tabassum, J.H. Jang, M. Abu-Omar, S.L. Scott, S. Suh, Degradation rates of plastics in the environment, ACS Sustain Chem Eng 8 (2020) 3494–3511. https://doi.org/10.1021/acssuschemeng.9b06635.

[4] M.R. Yates, C.Y. Barlow, Life cycle assessments of biodegradable, commercial biopolymers—A critical review, Resour Conserv Recycl 78 (2013) 54–66. https://doi.org/10.1016/j.resconrec.2013.06.010.

[5] A. Steinbüchel, B. Füchtenbusch, Bacterial and other biological systems for polyester production, Trends Biotechnol 16 (1998) 419–427. https://doi.org/10.1016/S0167-7799(98)01194-9.

[6] R.A. Ilyas, S.M. Sapuan, A. Kadier, M.S. Kalil, R. Ibrahim, M.S.N. Atikah, N.M. Nurazzi, A. Nazrin, C.H. Lee, M.N. Faiz Norrrahim, N.H. Sari, E. Syafri, H. Abral, L. Jasmani, M.I.J. Ibrahim, Properties and characterization of PLA, PHA, and other types of biopolymer composites, in: Advanced Processing, Properties, and Applications of Starch and Other Bio-Based Polymers, Elsevier, 2020: pp. 111–138. https://doi.org/10.1016/B978-0-12-819661-8.00008-1.

[7] M. Kumar, R. Rathour, R. Singh, Y. Sun, A. Pandey, E. Gnansounou, K.-Y. Andrew Lin, D.C.W. Tsang, I.S. Thakur, Bacterial polyhydroxyalkanoates: opportunities, challenges, and prospects, J Clean Prod 263 (2020) 121500. https://doi.org/10.1016/j.jclepro.2020.121500.

[8] M. Shabina, M. Afzal, S. Hameed, Bacterial polyhydroxyalkanoates-eco-friendly next generation plastic: production, biocompatibility, biodegradation, physical properties and applications, Green Chem Lett Rev 8 (2015) 56–77. https://doi.org/10.1080/17518253.2015.1109715.

[9] T. Hofmann, S. Ghoshal, N. Tufenkji, J.F. Adamowski, S. Bayen, Q. Chen, P. Demokritou, M. Flury, T. Hüffer, N.P. Ivleva, R. Ji, R.L. Leask, M. Maric, D.M. Mitrano, M. Sander, S. Pahl, M.C. Rillig, T.R. Walker, J.C. White, K.J. Wilkinson, Plastics can be used more sustainably in agriculture, Commun Earth Environ 4 (2023) 332. https://doi.org/10.1038/s43247-023-00982-4.

[10] T. Pulingam, J.N. Appaturi, T. Parumasivam, A. Ahmad, K. Sudesh, Biomedical Applications of Polyhydroxyalkanoate in Tissue Engineering, Polymers (Basel) 14 (2022) 2141. https://doi.org/10.3390/polym14112141.

[11] C.S. Wu, Controlled release evaluation of bacterial fertilizer using polymer composites as matrix, Journal of Controlled Release 132 (2008) 42–48. https://doi.org/10.1016/j.jconrel.2008.08.015.

[12] K.Y. Sen, M.H. Hussin, S. Baidurah, Biosynthesis of poly(3-hydroxybutyrate) (PHB) by Cupriavidus necator from various pretreated molasses as carbon source, Biocatal Agric Biotechnol 17 (2019) 51–59. https://doi.org/10.1016/j.bcab.2018.11.006.

[13] N. Poomipuk, A. Reungsang, P. Plangklang, Poly-β-hydroxyalkanoates production from cassava starch hydrolysate by Cupriavidus sp. KKU38, Int J Biol Macromol 65 (2014) 51–64. https://doi.org/10.1016/j.ijbiomac.2014.01.002.

[14] S.K. Ghosh, Utilization and management of bioresources, Springer Singapore, Singapore, 2018. https://doi.org/10.1007/978-981-10-5349-8.

[15] N. Poomipuk, A. Reungsang, P. Plangklang, Poly-β-hydroxyalkanoates production from cassava starch hydrolysate by Cupriavidus sp. KKU38, Int J Biol Macromol 65 (2014) 51–64. https://doi.org/10.1016/j.ijbiomac.2014.01.002.

[16] S. Vigneswari, M.S.M. Noor, T.S.M. Amelia, K. Balakrishnan, A. Adnan, K. Bhubalan, A.-A.A. Amirul, S. Ramakrishna, Recent Advances in the Biosynthesis of Polyhydroxyalkanoates from Lignocellulosic Feedstocks, Life 11 (2021) 807. https://doi.org/10.3390/life11080807.

[17] G. Pesante, N. Frison, Recovery of bio-based products from PHA-rich biomass obtained from biowaste: A review, Bioresour Technol Rep 21 (2023). https://doi.org/10.1016/j.biteb.2023.101345.

[18] C.A. Cardona Alzate, J.C. Solarte Toro, Á.G. Peña, Fermentation, thermochemical and catalytic processes in the transformation of biomass through efficient biorefineries, Catal Today 302 (2018) 61–72. https://doi.org/10.1016/j.cattod.2017.09.034.

[19] A. Muscat, E.M. de Olde, I.J.M. de Boer, R. Ripoll-Bosch, The battle for biomass: A systematic review of food-feed-fuel competition, Glob Food Sec 25 (2020). https://doi.org/10.1016/j.gfs.2019.100330.

[20] M.K. Awasthi, V. Kumar, V. Yadav, S. Sarsaiya, S.K. Awasthi, R. Sindhu, P. Binod, V. Kumar, A. Pandey, Z. Zhang, Current state of the art biotechnological strategies for conversion of watermelon wastes residues to biopolymers production: A review, Chemosphere 290 (2022) 133310. https://doi.org/10.1016/j.chemosphere.2021.133310.

[21] C. Hierro-Iglesias, A. Chimphango, P. Thornley, A. Fernández-Castané, Opportunities for the development of cassava waste biorefineries for the production of polyhydroxyalkanoates in Sub-Saharan Africa, Biomass Bioenergy 166 (2022) 106600. https://doi.org/10.1016/j.biombioe.2022.106600.

[22] S. Obruca, P. Benesova, J. Oborna, I. Marova, Application of protease-hydrolyzed whey as a complex nitrogen source to increase poly(3-hydroxybutyrate) production from oils by Cupriavidus necator, Biotechnol Lett 36 (2014) 775–781. https://doi.org/10.1007/s10529-013-1407-z.

[23] P. Marciniak, J. Możejko-Ciesielska, What Is New in the Field of Industrial Wastes Conversion into Polyhydroxyalkanoates by Bacteria?, Polymers (Basel) 13 (2021) 1731. https://doi.org/10.3390/polym13111731.

[24] A. Asante-Pok, Analysis of incentives and disincentives for cassava in Nigeria, 2013.

[25] A.M. Bazzanella, F. Ausfelder, Low carbon energy and feedstock for the European chemical industry, 2017. www.dechema.de.

[26] O.A. Adebo, I. Gabriela Medina-Meza, Impact of Fermentation on the Phenolic Compounds and Antioxidant Activity of Whole Cereal Grains: A Mini Review, Molecules 25 (2020) 927. https://doi.org/10.3390/molecules25040927.

[27] B. Nambisan, Strategies for elimination of cyanogens from cassava for reducing toxicity and improving food safety, Food and Chemical Toxicology 49 (2011) 690–693. https://doi.org/10.1016/j.fct.2010.10.035.

[28] R. Geyer, J.R. Jambeck, K.L. Law, Production, use, and fate of all plastics ever made, Sci Adv 3 (2017) 25–29. https://doi.org/10.1126/sciadv.1700782.

[29] UNECA, Fossil Fuels in Africa in the Context of a Carbon Constrained Future, 2011.

[30] Sub-Saharan Africa, Paradox of Progress. Sub-Saharan Africa (2017). https://www.dni.gov/index.php/the-next-five-years/sub-saharan-africa (accessed May 5, 2020).

[31] Ellen MacArthur Foundation, Completing the picture: how the circular economy tackles climate change, 2019. www.ellenmacarthurfoundation.org/publications.

[32] P.W. Owen, Renewable energy for sustainable rural development: significant potential synergies, but mostly unrealised, 2018.

[33] L. Pelkmans, What does net-zero emissions by 2050 mean for bioenergy and land use?, 2010.

[34] P. Sekoai, K. Yoro, Biofuel development initiatives in Sub-Saharan Africa: opportunities and challenges, Climate 4 (2016) 33. https://doi.org/10.3390/cli4020033.

[35] A.M. Szyniszewska, CassavaMap, a fine-resolution disaggregation of cassava production and harvested area in Africa in 2014, Sci Data 7 (2020) 159. https://doi.org/10.1038/s41597-020-0501-z.

[36] WACOMP, Cassava, (2020).

[37] N. Prakobboon, M.M. Vahdati, M. Shahrestani, An environmental impact assessment of the management of cassava waste : A case study in Thailand, International Journal of Biomass & Renewables 7 (2018) 18–29.

[38] S. Li, Y. Cui, Y. Zhou, Z. Luo, J. Liu, M. Zhao, The industrial applications of cassava: current status, opportunities and prospects, J Sci Food Agric 97 (2017) 2282–2290. https://doi.org/10.1002/jsfa.8287.

[39] OECD, Global Plastics Outlook, OECD, 2022. https://doi.org/10.1787/aa1edf33-en.

[40] J. Saghir, J. Santoro, Urbanization in Sub-Saharan Africa. Meeting challenges by bridging stakeholders, Center for Strategic & International Studies (2018) 1–7. https://www.csis.org/analysis/urbanization-sub-saharan-africa.

[41] J.O. Babayemi, I.C. Nnorom, O. Osibanjo, R. Weber, Ensuring sustainability in plastics use in Africa: consumption, waste generation, and projections, Environ Sci Eur 31 (2019). https://doi.org/10.1186/s12302-019-0254-5.

[42] K.-B. Lange, Bioplastics market data update, 2019.

[43] M. Rabnawaz, I. Wyman, R. Auras, S. Cheng, A roadmap towards green packaging: the current status and future outlook for polyesters in the packaging industry, Green Chem. 19 (2017) 4737–4753. https://doi.org/10.1039/C7GC02521A.

[44] K.-B. Lange, Bioplastics market data update, 2019.

[45] E. Bugnicourt, P. Cinelli, A. Lazzeri, V. Alvarez, Polyhydroxyalkanoate (PHA): review of synthesis, characteristics, processing and potential applications in packaging, Express Polym Lett 8 (2014) 791–808. https://doi.org/10.3144/expresspolymlett.2014.82.

[46] W. Chen, Y.W. Tong, PHBV microspheres as neural tissue engineering scaffold support neuronal cell growth and axon–dendrite polarization, Acta Biomater 8 (2012) 540–548. https://doi.org/10.1016/j.actbio.2011.09.026.

[47] J. Yu, L.X.L. Chen, The greenhouse gas emissions and fossil energy requirement of bioplastics from cradle to gate of a biomass refinery, Environ Sci Technol 42 (2008) 6961–6966. https://doi.org/10.1021/es7032235.

[48] A.H. Tullo, PHA: A Biopolymer Whose Time Has Finally Come, (2019). https://cen.acs.org/business/biobased-chemicals/PHA-biopolymer-whose-time-finally/97/i35 (accessed November 24, 2020).

[49] V. Popa, I. Volf, I. Biomass for Fuels and Biomaterials. Biomass as renewable raw material to obtain bioproducts of high-tech value, Elsevier, 2018.

[50] M. Zhang, L. Xie, Z. Yin, S.K. Khanal, Q. Zhou, Biorefinery approach for cassava-based industrial wastes: current status and opportunities, Bioresour Technol 215 (2016) 50–62. https://doi.org/10.1016/j.biortech.2016.04.026.

[51] S.M. Ioannidou, C. Pateraki, D. Ladakis, H. Papapostolou, M. Tsakona, A. Vlysidis, I.K. Kookos, A. Koutinas, Sustainable production of bio-based chemicals and polymers via integrated biomass refining and bioprocessing in a circular bioeconomy context, Bioresour Technol 307 (2020) 123093. https://doi.org/10.1016/j.biortech.2020.123093.

[52] J. Moncada, J.A. Tamayo, C.A. Cardona, Integrating first, second, and third generation biorefineries: incorporating microalgae into the sugarcane biorefinery, Chem Eng Sci 118 (2014) 126–140. https://doi.org/10.1016/j.ces.2014.07.035.

[53] UNIDO, Industrial development in least developed countries, 2018. https://www.unido.org/api/opentext/documents/download/12831761/unido-file-12831761.

[54] D. Andrews, The circular economy, design thinking and education for sustainability, Local Economy: The Journal of the Local Economy Policy Unit 30 (2015) 305–315. https://doi.org/10.1177/0269094215578226.

[55] C.D. Botero, D.L. Restrepo, C.A. Cardona, A comprehensive review on the implementation of the biorefinery concept in biodiesel production plants, Biofuel Research Journal 4 (2017) 691–703. https://doi.org/10.18331/BRJ2017.4.3.6.

[56] P. Desmond, M. Asamba, Accelerating the transition to a circular economy in Africa: case studies from Kenya and South Africa. The circular economy and the global south. Sustainable lifestyles and green industrial development, Routledge, 2019. https://doi.org/https://doi.org/10.4324/9780429434006.

[57] V. Mathioudakis, P.W. Gerbens-Leenes, T.H. Van der Meer, A.Y. Hoekstra, The water footprint of second-generation bioenergy: a comparison of biomass feedstocks and conversion techniques, J Clean Prod 148 (2017) 571–582. https://doi.org/10.1016/j.jclepro.2017.02.032.

[58] J. Moncada, J.A. Tamayo, C.A. Cardona, Integrating first, second, and third generation biorefineries: incorporating microalgae into the sugarcane biorefinery, Chem Eng Sci 118 (2014) 126–140. https://doi.org/10.1016/j.ces.2014.07.035.

[59] M. Kumar, R. Rathour, R. Singh, Y. Sun, A. Pandey, E. Gnansounou, K.-Y. Andrew Lin, D.C.W. Tsang, I.S. Thakur, Bacterial polyhydroxyalkanoates: opportunities, challenges, and prospects, J Clean Prod 263 (2020) 121500. https://doi.org/10.1016/j.jclepro.2020.121500.

[60] X. Xiong, I.K.M. Yu, D.C.W. Tsang, N.S. Bolan, Y. Sik Ok, A.D. Igalavithana, M.B. Kirkham, K.-H. Kim, K. Vikrant, Value-added chemicals from food supply chain wastes: state-of-the-art review and future prospects, Chemical Engineering Journal 375 (2019) 121983. https://doi.org/10.1016/j.cej.2019.121983.

[61] T.M. Mata, A.A. Martins, N.S. Caetano, Microalgae for biodiesel production and other applications: a review, Renewable and Sustainable Energy Reviews 14 (2010) 217–232. https://doi.org/10.1016/j.rser.2009.07.020.

[62] Z. Liu, K. Wang, Y. Chen, T. Tan, J. Nielsen, Third-generation biorefineries as the means to produce fuels and chemicals from CO2, Nat Catal 3 (2020) 274–288. https://doi.org/10.1038/s41929-019-0421-5.

[63] J.C. Magalhães Pires, A.L. Da Cunha Gonçalves, Bioenergy with carbon capture and storage: using Natural Resources for Sustainable Development, Academic Press, 2019. https://doi.org/https://doi.org/10.1016/C2017-0-04413-0.

[64] Biofuture Platform, Creating the biofuture: a report on the state of the low carbon bioeconomy, 2018.

[65] BBIJU, Olive leaf mutli-product cascade based biorefinery, (2021). https://www.bbi.europa.eu/projects/oleaf4value (accessed June 28, 2021).

[66] Vivergofuels, (2019). https://vivergofuels.com/e10-the-greener-fuel/ (accessed November 24, 2020).

[67] S. Blanco-Rosete, C. Webb, Emerging biorefinery markets: global context and prospects for Latin America, Biofuels, Bioproducts and Biorefining (2008) 331–342. https://doi.org/10.1002/bbb.

[68] P. Sekoai, K. Yoro, Biofuel development initiatives in Sub-Saharan Africa: opportunities and challenges, Climate 4 (2016) 33. https://doi.org/10.3390/cli4020033.

[69] Energy Commission, Bioenergy policy for Ghana, 2010.

[70] S.A. Department of Science and Technology, The Bio-economy Strategy is an initiative of the Department of Science and Technology, South Africa., 2013.

[71] S.A. Department of Science and Technology, The Bio-economy Strategy is an initiative of the Department of Science and Technology, South Africa., 2013.

[72] L. Smith, Plastic waste disposal, 2019. https://commonslibrary.parliament.uk/.

[73] IRENA, Biofuel potential in Southeast Asia: raising food yields, reducing food waste and utilising residues, 2017.

[74] Innovative Jatropha biofuel production in Malawi, (2013). https://www.engineeringnews.co.za/article/innovative-jatropha-biofuel-production-in-malawi-2013-07-05 (accessed May 13, 2020).

[75] B. Amigun, J.K. Musango, W. Stafford, Biofuels and sustainability in Africa, Renewable and Sustainable Energy Reviews 15 (2011) 1360–1372. https://doi.org/10.1016/j.rser.2010.10.015.

[76] W. Sawahel, Brazil and India join Senegal for biofuel production - SciDev.Net, (2006). https://www.scidev.net/global/cooperation/news/brazil-and-india-join-senegal-for-biofuel-producti.html (accessed May 14, 2020).

[77] M. Kempf, Jatropha production in semi-arid areas of Tanzania Is the growing and processing of Jatropha in the semi-arid Central Corridor of Tanzania a way to improve the income of rural households and thereby enhance their livelihood? A feasibility study, 2007.

[78] D. Banks, J. Schäffler, The potential contribution of renewable in south africa., 2005.

[79] D. Callo-Concha, H. Jaenicke, C.B. Schmitt, M. Denich, Advances in food and non-food biomass production, processing and use in Sub-Saharan Africa, MDPI, 2020. https://doi.org/10.3390/books978-3-03928-669-0.

[80] N. Hashim, How knowledge, policy planning, and implementation succeed or fail: the jatropha projects in Tanzania, Journal of African Business 15 (2014) 169–183. https://doi.org/10.1080/15228916.2014.956640.

[81] IEA, How competitive is biofuel production in Brazil and the United States?, (2018). https://www.iea.org/articles/how-competitive-is-biofuel-production-in-brazil-and-the-united-states (accessed January 17, 2021).

[82] L.-J. Vandi, C. Chan, A. Werker, D. Richardson, B. Laycock, S. Pratt, Wood-PHA composites: mapping opportunities, Polymers (Basel) 10 (2018) 751. https://doi.org/10.3390/polym10070751.

[83] M. Yang, N.R. Baral, B.A. Simmons, J.C. Mortimer, P.M. Shih, C.D. Scown, Accumulation of high-value bioproducts in planta can improve the economics of advanced biofuels, Proc Natl Acad Sci U S A 117 (2020) 27061. https://doi.org/10.1073/pnas.2018562117.

[84] D. Lestari, E. Zvinavashe, J.P.M. Sanders, Economic valuation of potential products from Jatropha seed in five selected countries: Zimbabwe, Tanzania, Mali, Indonesia, and The Netherlands, Biomass Bioenergy 74 (2015) 84–91. https://doi.org/10.1016/j.biombioe.2014.12.011.

[85] M. Bokanga, Cassava: post-harvest operations, 1999.

[86] A.D. Uchechukwu-Agua, O.J. Caleb, U.L. Opara, Postharvest handling and storage of fresh cassava root and products: a review, Food Bioproc Tech 8 (2015) 729–748. https://doi.org/10.1007/s11947-015-1478-z.

[87] M. Zaman, Cassava Production Guidelines for Foof Security and Adaptation to Climate Change in Asia and Africa, 2018.

[88] M. Bokanga, Cassava: post-harvest operations, 1999.

[89] D. Olukanni, T. Olatunji, Cassava waste management and biogas generation potential in selected local government areas in Ogun State, Nigeria, Recycling 3 (2018) 58. https://doi.org/10.3390/recycling3040058.

[90] M. Zaman, Cassava production guidelines for food security and adaptation to climate change in Asia and Africa, 2018.

[91] I. Ekop, Simonyan. K.J, E.T. Evwierhoma, Utilization of cassava wastes for value added products: an overview, International Journal of Scientific Engineering and Science 3 (2019) 31–39. https://doi.org/10.5281/zenodo.2556466.

[92] S.K. Ghosh, Utilization and management of bioresources, Springer Singapore, Singapore, 2018. https://doi.org/10.1007/978-981-10-5349-8.

[93] O.L. Ki, A. Kurniawan, C.X. Lin, Y.H. Ju, S. Ismadji, Bio-oil from cassava peel: a potential renewable energy source, Bioresour Technol 145 (2013) 157–161. https://doi.org/10.1016/j.biortech.2013.01.122.

[94] A. Asante-Pok, Analysis of incentives and disincentives for cassava in Nigeria, 2013.

[95] D. Olukanni, T. Olatunji, Cassava waste management and biogas generation potential in selected local government areas in Ogun State, Nigeria, Recycling 3 (2018) 58. https://doi.org/10.3390/recycling3040058.

[96] G.S. Aruwajoye, F.D. Faloye, E.G. Kana, Soaking assisted thermal pretreatment of cassava peels wastes for fermentable sugar production: Process modelling and optimization, Energy Convers Manag 150 (2017) 558–566. https://doi.org/10.1016/j.enconman.2017.08.046.

[97] P. Zong, Y. Jiang, Y. Tian, J. Li, M. Yuan, Y. Ji, M. Chen, D. Li, Y. Qiao, Pyrolysis behavior and product distributions of biomass six group components: Starch, cellulose, hemicellulose, lignin, protein and oil, Energy Convers Manag 216 (2020) 112777. https://doi.org/10.1016/j.enconman.2020.112777.

[98] I. Ekop, Simonyan. K.J, E.T. Evwierhoma, Utilization of cassava wastes for value added products: an overview, International Journal of Scientific Engineering and Science 3 (2019) 31–39. https://doi.org/10.5281/zenodo.2556466.

[99] L.P.S. Vandenberghe, C.R. Soccol, A. Pandey, J.-M. Lebeault, Solid-state fermentation for the synthesis of citric acid by Aspergillus niger, Bioresour Technol 74 (2000) 175–178. https://doi.org/10.1016/S0960-8524(99)00107-8.

[100] D.G. Martinez, A. Feiden, R. Baricatti, K.R. de F. Zara, Ethanol production from waste of cassava processing, Applied Sciences (Switzerland) 8 (2018) 1–8. https://doi.org/10.3390/app8112158.

[101] A.B.P. Medeiros, A. Pandey, R.J.S. Freitas, P. Christen, C.R. Soccol, Optimization of the production of aroma compounds by Kluyveromyces marxianus in solid-state fermentation using factorial

design and response surface methodology, Biochem Eng J 6 (2000) 33–39. https://doi.org/10.1016/S1369-703X(00)00065-6.

[102] S. Chavadej, T. Wangmor, K. Maitriwong, P. Chaichirawiwat, P. Rangsunvigit, P. Intanoo, Separate production of hydrogen and methane from cassava wastewater with added cassava residue under a thermophilic temperature in relation to digestibility, J Biotechnol 291 (2019) 61–71. https://doi.org/10.1016/j.jbiotec.2018.11.015.

[103] T.D. Kusworo, Biogas production from cassava starch effluent using microalgae as biostabilisator, International Journal of Science and Engineering 2 (2011) 4–8. https://doi.org/10.12777/ijse.2.1.4-8.

[104] E. Ekeledo, S. Latif, A. Abass, J. Müller, Antioxidant potential of extracts from peels and stems of yellow-fleshed and white cassava varieties, Int J Food Sci Technol 56 (2021) 1333–1342. https://doi.org/10.1111/ijfs.14814.

[105] P. Wongsirichot, M. Gonzalez-Miquel, J. Winterburn, Holistic valorization of rapeseed meal utilizing green solvents extraction and biopolymer production with Pseudomonas putida, J Clean Prod 230 (2019) 420–429. https://doi.org/10.1016/j.jclepro.2019.05.104.

[106] A. Anukam, J. Berghel, Biomass Pretreatment and Characterization: A Review, in: Biotechnological Applications of Biomass, IntechOpen, 2021. https://doi.org/10.5772/intechopen.93607.

[107] J. Cai, Y. He, X. Yu, S.W. Banks, Y. Yang, X. Zhang, Y. Yu, R. Liu, A. V. Bridgwater, Review of physicochemical properties and analytical characterization of lignocellulosic biomass, Renewable and Sustainable Energy Reviews 76 (2017) 309–322. https://doi.org/10.1016/j.rser.2017.03.072.

[108] R. García, C. Pizarro, A.G. Lavín, J.L. Bueno, Characterization of Spanish biomass wastes for energy use, Bioresour Technol 103 (2012) 249–258. https://doi.org/10.1016/j.biortech.2011.10.004.

[109] P. Koczoń, J.T. Hołaj-Krzak, B.K. Palani, T. Bolewski, J. Dąbrowski, B.J. Bartyzel, E. Gruczyńska-Sękowska, The Analytical Possibilities of FT-IR Spectroscopy Powered by Vibrating Molecules, Int J Mol Sci 24 (2023). https://doi.org/10.3390/ijms24021013.

[110] Z.U. Rehman, J.S. Vrouwenvelder, P.E. Saikaly, Physicochemical Properties of Extracellular Polymeric Substances Produced by Three Bacterial Isolates From Biofouled Reverse Osmosis Membranes, Front Microbiol 12 (2021) 1–13. https://doi.org/10.3389/fmicb.2021.668761.

[111] T.R. Sarker, R. Azargohar, A.K. Dalai, M. Venkatesh, Physicochemical and Fuel Characteristics of Torrefied Agricultural Residues for Sustainable Fuel Production, Energy & Fuels 34 (2020) 14169–14181. https://doi.org/10.1021/acs.energyfuels.0c02121.

[112] A. Anukam, S. Mamphweli, P. Reddy, E. Meyer, O. Okoh, Pre-processing of sugarcane bagasse for gasification in a downdraft biomass gasifier system: A comprehensive review, Renewable and Sustainable Energy Reviews 66 (2016) 775–801. https://doi.org/10.1016/j.rser.2016.08.046.

[113] A.K. Kumar, S. Sharma, Recent updates on different methods of pretreatment of lignocellulosic feedstocks: a review, Bioresour Bioprocess 4 (2017). https://doi.org/10.1186/s40643-017-0137-9.

[114] D.W.S. Wong, Amylolytic Enzymes, in: Food Enzymes, Springer US, Boston, MA, 1995: pp. 37–84. https://doi.org/10.1007/978-1-4757-2349-6_3.

[115] C.H.A. Che Hussian, W.Y. Leong, Thermostable enzyme research advances: a bibliometric analysis, Journal of Genetic Engineering and Biotechnology 21 (2023) 37. https://doi.org/10.1186/s43141-023-00494-w.

[116] K.L. Kindle, Characteristics and production of thermostable α-amylase, Appl Biochem Biotechnol 8 (1983) 153–170. https://doi.org/10.1007/BF02778096.

[117] P. Kumar, T. Satyanarayana, Microbial glucoamylases: characteristics and applications, Crit Rev Biotechnol 29 (2009) 225–255. https://doi.org/10.1080/07388550903136076.

[118] H.M. El Mashad, L. Zhao, R. Zhang, Z. Pan, Integrated Processing Technologies for Food and Agricultural By-Products, 2019.

[119] B.B. Network, Pre-treatments to enhance the enzymatic saccharification of lignocellulose: technological and economic aspects Commissioned by the, n.d. https://angliasciencewriting.com/.

[120] H. Chen, Lignocellulose biorefinery feedstock engineering, in: Lignocellulose Biorefinery Engineering, Elsevier, 2015: pp. 37–86. https://doi.org/10.1016/B978-0-08-100135-6.00003-X.

[121] J. Fuchs, J.C. Schmid, S. Müller, A.M. Mauerhofer, F. Benedikt, H. Hofbauer, The impact of gasification temperature on the process characteristics of sorption enhanced reforming of biomass, Biomass Convers Biorefin 10 (2020) 925–936. https://doi.org/10.1007/s13399-019-00439-9.

[122] W.N.W. Salleh, A.F. Ismail, 1.13 Preparation of Carbon Membranes for Gas Separation, in: Comprehensive Membrane Science and Engineering, Elsevier, 2017: pp. 330–357. https://doi.org/10.1016/B978-0-12-409547-2.12241-3.

[123] R. Chatterjee, B. Sajjadi, W.Y. Chen, D.L. Mattern, N. Hammer, V. Raman, A. Dorris, Effect of Pyrolysis Temperature on PhysicoChemical Properties and Acoustic-Based Amination of Biochar for Efficient CO2 Adsorption, Front Energy Res 8 (2020). https://doi.org/10.3389/fenrg.2020.00085.

[124] T. Tsoutsos, D. Bethanis, Optimization of the dilute acid hydrolyzator for cellulose-to-bioethanol saccharification, Energies (Basel) 4 (2011) 1601–1623. https://doi.org/10.3390/en4101601.

[125] R. Bayitse, X. Hou, A.-B. Bjerre, F.K. Saalia, Optimisation of enzymatic hydrolysis of cassava peel to produce fermentable sugars, AMB Express 5 (2015) 60. https://doi.org/10.1186/s13568-015-0146-z.

[126] K. Yoonan, J. Kongkiattikajorn, A Study of Optimal Conditions for Reducing Sugars Production, Kasetsart Journal: Natural Science 35 (2004) 29–35.

[127] E.O. Ajala, M.A. Ajala, I.A. Tijani, A.A. Adebisi, I. Suru, Kinetics modelling of acid hydrolysis of cassava (Manihot esculanta Cranz) peel and its hydrolysate chemical characterisation, J King Saud Univ Sci 32 (2020) 2284–2292. https://doi.org/10.1016/j.jksus.2020.03.003.

[128] A.L. Woiciechowski, S. Nitsche, A. Pandey, C.R. Soccol, Acid and enzymatic hydrolysis to recover reducing sugars from cassava bagasse: an economic study, Brazilian Archives of Biology and Technology 45 (2002) 393–400. https://doi.org/10.1590/S1516-89132002000300018.

[129] D. Montané, High-temperature dilute-acid hydrolysis of olive stones for furfural production, Biomass Bioenergy 22 (2002) 295–304. https://doi.org/10.1016/S0961-9534(02)00007-7.

[130] A. Pandey, C.R. Soccol, P. Nigam, V.T. Soccol, L.P.S. Vandenberghe, R. Mohan, Biotechnological potential of agroindustrial residues. II: cassava bagasse, Bioresour Technol 74 (2000) 81–87. https://doi.org/10.1016/S0960-8524(99)00143-1.

[131] V. Okudoh, C. Trois, T. Workneh, S. Schmidt, The potential of cassava biomass and applicable technologies for sustainable biogas production in South Africa: a review, Renewable and Sustainable Energy Reviews 39 (2014) 1035–1052. https://doi.org/10.1016/j.rser.2014.07.142.

[132] A. Parmar, B. Sturm, O. Hensel, Crops that feed the world: production and improvement of cassava for food, feed, and industrial uses, Food Secur 9 (2017) 907–927. https://doi.org/10.1007/s12571-017-0717-8.

[133] N. Thongchul, S. Navankasattusas, S.-T. Yang, Production of lactic acid and ethanol by Rhizopus oryzae integrated with cassava pulp hydrolysis, Bioprocess Biosyst Eng 33 (2010) 407–416. https://doi.org/10.1007/s00449-009-0341-x.

[134] X. Shi, Y. Chen, H. Ren, D. Liu, T. Zhao, N. Zhao, H. Ying, Economically enhanced succinic acid fermentation from cassava bagasse hydrolysate using Corynebacterium glutamicum immobilized in porous polyurethane filler, Bioresour Technol 174 (2014) 190–197. https://doi.org/10.1016/j.biortech.2014.09.137.

[135] M.K. Mtunguja, D.M. Beckles, H.S. Laswai, J.C. Ndunguru, N.J. Sinha, Opportunities to commercialize cassava production for poverty alleviation and improved food security in Tanzania, African Journal of Food, Agriculture, Nutrition and Development 19 (2019) 13928–13946. https://doi.org/10.18697/AJFAND.84.BLFB1037.

[136] M.O. Aremu, S.K. Layokun, B.O. Solomon, Production of Poly (3-hydroxybutyrate) from cassava starch hydrolysate by Pseudomonas aeruginosa NCIB 950, American Journal of Scientific and Industrial Research 1 (2010) 421–426. https://doi.org/10.5251/ajsir.2010.1.3.421.426.

[137] M.R. Yates, C.Y. Barlow, Life cycle assessments of biodegradable, commercial biopolymers—A critical review, Resour Conserv Recycl 78 (2013) 54–66. https://doi.org/10.1016/j.resconrec.2013.06.010.

[138] J. Lu, R.C. Tappel, C.T. Nomura, Mini-review: biosynthesis of Poly(hydroxyalkanoates), Polymer Reviews 49 (2009) 226–248. https://doi.org/10.1080/15583720903048243.

[139] K.W. Meereboer, M. Misra, A.K. Mohanty, Review of recent advances in the biodegradability of polyhydroxyalkanoate (PHA) bioplastics and their composites, Green Chemistry 22 (2020) 5519–5558. https://doi.org/10.1039/d0gc01647k.

[140] X. Fei, J. Wang, X. Zhang, Z. Jia, Y. Jiang, X. Liu, Recent Progress on Bio-Based Polyesters Derived from 2,5-Furandicarbonxylic Acid (FDCA), Polymers (Basel) 14 (2022) 625. https://doi.org/10.3390/polym14030625.

[141] Markets and Markets, Polyhydroxyalkanoate (PHA) market by type (short chain length, medium chain length), production method (sugar fermentation, vegetable oil fermentation, methane fermentation), application, and region-global forecast to 2024, 2019.

[142] Knowledge Hub, Hya Bioplastics - Biodegradable packaging from plants, (2021). https://knowledge-hub.circle-lab.com/article/7874?n=Hya-Bioplastics---Biodegradable-packaging-from-plants.

[143] Plastics Technology, Prices bottom out for polyolefins; PET, PS, PVC move up, (2017). https://www.ptonline.com/articles/prices-bottom-out-for-polyolefins-pet-ps-pvc-move-up (accessed May 6, 2020).

[144] C. Kourmentza, J. Plácido, N. Venetsaneas, A. Burniol-Figols, C. Varrone, H.N. Gavala, M.A.M. Reis, Recent advances and challenges towards sustainable Polyhydroxyalkanoate (PHA) production, Bioengineering 4 (2017) 55. https://doi.org/10.3390/bioengineering4020055.

[145] D. Jendrossek, R. Handrick, Microbial degradation of polyhydroxyalkanoates, Annu Rev Microbiol 56 (2002) 403–432. https://doi.org/10.1146/annurev.micro.56.012302.160838.

[146] D. Jendrossek, R. Handrick, Microbial degradation of polyhydroxyalkanoates, Annu Rev Microbiol 56 (2002) 403–432. https://doi.org/10.1146/annurev.micro.56.012302.160838.

[147] B. Kunasundari, K. Sudesh, Isolation and recovery of microbial polyhydroxyalkanoates, Express Polym Lett 5 (2011) 620–634. https://doi.org/10.3144/expresspolymlett.2011.60.

[148] K. Sudesh, H. Abe, Y. Doi, Synthesis, structure and properties of polyhydroxyalkanoates: biological polyesters, Progress in Polymer Science (Oxford) 25 (2000) 1503–1555. https://doi.org/10.1016/S0079-6700(00)00035-6.

[149] Q. Zhuang, Q. Wang, Q. Liang, Q. Qi, Synthesis of polyhydroxyalkanoates from glucose that contain medium-chain-length monomers via the reversed fatty acid β-oxidation cycle in Escherichia coli, Metab Eng 24 (2014) 78–86. https://doi.org/10.1016/j.ymben.2014.05.004.

[150] J. Gao, J.A. Ramsay, B.A. Ramsay, Fed-batch production of poly-3-hydroxydecanoate from decanoic acid, J Biotechnol 218 (2016) 102–107. https://doi.org/10.1016/j.jbiotec.2015.12.012.

[151] A. Sukan, I. Roy, T. Keshavarz, Agro-industrial waste materials as substrates for the production of poly(3-hydroxybutyric acid), J Biomater Nanobiotechnol 05 (2014) 229–240. https://doi.org/10.4236/jbnb.2014.54027.

[152] A. Steinbüchel, Molecular basis for biosynthesis and accumulation of polyhydroxyalkanoic acids in bacteria, FEMS Microbiol Lett 103 (1992) 217–230. https://doi.org/10.1016/0378-1097(92)90313-D.

[153] S. Obruca, P. Sedlacek, E. Slaninova, I. Fritz, C. Daffert, K. Meixner, Z. Sedrlova, M. Koller, Novel unexpected functions of PHA granules, Appl Microbiol Biotechnol 104 (2020) 4795–4810. https://doi.org/10.1007/s00253-020-10568-1.

[154] D. Jendrossek, Polyhydroxyalkanoate granules are complexsSubcellular organelles (carbonosomes), J Bacteriol 191 (2009) 3195–3202. https://doi.org/10.1128/JB.01723-08.

[155] D. Jendrossek, D. Pfeiffer, New insights in the formation of polyhydroxyalkanoate granules (carbonosomes) and novel functions of poly(3-hydroxybutyrate), Environ Microbiol 16 (2014) 2357–2373. https://doi.org/10.1111/1462-2920.12356.

[156] A. Steinbüchel, Molecular basis for biosynthesis and accumulation of polyhydroxyalkanoic acids in bacteria, FEMS Microbiol Lett 103 (1992) 217–230. https://doi.org/10.1016/0378-1097(92)90313-D.

[157] H. Moralejo-Gárate, R. Kleerebezem, A. Mosquera-Corral, M.C.M. van Loosdrecht, Impact of oxygen limitation on glycerol-based biopolymer production by bacterial enrichments, Water Res 47 (2013) 1209–1217. https://doi.org/10.1016/j.watres.2012.11.039.

[158] C. Kourmentza, I. Ntaikou, G. Lyberatos, M. Kornaros, Polyhydroxyalkanoates from Pseudomonas sp. using synthetic and olive mill wastewater under limiting conditions, Int J Biol Macromol 74 (2015) 202–210. https://doi.org/10.1016/j.ijbiomac.2014.12.032.

[159] S.K. Bhatia, J.-H. Kim, M.-S. Kim, J. Kim, J.W. Hong, Y.G. Hong, H.-J. Kim, J.-M. Jeon, S.-H. Kim, J. Ahn, H. Lee, Y.-H. Yang, Production of (3-hydroxybutyrate-co-3-hydroxyhexanoate) copolymer from coffee waste oil using engineered Ralstonia eutropha, Bioprocess Biosyst Eng 41 (2018) 229–235. https://doi.org/10.1007/s00449-017-1861-4.

[160] B.H.A. Rehm, Polyester synthases: natural catalysts for plastics, Biochemical Journal 376 (2003) 15–33. https://doi.org/10.1042/BJ20031254.

[161] M.S. Morlino, R. Serna García, F. Savio, G. Zampieri, T. Morosinotto, L. Treu, S. Campanaro, Cupriavidus necator as a platform for polyhydroxyalkanoate production: An overview of strains, metabolism, and modeling approaches, Biotechnol Adv 69 (2023) 108264. https://doi.org/10.1016/j.biotechadv.2023.108264.

[162] L. Zhang, Z. Jiang, T.-H. Tsui, K.-C. Loh, Y. Dai, Y.W. Tong, A Review on Enhancing Cupriavidus necator Fermentation for Poly(3-hydroxybutyrate) (PHB) Production From Low-Cost Carbon Sources, Front Bioeng Biotechnol 10 (2022). https://doi.org/10.3389/fbioe.2022.946085.

[163] M.J. de Smet, G. Eggink, B. Witholt, J. Kingma, H. Wynberg, Characterization of intracellular inclusions formed by Pseudomonas oleovorans during growth on octane, J Bacteriol 154 (1983) 870–878. https://doi.org/10.1128/jb.154.2.870-878.1983.

[164] S.Y. Choi, M.N. Rhie, H.T. Kim, J.C. Joo, I.J. Cho, J. Son, S.Y. Jo, Y.J. Sohn, K.-A. Baritugo, J. Pyo, Y. Lee, S.Y. Lee, S.J. Park, Metabolic engineering for the synthesis of polyesters: a 100-year journey from polyhydroxyalkanoates to non-natural microbial polyesters, Metab Eng 58 (2020) 47–81. https://doi.org/10.1016/j.ymben.2019.05.009.

[165] Y. Gao, C. Liu, Y. Ding, C. Sun, R. Zhang, M. Xian, G. Zhao, Development of genetically stable Escherichia coli strains for poly(3-hydroxypropionate) production, PLoS One 9 (2014) e97845. https://doi.org/10.1371/journal.pone.0097845.

[166] S. Obruca, P. Benesova, J. Oborna, I. Marova, Application of protease-hydrolyzed whey as a complex nitrogen source to increase poly(3-hydroxybutyrate) production from oils by Cupriavidus necator, Biotechnol Lett 36 (2014) 775–781. https://doi.org/10.1007/s10529-013-1407-z.

[167] M. Miranda De Sousa Dias, M. Koller, D. Puppi, A. Morelli, F. Chiellini, G. Braunegg, Fed-batch synthesis of poly(3-hydroxybutyrate) and poly(3-hydroxybutyrate-co-4-hydroxybutyrate) from sucrose and 4-hydroxybutyrate precursors by Burkholderia sacchari strain DSM 17165, Bioengineering 4 (2017) 36. https://doi.org/10.3390/bioengineering4020036.

[168] J. Gao, J.A. Ramsay, B.A. Ramsay, Fed-batch production of poly-3-hydroxydecanoate from decanoic acid, J Biotechnol 218 (2016) 102–107. https://doi.org/10.1016/j.jbiotec.2015.12.012.

[169] P. Kanjanachumpol, S. Kulpreecha, V. Tolieng, N. Thongchul, Enhancing polyhydroxybutyrate production from high cell density fed-batch fermentation of Bacillus megaterium BA-019, Bioprocess Biosyst Eng 36 (2013) 1463–1474. https://doi.org/10.1007/s00449-013-0885-7.

[170] J.-W. Hong, H.-S. Song, Y.-M. Moon, Y.-G. Hong, S.K. Bhatia, H.-R. Jung, T.-R. Choi, S. Yang, H.-Y. Park, Y.-K. Choi, Y.-H. Yang, Polyhydroxybutyrate production in halophilic marine bacteria Vibrio proteolyticus isolated from the Korean peninsula, Bioprocess Biosyst Eng 42 (2019) 603–610. https://doi.org/10.1007/s00449-018-02066-6.

[171] Y. Gao, C. Liu, Y. Ding, C. Sun, R. Zhang, M. Xian, G. Zhao, Development of genetically stable Escherichia coli strains for poly(3-hydroxypropionate) production, PLoS One 9 (2014) e97845. https://doi.org/10.1371/journal.pone.0097845.

[172] R. Shen, J. Yin, J.-W. Ye, R.-J. Xiang, Z.-Y. Ning, W.-Z. Huang, G.-Q. Chen, Promoter engineering for enhanced P(3HB- co -4HB) production by Halomonas bluephagenesis, ACS Synth Biol 7 (2018) 1897–1906. https://doi.org/10.1021/acssynbio.8b00102.

[173] I. Orita, K. Nishikawa, S. Nakamura, T. Fukui, Biosynthesis of polyhydroxyalkanoate copolymers from methanol by Methylobacterium extorquens AM1 and the engineered strains under cobalt-deficient conditions, Appl Microbiol Biotechnol 98 (2014) 3715–3725. https://doi.org/10.1007/s00253-013-5490-9.

[174] R. V. Nonato, P.E. Mantelatto, C.E.V. Rossell, Integrated production of biodegradable plastic, sugar and ethanol, Appl Microbiol Biotechnol 57 (2001) 1–5. https://doi.org/10.1007/s002530100732.

[175] H. Jørgensen, J.B. Kristensen, C. Felby, Enzymatic conversion of lignocellulose into fermentable sugars: challenges and opportunities, Biofuels, Bioproducts and Biorefining 1 (2007) 119–134. https://doi.org/10.1002/bbb.4.

[176] T. Volova, E. Kiselev, O. Vinogradova, E. Nikolaeva, A. Chistyakov, A. Sukovatiy, E. Shishatskaya, A glucose-utilizing strain, Cupriavidus euthrophus B-10646: growth kinetics, characterization and synthesis of multicomponent PHAs, PLoS One 9 (2014) e87551. https://doi.org/10.1371/journal.pone.0087551.

[177] B.B. Salgaonkar, K. Mani, J.M. Bragança, Sustainable bioconversion of cassava waste to poly(3-hydroxybutyrate-co-3-hydroxyvalerate) by Halogeometricum borinquense strain E3, J Polym Environ 27 (2019) 299–308. https://doi.org/10.1007/s10924-018-1346-9.

[178] D.A. da Silva, R.V. Antonio, J.M. Rossi, R. da S. Pena, Production of medium-chain-length polyhydroxyalkanoate by Pseudomonas oleovorans grown in sugary cassava extract supplemented with andiroba oil, Food Science and Technology (Campinas) 34 (2014) 738–745. https://doi.org/10.1590/1678-457X.6465.

[179] A. Farghaly, A.M. Enitan, S. Kumari, F. Bux, A. Tawfik, Polyhydroxyalkanoates production from fermented paperboard mill wastewater using acetate-enriched bacteria, Clean Technol Environ Policy 19 (2017) 935–947. https://doi.org/10.1007/s10098-016-1286-9.

[180] F. Ahmadi, A.A. Zinatizadeh, A. Asadi, T. McKay, S. Azizi, Simultaneous carbon and nutrients removal and PHA production in a novel single air lift bioreactor treating an industrial wastewater, Environ Technol Innov 18 (2020) 100776. https://doi.org/10.1016/j.eti.2020.100776.

[181] M.K. Gouda, A.E. Swellam, S.H. Omar, Production of PHB by a Bacillus megaterium strain using sugarcane molasses and corn steep liquor as sole carbon and nitrogen sources, Microbiol Res 156 (2001) 201–207. https://doi.org/10.1078/0944-5013-00104.

[182] F. Ahmadi, A.A. Zinatizadeh, A. Asadi, The effect of different operational strategies on polyhydroxyalkanoates (PHAs) production at short-term biomass enrichment, J Environ Chem Eng 8 (2020) 103531. https://doi.org/10.1016/j.jece.2019.103531.

[183] Research and Markets, Global polyhydroxyalkanoate (PHA) market analysis & trends - Industry forecast to 2025, 2017.

[184] European Bioplastics, Bioplastics market development update 2023, (n.d.).

[185] Research and Markets, Global polyhydroxyalkanoate (PHA) market analysis & trends - Industry forecast to 2025, 2017.

[186] C. Nielsen, A. Rahman, A.U. Rehman, M.K. Walsh, C.D. Miller, Food waste conversion to microbial polyhydroxyalkanoates, Microb Biotechnol 10 (2017) 1338–1352. https://doi.org/10.1111/1751-7915.12776.

[187] R.K. Padi, A. Chimphango, Feasibility of commercial waste biorefineries for cassava starch industries: techno-economic assessment, Bioresour Technol 297 (2020) 122461. https://doi.org/10.1016/j.biortech.2019.122461.

[188] R.K. Padi, A. Chimphango, Feasibility of commercial waste biorefineries for cassava starch industries: Techno-economic assessment, Bioresour Technol 297 (2020) 122461. https://doi.org/10.1016/j.biortech.2019.122461.

[189] M.K. Patel, A. Bechu, J.D. Villegas, M. Bergez-Lacoste, K. Yeung, R. Murphy, J. Woods, O.N. Mwabonje, Y. Ni, A.D. Patel, J. Gallagher, D. Bryant, Second-generation bio-based plastics are becoming a reality - Non-renewable energy and greenhouse gas (GHG) balance of succinic acid-based plastic end products made from lignocellulosic biomass, Biofuels, Bioproducts and Biorefining 12 (2018) 426–441. https://doi.org/10.1002/bbb.1849.

[190] G. Du, L. Liu, J. Chen, White biotechnology for organic acids, in: Industrial Borefineries & White Biotechnology, Elsevier, 2015: pp. 409–444.

[191] Grand View Research, Key companies & market share insights succinic acid market report scope, 2016.

[192] Markets and Markets, Bioethanol market by feedstock (starch based, sugar based, cellulose based), end-use industry (transportation, pharmaceuticals, cosmetics, alcoholic beverages), fuel blend (E5, E10, E15 to E70, E75 & E85), and region - Global forecast to 2025, 2020.

[193] X.Z. Tang, P. Kumar, S. Alavi, K.P. Sandeep, Recent advances in biopolymers and biopolymer-based nanocomposites for food packaging materials, Crit Rev Food Sci Nutr 52 (2012) 426–442. https://doi.org/10.1080/10408398.2010.500508.

[194] K.G. Harding, J.S. Dennis, H. von Blottnitz, S.T.L. Harrison, Environmental analysis of plastic production processes: comparing petroleum-based polypropylene and polyethylene with biologically-based poly-β-hydroxybutyric acid using life cycle analysis, J Biotechnol 130 (2007) 57–66. https://doi.org/10.1016/j.jbiotec.2007.02.012.

[195] S. Kim, B.E. Dale, Energy and greenhouse gas profiles of polyhydroxybutyrates derived from corn grain: a life cycle perspective, Environ Sci Technol 42 (2008) 7690–7695. https://doi.org/10.1021/es8004199.

[196] Z.W. Zhong, B. Song, C.X. Huang, Environmental impacts of three polyhydroxyalkanoate (PHA) manufacturing processes, Materials and Manufacturing Processes 24 (2009) 519–523. https://doi.org/10.1080/10426910902740120.

[197] C.R. Álvarez-Chávez, S. Edwards, R. Moure-Eraso, K. Geiser, Sustainability of bio-based plastics: general comparative analysis and recommendations for improvement, J Clean Prod 23 (2012) 47–56. https://doi.org/10.1016/j.jclepro.2011.10.003.

[198] A. Kendall, A life cycle assessment of biopolymer production from material recovery facility residuals, Resour Conserv Recycl 61 (2012) 69–74. https://doi.org/10.1016/j.resconrec.2012.01.008.

[199] A. Kendall, A life cycle assessment of biopolymer production from material recovery facility residuals, Resour Conserv Recycl 61 (2012) 69–74. https://doi.org/10.1016/j.resconrec.2012.01.008.

[200] C. Isola, H.L. Sieverding, R. Raghunathan, M.P. Sibi, D.C. Webster, J. Sivaguru, J.J. Stone, Life cycle assessment of photodegradable polymeric material derived from renewable bioresources, J Clean Prod 142 (2017) 2935–2944. https://doi.org/10.1016/j.jclepro.2016.10.177.

[201] K. Yoonan, J. Kongkiattikajorn, A Study of Optimal Conditions for Reducing Sugars Production, Kasetsart Journal: Natural Science 35 (2004) 29–35.

[202] Z.L. Liu, P.J. Slininger, B.S. Dien, M.A. Berhow, C.P. Kurtzman, S.W. Gorsich, Adaptive response of yeasts to furfural and 5-hydroxymethylfurfural and new chemical evidence for HMF conversion to 2,5-bis-hydroxymethylfuran, J Ind Microbiol Biotechnol 31 (2004) 345–352. https://doi.org/10.1007/s10295-004-0148-3.

[203] C. Arce, L. Kratky, Mechanical pretreatment of lignocellulosic biomass toward enzymatic/fermentative valorization, IScience 25 (2022). https://doi.org/10.1016/j.isci. 2022.104610.

[204] S. Susanti, D. Al Karoma, D. Mulyani, M. Masruri, Physical Properties and Characterization of Cassava Peel Waste Modified by Esterification, The Journal of Pure and Applied Chemistry Research 6 (2017) 255–260. https://doi.org/10.21776/ub.jpacr.2017.006.03.346.

[205] S. Widiarto, S.D. Yuwono, A. Rochliadi, I.M. Arcana, Preparation and Characterization of Cellulose and Nanocellulose from Agro-industrial Waste - Cassava Peel, IOP Conf Ser Mater Sci Eng 176 (2017) 012052. https://doi.org/10.1088/1757-899X/176/1/012052.

[206] Z. Daud, H. Awang, A.S.M. Kassim, M.Z.M. Hatta, A.M. Aripin, Comparison of Pineapple Leaf and Cassava Peel by Chemical Properties and Morphology Characterization, Adv Mat Res 974 (2014) 384–388. https://doi.org/10.4028/www.scientific.net/AMR.974.384.

[207] R. Kayiwa, H. Kasedde, M. Lubwama, J.B. Kirabira, Characterization and pre-leaching effect on the peels of predominant cassava varieties in Uganda for production of activated carbon, Current Research in Green and Sustainable Chemistry 4 (2021) 100083. https://doi.org/10.1016/j.crgsc.2021.100083.

[208] S. Widiarto, E. Pramono, Suharso, A. Rochliadi, I.M. Arcana, Cellulose Nanofibers Preparation from Cassava Peels via Mechanical Disruption, Fibers 7 (2019) 44. https://doi.org/10.3390/fib7050044.

[209] M. Asadieraghi, W.M.A. Wan Daud, Characterization of lignocellulosic biomass thermal degradation and physiochemical structure: Effects of demineralization by diverse acid solutions, Energy Convers Manag 82 (2014) 71–82. https://doi.org/10.1016/j.enconman.2014.03.007.

[210] G.S. Aruwajoye, F.D. Faloye, E.G. Kana, Process Optimisation of Enzymatic Saccharification of Soaking Assisted and Thermal Pretreated Cassava Peels Waste for Bioethanol Production, Waste Biomass Valorization 11 (2020) 2409–2420. https://doi.org/10.1007/s12649-018-00562-0.

[211] S. Idris, R. Shamsudin, M.Z.M. Nor, M.N. Mokhtar, S.S. Abdul Gani, Physicochemical composition of different parts of cassava (Manihot esculenta Crantz) plant, Food Res 4 (2020) 78–84. https://doi.org/10.26656/fr.2017.4(S1).S33.

[212] H.-S. Kim, S. Kim, H.-J. Kim, H.-S. Yang, Thermal properties of bio-flour-filled polyolefin composites with different compatibilizing agent type and content, Thermochim Acta 451 (2006) 181–188. https://doi.org/10.1016/j.tca.2006.09.013.

[213] S. Ismail, N. Mansor, Z. Man, A Study on Thermal Behaviour of Thermoplastic Starch Plasticized by [Emim] Ac and by [Emim] Cl, Procedia Eng 184 (2017) 567–572. https://doi.org/10.1016/j.proeng.2017.04.138.

[214] M. Poletto, A.J. Zattera, M.M.C. Forte, R.M.C. Santana, Thermal decomposition of wood: Influence of wood components and cellulose crystallite size, Bioresour Technol 109 (2012) 148–153. https://doi.org/10.1016/j.biortech.2011.11.122.

[215] X. Liu, Y. Wang, L. Yu, Z. Tong, L. Chen, H. Liu, X. Li, Thermal degradation and stability of starch under different processing conditions, Starch - Stärke 65 (2013) 48–60. https://doi.org/10.1002/star.201200198.

[216] L. Hu, X.-Y. Wei, X.-H. Guo, H.-P. Lv, G.-H. Wang, Investigation on the kinetic behavior, thermodynamic and volatile products analysis of chili straw waste pyrolysis, J Environ Chem Eng 9 (2021) 105859. https://doi.org/10.1016/j.jece.2021.105859.

[217] A. Al-Rumaihi, P. Parthasarathy, A. Fernandez, T. Al-Ansari, H.R. Mackey, R. Rodriguez, G. Mazza, G. McKay, Thermal degradation characteristics and kinetic study of camel manure pyrolysis, J Environ Chem Eng 9 (2021). https://doi.org/10.1016/j.jece.2021.106071.

[218] K. Aup-Ngoen, M. Noipitak, Effect of carbon-rich biochar on mechanical properties of PLA-biochar composites, Sustain Chem Pharm 15 (2020) 100204. https://doi.org/10.1016/j.scp.2019.100204.

[219] J.B. Sluiter, K.P. Michel, B. Addison, Y. Zeng, W. Michener, A.L. Paterson, F.A. Perras, E.J. Wolfrum, Direct determination of cellulosic glucan content in starch-containing samples, Cellulose 28 (2021) 1989–2002. https://doi.org/10.1007/s10570-020-03652-2.

[220] L. Wei, T. Yan, Y. Wu, H. Chen, B. Zhang, Optimization of alkaline extraction of hemicellulose from sweet sorghum bagasse and its direct application for the production of acidic xylooligosaccharides by Bacillus subtilis strain MR44, PLoS One 13 (2018) e0195616. https://doi.org/10.1371/journal.pone.0195616.

[221] J. Kong-Win Chang, X. Duret, V. Berberi, H. Zahedi-Niaki, J.-M. Lavoie, Two-Step Thermochemical Cellulose Hydrolysis With Partial Neutralization for Glucose Production, Front Chem 6 (2018). https://doi.org/10.3389/fchem.2018.00117.

[222] I.K. Hindrichsen, M. Kreuzer, J. Madsen, K.E.B. Knudsen, Fiber and Lignin Analysis in Concentrate, Forage, and Feces: Detergent Versus Enzymatic-Chemical Method, J Dairy Sci 89 (2006) 2168–2176. https://doi.org/10.3168/jds.S0022-0302(06)72287-1.

[223] N. Paksung, J. Pfersich, P.J. Arauzo, D. Jung, A. Kruse, Structural Effects of Cellulose on Hydrolysis and Carbonization Behavior during Hydrothermal Treatment, ACS Omega 5 (2020) 12210–12223. https://doi.org/10.1021/acsomega.0c00737.

[224] V. Pasangulapati, K.D. Ramachandriya, A. Kumar, M.R. Wilkins, C.L. Jones, R.L. Huhnke, Effects of cellulose, hemicellulose and lignin on thermochemical conversion characteristics of the selected biomass, Bioresour Technol 114 (2012) 663–669. https://doi.org/10.1016/j.biortech.2012.03.036.

[225] T.C. Egbosiuba, Biochar and bio-oil fuel properties from nickel nanoparticles assisted pyrolysis of cassava peel, Heliyon 8 (2022) e10114. https://doi.org/10.1016/j.heliyon.2022.e10114.

[226] S. Sukarni, M.R. Ramadhan, Pyrolytic Characteristics and Kinetic Parameters Evaluation of Cassava Stalks Using Thermogravimetric Analyzer, Key Eng Mater 851 (2020) 137–141. https://doi.org/10.4028/www.scientific.net/KEM.851.137.

[227] H.I. Owamah, Biosorptive removal of Pb(II) and Cu(II) from wastewater using activated carbon from cassava peels, J Mater Cycles Waste Manag 16 (2014) 347–358. https://doi.org/10.1007/s10163-013-0192-z.

[228] J. Fonseca, A. Albis, A.R. Montenegro, Evaluation of zinc adsorption using cassava peels (Manihot esculenta) modified with citric acid, Contemporary Engineering Sciences 11 (2018) 3575–3585. https://doi.org/10.12988/ces.2018.87364.

[229] M.F. Aller, Biochar properties: Transport, fate, and impact, Crit Rev Environ Sci Technol 46 (2016) 1183–1296. https://doi.org/10.1080/10643389.2016.1212368.

[230] N.S. Pooja, G. Padmaja, Enhancing the Enzymatic Saccharification of Agricultural and Processing Residues of Cassava through Pretreatment Techniques, Waste Biomass Valorization 6 (2015) 303–315. https://doi.org/10.1007/s12649-015-9345-8.

[231] N.S. Pooja, M.S. Sajeev, M.L. Jeeva, G. Padmaja, Bioethanol production from microwave-assisted acid or alkali-pretreated agricultural residues of cassava using separate hydrolysis and fermentation (SHF), 3 Biotech 8 (2018) 69. https://doi.org/10.1007/s13205-018-1095-4.

[232] M.U. Ude, I. Oluka, P.C. Eze, Optimization and kinetics of glucose production via enzymatic hydrolysis of mixed peels, Journal of Bioresources and Bioproducts 5 (2020) 283–290. https://doi.org/10.1016/j.jobab.2020.10.007.

[233] P. Alain, K. Nanssou, Y. Jiokap, Pretreatment of cassava stems and peelings by thermohydrolysis to enhance hydrolysis yield of cellulose in bioethanol production process, Renew Energy 97 (2016) 252–265. https://doi.org/10.1016/j.renene.2016.05.050.

[234] C.O. Ofuya, S.N. Obilor, The suitability of fermented cassava peel as a poultry feedstuff, Bioresour Technol 44 (1993) 101–104. https://doi.org/10.1016/0960-8524(93)90181-A.

[235] E. Menya, P.W. Olupot, H. Storz, M. Lubwama, Y. Kiros, Characterization and alkaline pretreatment of rice husk varieties in Uganda for potential utilization as precursors in the production of activated carbon and other value-added products, Waste Management 81 (2018) 104–116. https://doi.org/10.1016/j.wasman.2018.09.050.

[236] C. Tejada-Tovar, A.D. Gonzalez-Delgado, A. Villabona-Ortiz, Characterization of Residual Biomasses and Its Application for the Removal of Lead Ions from Aqueous Solution, Applied Sciences 9 (2019) 4486. https://doi.org/10.3390/app9214486.

[237] S. Kim, Diffusion of sulfuric acid within lignocellulosic biomass particles and its impact on dilute-acid pretreatment, Bioresour Technol 83 (2002) 165–171. https://doi.org/10.1016/S0960-8524(01)00197-3.

[238] G. Lee, S. In Park, H. Yi Shin, H.-I. Joh, S.-S. Kim, S. Lee, Simultaneous reactions of sulfonation and condensation for high-yield conversion of polystyrene into carbonaceous material, Journal of Industrial and Engineering Chemistry 122 (2023) 426–436. https://doi.org/10.1016/j.jiec.2023.02.042.

[239] E. Lizundia, F. Luzi, D. Puglia, Organic waste valorisation towards circular and sustainable biocomposites, Green Chemistry 24 (2022) 5429–5459. https://doi.org/10.1039/D2GC01668K.

[240] A. Parihar, J. Vongsvivut, S. Bhattacharya, Synchrotron-Based Infra-Red Spectroscopic Insights on Thermo-Catalytic Conversion of Cellulosic Feedstock to Levoglucosenone and Furans, ACS Omega 4 (2019) 8747–8757. https://doi.org/10.1021/acsomega.8b03681.

[241] M.N. Ikhwan Musa, T. Marimuthu, H.N. Mohd Rashid, K.P. Sambasevam, Development of pH indicator film composed of corn starch-glycerol and anthocyanin from hibiscus sabdariffa, Malaysian Journal of Chemistry 22 (2020) 19–24.

[242] F. Hu, A. Ragauskas, Suppression of pseudo-lignin formation under dilute acid pretreatment conditions, RSC Adv. 4 (2014) 4317–4323. https://doi.org/10.1039/C3RA42841A.

[243] M. Becker, K. Ahn, M. Bacher, C. Xu, A. Sundberg, S. Willför, T. Rosenau, A. Potthast, Comparative hydrolysis analysis of cellulose samples and aspects of its application in conservation science, Cellulose 28 (2021) 8719–8734. https://doi.org/10.1007/s10570-021-04048-6.

[244] S. Mohd-Asharuddin, N. Othman, N.S. Mohd Zin, H.A. Tajarudin, A Chemical and Morphological Study of Cassava Peel: A Potential Waste as Coagulant Aid, MATEC Web of Conferences 103 (2017) 06012. https://doi.org/10.1051/matecconf/201710306012.

[245] M.I. Ruiz, C.I. Sanchez, R.G. Torrres, D.R. Molina, Enzymatic hydrolysis of cassava starch for production of bioethanol with a colombian wild yeast strain, J Braz Chem Soc 22 (2011) 2337–2343. https://doi.org/10.1590/S0103-50532011001200014.

[246] J.I. Ona, P.J. Halling, M. Ballesteros, Enzyme hydrolysis of cassava peels: treatment by amylolytic and cellulolytic enzymes, Biocatal Biotransformation 37 (2019) 77–85. https://doi.org/10.1080/10242422.2018.1551376.

[247] J.I. Ona, P.J. Halling, M. Ballesteros, Enzyme hydrolysis of cassava peels: treatment by amylolytic and cellulolytic enzymes, Biocatal Biotransformation 37 (2019) 77–85. https://doi.org/10.1080/10242422.2018.1551376.

[248] R. Johnson, G. Padmaja, Comparative Studies on the Production of Glucose and High Fructose Syrup from Tuber Starches, International Research Journal of Biological Sciences 2 (2013) 68–75. www.isca.me.

[249] W.-P. Dorleku, R. Bayitse, A.C.H. Hansen, F.K. Saalia, A.-B. Bjerre, Response surface optimisation of enzymatic hydrolysis of cassava peels without chemical and hydrothermal pretreatment, Biomass Convers Biorefin (2022). https://doi.org/10.1007/s13399-021-02201-6.

[250] A. McIntosh, J. Pontius, Tools and Skills, in: Case Studies for Integrating Science and the Global Environment, Elsevier, 2017: pp. 1–112. https://doi.org/10.1016/B978-0-12-801712-8.00001-9.

[251] A.L. Woiciechowski, S. Nitsche, A. Pandey, C.R. Soccol, Acid and enzymatic hydrolysis to recover reducing sugars from cassava bagasse: An economic study, Brazilian Archives of Biology and Technology 45 (2002) 393–400. https://doi.org/10.1590/S1516-89132002000300018.

[252] B. Saekhow, S. Chookamlang, A. Na-u-dom, N. Leksawasdi, V. Sanguanchaipaiwong, Enzymatic hydrolysis of cassava stems for butanol production of isolated Clostridium sp., Energy Reports 6 (2020) 196–201. https://doi.org/10.1016/j.egyr.2019.08.042.

[253] A.A. Olanbiwoninu, S.A. Odunfa, Enhancing the Production of Reducing Sugars from Cassava Peels by Pretreatment Methods, 2 (2012).

[254] O.E. Onyelucheya, J.T. Nwabanne, C.M. Onyelucheya, O.E. Adeyemo, Acid Hydrolysis Of Cassava Peel, 5 (2016) 184–187.

[255] D.C. Montgomery, MONT, in: Catalysis from A to Z, Wiley, 2020. https://doi.org/10.1002/9783527809080.cataz11063.

[256] J.R. Wagner, E.M. Mount, H.F. Giles, Design of Experiments, in: Extrusion, Elsevier, 2014: pp. 291–308. https://doi.org/10.1016/B978-1-4377-3481-2.00025-9.

[257] N.S. Neta, A.M. Peres, J.A. Teixeira, L.R. Rodrigues, Maximization of fructose esters synthesis by response surface methodology, N Biotechnol 28 (2011) 349–355. https://doi.org/10.1016/j.nbt.2011.02.007.

[258] S. Dong, M.J. Bortner, M. Roman, Analysis of the sulfuric acid hydrolysis of wood pulp for cellulose nanocrystal production: A central composite design study, Ind Crops Prod 93 (2016) 76–87. https://doi.org/10.1016/j.indcrop.2016.01.048.

[259] G.L. Miller, Use of Dinitrosalicylic Acid Reagent for Determination of Reducing Sugar, Anal Chem 31 (1959) 426–428. https://doi.org/10.1021/ac60147a030.

[260] R. Bayitse, X. Hou, A.B. Bjerre, F.K. Saalia, Optimisation of enzymatic hydrolysis of cassava peel to produce fermentable sugars, AMB Express 5 (2015). https://doi.org/10.1186/s13568-015-0146-z.

[261] C. Virunanon, C. Ouephanit, V. Burapatana, Cassava pulp enzymatic hydrolysis process as a preliminary step in bio-alcohols production from waste starchy resources, J Clean Prod 39 (2013) 273–279. https://doi.org/10.1016/j.jclepro.2012.07.055.

[262] R.M. Collares, L.V.S. Miklasevicius, M.M. Bassaco, N.P.G. Salau, M.A. Mazutti, D.A. Bisognin, L.M. Terra, Optimization of enzymatic hydrolysis of cassava to obtain fermentable sugars, J Zhejiang Univ Sci B 13 (2012) 579–586. https://doi.org/10.1631/jzus.B1100297.

[263] Z. Barati, S. Latif, J. Müller, Enzymatic hydrolysis of cassava peels as potential pre-treatment for peeling of cassava tubers, Biocatal Agric Biotechnol 20 (2019) 101247. https://doi.org/10.1016/j.bcab.2019.101247.

[264] P.K. Robinson, Enzymes: principles and biotechnological applications, Essays Biochem 59 (2015) 1–41. https://doi.org/10.1042/bse0590001.

[265] K.S. Siddiqui, H. Ertan, A. Poljak, W.J. Bridge, Evaluating Enzymatic Productivity—The Missing Link to Enzyme Utility, Int J Mol Sci 23 (2022) 6908. https://doi.org/10.3390/ijms23136908.

[266] E.I. Kashcheyeva, Y.A. Gismatulina, G.F. Mironova, E.K. Gladysheva, V. V. Budaeva, E.A. Skiba, V.N. Zolotuhin, N.A. Shavyrkina, A.N. Kortusov, A.A. Korchagina, Properties and Hydrolysis Behavior of Celluloses of Different Origin, Polymers (Basel) 14 (2022) 3899. https://doi.org/10.3390/polym14183899.

[267] I. Ben Taher, P. Fickers, S. Chniti, M. Hassouna, Optimization of enzymatic hydrolysis and fermentation conditions for improved bioethanol production from potato peel residues, Biotechnol Prog 33 (2017) 397–406. https://doi.org/10.1002/btpr.2427.

[268] S. Sun, L. Zhang, F. Liu, X. Fan, R.-C. Sun, One-step process of hydrothermal and alkaline treatment of wheat straw for improving the enzymatic saccharification, Biotechnol Biofuels 11 (2018) 137. https://doi.org/10.1186/s13068-018-1140-x.

[269] E. Akponah, O.O. Akpomie, O.O. Akponah, E. And Akpomie, Analysis of the suitability of yam , potato and cassava root peels for bioethanol production using Saccharomyces cerevisae, International Research Journal of Microbiology 2 (2011) 393–398. http://interesjournal.org/IRJM/Pdf/2011/November/Akponah and Akpomie.pdf.

[270] K. Chiodza, N.J. Goosen, Influence of mixing speed, solids concentration and enzyme dosage on dry solids yield and protein recovery during enzymatic hydrolysis of sardine (Sardina pilchardus) processing by-products using Alcalase 2.4L: a multivariable optimisation approach, Biomass Convers Biorefin (2023). https://doi.org/10.1007/s13399-023-03829-2.

[271] F.J. Warren, B. Zhang, G. Waltzer, M.J. Gidley, S. Dhital, The interplay of α-amylase and amyloglucosidase activities on the digestion of starch in in vitro enzymic systems, Carbohydr Polym 117 (2015) 192–200. https://doi.org/10.1016/j.carbpol.2014.09.043.

[272] T.C. Nguyen, S. Chu-ky, H.N. Luong, H. Van Nguyen, Effect of Pretreatment Methods on Enzymatic Kinetics of Ungelatinized Cassava Flour Hydrolysis, Catalysts 10 (2020) 760. https://doi.org/10.3390/catal10070760.

[273] H. Kong, X. Yang, Z. Gu, Z. Li, L. Cheng, Y. Hong, C. Li, Heat pretreatment improves the enzymatic hydrolysis of granular corn starch at high concentration, Process Biochemistry 64 (2018) 193–199. https://doi.org/10.1016/j.procbio.2017.09.021.

[274] Z. Abidin, E. Saraswati, T. Naid, Bioethanol production fromwaste of the cassava peel (Manihot eculenta) by acid hydrolysis and fermentation process, Int J Pharmtech Res 6 (2014) 1209–1212.

[275] O. Vega-Castro, E. León, M. Arias, M.T. Cesario, F. Ferreira, M.M.R. da Fonseca, A. Segura, P. Valencia, R. Simpson, H. Nuñez, J. Contreras-Calderon, Characterization and Production of a Polyhydroxyalkanoate from Cassava Peel Waste: Manufacture of Biopolymer Microfibers by Electrospinning, J Polym Environ 29 (2021) 187–200. https://doi.org/10.1007/s10924-020-01861-1.

[276] W. Deng, Y. Feng, J. Fu, H. Guo, Y. Guo, B. Han, Z. Jiang, L. Kong, C. Li, H. Liu, P.T.T. Nguyen, P. Ren, F. Wang, S. Wang, Y. Wang, Y. Wang, S.S. Wong, K. Yan, N. Yan, X. Yang, Y. Zhang, Z. Zhang, X. Zeng, H. Zhou, Catalytic conversion of lignocellulosic biomass into chemicals and fuels, Green Energy & Environment 8 (2023) 10–114. https://doi.org/10.1016/j.gee.2022.07.003.

[277] J.L. Crespo-mariño, E.M. Eds, High performance computing, Aircraft Engineering and Aerospace Technology 77 (2005) 393–400. https://doi.org/10.1108/aeat.2005.12777dab.008.

[278] N. Boudechiche, H. Yazid, M. Trari, Z. Sadaoui, Valorization of Crataegus azarolus stones for the removal of textile anionic dye by central composite rotatable design using cubic model: optimization, isotherm, and kinetic studies, Environmental Science and Pollution Research 24 (2017) 19609–19623. https://doi.org/10.1007/s11356-017-9606-0.

[279] J.F. Kennedy, L. Quinton, Essentials of Carbohydrate Chemistry and Biochemistry, Carbohydr Polym 47 (2002) 87. https://doi.org/10.1016/S0144-8617(01)00274-0.

[280] S. Gámez, J.J. González-Cabriales, J.A. Ramírez, G. Garrote, M. Vázquez, Study of the hydrolysis of sugar cane bagasse using phosphoric acid, J Food Eng 74 (2006) 78–88. https://doi.org/10.1016/j.jfoodeng.2005.02.005.

[281] V.B. Agbor, N. Cicek, R. Sparling, A. Berlin, D.B. Levin, Biomass pretreatment: Fundamentals toward application, Biotechnol Adv 29 (2011) 675–685. https://doi.org/10.1016/j.biotechadv.2011.05.005.

[282] D. Jendrossek, D. Pfeiffer, New insights in the formation of polyhydroxyalkanoate granules (carbonosomes) and novel functions of poly(3-hydroxybutyrate), Environ Microbiol 16 (2014) 2357–2373. https://doi.org/10.1111/1462-2920.12356.

[283] A. Fernández-Castané, H. Li, O.R.T. Thomas, T.W. Overton, Flow cytometry as a rapid analytical tool to determine physiological responses to changing O2 and iron concentration by Magnetospirillum gryphiswaldense strain MSR-1, Sci Rep 7 (2017) 1–11. https://doi.org/10.1038/s41598-017-13414-z.

[284] C. Hierro-Iglesias, M. Masó-Martínez, J. Dulai, K.J. Chong, P.H. Blanco-Sanchez, A. Fernández-Castané, Magnetotactic Bacteria-Based Biorefinery: Potential for Generating Multiple Products from a Single Fermentation, ACS Sustain Chem Eng 9 (2021) 10537–10546. https://doi.org/10.1021/acssuschemeng.1c02435.

[285] D. Crutchik, O. Franchi, L. Caminos, D. Jeison, M. Belmonte, A. Pedrouso, A. Val del Rio, A. Mosquera-Corral, J.L. Campos, Polyhydroxyalkanoates (PHAs) production: A feasible economic option for the treatment of sewage sludge in municipalwastewater treatment plants?, Water (Switzerland) 12 (2020) 1–12. https://doi.org/10.3390/W12041118.

[286] L.S. Serafim, P.C. Lemos, M.G.E. Albuquerque, M.A.M. Reis, Strategies for PHA production by mixed cultures and renewable waste materials, Appl Microbiol Biotechnol 81 (2008) 615–628. https://doi.org/10.1007/s00253-008-1757-y.

[287] D. Tan, Y. Wang, Y. Tong, G.-Q. Chen, Grand Challenges for Industrializing Polyhydroxyalkanoates (PHAs), Trends Biotechnol 39 (2021) 953–963. https://doi.org/10.1016/j.tibtech.2020.11.010.

[288] K. Wang, A.M. Hobby, Y. Chen, A. Chio, B.M. Jenkins, R. Zhang, Techno-Economic Analysis on an Industrial-Scale Production System of Polyhydroxyalkanoates (PHA) from Cheese By-Products by Halophiles, Processes 10 (2021) 17. https://doi.org/10.3390/pr10010017.

[289] A. Getachew, F. Woldesenbet, Production of biodegradable plastic by polyhydroxybutyrate (PHB) accumulating bacteria using low cost agricultural waste material, BMC Res Notes 9 (2016) 509. https://doi.org/10.1186/s13104-016-2321-y.

[290] V. Saranya, Poornimakkani, M.S. Krishnakumari, P. Suguna, C. Binuramesh, P. Abirami, V. Rajeswari, K.B. Ramachandran, R. Shenbagarathai, Quantification of Intracellular Polyhydroxyalkanoates by Virtue of Personalized Flow Cytometry Protocol, Curr Microbiol 65 (2012) 589–594. https://doi.org/10.1007/s00284-012-0198-0.

[291] J. Jackie, C.K. Chua, D.C.Y. Chong, S.Y. Lim, S.F.Y. Li, Rapid and Sensitive Direct Detection of Endotoxins by Pyrolysis–Gas Chromatography–Mass Spectrometry, ACS Omega 6 (2021) 15192–15198. https://doi.org/10.1021/acsomega.1c01446.

[292] M. Barea-Sepúlveda, H. Duarte, M.J. Aliaño-González, A. Romano, B. Medronho, Total Ion Chromatogram and Total Ion Mass Spectrum as Alternative Tools for Detection and Discrimination (A Review), Chemosensors 10 (2022) 465. https://doi.org/10.3390/chemosensors10110465.

[293] K.M. McKinnon, Flow cytometry: An overview, Curr Protoc Immunol 2018 (2018) 5.1.1-5.1.11. https://doi.org/10.1002/cpim.40.

[294] R. Zuriani, S. Vigneswari, M.N.M. Azizan, M.I.A. Majid, A.A. Amirul, A high throughput Nile red fluorescence method for rapid quantification of intracellular bacterial polyhydroxyalkanoates, Biotechnology and Bioprocess Engineering 18 (2013) 472–478. https://doi.org/10.1007/s12257-012-0607-z.

[295] A.A. Amirul, A.R.M. Yahya, K. Sudesh, M.N.M. Azizan, M.I.A. Majid, Biosynthesis of poly(3-hydroxybutyrate-co-4-hydroxybutyrate) copolymer by Cupriavidus sp. USMAA1020 isolated from Lake Kulim, Malaysia, Bioresour Technol 99 (2008) 4903–4909. https://doi.org/10.1016/j.biortech.2007.09.040.

[296] P. Spiekermann, B.H.A. Rehm, R. Kalscheuer, D. Baumeister, A. Steinbüchel, A sensitive, viable-colony staining method using Nile red for direct screening of bacteria that accumulate polyhydroxyalkanoic acids and other lipid storage compounds, Arch Microbiol 171 (1999) 73–80. https://doi.org/10.1007/s002030050681.

[297] V. Gorenflo, A. Steinbüchel, S. Marose, M. Rieseberg, T. Scheper, Quantification of bacterial polyhydroxyalkanoic acids by Nile red staining, Appl Microbiol Biotechnol 51 (1999) 765–772. https://doi.org/10.1007/s002530051460.

[298] I. Vizcaino-Caston, C.A. Kelly, A.V.L. Fitzgerald, G.A. Leeke, M. Jenkins, T.W. Overton, Development of a rapid method to isolate polyhydroxyalkanoates from bacteria for screening studies, J Biosci Bioeng 121 (2016) 101–104. https://doi.org/10.1016/j.jbiosc.2015.04.021.

[299] F. Garcia-Ochoa, E. Gomez, Bioreactor scale-up and oxygen transfer rate in microbial processes: An overview, Biotechnol Adv 27 (2009) 153–176. https://doi.org/10.1016/j.biotechadv.2008.10.006.

[300] F. Garcia-Ochoa, E. Gomez, V.E. Santos, J.C. Merchuk, Oxygen uptake rate in microbial processes: An overview, Biochem Eng J 49 (2010) 289–307. https://doi.org/10.1016/j.bej.2010.01.011.

[301] V. Riis, W. Mai, Gas chromatographic determination of poly-β-hydroxybutyric acid in microbial biomass after hydrochloric acid propanolysis, J Chromatogr A 445 (1988) 285–289. https://doi.org/10.1016/S0021-9673(01)84535-0.

[302] P. Dey, V. Rangarajan, Improved fed-batch production of high-purity PHB (poly-3 hydroxy butyrate) by Cupriavidus necator (MTCC 1472) from sucrose-based cheap substrates under response surface-optimized conditions, 3 Biotech 7 (2017) 1–14. https://doi.org/10.1007/s13205-017-0948-6.

[303] D. Kucera, P. Benesova, P. Ladicky, M. Pekar, P. Sedlacek, S. Obruca, Production of polyhydroxyalkanoates using hydrolyzates of spruce sawdust: Comparison of hydrolyzates detoxification by application of overliming, active carbon, and lignite, Bioengineering 4 (2017). https://doi.org/10.3390/bioengineering4020053.

[304] A. Fernández-Castané, H. Li, O.R.T. Thomas, T.W. Overton, Development of a simple intensified fermentation strategy for growth of Magnetospirillum gryphiswaldense MSR-1: Physiological responses to changing environmental conditions, N Biotechnol 46 (2018) 22–30. https://doi.org/10.1016/j.nbt.2018.05.1201.

[305] M.H. Nicolaisen, J. Bælum, C.S. Jacobsen, J. Sørensen, Transcription dynamics of the functional tfdA gene during MCPA herbicide degradation by Cupriavidus necator AEO106 (pRO101) in agricultural soil, Environ Microbiol 10 (2008) 571–579. https://doi.org/10.1111/j.1462-2920.2007.01476.x.

[306] S. Martinez, E. Déziel, Changes in polyhydroxyalkanoate granule accumulation make optical density measurement an unreliable method for estimating bacterial growth in Burkholderia thailandensis, Can J Microbiol 66 (2020) 256–262. https://doi.org/10.1139/cjm-2019-0342.

[307] J. Xia, G. Wang, J. Lin, Y. Wang, J. Chu, Y. Zhuang, S. Zhang, Advances and Practices of Bioprocess Scale-up, in: Adv Biochem Eng Biotechnol, Springer Science and Business Media Deutschland GmbH, 2015: pp. 137–151. https://doi.org/10.1007/10_2014_293.

[308] D.H. Vu, A. Mahboubi, A. Root, I. Heinmaa, M.J. Taherzadeh, D. Åkesson, Thorough Investigation of the Effects of Cultivation Factors on Polyhydroalkanoates (PHAs) Production by Cupriavidus necator from Food Waste-Derived Volatile Fatty Acids, Fermentation 8 (2022) 605. https://doi.org/10.3390/fermentation8110605.

[309] L.E. Mcdaniel, E.G. Bailey, Effect of Shaking Speed and Type of Closure on Shake Flask Cultures, 1969.

[310] E.E. Uchendu, M.R. Shukla, B.M. Reed, D.C.W. Brown, P.K. Saxena, Improvement of Ginseng by In Vitro Culture, in: Comprehensive Biotechnology, Elsevier, 2011: pp. 317–329. https://doi.org/10.1016/B978-0-08-088504-9.00251-8.

[311] S.K. Singh, S.K. Singh, V.R. Tripathi, S.K. Khare, S.K. Garg, Comparative one-factor-at-a-time, response surface (statistical) and bench-scale bioreactor level optimization of thermoalkaline protease production from a psychrotrophic Pseudomonas putida SKG-1 isolate, Microb Cell Fact 10 (2011) 114. https://doi.org/10.1186/1475-2859-10-114.

[312] Md.Z. Alam, N.A. Kabbashi, S.N.I.S. Hussin, Production of bioethanol by direct bioconversion of oil-palm industrial effluent in a stirred-tank bioreactor, J Ind Microbiol Biotechnol 36 (2009) 801–808. https://doi.org/10.1007/s10295-009-0554-7.

[313] M. Michelin, M. de L.T. de M. Polizeli, D.P. da Silva, D.S. Ruzene, A.A. Vicente, J.A. Jorge, H.F. Terenzi, J.A. Teixeira, Production of xylanolytic enzymes by Aspergillus terricola in stirred tank and airlift tower loop bioreactors, J Ind Microbiol Biotechnol 38 (2011) 1979–1984. https://doi.org/10.1007/s10295-011-0987-7.

[314] A. Berenjian, Bioreactor Scale-Up, in: 2020: pp. C1–C1. https://doi.org/10.1007/978-3-030-16230-6_11.

[315] L. Qu, L.-J. Ren, G.-N. Sun, X.-J. Ji, Z.-K. Nie, H. Huang, Batch, fed-batch and repeated fed-batch fermentation processes of the marine thraustochytrid Schizochytrium sp. for producing

docosahexaenoic acid, Bioprocess Biosyst Eng 36 (2013) 1905–1912. https://doi.org/10.1007/s00449-013-0966-7.

[316] Md.S.I. Mozumder, H. De Wever, E.I.P. Volcke, L. Garcia-Gonzalez, A robust fed-batch feeding strategy independent of the carbon source for optimal polyhydroxybutyrate production, Process Biochemistry 49 (2014) 365–373. https://doi.org/10.1016/j.procbio.2013.12.004.

[317] E. Carsanba, M. Pintado, C. Oliveira, Fermentation Strategies for Production of Pharmaceutical Terpenoids in Engineered Yeast, Pharmaceuticals 14 (2021) 295. https://doi.org/10.3390/ph14040295.

[318] S. Ganeshan, S.H. Kim, V. Vujanovic, Scaling-up production of plant endophytes in bioreactors: concepts, challenges and perspectives, Bioresour Bioprocess 8 (2021) 63. https://doi.org/10.1186/s40643-021-00417-y.

[319] J.M.B.T. Cavalheiro, M.C.M.D. de Almeida, C. Grandfils, M.M.R. da Fonseca, Poly(3-hydroxybutyrate) production by Cupriavidus necator using waste glycerol, Process Biochemistry 44 (2009) 509–515. https://doi.org/10.1016/j.procbio.2009.01.008.

[320] R.R. Dalsasso, F.A. Pavan, S.E. Bordignon, G.M.F. de Aragão, P. Poletto, Polyhydroxybutyrate (PHB) production by Cupriavidus necator from sugarcane vinasse and molasses as mixed substrate, Process Biochemistry 85 (2019) 12–18. https://doi.org/10.1016/j.procbio.2019.07.007.

[321] D. Nygaard, O. Yashchuk, D.G. Noseda, B. Araoz, É.B. Hermida, Improved fermentation strategies in a bioreactor for enhancing poly(3-hydroxybutyrate) (PHB) production by wild type Cupriavidus necator from fructose, Heliyon 7 (2021). https://doi.org/10.1016/j.heliyon.2021.e05979.

[322] Juan Moreno-Cid, Tuuli Inkeri Pöllänen, Carmen García Álvarez, Fuensanta Verdú, How to use the microbial respiration in the aerobic fermentation process: OUR, CER, and RQ determination with bionet bBREATH, 2021.

[323] R. Lin, J. Cheng, L. Ding, W. Song, J. Zhou, K. Cen, Inhibitory effects of furan derivatives and phenolic compounds on dark hydrogen fermentation, Bioresour Technol 196 (2015) 250–255. https://doi.org/10.1016/j.biortech.2015.07.097.

[324] V. Kachrimanidou, A. Vlysidis, N. Kopsahelis, I.K. Kookos, Increasing the volumetric productivity of fermentative ethanol production using a fed-batch vacuferm process, Biomass Convers Biorefin 11 (2021) 673–680. https://doi.org/10.1007/s13399-020-00673-6.

[325] S. Khanna, A.K. Srivastava, Statistical media optimization studies for growth and PHB production by Ralstonia eutropha, Process Biochemistry 40 (2005) 2173–2182. https://doi.org/10.1016/j.procbio.2004.08.011.

[326] E. Palmqvist, B. Hahn-Hägerdal, Fermentation of lignocellulosic hydrolysates. II: inhibitors and mechanisms of inhibition, Bioresour Technol 74 (2000) 25–33. https://doi.org/10.1016/S0960-8524(99)00161-3.

[327] R. Tang, C. Weng, X. Peng, Y. Han, Metabolic engineering of Cupriavidus necator H16 for improved chemoautotrophic growth and PHB production under oxygen-limiting conditions, Metab Eng 61 (2020) 11–23. https://doi.org/10.1016/j.ymben.2020.04.009.

[328] J. Yu, Y. Lu, Carbon dioxide fixation by a hydrogen-oxidizing bacterium: Biomass yield, reversal respiratory quotient, stoichiometric equations and bioenergetics, Biochem Eng J 152 (2019) 107369. https://doi.org/10.1016/j.bej.2019.107369.

[329] J. Wang, S. Liu, J. Huang, R. Cui, Y. Xu, Z. Song, Genetic engineering strategies for sustainable polyhydroxyalkanoate (PHA) production from carbon-rich wastes, Environ Technol Innov 30 (2023) 103069. https://doi.org/10.1016/j.eti.2023.103069.

[330] R. Shen, J. Yin, J.-W. Ye, R.-J. Xiang, Z.-Y. Ning, W.-Z. Huang, G.-Q. Chen, Promoter engineering for enhanced P(3HB- co -4HB) production by Halomonas bluephagenesis, ACS Synth Biol 7 (2018) 1897–1906. https://doi.org/10.1021/acssynbio.8b00102.

[331] K. Sangkharak, P. Prasertsan, The production of polyhydroxyalkanoate by Bacillus licheniformis using sequential mutagenesis and optimization, Biotechnology and Bioprocess Engineering 18 (2013) 272–279. https://doi.org/10.1007/s12257-012-0615-z.

[332] Y.-G. Lee, Y.-S. Jin, Y.-L. Cha, J.-H. Seo, Bioethanol production from cellulosic hydrolysates by engineered industrial Saccharomyces cerevisiae, Bioresour Technol 228 (2017) 355–361. https://doi.org/10.1016/j.biortech.2016.12.042.

[333] S. Baei, G.D. Najafpour, H. Younesi, F. Tabandeh, H. Issazadeh, M. Khodabandeh, Growth kinetic parameters and biosynthesis of polyhydroxybutyrate in Cupriavidus necator DSMZ 545 on selected substrates, Chemical Industry and Chemical Engineering Quarterly 17 (2011) 1–8. https://doi.org/10.2298/CICEQ100216043B.

[334] C. Boy, J. Lesage, S. Alfenore, S.E. Guillouet, N. Gorret, Investigation of the robustness of Cupriavidus necator engineered strains during fed-batch cultures, AMB Express 11 (2021). https://doi.org/10.1186/s13568-021-01307-4.

[335] Lic. Daiana Nygaard, Elida Hermida, Oxana Yashchuk, Scalable production of polyhydroxybutyrate biopolymer from Cupriavidus necator ATCC 17697, 2019.

[336] Haydn Rhys Ingram, Production of Polyhydroxyalkanoate Copolymers by Cupriavidus necator using Spent Coffee Grounds as a Sustainable Feedstock, 2022.

[337] S. Milker, A. Sydow, I. Torres-Monroy, G. Jach, F. Faust, L. Kranz, L. Tkatschuk, D. Holtmann, Gram-scale production of the sesquiterpene α-humulene with *Cupriavidus necator*, Biotechnol Bioeng 118 (2021) 2694–2702. https://doi.org/10.1002/bit.27788.

[338] E. Grousseau, E. Blanchet, S. Déléris, M.G.E. Albuquerque, E. Paul, J.-L. Uribelarrea, Phosphorus limitation strategy to increase propionic acid flux towards 3-hydroxyvaleric acid monomers in Cupriavidus necator, Bioresour Technol 153 (2014) 206–215. https://doi.org/10.1016/j.biortech.2013.11.072.

[339] E. Grousseau, E. Blanchet, S. Déléris, M.G.E. Albuquerque, E. Paul, J.-L. Uribelarrea, Impact of sustaining a controlled residual growth on polyhydroxybutyrate yield and production kinetics in Cupriavidus necator, Bioresour Technol 148 (2013) 30–38. https://doi.org/10.1016/j.biortech.2013.08.120.

Appendices

Appendix A

A1 Acid hydrolysis optimisation using response surface methodology: glucose concentration response.

Analogous to the CCD presented in *Chapter 4.3.2.2 Acid hydrolysis optimization using response surface methodology*, a CCD was conducted to investigate the effect of three variables on the glucose concentration in the hydrolysate. The variables under investigation were H_2SO_4 concentration, hydrolysis time and hydrolysis temperature. The experimental results and the corresponding independent factors are shown in Table A1.1.

Table A1. 1 Central Composite Design (CCD) used in this study for the optimization along with experimental values of the response glucose concentration.

Run	Factor x_1 [H_2SO_4] (M)	Factor x_2 Time (min)	Factor x_3 Temperature (°C)	Response glucose concentration (g/L)
1	-1	1	-1	20.0
2	-1	1	1	48.2
3	-1	-1	1	54.6
4	-1	-1	-1	2.4
5	1	-1	1	47.1
6	1	-1	-1	22.0
7	1	1	-1	54.6
8	1	1	1	53.2
9	-1.68	0	0	1.7
10	1.68	0	0	47.5
11	0	-1.68	0	51.5
12	0	0	-1.68	2.8
13	0	0	1.68	44.1
14	0	1.68	0	46.0
15	0	0	0	48.7
16	0	0	0	49.9
17	0	0	0	48.7
18	0	0	0	36.0
19	0	0	0	52.3
20	0	0	0	40.8

The data from table A1.1 underwent analysis using ANOVA in Design Expert. The results of the ANOVA test are presented in Table A1.2. This model exhibited a coefficient of variation (CV) of 22.5%, which lies above an acceptable limit of 15% [277]. Furthermore, the fitness of the model was evaluated through the coefficient of determination R^2. In this case, an R^2 of 0.88 was obtained,

indicating that the variables account for over 88% of the variation, and that the model cannot explain less than 12% of the total variance. Adequate precision measures the signal-to-noise ratio, and values greater than 4 are desirable. The ratio of 9.45 indicates that the signal is adequate for the model, which can be used to navigate the design space. However, the adjusted R^2 (0.78) is not in reasonable agreement with the predicted R^2 (0.26), showing a difference greater than 0.2 [255]. Despite obtaining less favourable statistical metrics compared to those achieved for the TRS response model detailed in Chapter 4.3.2.2, the ANOVA analysis presented in this section also resulted in a statistically significant model, as indicated by a p-value of 0.001. Moreover, the lack of fit for this model was not significant, with a p-value of 0.09. Consequently, we proceeded with the validation of the model.

Table A1. 2 Analysis of variance (ANOVA) for the central composite design quadratic model for the glucose concentration response. x1: H2SO4 concentration; x2: time; x3: temperature.

Source	Sum of squares	df	Mean square	F-value	p-value
Model	5687.29	9	631.92	8.3	0.001
x_1	1164.71	1	1164.71	15.3	0.003
x_2	185.06	1	185.06	2.4	0.15
x_3	1974.56	1	1974.56	25.9	0.0005
x_1x_2	175.13	1	175.13	2.3	0.16
x_1x_3	553.28	1	553.28	7.3	0.02
x_2x_3	285.25	1	285.25	3.8	0.08
x_1^2	632.70	1	632.70	8.3	0.016
x_2^2	52.89	1	52.89	0.69	0.42
x_3^2	717.12	1	717.12	9.4	0.01
Residual	761.57	10	76.16	-	-
Lack of fit	598.28	5	119.66	3.7	0.09
Pure error	163.30	5	32.66	-	-
Cor Total	6448.85	19	-	-	-

C.V = 22.5%; R^2 = 0.88; Adj R^2 = 0.78; Pred R^2 = 0.26; Adeq Precision = 9.45

The validation was carried out under the same hydrolysis conditions presented in Chapter 4.3.2.2: 2.2 M H2SO4, 150 min and 102 °C. Under these conditions, a glucose concentration of 42.7 g/L was obtained, while the expected value was 52.6 g/L. This discrepancy results in an error of 19% which lies above the acceptable limit of 15%.

Despite efforts to optimise the model by eliminating insignificant factors and introducing higher-order terms, our attempts did not yield a robust and reliable model.

Therefore, while the ANOVA test showed a significant model, various statistical indicators here presented, including the CV, R^2 and the difference between the predicted and adjusted R^2 demonstrated room for improvement. This fact is supported by Figure A1.1, where the predicted vs. actual values plot, shows that most of the points are not close to the line. Moreover, the 19% error in the validation experiment further reinforced the need for enhancing the model to establish its reliability for predicting reliable data.

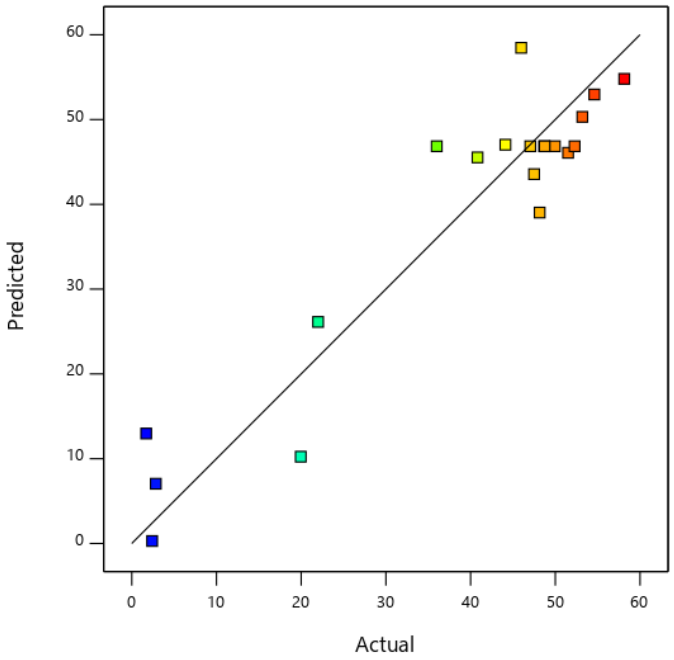

Figure A1. 1 Glucose concentration predicted vs. actual values plot

A2. Total reducing sugars (TRS) determination method

Figure A2.1 illustrates the calibration curve used throughout the thesis to determine the concentration of total reducing sugars (TRS) in the samples using the Di-nitrosalicylic acid (DNS) test. The absorbance values of the samples were interpolated using the provided calibration curve, which was constructed using pure synthetic D-(+)-glucose (CAS 2280-44-6) as a reference compound for calculating the TRS concentration. The equation was:

$y = 0.3984x$

where y is the TRS concentration and x is the absorbance measured.

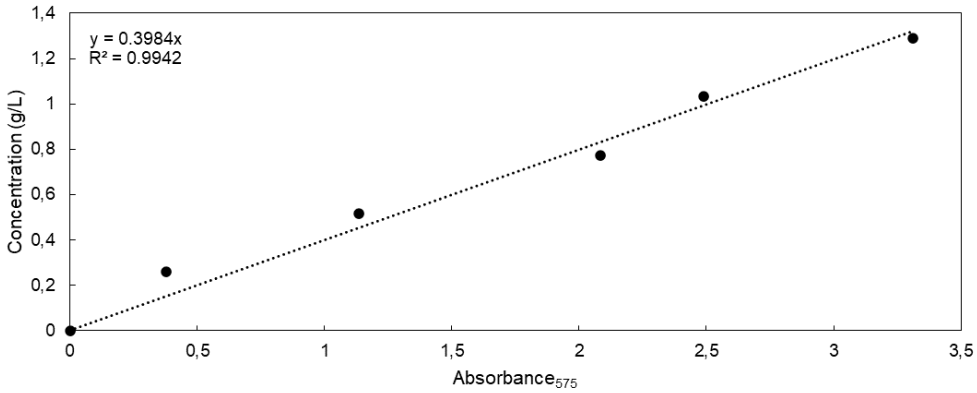

Figure A2. 1 Calibration curve for the determination of total reducing sugars (TRS)

Figure A2.2 shows a representative image displaying four samples containing varying TRS concentrations. These samples are arranged in ascending order from the lowest concentration to the highest concentrated, as determined through the DNS test.

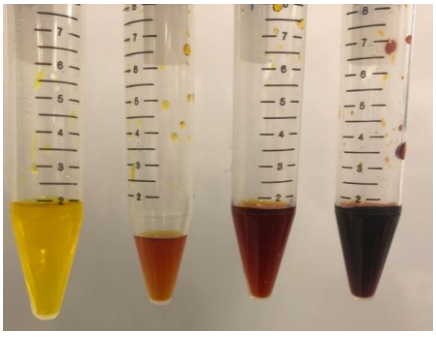

Figure A2. 2 Representative samples containing ascending concentrations of total reducing sugars determined through the Di-nitrosalicylic acid (DNS) test.

Appendix B

B1. Correlation determination between OD_{600} measurements and dry cell weight (DCW)

Figure B1.1 illustrates the correlation between OD_{600} values and dry cell weight (DCW) concentration. As depicted in Figure B1.1, $1OD_{600}$ is equivalent to 0.2941 g/L of DCW. The establishment of this robust correlation (R^2=0.9786) simplifies future experiments due to the ease of OD_{600} measurements in comparison to the quantification of DCW.

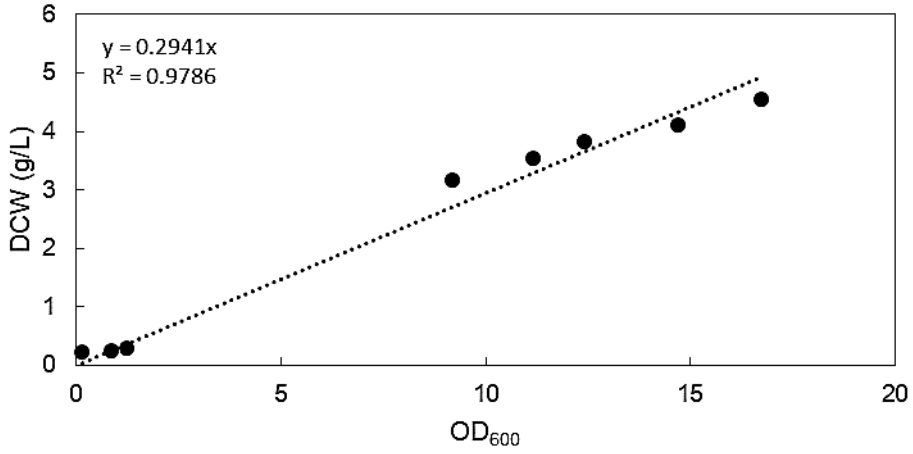

Figure B1. 1 Correlation between OD_{600} and microbial dry cell weight (DCW) of *Cupriavidus necator* cultures. DCW (g/L) = 0.2941 x OD_{600}. R^2=0.9786

B2 Determination of polyhydroxyalkanoates concentration through GC-MS

Figure B2.1 depicts the calibration curves for the quantification of 3-hydroxybutiric acid (Figure B2.1A) and 3-hydroxyvaleric-acid (Figure B2.1B). These two monomers the monomers constitute the building blocks of the of poly(3-hydroxybutyric acid-*co*-3-hydroxyvaleric acid (PHBV), which is the specific PHA detected throughout this thesis.

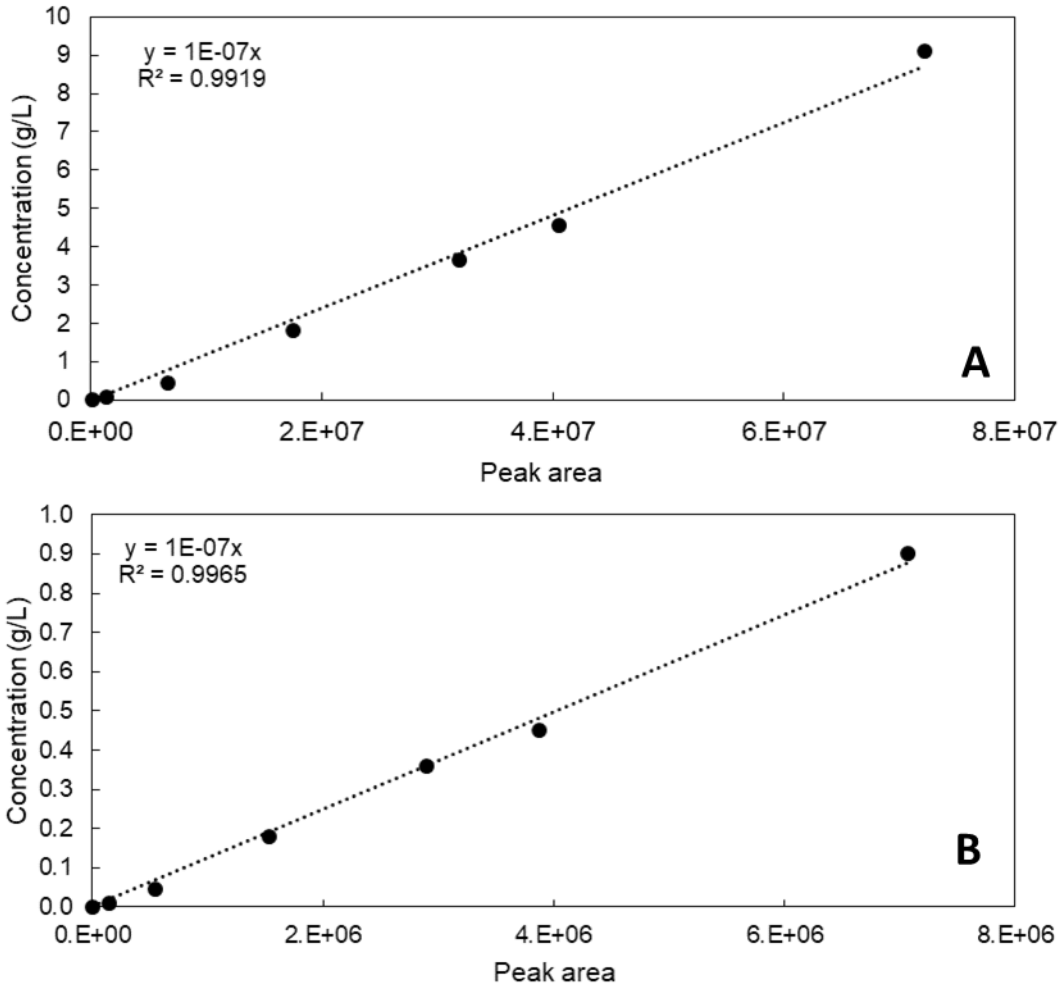

Figure B2. 1 Calibration curves for the calculation of polyhydroxybutyrate (PHB) (A), and polyhydroxyvalerate (PHV) (B) concentration.

Figure B2.2 shows two representative GC-MS chromatograms of a PHBV standard sample (Figure B2.2 A1) and a PHBV sample synthesised through *C. necator* fermentation (Figure B2.2 A2). B2.2 B1 also includes the molecular representations of the compounds corresponding to each peak. Furthermore, the mass spectroscopy spectra of 3-hydroxybutyric acid obtained in this study and the theoretical one is presented in Figure B2.2 B1 and B2, respectively. The same information regarding 3-hydroxyvaleric acid is presented in Figure B2.2 C1 and C2.

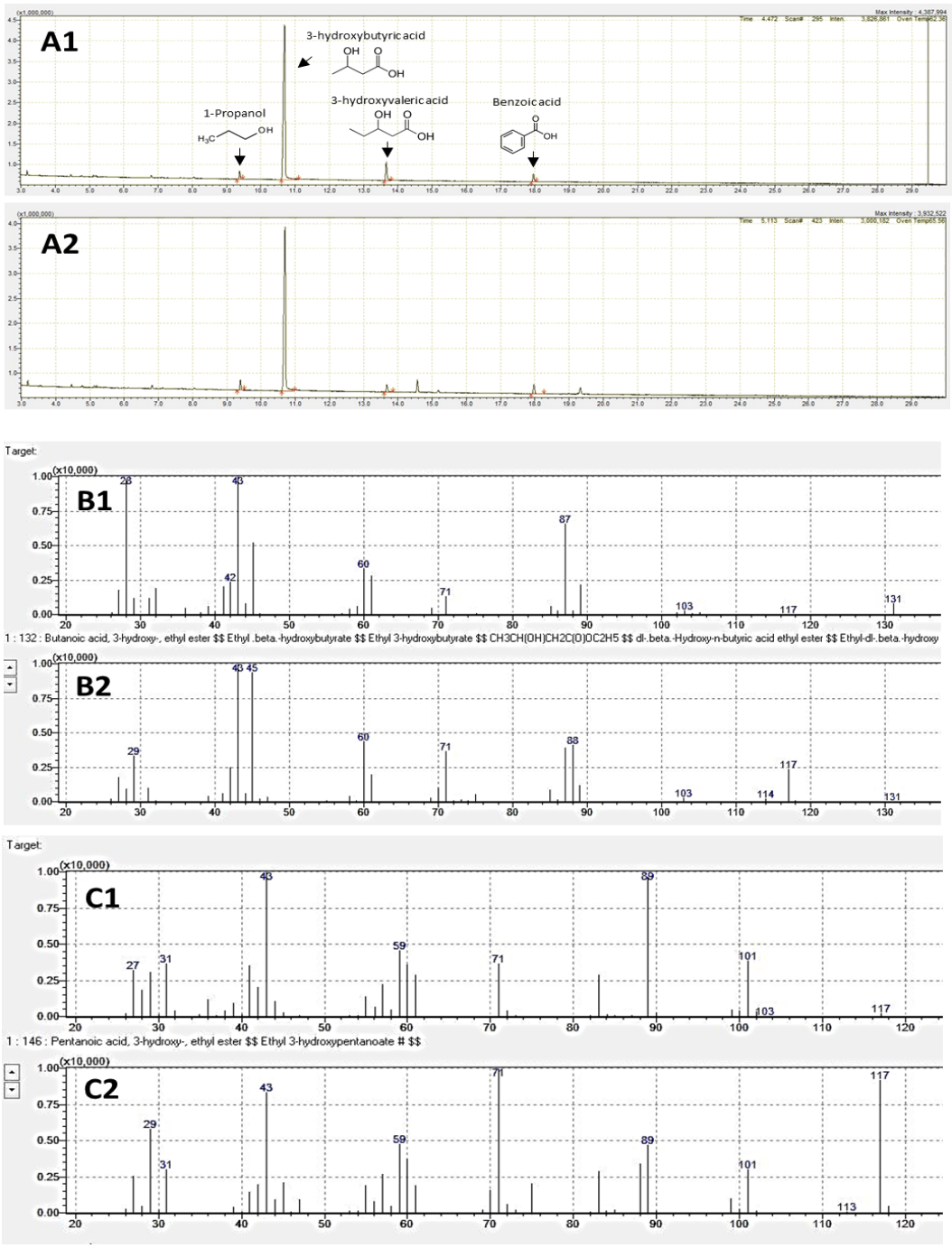

Figure B2. 2 GC-MS spectra of commercial poly(3-hydroxybutyric acid-*co*-3-hydroxyvaleric acid) (A1); PHBV synthesised via Cupriavidus necator fermentation using cassava peel hydrolysate at flask scale (A2); mass spectroscopy spectra of 3-hydroxybutyric acid resultant from the present study (B1); along with its theoretical spectrum (B2); mass spectroscopy spectra of 3-hydroxyvaleric acid resultant from the present study (C1); along with its theoretical spectrum (C2).

B3. Correlation between PHA concentration (%) and pyrromethene-546 fluorescence values

Figure B3.1 displays the correlation between the PHA concentration (%), as determined by GC-MS analysis, and the corresponding Pyr-546 values measured using FCM.

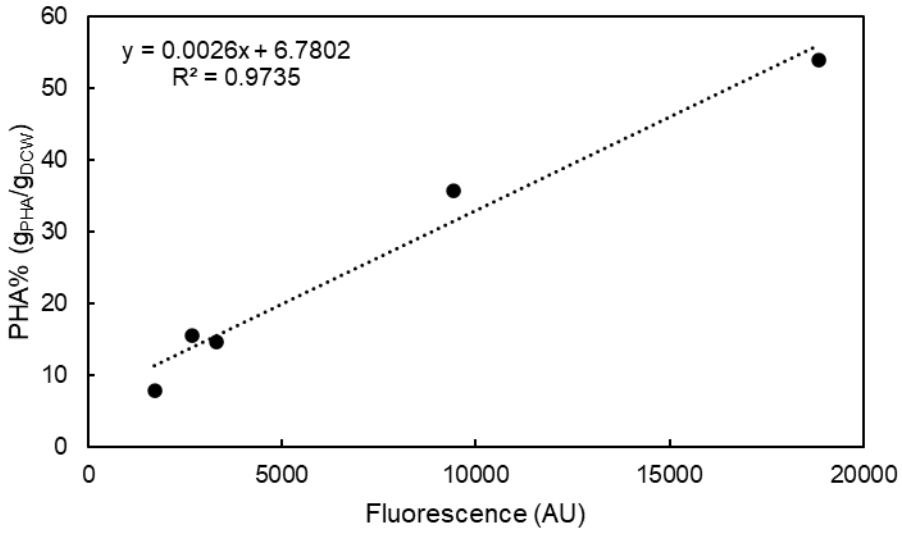

Figure B3. 1 Correlation between PHA concentration (%) quantified using GC-MS and fluorescence values from flow cytometry (FCM) after pyrromethene-546 (Pyr-546) staining. AU: arbitrary units.

B4. Pyrromethene-546 fluorescence histograms from the polyhydroxyalkanoates-staining optimisation

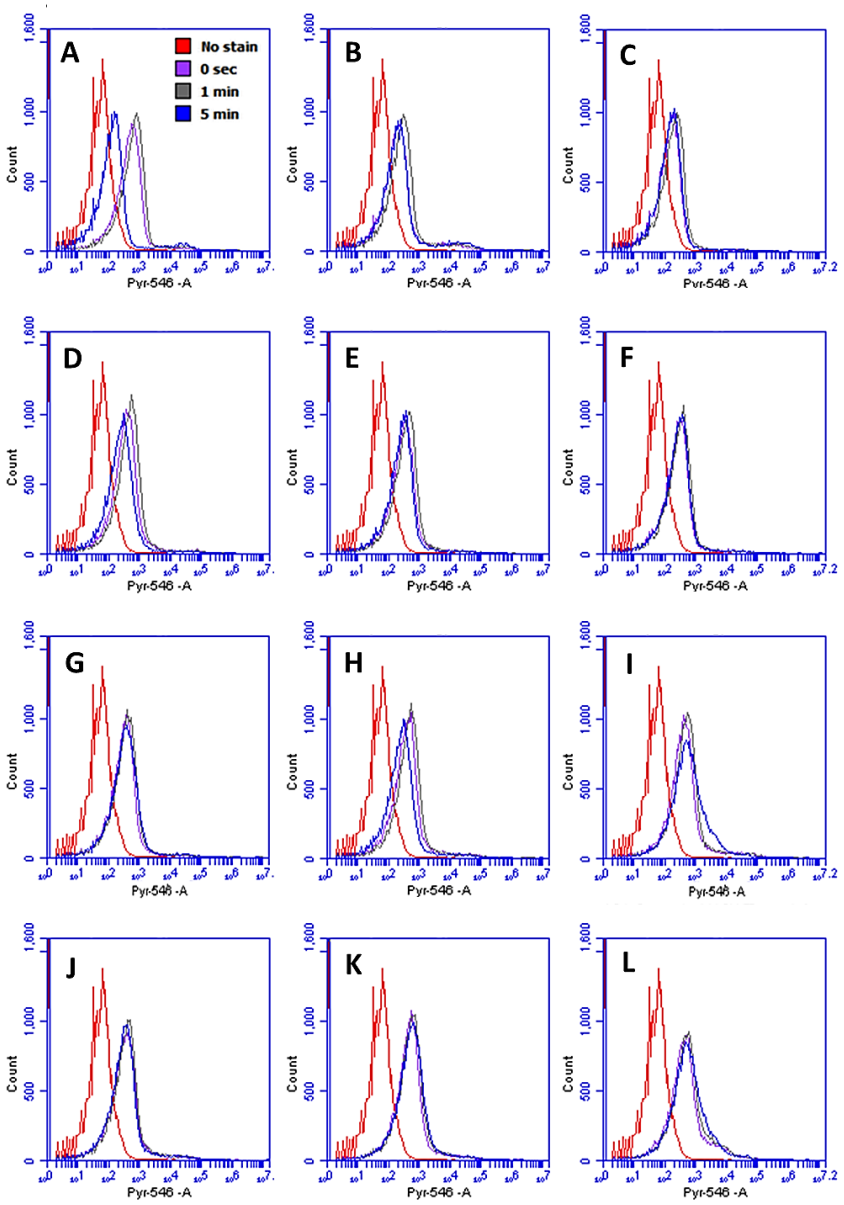

Figure B4. 1 Histograms showing fluorescence intensity of *Cupriavidus necator* stained with varying pyr-546 concentrations (A) 0.05 mg/mL, 100 % DMSO; (B) 0.05 mg/mL, 20/80 (% v/v) EtOH/DMSO; (C) 0.05 mg/mL, 40/60 (% v/v) EtOH/DMSO; (D) 0.05 mg/mL, 60/40 (% v/v) EtOH/DMSO; (E) 0.1 mg/mL, 100 % DMSO; (F) 0.1 mg/mL, 20/80 (% v/v) EtOH/DMSO;(G) 0.1 mg/mL, 40/60 (% v/v) EtOH/DMSO; (H) 0.1 mg/mL, 60/40 (% v/v) EtOH/DMSO; (I) 0.2 mg/mL, 100 % DMSO; (J) 0.2 mg/mL, 20/80 (% v/v) EtOH/DMSO; (K) 0.2 mg/mL, 40/60 (% v/v) EtOH/DMSO; (L) 0.2 mg/mL, 60/40 20/80 (% v/v) EtOH/DMSO, and different incubation times of 0 min (purple); 1 min (grey); and 5 min (blue). The red histogram present in all the plots represents the non-stained sample.

B5. Pyrromethene-546 fluorescence histograms from the *Cupriavidus necator* growth and PHA production screening experiment from cassava peel hydrolysates

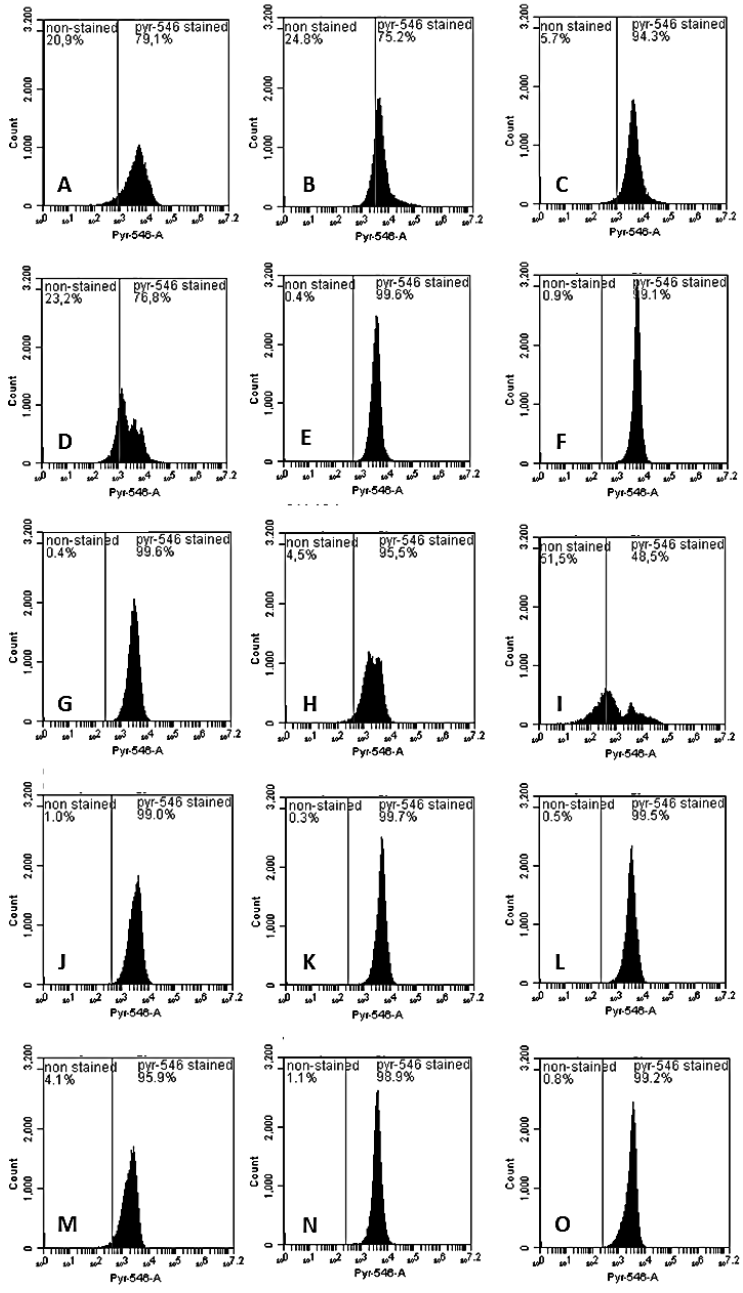

Figure B5. 1 Analysis of polyhydroxyalkanoates (PHA) production by *Cupriavidus necator (C. necator)* after Pyr-546 staining (A) 0.6 M, 182 min, 72 ºC; (B) 0.6M, 182 min, 107 ºC; (C) 0.6M, 58 min, 107 ºC, (D) 0.6 M, 58 min, 72 ºC; (E) 2.4M, 58 min, 107 ºC; (F) 2.4M 58 min, 72 ºC; (G) 2.4M, 182 min, 72 ºC; (H) 2.4M, 182 min, 107 ºC, (I) 0.01M, 120 min, 90 ºC,(J) 3M, 120 min, 90 ºC; (K) 1.5M, 15 min, 90 ºC; (L) 1.5M, 120 min, 60 ºC; (M) 1.5M, 120 min, 120 ºC; (N) 1.5M, 225 min, 90 ºC; (O) 1.5M, 120 min, 90 ºC.

B6. Size and complexity histograms from the *Cupriavidus necator* growth and PHA production screening experiment from cassava peel hydrolysates

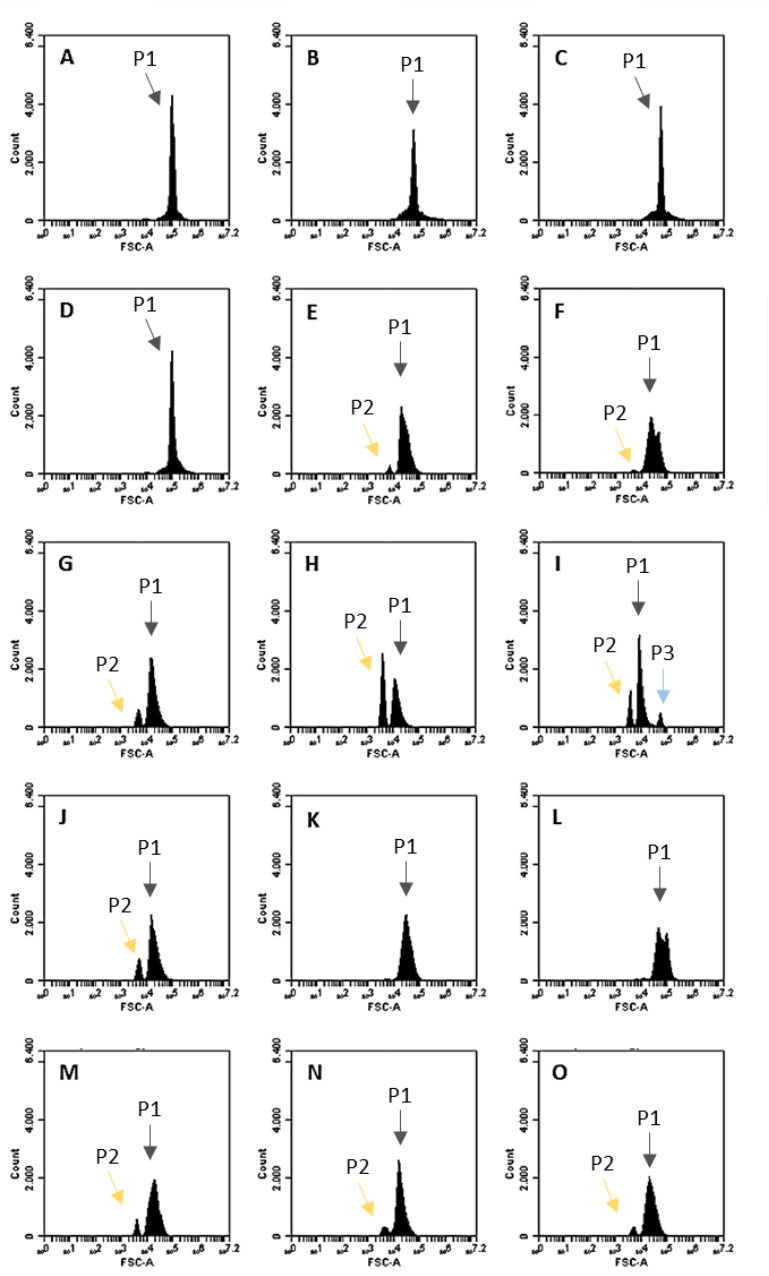

Figure B6. 1 Analysis of *Cupriavidus necator (C. necator)* size through forward scatter (FSC) using flow cytometry (FCM). (A) 0.6 M, 182 min, 72 ºC; (B) 0.6M, 182 min, 107 ºC; (C) 0.6M, 58 min, 107 ºC, (D) 0.6 M, 58 min, 72 ºC; (E) 2.4M, 58 min, 107 ºC; (F) 2.4M 58 min, 72 ºC; (G) 2.4M, 182 min, 72 ºC; (H) 2.4M, 182 min, 107 ºC, (I) 0.01M, 120 min, 90 ºC,(J) 3M, 120 min, 90 ºC; (K) 1.5M, 15 min, 90 ºC; (L) 1.5M, 120 min, 60 ºC; (M) 1.5M, 120 min, 120 ºC; (N) 1.5M, 225 min, 90 ºC; (O) 1.5M, 120 min, 90 ºC (n=3). P1: population 1; P2: population 2; and P3: population 3.

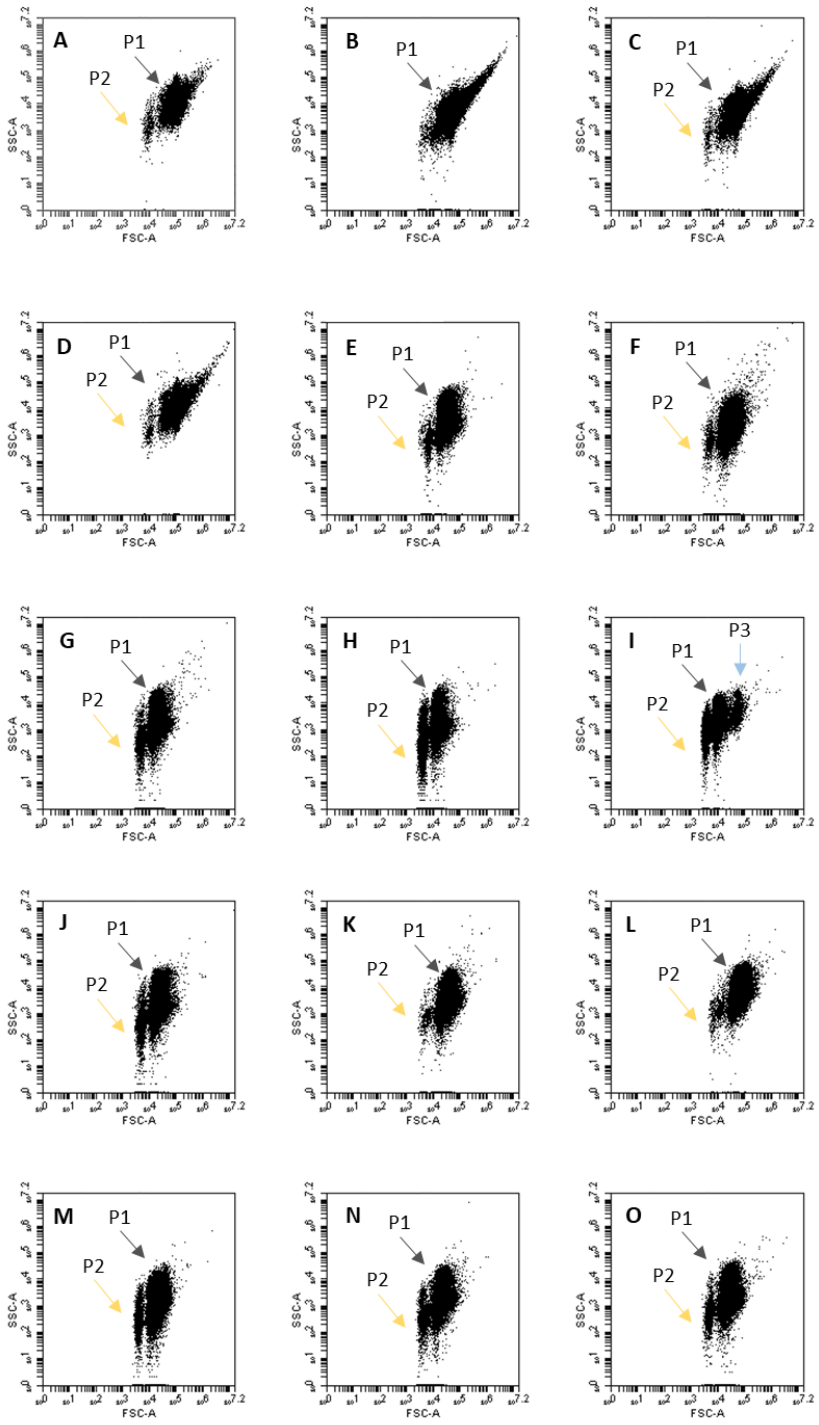

Figure B6. 2 Analysis of *Cupriavidus necator (C. necator)* size through forward scatter (FSC-A axis) and complexity through size scatter (SSC-A axis) using flow cytometry (FCM). (A) 0.6 M, 182 min, 72 ºC; (B) 0.6M, 182 min, 107 ºC; (C) 0.6M, 58 min, 107 ºC, (D) 0.6 M, 58 min, 72 ºC; (E) 2.4M, 58 min, 107 ºC; (F) 2.4M 58 min, 72 ºC; (G) 2.4M, 182 min, 72 ºC; (H) 2.4M, 182 min, 107 ºC, (I) 0.01M, 120 min, 90 ºC,(J) 3M, 120 min, 90 ºC; (K) 1.5M, 15 min, 90 ºC; (L) 1.5M, 120 min, 60 ºC; (M) 1.5M, 120 min, 120 ºC; (N) 1.5M, 225 min, 90 ºC; (O) 1.5M, 120 min, 90 ºC (n=3). P1: population 1; P2: population 2; and P3: population 3.